Cardiac Energy Metabolism and the Role of SGLT2 Inhibitors in Heart Failure

by

Nikole J Byrne

A thesis submitted in partial fulfillment of the requirements for the degree of

Doctor of Philosophy

Medical Science – Pediatrics

University of Alberta

Abstract

Heart failure (HF) is a condition where the cardiac muscle exhibits contractile dysfunction, limiting its ability to deliver adequate amounts of oxygen to organs throughout the body. Despite improved survival seen with pharmacological and mechanical treatment strategies, HF patients continue to experience high hospitalization and mortality rates, resulting in poor quality of life and a significant burden on healthcare. As such, the need for better therapies for HF has helped expand our understanding of the development and progression of the disease, including the role that metabolic perturbances may play. Particularly, it is becoming more evident that cardiac substrate metabolism is impaired at the transcriptional level of metabolic enzymes, playing an important role in HF pathogenesis. Researchers, therefore, believe that therapeutic approaches designed to optimize cardiac energy production may be beneficial in the treatment and management of clinical HF. However, whether or not this loss of metabolic flexibility in the failing heart is permanent and thus cannot be corrected by interventions remains unclear.

In addition, the sodium/glucose cotransporter (SGLT) 2 inhibitor, empagliflozin, has been shown to profoundly reduce cardiovascular mortality and HF hospitalization in diabetic patients with high-risk of cardiovascular disease. Of importance, empagliflozin is thought to exert cardiovascular benefit upon improving substrate availability and myocardial energetics, and therefore may be of benefit in established HF even in the absence of diabetes. Furthermore, empagliflozin has also been shown to induce hemodynamic, diuretic and anti-inflammatory effects in the setting of diabetes, highlighting additional mechanisms that may be involved in facilitating these profound cardiovascular improvements.

In order to better understand the role of cardiac substrate metabolism and/or the effects of empagliflozin in the regression of HF, we used an experimental model of pressure overload, where the transverse aorta is constricted to induce HF. In the first set of experiments, debanding (DB) surgery was performed to remove the aortic constriction once systolic cardiac function had severely declined (ejection fraction < 30%) and both fatty acid and glucose oxidation were significantly impaired. At 1- and 3- weeks following DB, cardiac remodeling, systolic and diastolic function, myocardial substrate metabolism and expression of markers of hypertrophy/HF and metabolic genes were assessed. In another set of experiments, mice with moderate HF (ejection fraction < 45%) were treated with 10 mg/kg/day empagliflozin via oral gavage for two weeks to determine whether empagliflozin improves cardiac remodeling, systolic and diastolic function in the absence of diabetes. We also explored whether empagliflozin induces changes in circulating ketone bodies, cardiac substrate oxidation or increased cardiac ATP production in nondiabetic HF. Lastly, we further investigated whether empagliflozin induced beneficial outcomes associated with improved hemodynamics, diuretic effects and anti-inflammation responses in the heart.

We observed that following reversal of the elevated aortic afterload in HF, there is near complete recovery of systolic and diastolic function by 3-weeks following DB and transcriptional levels of several markers for hypertrophy/HF were restored to that observed in control hearts. Of note, myocardial oxidation of both glucose and fatty acids was restored at 1-week post-DB, leading us to believe that normalization of cardiac substrate utilization precedes full recovery of contractile function in the regression of HF. In addition, treatment with empagliflozin was found to blunt the decline in systolic dysfunction in mice with HF in the absence of diabetes. Surprisingly, these

beneficial effects of empagliflozin in HF were not associated with any improvements in myocardial glucose, fatty acid or ketone metabolism. Furthermore, since the cardiac benefit of empagliflozin in HF in the absence of diabetes occurred without elevating circulating ketone bodies, weight loss, hemodynamic improvements or altering electrolyte concentrations, it is apparent that these prevailing theories may not be essential to the cardiovascular benefits of empagliflozin. Nonetheless, we show for the first time that empagliflozin reduces cardiac inflammation in a nondiabetic setting via reduced activation of the nucleotide-binding domain-like receptor protein 3 (NLRP3) inflammasome, and this occurs in a Ca^{2+}-dependent manner, independent of renal SGTL2 inhibition. Altogether, these data suggest that although improvements in myocardial energetics may be beneficial to the failing heart, increasing cardiac energy production is not a pre-requisite to improving cardiac contractile function. Furthermore, these findings provide important translational clues for the ongoing studies of SGLT2 inhibitors in diabetic and nondiabetic patients with HF.

Preface

This thesis is an original work by Byrne NJ. The research project, of which this thesis is a part, received research ethics approve from the University of Alberta Institutional Animal Care and Use Committee and conform to the Guide for the Care and Use of Laboratory Animals published by the U.S. National Institutes of Health (8th edition, revised 2011).

Chapter 2 has been published as Byrne NJ, Levasseur J, Sung MM, Masson G, Boisvenue J, Young ME, Dyck JRB. Normalization of Cardiac Substrate Utilization and Left Ventricular Hypertrophy Precede Functional Recovery in Heart Failure Regression. *Cardiovascular Research*. 2016; 110(2):249-57. For this project, I was the primary researcher responsible for all decision-making regarding the course of the study. This included contributing to the conception and design of the experimental paradigm with Levasseur JL and Dyck JRB and organizing all experiments. Levasseur J performed surgeries, Beker D performed echocardiography, Masson G performed the isolated working heart perfusions, and I interpreted all resulting data (including analysis of echocardiography images) from aforementioned experiments. Furthermore, I executed *in vivo* experiments (indirect calorimetry, treadmill running) and performed immunoblot analysis. I also wrote the published manuscript with the editing assistance of Dyck JRB.

Chapter 3 has been published as Byrne NJ, Parajuli N, Levasseur JL, Boisvenue J, Beker DL, Masson G, Fedak PWM, Verma S and Dyck JRB. Empagliflozin Prevents Worsening of Cardiac Function in an Experimental Model of Pressure Overload-Induced Heart Failure. *JACC: Basic to Translational Science*. 2017;2:347-354. For this project, I was the primary researcher responsible

for all decision-making regarding the course of the study. This included contributing to the conception and design of the experimental paradigm with Levasseur J and Dyck JRB and organizing all experiments. Levasseur J performed surgeries, Beker D performed echocardiography, Masson G performed the isolated working heart perfusions, and I interpreted all resulting data (including analysis of echocardiography images) from aforementioned experiments. I also wrote the published manuscript with the editing assistance of Dyck JRB.

Chapter 4 is a manuscript under revision at the *Journal of the American College of Cardiology*: Byrne NJ, Matsumura N, Alma'ayah Z, Ferdaoussi M, Takahara S, Darwesh AM, Levasseur JL, Jahng JWS, Vos D, Parajuli N, El-Kadi AOS, Braam B, Young ME, Light PE, Verma S, Sweeney G, Seubert JM, Dyck JRB. Empagliflozin Improves Cardiac Function in Heart Failure by Suppressing Activation of the NLRP3 Inflammasome. For this project, I was the primary researcher responsible for all decision-making regarding the course of the study. This included contributing to the conception and design of the experimental paradigm with Levasseur J and Dyck JRB and organizing all experiments. Levasseur J performed surgeries, Beker D performed echocardiography, Masson G performed the isolated working heart perfusions, Zhuang W performed flame photometry, Jahng JWS performed confocal immunofluorescence, Darwesh AM performed Langendorff heart perfusions, Alma'ayah Z and Ferdaoussi M performed cell culture and RT-PCR experiments and I interpreted all resulting data from aforementioned experiments. Matsumura N performed remaining *in vivo* rat work and I performed remaining *in vivo* mouse work including urine collection, blood glucose and ketone measurements and indirect calorimetry. I also wrote the published manuscript with the editing assistance of Dyck JRB.

Dedication

This thesis is dedicated to my grandfather, Lawrence Kwiatkowski, who always encouraged me to ask questions and inspired me to never stop learning.

Acknowledgements

My sincere thanks to my supervisor, Dr. Jason RB Dyck, for his mentorship and guidance in completing this research and furthering my career. The many opportunities he has provide me to share my work internationally and pursue future endeavors has allowed me to continue to grow as a research scientist.

I would like to express my gratitude to my committee members, Dr. Gary D Lopaschuk, Dr. Peter E Light and Dr. Richard Lehner, for their valuable time and insight. Your input and guidance have been enlightening throughout my graduate studies.

A special thank you to Jody Levasseur, who not only contributed her expertise to the research throughout my graduate studies, but also provided countless hours of support outside of lab work. Thank you to my fellow lab members Donna Beker, Miranda M Sung, Grant Masson, Nobutoshi Matsumura, Zaid Alma'ayah, Mourad Ferdaoussi, Shingo Takahara, Ian Robertson, Amy Barr, Jamie Boisvenue, Carrie Soltys, Dyonne Vos, Nirmal Parajuli, who have contributed greatly to my education and experience throughout the years. Thank you to the volunteer and summer students in our lab for their friendship and allowing me the opportunity to gain mentorship experience: Richelle Edwards, Marc Mullen, Mya Schmidt, Abrar Alam. Thank you to our collaborators, Ahmed M Darwesh, James Won Suk Jahng, Gary Sweeney, John M Seubert, Branko Braam, Subhodh Verma, Martin E Young, Ayman OS El-Kadi, Paul WM Fedak, who have contributed greatly to the work presented in this thesis.

I am especially grateful to my mother, Barb Byrne, who always inquired enthusiastically about my research and supported me in a number of ways throughout the years. Thank you to my entire family and friends, particularly Sandy White, Richelle Edwards and Reece Levasseur, for your constant emotional support and encouragement, especially during the most stressful times.

I would also like to thank Alberta Innovates for the Graduate Studentship, the Faculty of Medicine & Dentistry for the Motyl Graduate Studentship in Cardiac Sciences and the Faculty of Graduate Studies and Research for the Queen Elizabeth II Graduate Scholarship.

Table of Contents

List of Tables

List of Figures

List of Abbreviations

βOHB = beta-hydroxybutyrate

4E-BP1 = eukaryotic translation initiation factor 4E

A = late mitral inflow

AAC = abdominal aortic constriction

AB = aortic banding

ACC = acetyl-CoA carboxylase

ACE = angiotensin-converting-enzyme

AKT = protein kinase B

AMPK = 5′ adenosine monophosphate-activated protein kinase

ANGII = angiotensin II

ANP = atrial natriuretic peptide

ANOVA = analysis of variance

ASC = apoptosis-associated speck-like protein containing caspase-recruitment domain

ATGL = adipose triglyceride lipase

ATP = adenosine triphosphate

AU = arbitrary units

BDH1 = beta-hydroxybutyrate dehydrogenase 1

BNP = brain natriuretic peptide

BP = blood pressure

BSA = bovine serum albumin

CANTOS = canakinumab anti-inflammatory thrombosis outcomes study

CANVAS = canagliflozin cardiovascular assessment study

CASP1 = caspase 1

CA^{2+} = calcium ion

CDNA = complementary deoxyribonucleic acid

COA = coenzyme A

CO = cardiac output

COL1α1 = collagen type I alpha-1

COL3α1 = collagen type III alpha-1

CPT = carnitine palmitoyltransferase

CVD = cardiovascular disease

DAMP = damage-associated molecular patterns

DAPI = 4′,6-diamidino-2-phenylindole

DB = debanding

DECLARE-TIMI58 = dapagliflozin on the incidence of cardiovascular events

DMSO = dimethyl sulfoxide

DP = developed pressure

DPP-4 = dipeptidyl peptidase-4

DP/DT_{MAX} = rate of contraction

DP/DT_{MIN} = rate of relaxation

E = early mitral inflow

E′ = tissue Doppler mitral annulus velocity

ECM = extracellular matrix

EMPA = empagliflozin

EMPA-REG Outcome = empagliflozin cardiovascular outcome event trial in type 2 diabetes mellitus patients

EF = ejection fraction

ET = ejection time

ETC = electron transport chain

$FADH_2$ = flavin adenine dinucleotide

FA = fatty acid

FAT/CD36 = fatty acid translocase

FFA = free fatty acid

FS = fractional shortening

GAPDH = glyceraldehyde 3-phosphate dehydrogenase

GLUT = glucose transporter

GSK3β = glycogen synthase kinase 3-beta

H^+ = hydrogen ion

HBA_{1c} = hemoglobin A1c

HDAC = histone deacetylase

HDL = high-density lipoprotein

HF = heart failure

HFPEF = HF with preserved EF

HFREF = HF with reduced EF

HR = heart rate

HW/TL = heart weight normalized to tibia length

IL = interleukin

IVCT = isovolumic contraction time

IVRT = isovolumic relaxation time

IVS = interventricular septum

I/R = ischemia/reperfusion

K^+ = potassium ion

K_D = dissociation constant

KO = knockout

LA = left atrial

LCAD = long-chain acyl-CoA dehydrogenase

LDL = low-density lipoprotein

LV = left ventricular

LVDP = LV developed pressure

LVEDP = LV end-diastolic pressure

LVEDV = LV end-diastolic volume

LVESV = LV end-systolic volume

LVID = LV internal diameter

LPS = lipopolysaccharide

LV = left ventricular

LVPW = LV posterior wall

MAC3 = lysosomal-associated membrane protein 2

MCAD = medium-chain acyl-CoA dehydrogenase

MCD = malonyl-CoA decarboxylase

MCP = monocyte chemoattractant peptide

MEE = myocardial external energy efficiency

MHC = myosin heavy chain

MI = myocardial infarction

MRNA = messenger ribonucleic acid

MTOR = mammalian target of rapamycin

MTT = 3-[4,5-dimethylthiazol-2-yl]-2,5-diphenyltetrazoliumbromide

MV = mitral valve

M-MODE = motion mode

M0 = naïve macrophage

M1 = pro-inflammatory macrophage

M2 = pro-fibrotic macrophage

NADH = nicotinamide adenine dinucleotide

NA^+ = sodium ion

NCX = sarcolemmal and mitochondrial Na^+/Ca^{2+} exchanger

NLRP3 = nucleotide-binding domain-like receptor protein 3

NFκB = nuclear factor kappa-light-chain-enhancer of activated B cells

NHE = Na^+/H^+ exchanger

RT-PCR = real-time polymerase chain reaction

PBS = phosphate buffered saline

PDH = pyruvate dehydrogenase

PDK = pyruvate dehydrogenase kinase

PGC1α: peroxisomal proliferator activated receptor-g coactivator 1-alpha

PPARα: peroxisome proliferator activated receptor-alpha

PSP = peak systolic pressure

P/O = phosphate/oxygen

RAPTOR = regulatory-associated protein of mTOR

RER = respiratory exchange ratio

RNA = ribonucleic acid

SCOT = succinyl-CoA:3-oxaloacid-CoAtransferase

SEM = standard error of the mean

SERCA2a = sarco/endoplasmic reticulum Ca^{2+} adenosine triphosphatase-2a

SGLT2 = Na^{+}/glucose cotransporter 2

SV = stroke volume

S6 = ribosomal protein S6

TAC = transverse aortic constriction

TCA = tricarboxylic acid

TNFα = tumor necrosis factor-alpha

TXNIP = thioredoxin-interacting protein

VCO_2 = carbon dioxide production

VO_2 = oxygen consumption

VO_2MAX = maximal oxygen consumption

VW/TL = ventricle weight normalized to tibia length

WGA = wheat germ agglutinin

Chapter One

Literature Review

1.1 Introduction to Heart Failure

1.1.1 Overview

Heart failure (HF) is a debilitating, chronic disorder affecting over 28 million people worldwide, resulting in a significant burden on healthcare (1,2). Defined as the heart's inability to deliver adequate amounts of oxygen to the peripheries, HF most commonly appears as a shortness of breath, peripheral edema and limited exercise tolerance, significantly impacting one's quality of life. Of importance, HF is most often a result of systemic hypertension (3,4) diabetes mellitus (5), myocardial infarction (MI) (6-8) or sepsis (9,10). However, for the purpose of this thesis, HF will refer to non-ischemic HF resulting from conditions of pressure-overload, such as high systolic blood pressure (BP) or aortic stenosis, in the absence of diabetes and/or obesity.

The underlying pathogenesis of HF involves changes to renal hemodynamics, leading to sodium and fluid retention and activation of the sympathetic nervous system in attempt to normalize wall stress and maintain cardiac output through increased stroke volume (SV) and heart rate (HR). In response to this pressure-overload, the heart adapts by increasing muscle mass. This process, commonly referred to as left ventricular (LV) hypertrophy, is initially compensatory, but eventually transitions to a decompensated form of hypertrophy, ultimately resulting in cardiac dysfunction (11,12). At the cellular level, the myocardium appears to revert back to expression of fetal gene patterns, which is considered to serve as a biomarker of cardiac hypertrophy/dysfunction (13,14). Particularly, the induction of atrial and brain natriuretic peptide (ANP and BNP, respectively), reduction of the contractile protein, sarco/endoplasmic reticulum Ca^{2+} adenosine

triphosphatase-2a (SERCA2a), and a switch from α- to β- myosin heavy chain (MHC) are features of the failing heart (15-20). Furthermore, induction of the protein kinase B (Akt)/mammalian target of rapamycin (mTOR)/Raptor pathway and downstream substrates, ribosomal protein S6 (S6) and eukaryotic initiation factor 4E-binding protein (4E-BP), have been previously described as molecular markers of hypertrophic growth in response to pressure-overload (21). In addition, the structural remodeling that results from pressure-overload can be assessed by motion mode (M-mode) echocardiography, measured as increases in overall LV mass, interventricular septum and LV posterior wall (IVS and LVPW, respectively) thicknesses, LV internal diameter (LVID), LV volume and left atrial (LA) diameter.

LV dysfunction can be described as either systolic or diastolic in nature, characterized by impaired contraction or relaxation properties of the heart, respectively. Systolic dysfunction, determined by impaired pump function, is evident by reductions in LV ejection fraction (EF) or fractional shortening (FS). Additional functional parameters, such as CO and SV, are also indicators of reduced cardiac contractility. Diastolic dysfunction is a result of ventricular stiffness, which significantly impairs the relaxation properties of the heart, resulting in impaired LV filling properties. Deranged filling patterns can also be detected by echocardiography, measured by alterations in the ratio of early and late mitral inflow (E and A wave, respectively) and the ratio of the E wave to the tissue Doppler mitral annulus velocity (E′) (22,23). Traditionally, echocardiographic measurement of the LV EF is used to define HF, but more recently HF has become divided into two groups, classified as HF with reduced EF (HFrEF; EF <40%) or preserved EF (HFpEF; EF >50%) based on the presence or absence of impaired systolic dysfunction,

respectively (24). HFrEF and HFpEF each account for approximately half the patients diagnosed with HF (25), although the differences are not completely understood.

To date, the diagnosis and treatment of HFpEF has been challenging, and efficacious therapies are still lacking. However, current treatment strategies for HFrEF include pharmacological strategies to target neurohormonal suppression or regulate hemodynamics and/or volume overload (such as angiotensin-converting-enzyme (ACE) inhibitors, β-blockers, diuretics) or mechanical strategies including LV assist devices or resynchronization therapy. However, cardiac transplantation provides the greatest survival outcomes. Despite improvements in survival seen with these therapies, HFrEF and HFpEF have a 5-year mortality of 75.3% and 75.7%, respectively (26). More recently, it has become evident that disturbances in myocardial energy production are thought to contribute to worsening of cardiac dysfunction in HF (27). As such, therapeutic approaches designed to optimize cardiac energy production have become of increasing interest.

1.1.2 Animal models

In order to better understand the extremely complex syndrome of HF, both animal models and isolated cells and organs provide beneficial tools to simplify the research question. Particularly, the convenience and cost of small animal models, as well as the simplicity of genetic manipulation, provide rationale for using this tool to explore clinical research questions in order to gain specific insight into the human syndrome. However, in order to fully translate scientific findings and implement new therapeutic options into a clinical setting, it is important to understand the concern

of physiological applicability and ensure the chosen experimental model is appropriate for the experimental design.

The most common mouse model of HF is induced by surgical constriction of the aorta either on the ascending aorta (aortic banding; AB) or transverse aorta (TAC). These models are particularly advantageous in that they very closely replicate clinical aortic stenosis, where a fixed aortic band mimics calcification/stiffening of the aortic valve, resulting in increased aortic afterload. Typically, the TAC model is characterized by early adaptive cardiac remodeling, particularly LV hypertrophy, which progresses to maladaptive remodeling and overt cardiac dysfunction at approximately 3-4 weeks in a relatively young mouse (28-31). Particularly, the morphological and molecular changes of the heart induced by pressure-overload enable researchers to explore the underlying mechanisms of HF and gain insight into new therapeutic targets. However, there exists a great deal of variability in the severity of cardiac hypertrophy/HF resulting from this model, which can largely be accounted to differences in sex, age and/or strain of mice, as well as technical differences between research facilities (*i.e.* placement and constriction of ligature). Furthermore, since cardiac dysfunction is induced in an acute manner using this model, as opposed to the slow progression of pressure overload observed in patients, it particularly provides insight to the early effects of the insult. Alternatively, the constriction can also be placed on the abdominal aorta (AAC), inducing a more gradual restriction to aortic flow, yet requires a greater duration of time following surgery to achieve the transition from cardiac hypertrophy to overt cardiac dysfunction (32-34), making it more difficult to use as a model of established HF.

Another manner to induce pressure-overload is by utilizing animal models with hypertension. For example, certain rodent models spontaneously develop hypertension, which can lead to cardiac remodeling and dysfunction with time (35,36). In addition, other strains appear to be sensitive to sodium intake and develop concentric LV hypertrophy (37) and/or HFpEF (38) in response to long-term high-salt feeding. The benefit of these models are the lack of surgical complications and gradual onset of hypertension, which more closely mimics the transition from hypertrophy to HF seen in humans. Finally, stimulation with agents that have been shown to induce hypertension, such as angiotensin II (AngII), isoproterenol or phenylephrine, has also been used to study cardiac hypertrophy and the resulting myocardial dysfunction (39-41).

HF is also commonly induced by permanent coronary ligation (42-45) or ischemia/reperfusion (I/R) (46-49) to imitate MI, as well as induced in the setting of obesity, insulin resistance and type 2 diabetes (50-53). These rodent models feature the complex interactions that occur with comorbidities in human HF; however, this thesis will primarily focus on exploring the pathogenesis of non-ischemic HF in the absence of diabetes and/or obesity. Therefore, the experimental models used in these studies represent a simplified condition of HF without the complications associated with MI or high-fat diet-induced cardiac dysfunction. Altogether, while there are significant differences between human heart failure and experimental models, many common features in the HF phenotype enable important observations of the physiological and energetic effects of cardiac dysfunction. In addition, we combine results from two different rodent models of HF in order to provide additional insight into varying forms of human HF.

1.2 Cardiac Substrate Utilization in the Normal and Failing Heart

In order to pump >7000 L/day of blood for basic functioning, the human heart must produce an abundance of energy to ensure proper cardiac contraction and relaxation. This energy comes in the form of high-energy phosphate molecules, adenosine triphosphate (ATP), over 95% of which is produced by mitochondrial oxidative phosphorylation in the cardiomyocyte in a healthy human heart. More specifically, the β-oxidation of fatty acids (FAs) accounts for roughly 60-90% of acetyl coenzyme A (CoA) in the tricarboxylic acid (TCA) cycle, while the oxidation of pyruvate from both glycolysis and lactate oxidation accounts for 10-40% and other minor substrates (including ketone bodies) supply the rest (27,54-56) **(Figure 1.1)**. However, under metabolically demanding conditions, where HR and/or BP are elevated, such as exercise, there appears to be an increase in myocardial glucose uptake (57). The adaptability of the cardiomyocyte, therefore, enables the heart to switch between energy substrates based on availability and energy demand. In this manner, glucose and FAs are considered to compete as substrates through a process referred to as the "Randle cycle" (58). Nevertheless, it is believed that in HF, this metabolic flexibility is impaired resulting in insufficient energy output and, consequently, impaired cardiac contractility. The failing heart has therefore been referred to as an "engine out of fuel" (59). More specifically, ATP production is estimated to be reduced by up to 40% compared to the normal heart. However, the exact profile of metabolic changes in HF remain controversial and vary largely depending on the type and duration of HF as well as the experimental model used. Nonetheless, there has been considerable effort in better understanding cardiac substrate utilization in HF in order to design therapeutic strategies to modulate the use of specific substrates in hopes of optimizing cardiac energy production. However, a body of evidence suggests that this metabolic remodelling, or

impaired cardiac substrate utilization in HF, is thought to occur at the transcriptional level of genes encoding regulatory enzymes involved in substrate metabolism. As such, it is unclear whether or not this genetic reprogramming, and therefore metabolic inflexibility, can be reversed in established HF. Altogether, this begs the question of whether targeting metabolic pathways has any treatment potential in the failing heart.

1.2.1 Glucose metabolism

Glucose is taken up into the cardiomyocytes by the cardiac glucose transporters (GLUTs) and is used as a substrate for glycolysis to form pyruvate or stored in the form of lactate **(Figure 1.1)**. Glycolysis itself produces 2 molecules of ATP and the resulting pyruvate is further converted to acetyl-CoA by the rate limiting enzyme, pyruvate dehydrogenase (PDH), which is phosphorylated/inhibited by PDH kinase (PDK). Requiring 6 molecules of O_2 and yielding ~31 ATP molecules in the TCA cycle, glucose is, in theory, the most efficient energy substrate with a phosphate/oxygen (P/O) ratio of 2.58 (60).

Although the non-ischemic failing heart may not have a shortage in oxygen transport compared to the ischemic failing heart (61), it is generally believed that rate of glycolysis, an anaerobic metabolic process, is increased both in experimental models (62-65) and human HF (66). This shift in energy production toward glycolysis is another manner in which the failing heart resembles the fetal heart. Interestingly, although glycolysis rates are normally coupled to rates of glucose oxidation, this is not necessarily the case in HF, where the contribution of glucose oxidation to the energy production of the failing heart is reduced (32,39,67-69). This impairment in glucose

oxidation is thought to be due a result of impaired mitochondrial oxidative capacity, as well as reduced expression and activity of PDH (32,39,67,68) and is considered to precede impaired cardiac dysfunction (32). Nonetheless, reduced glucose oxidation is not entirely consistent in all experimental models of HF (62,64,70,71) and, therefore, requires further clarification. Regardless, there is evidence that increasing glucose oxidation may be a therapeutic approach to improve function in the failing heart. Particularly, indirect stimulation of PDH by dichloroacetate is shown to reduce LV hypertrophy/HF (72). Furthermore, indirect stimulation of glucose oxidation via decreased FA oxidation (73) may improve the uncoupling of glycolysis to glucose oxidation, thereby reducing intracellular acidosis in ischemic heart disease (74-76); however, the potential benefit in non-ischemic heart disease remains to be elucidated.

1.2.2 Fatty acid metabolism

Circulating free FAs (FFAs) are transported into the cardiomyocyte either by passive diffusion or via the FA translocase (FAT, or CD36) and are first converted to long-chain fatty acyl-CoA **(Figure 1.1)**. Carnitine palmitoyltransferase I and II (CPTI/II) then facilitate their transport, in the form of long-chain acylcarnitine, across the outer and inner mitochondrial membranes to the TCA cycle (77,78), where oxidation of one FA molecule produces approximately 105 ATP molecules (based on palmitate as representative FA). Central players in the regulation of FA transport and oxidation include: acetyl-CoA carboxylase (ACC), which catalyzes the conversion of acetyl-CoA to malonyl-CoA to negatively regulate the activity of CPT1 (79); malonyl-CoA decarboxylase (MCD), which catalyzes the degradation of malonyl-CoA, thereby promoting FA transport to the mitochondria; 5′ adenosine monophosphate-activated protein kinase (AMPK), which

phosphorylates/inactivates ACC in response to decreases in energy state (80,81); acyl-CoA dehydrogenases [particularly long and medium chain (LCAD and MCAD, respectively)], which catalyze the initial step of β-oxidation; and peroxisome proliferator-activated receptor-alpha (PPARα) and peroxisome proliferator-activated receptor gamma coactivator 1-alpha (PGC1α), transcriptional coactivators that regulate the expression of genes involved in FA metabolism. Requiring 23 molecules of O_2, FAs are considered to be the least efficient energy substrate having a P/O ratio of 2.33 (60).

Of note, AMPK is considered to be the "energy sensor" of the heart with various physiological roles but is thought to play a considerable part in the progression of HF. Although its activity has been shown to be both reduced and elevated in failing hearts of both mice and humans (82-87), it is often used as a marker of energy status and has also been considered as a potential pharmacological target to modulate FA utilization in HF. Interestingly, FA uptake and oxidation rates have been shown to be both increased (88-90) and decreased (91,92) in humans with various degrees of cardiomyopathy. However, accelerated rates of lipolysis have also been shown in HF (69,93,94), leading to increased circulating FA levels and enhancing FA uptake and oxidation by the heart (88,89). Nonetheless, this inconsistency continues with experimental models of AngII-, TAC- or MI-induced cardiac dysfunction showing that FA oxidation rates are unchanged (41,70,71) or reduced (31,95-97). Although the effect of HF on myocardial FA oxidation rates remain unclear, it appears that transcript and protein expression of enzymes involved in FA uptake (FAT/CD36) (98-100), transport (CPT1) (71), oxidation (LCAD and MCAD) (71,101,102) and transcriptional control of FA metabolic genes (PPARα and PGC1α) (103,104) are generally down-regulated in HF. However, pharmacological interventions aimed at increasing cardiac FA uptake

could result in intramyocardial lipid accumulation in the heart and resulting lipotoxicity. Moreover, since FA oxidation requires larger oxygen consumption than glucose oxidation, it stands to reason that inhibiting FA oxidation may be a reasonable approach to modulating cardiac energy metabolism in HF. For example, agents such as trimetazidine and perhexiline have been shown to improve cardiac contractile function upon direct inhibition of FA oxidation (105,106).

1.2.3 Ketone body metabolism

Under conditions of low glucose (low insulin/glucagon ratio), such as exercise or fasting, the liver diverts acetyl-CoA from the breakdown of FAs to form acetoacetate and β-hydroxybutyrate (βOHB), commonly referred to as ketone bodies, in a process known as hepatic ketogenesis **(Figure 1.1)**. Ketone bodies are taken up by most organs, including the brain, heart and skeletal muscle, relative to their circulating concentration (107), and provide an alternate fuel source to glucose and FAs; in fact, the myocardium consumes the highest rate of ketone bodies per unit mass of all organs (107-109). Particularly in the heart, βOHB is extracted at far higher rates than glucose and FAs (20 times and roughly double, respectively) (110), and is converted to acetyl-CoA for the TCA cycle, where the rate limiting enzyme is succinyl-CoA:3-oxaloacid-CoAtransferase (SCOT) (109). It is estimated that ketone bodies contribute approximately 10-15% of the heart's total oxidative metabolism (52,111,112), and are considered to have oxygen sparing effects compared to FAs, with a P/O ratio of ~2.50 (60). In fact, the presence of ketone bodies has been shown to improve myocardial work efficiency by competing with glucose and FAs (113,114).

Despite minimal contribution to the heart's total energy production under normal conditions, the role of ketone bodies in the failing heart is still under debate. Interestingly, ketone bodies are elevated in the blood of HF patients (115,116), although this depends on the severity and type of HF (*i.e.* HFrEF versus HFpEF) (117). On the other hand, ketone bodies are found to be decreased in the failing myocardium associated with an increase in the ketogenic intermediate, β-hydroxybutyryl-CoA (118), indicating a state of enhanced ketone body utilization in HF. However, another study demonstrated that use of circulating ketone bodies is reduced in skeletal-muscle but unchanged in the myocardium of patients with HF (119). Nonetheless, expression of the enzymes SCOT and beta-hydroxybutyrate dehydrogenase 1 (BDH1), key in the myocardial oxidation of βOHB, are also increased in the failing myocardium (118,120). It has been proposed, however, that enhanced βOHB oxidation may impede the production of acetyl-CoA for the TCA cycle by other substrates **(Figure 1.1)** (114,121) and consequently cause a reduction in overall mitochondrial oxidative phosphorylation (122). Furthermore, this decrease in glucose oxidation may further reduce cardiac efficiency. As such, it remains unclear as to whether enhanced myocardial ketone body oxidation is an adaptive or maladaptive process and whether or not chronically elevated βOHB would result in improved or worsening of cardiac function in the failing heart. In support of elevating circulating ketones as a therapeutic strategy for HF, recent work has demonstrated beneficial hemodynamic effects resulting from βOHB infusion (123).

1.2.4 Ketone bodies as signaling molecules

It has been well documented that FA & glucose intermediates impact various signaling pathways beyond their role as cardiac energy substrates. More recently, ketone bodies and their intermediates

have also been identified as having non-metabolic roles as signalling molecules. For example, ketone bodies were found to upregulate mitochondrial biogenesis as well as display antiarrhythmic properties by stabilizing cell membrane potential (124). In addition, βOHB is shown to have anti-hypertrophic and anti-oxidant (125) properties upon decreasing histone acetylation via inhibition of histone deacetylase (HDAC). Furthermore, βOHB is thought to modulate inflammation and immune cell function (125-130), which may, in part, explain the benefits of fasting, calorie restriction or a ketogenic diet. While these additional properties of ketone bodies may seem promising, it is worth mentioning that an increase in acetyl-CoA derived from ketone oxidation may result in hyperacetylation of mitochondrial proteins, potentially leading to the metabolic derangements evident in the failing heart (118,120). As such, a better understanding of the many roles of ketone bodies in the heart is required.

1.3 Cardiac Inflammation and Fibrosis in in Heart Failure

Although it was originally thought that inflammation was a secondary symptom of HF pathogenesis, it has more recently become accepted that cytokine signaling may play a mechanistic role in the development and progression of cardiac dysfunction (131). In fact, the Canakinumab Anti-Inflammatory Thrombosis Outcomes Study (CANTOS) trial recently demonstrated the therapeutic potential of targeting inflammatory pathways for treatment of cardiovascular (CV) disease (CVD) upon improving CV outcomes in patients with history of MI and elevated high-sensitivity C-reactive protein (132). While inflammation is well-recognized as a driver of atherosclerosis, its role in the development of HF is not clearly defined. Nonetheless, release and

expression of pro-inflammatory cytokines [interleukin (IL)-1, IL-6, IL-18, IL-1β and tumor necrosis factor-alpha (TNFα)] and chemokines [IL-8, monocyte chemoattractant peptide (MCP) 1] have been shown to increase in HF patients (133-135). In response to cellular damage, including hypertrophy, fibrosis and apoptosis which occur during myocardial injury, damage-associated molecular patterns (DAMPs) initiate the process of sterile inflammation (136-138). The nucleotide-binding oligomerization domain-like receptors protein 3 (NLRP3) inflammasome, a cytosolic protein complex, recognizes DAMPs, creating an activated inflammatory complex involving the adapter protein, apoptosis-associated speck-like protein containing caspase-recruitment domain (ASC) and pro-caspase 1 (139). The transcription of IL-1β and NLRP3 are referred to as the "priming" step, whereas assembly of the NLRP3 inflammasome complex results in activation of the enzyme caspase-1 (140,141), thereby promoting maturation of pro-inflammatory cytokines (mentioned above) (142,143) that trigger release of peripheral monocytes and other inflammatory cells (144,145). Cardiac fibroblasts, the main non-myocyte cell population in the heart, are also shown to play a role in sustaining inflammation upon production of the pro-inflammatory mediators, MCP1 and IL-8 (146) and facilitation of leukocyte migration. The role of the interaction between cardiac fibroblasts and myocytes has been well-documented in the development of cardiac contractile dysfunction (147). In addition, the thioredoxin-interacting protein (TXNIP) is an early response protein that has been recently implicated in the innate immune response via activation of the NLRP3 inflammasome (148,149). This positive-feedback loop is thought to magnify the inflammatory process, thereby accelerating progression of myocardial remodeling and worsening HF pathogenesis (136,150,151). Therefore, the NLRP3 inflammasome is considered to be a potent mediator of inflammation. As such, it is tempting to speculate that targeting the NLRP3 inflammasome may provide beneficial effects in HF. In support

of this, a pharmacological NLRP3 inhibitor was found to blunt the doxorubicin-induced decline in systolic cardiac function (152). Nonetheless, a better understanding of the role and potential therapeutic potential of the NLRP3 inflammation in HF is warranted.

Cardiac fibrosis, a form of repair where connective tissue is deposited in the injured myocardium, is thought to be tightly associated with inflammation (153,154). Importantly, both inflammation and fibrosis are thought to be key pathophysiological mechanisms in the development and progression of HF. Similar to compensatory cardiac hypertrophy, inflammation is initially a necessary physiological defence mechanism, but is suggested to progress fibrosis if persistent (155,156), consequently leading to cardiac stiffening and contractile dysfunction (157,158). Once exposed to initial pro-inflammatory signals secreted by cardiomyocytes following injury (159), macrophages assume a pro-inflammatory (M1) phenotype (160) and are involved in the maintenance of cardiac inflammation by secretion of pro-inflammatory cytokines and signaling neighboring fibroblasts (161). However, upon ingesting apoptotic neutrophils (162) and signaling by cytokines (particularly IL-13 and IL-4), macrophages are thought to undergo phenotypic changes from naïve (M0) to pro-fibrotic (M2) macrophages. Interestingly, there appears to be a direct association between cardiac M2 macrophages and MI in both humans and mice (163). Furthermore, M2 resident cardiac macrophages are thought to be essential to the development of AngII-induced myocardial fibrosis (164). In addition, myofibroblasts, which arise from cardiac fibroblasts and endothelial cells or circulating macrophages and monocytes, are responsible for secretion of extracellular matrix (ECM) components, leading to scar formation (165). Meanwhile, the pro-inflammatory cytokine, TNFα, has been implicated in the development of ECM remodeling and fibrosis (166), leading to cardiac hypertrophy/HF (167-169). In support of this,

genetic deletion of TNFα reduced the pressure overload-induced perivascular and interstitial collagen deposit in the heart (170,171). It has been proposed that TNFα mediates cardiac fibrosis upon promoting fibroblast activation (172) and the expression of the pro-fibrotic M2 macrophage phenotype (173). In summary, it is apparent that together inflammatory cells and fibroblasts contribute to the development of cardiac fibrosis and thus contractile impairments in HF. Particularly in the myocardium, increased expression of ECM proteins, such as collagen type I/III alpha-1 (Col1α1/Col3α1), and staining of collagen deposits indicate the degree of fibrotic remodeling.

1.4 Empagliflozin as a Novel Treatment Strategy for Heart Failure

1.4.1 Cardiovascular improvements in diabetes

The relationship between diabetes and HF is becoming increasingly well recognized, raising the interest in glucose-lowering therapy for treating CVD. However, the dipeptidyl peptidase-4 (DPP-4) inhibitors, sitagliptin, saxagliptin, and alogliptin, have either failed to demonstrated improvements in or even increased the risk of major adverse CV events in diabetic patients (174-176), raising concern regarding the therapeutic potential of anti-hyperglycemic agents. However, in 2015 Zinman *et al* (177) reported that anti-diabetic drug, empagliflozin, had striking and unexpected reductions in CV death and all-cause mortality by ~35-40% in patients with diabetes and high-risk of CVD. The multicenter Empagliflozin, CV Outcomes, and Mortality in Type 2 Diabetes (EMPA-REG Outcome) trial was primarily designed to assess CV safety of

empagliflozin at two doses (10 and 25 mg daily) over a median time of 2.6 years. Of importance, the benefit of empagliflozin occurred beyond optimal prevention strategies, as most patients were also undergoing treatment with antihypertensive or diuretic agents. More recently, the canagliflozin CV assessment study (CANVAS) and dapagliflozin on the incidence of CV events (DECLARE-TIMI58) trial similarly showed that the SGTL2 inhibitors, canagliflozin and dapagliflozin, respectively, also reduced risk of CV death or hospitalization for HF in type 2 diabetics with high risk of CVD (178,179); however, this occurred without improving the rate of all-cause mortality. Overall, these results have taken clinicians by surprise, raising numerous questions about the therapeutic potential of this class of drug, even in other forms of metabolic disease. In addition, since there appears to be no association between risk of HF and glycemic control (174-177,180), the underlying mechanisms for the profound CV improvements in response to treatment with empagliflozin, canagliflozin and dapagliflozin remain unknown.

1.4.2 Inhibition of sodium/glucose co-transporter 2

The "gliflozins" are a class of anti-diabetic drug designed to inhibit the primary sodium/glucose co-transporter (SGLT) 2, a low-affinity high-capacity transporter, which is prominently expressed in the proximal tubule of nephrons and is responsible for >90% of glucose reuptake (181-183). SGLT1, a high-affinity low-capacity transporter, is responsible for the other ~10% of glucose reabsorption at the distal segment of the proximal tubule (181,183). By preventing glucose reabsorption, SGLT2 inhibitors increase renal glucose excretion, thereby reducing circulating glucose levels, independent of insulin secretion and insulin action (184); as such, the risk of hypoglycemia is low (185). As expected, empagliflozin demonstrated modest improvements in

glycemic control, evident by reductions in hemoglobin A1c (HbA_{1c}) (177). In addition, empagliflozin induced modest weight loss, persistent reductions in systolic BP, decreased uric acid levels and caused a slight increase in levels of low- and high-density lipoprotein (LDL and HDL, respectively) cholesterol, as expected. Interestingly, these changes are thought to be insufficient to explain the outcomes (186-189).

1.4.3 Pharmacokinetics of empagliflozin

Empagliflozin has a high affinity (K_d = 57 nM) for SGLT2, which is slightly reduced in the presence of high glucose (20 mM) (190). However, the half-life of empagliflozin bound to SGLT2 (59 min) was unaffected by glucose concentration. Importantly, empagliflozin has the highest selectivity of SGLT2 over SGLT1 (>2500-fold; IC_{50} = 3.1 nM and 8300 nM, respectively) of all SGLT2 inhibitors (190,191). In addition, the dose-response curve of urinary glucose excretion demonstrates that higher doses of empagliflozin (3-10 mg/kg/day) in mice have no additional inhibitory effect on renal sodium reabsorption (192), suggesting there is no action on SGLT1 in this dose range. Of note, SGLT1, but not SGTL2, receptors are significantly expressed in cardiac tissue (181,193,194); empagliflozin is therefore unlikely to have any SGLT-related effects in the heart.

Although empagliflozin has slightly less affinity for mouse SGLT2 (IC_{50} = 1.9 nM), it is still highly selective over SGLT1 (~5,800-fold) (190,192). For *ex vivo* and *in vitro* experiments, the chosen concentration of empagliflozin (1 μM) is comparable to peak plasma concentrations seen in humans (~30-2500 nM) (177,195-202), has been previously reported to mediate effects in isolated

tissues (203-205), and is well below the IC_{50} of SGLT1 (190). Furthermore, the dose of 10 mg/kg/day empagliflozin used in our studies was chosen based on extensive work in rodent models demonstrating glycosuria, as well as beneficial renal and cardiac effects (50,52,206). This dose is within the range of that given to humans (10-100 mg) (196-200,202,207-209), based on the dose by factor method of allometric scaling used to extrapolate dose from animals to humans (210-212).[a] Additionally, a dosage of ~30-35 mg/kg/day empagliflozin in diet and 10 mg/kg/day by intraperitoneal injection resulted in free plasma concentrations of 1-2 nM and 20 nM in mice, respectively (192), which are well below the IC_{50} of SGLT1 (190). Altogether, these data clearly demonstrate that empagliflozin does not mediate any appreciable effects through SGLT1 inhibition at the dosage used throughout these studies.

1.4.4 Proposed mechanisms for cardiovascular benefit

1.4.4.1 Hemodynamic and renal effects

SGLT2 inhibitors not only induce early loss of urinary glucose, but also subsequently induces loss of sodium, evident by a persistent increase in hematocrit (213-215). It is also possible that the increase in hematocrit occurs as a result of stimulated erythropoiesis, as was seen by treatment with the SGLT2 inhibitor, dapagliflozin (216). Nonetheless, the diuretic hypothesis suggests that the combination of glucose and sodium loss may result in improved adaptations of renal vasculature and may result in both renal and cardiac benefit. By reducing extracellular fluid volume, empagliflozin is thought to reduce cardiac preload and afterload, thereby improving

[a] See Appendix A for extrapolated dose from humans to mice.

myocardial filling conditions. Interestingly, even modest reductions in BP can alleviate cardiac stress, which were also reported in the EMPA-REG Outcomes (177). In addition, as a result of hemoconcentration without an associated increase in HR, it is suggested that empagliflozin enhances oxygen delivery to tissues. Of note, the CV benefit of empagliflozin does not exactly match the profile of antihypertensive and diuretic therapy, which show smaller reductions in HF and mortality and a clear risk reduction in stroke than observed in the EMPA-REG Outcomes trial (217-219). As such, the drop in systolic and diastolic BP levels is unlikely to account solely for the rapid reductions in risk of HF but could indeed play a pivotal role.

1.4.4.2 Metabolic effects

In addition to moderating glycemic control, empagliflozin was also found to induce small decreases in body weight, primarily via reduced visceral fat (220-223), in patients with type 2 diabetes. Since reduced adiposity has been previously associated with reduced cardiometabolic risk (224), it stands to reason that empagliflozin may exert CV improvements upon producing a negative caloric balance and inducing weight loss (225). Furthermore, SGLT2 inhibitor-induced glycosuria coupled with hormonal changes, such as a rise in glucagon levels, have been shown to result in reduced glucose utilization and a subsequent shift toward increased lipid utilization **(Figure 1.2)** (226,227). Under such conditions, where the insulin/glucagon ratio is reduced, hepatic ketogenesis is enhanced (228). Of note, SGTL2 inhibition was found to accelerate lipolysis and increase circulating βOHB levels in diabetic rats (229-232) and humans (226,233). In addition, empagliflozin has also been shown to prevent hepatic lipid accumulation in obese mice (234,235) and increase plasma FA levels in type 2 diabetes, but not in nondiabetic controls (236). As such,

the “fuel hypothesis” suggests that empagliflozin may elevate levels of circulating FA and subsequently βOHB, thereby improving myocardial energetics and substrate efficiency upon using enhanced availability of βOHB as an alternate (and more efficient) substrate for the failing heart (120,237,238). However, it remains unclear why empagliflozin induces elevated circulating βOHB and whether or not βOHB is preferentially oxidized over glucose and FAs in the heart. In addition, it is worth mentioning that the development of diabetic ketoacidosis is a significant concern of SGLT2 inhibitors (239-241).

1.4.4.3 Anti-inflammatory effects

Based on the fact that intracellular glucose metabolism is thought to modulate inflammatory processes (242) and SGTL2 inhibitors regulate intracellular glucose metabolism, it has also been postulated that SGTL2 inhibitors may have anti-inflammatory effects (243,244). Particularly, reduced inflammation of the liver and kidney by empagliflozin, and other SGTL2 inhibitors (10,232,245) is thought to be associated with inhibition of the NLRP3 inflammasome (235,246). Particularly, there have been numerous accounts that SGLT2 inhibitors attenuate obesity- or diabetes- induced expression of pro-inflammatory properties in WAT, liver, kidney, pancreatic islets, the heart and the aortic root (10,234,235,246-249). In addition, treatment with an SGLT2 inhibitor was found to attenuate activation of NLRP3 inflammasome in macrophages in patients with type 2 diabetes and high CV risk (250). Furthermore, attenuated inflammation by the SGLT2 inhibitor, dapagliflozin, was associate with renal (247) and cardiac (249,251) benefits. Of note, βOHB is thought to inhibit NLRP3-activated inflammation (127), which may imply that anti-inflammatory effects of SGLT2 inhibitors are mediated through elevated circulating ketone bodies.

Although the anti-inflammatory properties of SGTL2 inhibitors via NLRP3 inflammasome suppression are well characterized in the setting of obesity and/or diabetes, their role in the context of CVD in the absence of hyperglycemia has yet to be elucidated. Moreover, since SGTL2 is not expressed at any significant levels in the heart (194), whether blunted activation of the cardiac NLRP3 inflammasome upon treatment with empagliflozin is direct or secondary to an overall metabolism effect has yet to be explored.

1.4.4.4 SGLT2-independent cardiac effects

Although SGLT1 is expressed in cardiac tissue (193,194), the circulating concentrations of empagliflozin are not sufficient to effect SGTL1 function (225); furthermore, dual SGLT1/2 inhibition has been shown to have detrimental consequences on cardiac function (252), and is therefore unlikely to explain the beneficial cardiac outcomes resulting from empagliflozin treatment. Nonetheless, although empagliflozin is known to regulate Na^+ and glucose handling in the kidney, it has also been shown to restore aberrant Na^+ and Ca^{2+} concentrations in cardiomyocytes isolated from rats and rabbits, in a glucose-independent manner (203). In fact, these effects appear to be mediated through direct inhibition of the cardiac Na^+/H^+ exchanger (NHE) 1, which plays a crucial role in regulating cardiac Ca^{2+} and Na^+ homeostasis for optimal cardiac rhythm and contraction (253,254). In addition, empagliflozin was recently shown to reduce sarcoplasmic reticulum Ca^{2+} leak (255) and directly increase expression of GLUT1, but not other cardiac GLUTs, in failing murine cardiomyocytes (256). Moreover, empagliflozin increased ATP content directly in rat cardiomyocytes and endothelial cells following hypoxia/reoxygenation injury (46). Lastly, empagliflozin reduced diastolic tension in ventricular trabecular isolated from

human failing hearts as well as in cardiomyocytes from diabetic and non-diabetic mice (257). Altogether, these findings suggest that empagliflozin may exert direct cardiac effects, independent of renal SGLT2 inhibition.

1.5 Hypothesis and Aims

In this thesis, we aim to investigate and characterize the changes in myocardial substrate metabolism during the regression of HF. Using an experimental model of pressure overload-induced HF (where EF <30% at approximately 3-4 weeks post-surgery), we will perform debanding (DB) surgery to remove the aortic constriction and yield a temporal profile of cardiac remodeling, systolic and diastolic function and associated myocardial energy metabolism for an additional 3 weeks. **We hypothesize that the genetic reprogramming of the metabolic pathways and energetic impairments in HF are irreversible in the regression of severe HF.**

Another aim of this thesis is to determine whether the anti-diabetic drug, empagliflozin, improves cardiac function in HF in the absence of diabetes. In order to do so, we will use an experimental model of pressure overload-induced HF (where EF <45% at approximately 2-3 post-surgery) treated with 10 mg/kg/day empagliflozin via oral gavage for an additional two weeks to determine changes in cardiac remodeling, systolic and diastolic function and cardiac fibrosis. **We hypothesize that empagliflozin improves cardiac systolic and diastolic dysfunction in overt HF, even in the absence of diabetes/obesity.** Furthermore, we wish to determine whether the beneficial effects of empagliflozin occur upon inducing a state of persistent hyperketonemia,

thereby providing a preferential fuel source for the failing myocardium. **As such, we hypothesize that empagliflozin enhances cardiac energy production via enhanced ketone body oxidation, ultimately improving cardiac contractile function.** We also aim to investigate other prevailing theories regarding the beneficial effects of empagliflozin in HF in the absence of diabetes, including improved hemodynamics, diuretic effects and reductions in cardiac inflammation via the NLRP3 inflammasome.

1.6 Figures

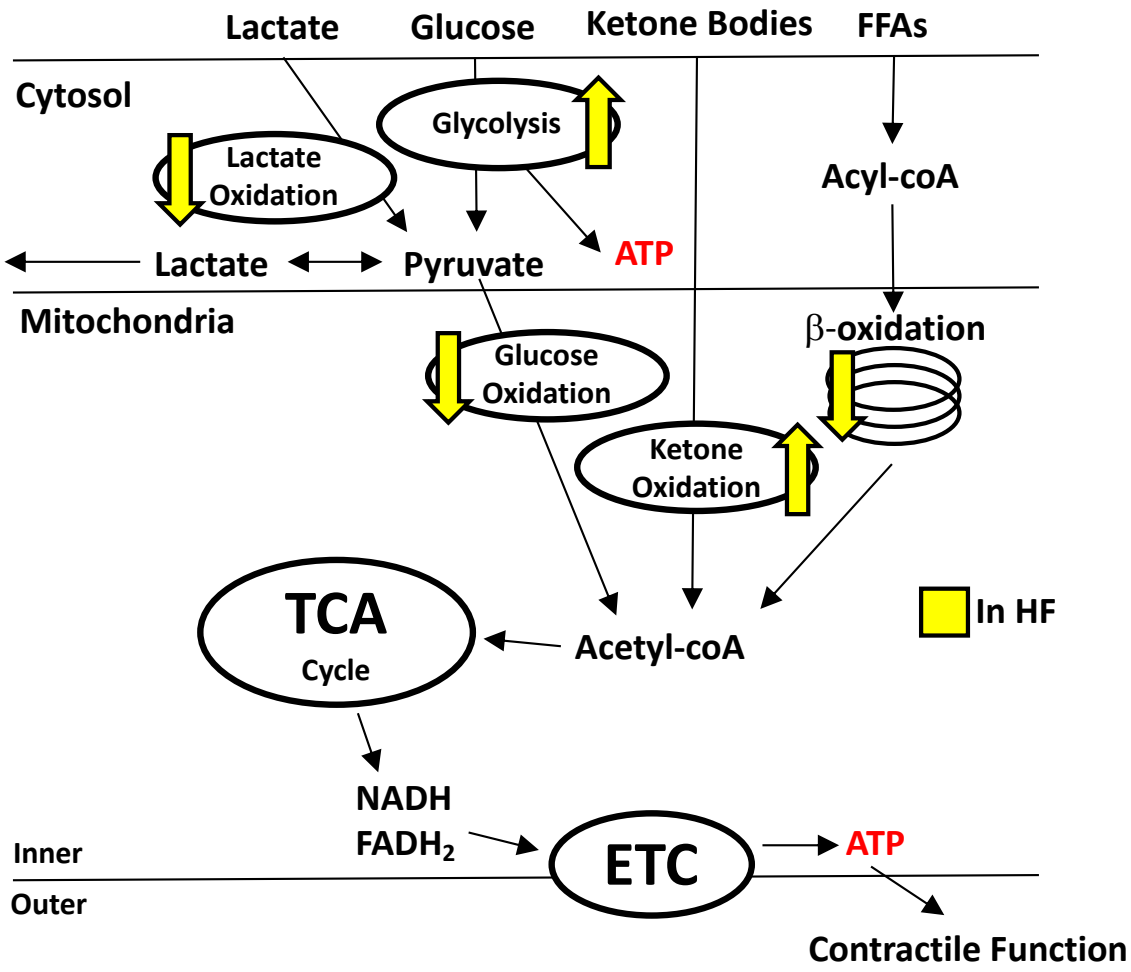

Figure 1.1. Cardiac Substrate Utilization in the Normal and Failing Heart. The β-oxidation of FAs accounts for roughly 60-90% of acetyl-CoA in the TCA cycle, while the oxidation of pyruvate from both glycolysis and lactate oxidation accounts for 10-40% and ketone bodies are considered a minor substrate. The failing heart is considered to be an "engine out of fuel" due to impaired metabolic flexibility resulting in insufficient ATP production. Glycolytic rates appear to be increased in HF, while the contribution of glucose oxidation and FAs is reduced. In addition, elevated levels of circulating ketone bodies in HF are thought enhance ketone body utilization in HF. ATP = adenosine triphosphate; COA = coenzyme A; ETC = electron transport chain; $FADH_2$ = flavin adenine dinucleotide; FFA = free fatty acid; HF = heart failure; NADH = nicotinamide adenine dinucleotide; TCA = tricarboxylic acid.

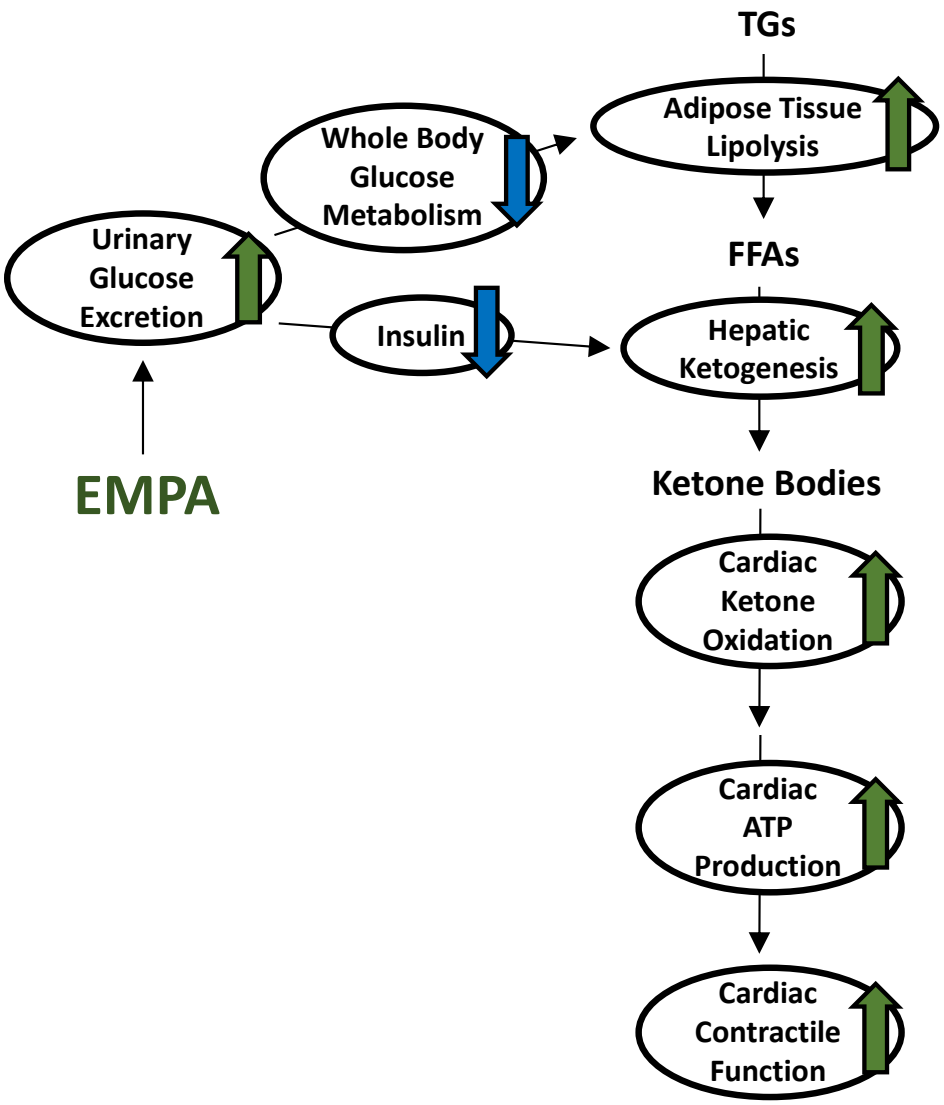

Figure 1.2. Empagliflozin "Fuel Hypothesis". Upon inducing glycosuria, empagliflozin is thought to cause a shift from whole body glucose utilization to lipid utilization, thereby accelerating adipose tissue lipolysis. Increased levels of circulation FA coupled with empagliflozin-induced hormonal changes are thought to enhance hepatic ketogenesis. The empagliflozin "fuel hypothesis", therefore, suggests that by elevating the level of circulating ketone bodies and subsequently increasing myocardial ketone body oxidation, cardiac energetics are improved, thus resulting in improved cardiac contractile function. EMPA = empagliflozin; FFA = free fatty acid; TGs = triglycerides.

1.7 References

1. Savarese G, Lund LH. Global Public Health Burden of Heart Failure. Card Fail Rev 2017;3:7-11.
2. Bleumink GS, Knetsch AM, Sturkenboom MC et al. Quantifying the heart failure epidemic: prevalence, incidence rate, lifetime risk and prognosis of heart failure The Rotterdam Study. Eur Heart J 2004;25:1614-9.
3. Ingelsson E, Bjorklund-Bodegard K, Lind L, Arnlov J, Sundstrom J. Diurnal blood pressure pattern and risk of congestive heart failure. JAMA 2006;295:2859-66.
4. Parati G, Esler M. The human sympathetic nervous system: its relevance in hypertension and heart failure. Eur Heart J 2012;33:1058-66.
5. Gilbert RE, Krum H. Heart failure in diabetes: effects of anti-hyperglycaemic drug therapy. Lancet 2015;385:2107-17.
6. Goldberg RJ, Spencer FA, Yarzebski J et al. A 25-year perspective into the changing landscape of patients hospitalized with acute myocardial infarction (the Worcester Heart Attack Study). Am J Cardiol 2004;94:1373-8.
7. Greenberg H, McMaster P, Dwyer EM, Jr. Left ventricular dysfunction after acute myocardial infarction: results of a prospective multicenter study. J Am Coll Cardiol 1984;4:867-74.
8. Velagaleti RS, Pencina MJ, Murabito JM et al. Long-term trends in the incidence of heart failure after myocardial infarction. Circulation 2008;118:2057-62.
9. Landesberg G, Gilon D, Meroz Y et al. Diastolic dysfunction and mortality in severe sepsis and septic shock. Eur Heart J 2012;33:895-903.

10. Tahara A, Kurosaki E, Yokono M et al. Effects of SGLT2 selective inhibitor ipragliflozin on hyperglycemia, hyperlipidemia, hepatic steatosis, oxidative stress, inflammation, and obesity in type 2 diabetic mice. European journal of pharmacology 2013;715:246-55.
11. Lorell BH. Transition from hypertrophy to failure. Circulation 1997;96:3824-7.
12. Frey N, Olson EN. Cardiac hypertrophy: the good, the bad, and the ugly. Annu Rev Physiol 2003;65:45-79.
13. Rajabi M, Kassiotis C, Razeghi P, Taegtmeyer H. Return to the fetal gene program protects the stressed heart: a strong hypothesis. Heart Fail Rev 2007;12:331-43.
14. Cappola TP. Molecular remodeling in human heart failure. J Am Coll Cardiol 2008;51:137-8.
15. Barry SP, Davidson SM, Townsend PA. Molecular regulation of cardiac hypertrophy. Int J Biochem Cell Biol 2008;40:2023-39.
16. Currie S, Smith GL. Enhanced phosphorylation of phospholamban and downregulation of sarco/endoplasmic reticulum Ca2+ ATPase type 2 (SERCA 2) in cardiac sarcoplasmic reticulum from rabbits with heart failure. Cardiovasc Res 1999;41:135-46.
17. Carniel E, Taylor MR, Sinagra G et al. Alpha-myosin heavy chain: a sarcomeric gene associated with dilated and hypertrophic phenotypes of cardiomyopathy. Circulation 2005;112:54-9.
18. Kiss E, Ball NA, Kranias EG, Walsh RA. Differential changes in cardiac phospholamban and sarcoplasmic reticular Ca(2+)-ATPase protein levels. Effects on Ca2+ transport and mechanics in compensated pressure-overload hypertrophy and congestive heart failure. Circ Res 1995;77:759-64.

19. Lowes BD, Minobe W, Abraham WT et al. Changes in gene expression in the intact human heart. Downregulation of alpha-myosin heavy chain in hypertrophied, failing ventricular myocardium. J Clin Invest 1997;100:2315-24.

20. Arai M, Matsui H, Periasamy M. Sarcoplasmic reticulum gene expression in cardiac hypertrophy and heart failure. Circ Res 1994;74:555-64.

21. Shende P, Plaisance I, Morandi C et al. Cardiac raptor ablation impairs adaptive hypertrophy, alters metabolic gene expression, and causes heart failure in mice. Circulation 2011;123:1073-82.

22. Oh JK, Appleton CP, Hatle LK, Nishimura RA, Seward JB, Tajik AJ. The noninvasive assessment of left ventricular diastolic function with two-dimensional and Doppler echocardiography. J Am Soc Echocardiogr 1997;10:246-70.

23. Nagueh SF, Smiseth OA, Appleton CP et al. Recommendations for the Evaluation of Left Ventricular Diastolic Function by Echocardiography: An Update from the American Society of Echocardiography and the European Association of Cardiovascular Imaging. Eur Heart J Cardiovasc Imaging 2016;17:1321-1360.

24. Yancy CW, Jessup M, Bozkurt B et al. 2013 ACCF/AHA guideline for the management of heart failure: a report of the American College of Cardiology Foundation/American Heart Association Task Force on Practice Guidelines. J Am Coll Cardiol 2013;62:e147-239.

25. Owan TE, Redfield MM. Epidemiology of diastolic heart failure. Prog Cardiovasc Dis 2005;47:320-32.

26. Shah KS, Xu H, Matsouaka RA et al. Heart Failure With Preserved, Borderline, and Reduced Ejection Fraction: 5-Year Outcomes. J Am Coll Cardiol 2017;70:2476-2486.

27. Stanley WC, Recchia FA, Lopaschuk GD. Myocardial substrate metabolism in the normal and failing heart. Physiol Rev 2005;85:1093-129.

28. Nagao M, Toh R, Irino Y et al. beta-Hydroxybutyrate elevation as a compensatory response against oxidative stress in cardiomyocytes. Biochem Biophys Res Commun 2016;475:322-8.

29. Hu P, Zhang D, Swenson L, Chakrabarti G, Abel ED, Litwin SE. Minimally invasive aortic banding in mice: effects of altered cardiomyocyte insulin signaling during pressure overload. Am J Physiol Heart Circ Physiol 2003;285:H1261-9.

30. Monnet E, Chachques JC. Animal models of heart failure: what is new? Ann Thorac Surg 2005;79:1445-53.

31. Sung MM, Das SK, Levasseur J et al. Resveratrol treatment of mice with pressure-overload-induced heart failure improves diastolic function and cardiac energy metabolism. Circulation Heart failure 2015;8:128-37.

32. Zhang L, Jaswal JS, Ussher JR et al. Cardiac insulin-resistance and decreased mitochondrial energy production precede the development of systolic heart failure after pressure-overload hypertrophy. Circ Heart Fail 2013;6:1039-48.

33. Hara M, Ono K, Hwang MW et al. Evidence for a role of mast cells in the evolution to congestive heart failure. J Exp Med 2002;195:375-81.

34. Wettschureck N, Rutten H, Zywietz A et al. Absence of pressure overload induced myocardial hypertrophy after conditional inactivation of Galphaq/Galpha11 in cardiomyocytes. Nat Med 2001;7:1236-40.

35. Bing OH, Brooks WW, Robinson KG et al. The spontaneously hypertensive rat as a model of the transition from compensated left ventricular hypertrophy to failure. J Mol Cell Cardiol 1995;27:383-96.

36. Heyen JR, Blasi ER, Nikula K et al. Structural, functional, and molecular characterization of the SHHF model of heart failure. Am J Physiol Heart Circ Physiol 2002;283:H1775-84.

37. Inoko M, Kihara Y, Morii I, Fujiwara H, Sasayama S. Transition from compensatory hypertrophy to dilated, failing left ventricles in Dahl salt-sensitive rats. The American journal of physiology 1994;267:H2471-82.

38. Klotz S, Hay I, Zhang G, Maurer M, Wang J, Burkhoff D. Development of heart failure in chronic hypertensive Dahl rats: focus on heart failure with preserved ejection fraction. Hypertension 2006;47:901-11.

39. Mori J, Alrob OA, Wagg CS, Harris RA, Lopaschuk GD, Oudit GY. ANG II causes insulin resistance and induces cardiac metabolic switch and inefficiency: a critical role of PDK4. Am J Physiol Heart Circ Physiol 2013;304:H1103-13.

40. Regan JA, Mauro AG, Carbone S et al. A mouse model of heart failure with preserved ejection fraction due to chronic infusion of a low subpressor dose of angiotensin II. Am J Physiol Heart Circ Physiol 2015;309:H771-8.

41. Mori J, Basu R, McLean BA et al. Agonist-induced hypertrophy and diastolic dysfunction are associated with selective reduction in glucose oxidation: a metabolic contribution to heart failure with normal ejection fraction. Circ Heart Fail 2012;5:493-503.

42. Mizuno M, Kuno A, Yano T et al. Empagliflozin normalizes the size and number of mitochondria and prevents reduction in mitochondrial size after myocardial infarction in diabetic hearts. Physiol Rep 2018;6:e13741.

43. Oshima H, Miki T, Kuno A et al. Empagliflozin, an SGLT2 Inhibitor, Reduced the Mortality Rate after Acute Myocardial Infarction with Modification of Cardiac Metabolomes and Antioxidants in Diabetic Rats. J Pharmacol Exp Ther 2019;368:524-534.

44. Reichert K, Colantuono B, McCormack I, Rodrigues F, Pavlov V, Abid MR. Murine Left Anterior Descending (LAD) Coronary Artery Ligation: An Improved and Simplified Model for Myocardial Infarction. J Vis Exp 2017.

45. Karwi QG, Zhang L, Wagg CS et al. Targeting the glucagon receptor improves cardiac function and enhances insulin sensitivity following a myocardial infarction. Cardiovasc Diabetol 2019;18:1.

46. Andreadou I, Efentakis P, Balafas E et al. Empagliflozin Limits Myocardial Infarction in Vivo and Cell Death in Vitro: Role of STAT3, Mitochondria, and Redox Aspects. Front Physiol 2017;8:1077.

47. Ussher JR, Wang W, Gandhi M et al. Stimulation of glucose oxidation protects against acute myocardial infarction and reperfusion injury. Cardiovasc Res 2012;94:359-69.

48. Frank A, Bonney M, Bonney S, Weitzel L, Koeppen M, Eckle T. Myocardial ischemia reperfusion injury: from basic science to clinical bedside. Semin Cardiothorac Vasc Anesth 2012;16:123-32.

49. Li S, Wu H, Han D et al. ZP2495 Protects against Myocardial Ischemia/Reperfusion Injury in Diabetic Mice through Improvement of Cardiac Metabolism and Mitochondrial

Function: The Possible Involvement of AMPK-FoxO3a Signal Pathway. Oxid Med Cell Longev 2018;2018:6451902.

50. Li C, Zhang J, Xue M et al. SGLT2 inhibition with empagliflozin attenuates myocardial oxidative stress and fibrosis in diabetic mice heart. Cardiovasc Diabetol 2019;18:15.

51. Calligaris SD, Lecanda M, Solis F et al. Mice long-term high-fat diet feeding recapitulates human cardiovascular alterations: an animal model to study the early phases of diabetic cardiomyopathy. PLoS One 2013;8:e60931.

52. Verma S, Rawat S, Ho KL et al. Empagliflozin Increases Cardiac Energy Production in Diabetes: Novel Translational Insights Into the Heart Failure Benefits of SGLT2 Inhibitors. JACC Basic Transl Sci 2018;3:575-587.

53. Habibi J, Aroor AR, Sowers JR et al. Sodium glucose transporter 2 (SGLT2) inhibition with empagliflozin improves cardiac diastolic function in a female rodent model of diabetes. Cardiovasc Diabetol 2017;16:9.

54. Huss JM, Kelly DP. Mitochondrial energy metabolism in heart failure: a question of balance. J Clin Invest 2005;115:547-55.

55. Rosano GM, Fini M, Caminiti G, Barbaro G. Cardiac metabolism in myocardial ischemia. Curr Pharm Des 2008;14:2551-62.

56. Depre C, Vanoverschelde JL, Taegtmeyer H. Glucose for the heart. Circulation 1999;99:578-88.

57. Kemppainen J, Fujimoto T, Kalliokoski KK, Viljanen T, Nuutila P, Knuuti J. Myocardial and skeletal muscle glucose uptake during exercise in humans. J Physiol 2002;542:403-12.

58. Randle PJ, Garland PB, Hales CN, Newsholme EA. The glucose fatty-acid cycle. Its role in insulin sensitivity and the metabolic disturbances of diabetes mellitus. Lancet 1963;1:785-9.

59. Neubauer S. The failing heart--an engine out of fuel. N Engl J Med 2007;356:1140-51.

60. Karwi QG, Uddin GM, Ho KL, Lopaschuk GD. Loss of Metabolic Flexibility in the Failing Heart. Front Cardiovasc Med 2018;5:68.

61. Dass S, Holloway CJ, Cochlin LE et al. No Evidence of Myocardial Oxygen Deprivation in Nonischemic Heart Failure. Circ Heart Fail 2015;8:1088-93.

62. Allard MF, Schonekess BO, Henning SL, English DR, Lopaschuk GD. Contribution of oxidative metabolism and glycolysis to ATP production in hypertrophied hearts. Am J Physiol 1994;267:H742-50.

63. Degens H, de Brouwer KF, Gilde AJ et al. Cardiac fatty acid metabolism is preserved in the compensated hypertrophic rat heart. Basic Res Cardiol 2006;101:17-26.

64. Akki A, Smith K, Seymour AM. Compensated cardiac hypertrophy is characterised by a decline in palmitate oxidation. Mol Cell Biochem 2008;311:215-24.

65. Nascimben L, Ingwall JS, Lorell BH et al. Mechanisms for increased glycolysis in the hypertrophied rat heart. Hypertension 2004;44:662-7.

66. Diakos NA, Navankasattusas S, Abel ED et al. Evidence of Glycolysis Up-Regulation and Pyruvate Mitochondrial Oxidation Mismatch During Mechanical Unloading of the Failing Human Heart: Implications for Cardiac Reloading and Conditioning. JACC Basic Transl Sci 2016;1:432-444.

67. Funada J, Betts TR, Hodson L et al. Substrate utilization by the failing human heart by direct quantification using arterio-venous blood sampling. PLoS One 2009;4:e7533.

68. Zhabyeyev P, Gandhi M, Mori J et al. Pressure-overload-induced heart failure induces a selective reduction in glucose oxidation at physiological afterload. Cardiovasc Res 2013;97:676-85.

69. Paolisso G, Gambardella A, Galzerano D et al. Total-body and myocardial substrate oxidation in congestive heart failure. Metabolism 1994;43:174-9.

70. Riehle C, Wende AR, Zaha VG et al. PGC-1beta deficiency accelerates the transition to heart failure in pressure overload hypertrophy. Circ Res 2011;109:783-93.

71. Osorio JC, Stanley WC, Linke A et al. Impaired myocardial fatty acid oxidation and reduced protein expression of retinoid X receptor-alpha in pacing-induced heart failure. Circulation 2002;106:606-12.

72. Kato T, Niizuma S, Inuzuka Y et al. Analysis of metabolic remodeling in compensated left ventricular hypertrophy and heart failure. Circ Heart Fail 2010;3:420-30.

73. Dyck JR, Cheng JF, Stanley WC et al. Malonyl coenzyme a decarboxylase inhibition protects the ischemic heart by inhibiting fatty acid oxidation and stimulating glucose oxidation. Circ Res 2004;94:e78-84.

74. Jaswal JS, Keung W, Wang W, Ussher JR, Lopaschuk GD. Targeting fatty acid and carbohydrate oxidation--a novel therapeutic intervention in the ischemic and failing heart. Biochim Biophys Acta 2011;1813:1333-50.

75. Dennis SC, Gevers W, Opie LH. Protons in ischemia: where do they come from; where do they go to? J Mol Cell Cardiol 1991;23:1077-86.

76. Lopaschuk GD, Ussher JR, Folmes CD, Jaswal JS, Stanley WC. Myocardial fatty acid metabolism in health and disease. Physiol Rev 2010;90:207-58.

77. McGarry JD, Brown NF. The mitochondrial carnitine palmitoyltransferase system. From concept to molecular analysis. Eur J Biochem 1997;244:1-14.

78. Murthy MS, Pande SV. Malonyl-CoA binding site and the overt carnitine palmitoyltransferase activity reside on the opposite sides of the outer mitochondrial membrane. Proc Natl Acad Sci U S A 1987;84:378-82.

79. Paulson DJ, Ward KM, Shug AL. Malonyl CoA inhibition of carnitine palmityltransferase in rat heart mitochondria. FEBS Lett 1984;176:381-4.

80. Hardie DG. Minireview: the AMP-activated protein kinase cascade: the key sensor of cellular energy status. Endocrinology 2003;144:5179-83.

81. Winder WW, Hardie DG. AMP-activated protein kinase, a metabolic master switch: possible roles in type 2 diabetes. Am J Physiol 1999;277:E1-10.

82. Lu TM, Tsai JY, Chen YC et al. Downregulation of Sirt1 as aging change in advanced heart failure. J Biomed Sci 2014;21:57.

83. Kim M, Shen M, Ngoy S, Karamanlidis G, Liao R, Tian R. AMPK isoform expression in the normal and failing hearts. J Mol Cell Cardiol 2012;52:1066-73.

84. Russell RR, 3rd, Li J, Coven DL et al. AMP-activated protein kinase mediates ischemic glucose uptake and prevents postischemic cardiac dysfunction, apoptosis, and injury. J Clin Invest 2004;114:495-503.

85. Tian R, Musi N, D'Agostino J, Hirshman MF, Goodyear LJ. Increased adenosine monophosphate-activated protein kinase activity in rat hearts with pressure-overload hypertrophy. Circulation 2001;104:1664-9.

86. Arad M, Seidman CE, Seidman JG. AMP-activated protein kinase in the heart: role during health and disease. Circ Res 2007;100:474-88.

87. Dyck JR, Lopaschuk GD. AMPK alterations in cardiac physiology and pathology: enemy or ally? J Physiol 2006;574:95-112.

88. Tuunanen H, Engblom E, Naum A et al. Decreased myocardial free fatty acid uptake in patients with idiopathic dilated cardiomyopathy: evidence of relationship with insulin resistance and left ventricular dysfunction. J Card Fail 2006;12:644-52.

89. Tuunanen H, Ukkonen H, Knuuti J. Myocardial fatty acid metabolism and cardiac performance in heart failure. Curr Cardiol Rep 2008;10:142-8.

90. Taylor M, Wallhaus TR, Degrado TR et al. An evaluation of myocardial fatty acid and glucose uptake using PET with [18F]fluoro-6-thia-heptadecanoic acid and [18F]FDG in Patients with Congestive Heart Failure. J Nucl Med 2001;42:55-62.

91. Neglia D, De Caterina A, Marraccini P et al. Impaired myocardial metabolic reserve and substrate selection flexibility during stress in patients with idiopathic dilated cardiomyopathy. Am J Physiol Heart Circ Physiol 2007;293:H3270-8.

92. Davila-Roman VG, Vedala G, Herrero P et al. Altered myocardial fatty acid and glucose metabolism in idiopathic dilated cardiomyopathy. J Am Coll Cardiol 2002;40:271-7.

93. Lommi J, Kupari M, Yki-Jarvinen H. Free fatty acid kinetics and oxidation in congestive heart failure. Am J Cardiol 1998;81:45-50.

94. Norrelund H, Wiggers H, Halbirk M et al. Abnormalities of whole body protein turnover, muscle metabolism and levels of metabolic hormones in patients with chronic heart failure. J Intern Med 2006;260:11-21.

95. Qanud K, Mamdani M, Pepe M et al. Reverse changes in cardiac substrate oxidation in dogs recovering from heart failure. Am J Physiol Heart Circ Physiol 2008;295:H2098-105.

96. Doenst T, Pytel G, Schrepper A et al. Decreased rates of substrate oxidation ex vivo predict the onset of heart failure and contractile dysfunction in rats with pressure overload. Cardiovasc Res 2010;86:461-70.

97. Lei B, Lionetti V, Young ME et al. Paradoxical downregulation of the glucose oxidation pathway despite enhanced flux in severe heart failure. J Mol Cell Cardiol 2004;36:567-76.

98. Heather LC, Howell NJ, Emmanuel Y et al. Changes in cardiac substrate transporters and metabolic proteins mirror the metabolic shift in patients with aortic stenosis. PLoS One 2011;6:e26326.

99. Umbarawan Y, Syamsunarno M, Koitabashi N et al. Myocardial fatty acid uptake through CD36 is indispensable for sufficient bioenergetic metabolism to prevent progression of pressure overload-induced heart failure. Sci Rep 2018;8:12035.

100. Sung MM, Byrne NJ, Kim TT et al. Cardiomyocyte-specific ablation of CD36 accelerates the progression from compensated cardiac hypertrophy to heart failure. Am J Physiol Heart Circ Physiol 2017;312:H552-H560.

101. Martin MA, Gomez MA, Guillen F et al. Myocardial carnitine and carnitine palmitoyltransferase deficiencies in patients with severe heart failure. Biochim Biophys Acta 2000;1502:330-6.

102. Sack MN, Rader TA, Park S, Bastin J, McCune SA, Kelly DP. Fatty acid oxidation enzyme gene expression is downregulated in the failing heart. Circulation 1996;94:2837-42.

103. Barger PM, Brandt JM, Leone TC, Weinheimer CJ, Kelly DP. Deactivation of peroxisome proliferator-activated receptor-alpha during cardiac hypertrophic growth. J Clin Invest 2000;105:1723-30.

104. Garnier A, Fortin D, Delomenie C, Momken I, Veksler V, Ventura-Clapier R. Depressed mitochondrial transcription factors and oxidative capacity in rat failing cardiac and skeletal muscles. J Physiol 2003;551:491-501.

105. Fragasso G, Palloshi A, Puccetti P et al. A randomized clinical trial of trimetazidine, a partial free fatty acid oxidation inhibitor, in patients with heart failure. J Am Coll Cardiol 2006;48:992-8.

106. Fragasso G, Perseghin G, De Cobelli F et al. Effects of metabolic modulation by trimetazidine on left ventricular function and phosphocreatine/adenosine triphosphate ratio in patients with heart failure. Eur Heart J 2006;27:942-8.

107. Balasse EO, Fery F. Ketone body production and disposal: effects of fasting, diabetes, and exercise. Diabetes Metab Rev 1989;5:247-70.

108. Cahill GF, Jr. Fuel metabolism in starvation. Annu Rev Nutr 2006;26:1-22.

109. Fukao T, Lopaschuk GD, Mitchell GA. Pathways and control of ketone body metabolism: on the fringe of lipid biochemistry. Prostaglandins Leukot Essent Fatty Acids 2004;70:243-51.

110. Ferrannini E, Santoro D, Bonadonna R, Natali A, Parodi O, Camici PG. Metabolic and hemodynamic effects of insulin on human hearts. Am J Physiol 1993;264:E308-15.

111. Rudolph W, Maas D, Richter J, Hasinger F, Hofmann H, Dohrn P. [on the Significance of Acetoacetate and Beta-Hydroxybutyrate in Human Myocardial Metabolism]. Klin Wochenschr 1965;43:445-51.

112. Camici PG, Marraccini P, Lorenzoni R et al. Coronary hemodynamics and myocardial metabolism in patients with syndrome X: response to pacing stress. J Am Coll Cardiol 1991;17:1461-70.

113. Sato K, Kashiwaya Y, Keon CA et al. Insulin, ketone bodies, and mitochondrial energy transduction. FASEB J 1995;9:651-8.

114. Kashiwaya Y, King MT, Veech RL. Substrate signaling by insulin: a ketone bodies ratio mimics insulin action in heart. Am J Cardiol 1997;80:50A-64A.

115. Lommi J, Kupari M, Koskinen P et al. Blood ketone bodies in congestive heart failure. J Am Coll Cardiol 1996;28:665-72.

116. Du Z, Shen A, Huang Y et al. 1H-NMR-based metabolic analysis of human serum reveals novel markers of myocardial energy expenditure in heart failure patients. PLoS One 2014;9:e88102.

117. Zordoky BN, Sung MM, Ezekowitz J et al. Metabolomic fingerprint of heart failure with preserved ejection fraction. PLoS One 2015;10:e0124844.

118. Bedi KC, Jr., Snyder NW, Brandimarto J et al. Evidence for Intramyocardial Disruption of Lipid Metabolism and Increased Myocardial Ketone Utilization in Advanced Human Heart Failure. Circulation 2016;133:706-16.

119. Janardhan A, Chen J, Crawford PA. Altered systemic ketone body metabolism in advanced heart failure. Tex Heart Inst J 2011;38:533-8.

120. Aubert G, Martin OJ, Horton JL et al. The Failing Heart Relies on Ketone Bodies as a Fuel. Circulation 2016;133:698-705.

121. Stanley WC, Meadows SR, Kivilo KM, Roth BA, Lopaschuk GD. beta-Hydroxybutyrate inhibits myocardial fatty acid oxidation in vivo independent of changes in malonyl-CoA content. Am J Physiol Heart Circ Physiol 2003;285:H1626-31.

122. Russell RR, 3rd, Taegtmeyer H. Changes in citric acid cycle flux and anaplerosis antedate the functional decline in isolated rat hearts utilizing acetoacetate. J Clin Invest 1991;87:384-90.

123. Nielsen R, Moller N, Gormsen LC et al. Cardiovascular Effects of Treatment with the Ketone Body 3-Hydroxybutyrate in Chronic Heart Failure Patients. Circulation 2019.

124. Cotter DG, Schugar RC, Crawford PA. Ketone body metabolism and cardiovascular disease. Am J Physiol Heart Circ Physiol 2013;304:H1060-76.

125. Shimazu T, Hirschey MD, Newman J et al. Suppression of oxidative stress by beta-hydroxybutyrate, an endogenous histone deacetylase inhibitor. Science 2013;339:211-4.

126. Fu SP, Li SN, Wang JF et al. BHBA suppresses LPS-induced inflammation in BV-2 cells by inhibiting NF-kappaB activation. Mediators Inflamm 2014;2014:983401.

127. Youm YH, Nguyen KY, Grant RW et al. The ketone metabolite beta-hydroxybutyrate blocks NLRP3 inflammasome-mediated inflammatory disease. Nat Med 2015;21:263-9.

128. Rahman M, Muhammad S, Khan MA et al. The beta-hydroxybutyrate receptor HCA2 activates a neuroprotective subset of macrophages. Nat Commun 2014;5:3944.

129. Gambhir D, Ananth S, Veeranan-Karmegam R et al. GPR109A as an anti-inflammatory receptor in retinal pigment epithelial cells and its relevance to diabetic retinopathy. Invest Ophthalmol Vis Sci 2012;53:2208-17.

130. Gambhir V, Yildiz C, Mulder R et al. The TLR2 agonists lipoteichoic acid and Pam3CSK4 induce greater pro-inflammatory responses than inactivated Mycobacterium butyricum. Cell Immunol 2012;280:101-7.

131. von Haehling S, Schefold JC, Lainscak M, Doehner W, Anker SD. Inflammatory biomarkers in heart failure revisited: much more than innocent bystanders. Heart Fail Clin 2009;5:549-60.

132. Ridker PM, Everett BM, Thuren T et al. Antiinflammatory Therapy with Canakinumab for Atherosclerotic Disease. N Engl J Med 2017;377:1119-1131.

133. Aukrust P, Ueland T, Lien E et al. Cytokine network in congestive heart failure secondary to ischemic or idiopathic dilated cardiomyopathy. Am J Cardiol 1999;83:376-82.

134. Testa M, Yeh M, Lee P et al. Circulating levels of cytokines and their endogenous modulators in patients with mild to severe congestive heart failure due to coronary artery disease or hypertension. J Am Coll Cardiol 1996;28:964-71.

135. Torre-Amione G, Kapadia S, Benedict C, Oral H, Young JB, Mann DL. Proinflammatory cytokine levels in patients with depressed left ventricular ejection fraction: a report from the Studies of Left Ventricular Dysfunction (SOLVD). J Am Coll Cardiol 1996;27:1201-6.

136. Bracey NA, Beck PL, Muruve DA et al. The Nlrp3 inflammasome promotes myocardial dysfunction in structural cardiomyopathy through interleukin-1beta. Exp Physiol 2013;98:462-72.

137. Mezzaroma E, Toldo S, Farkas D et al. The inflammasome promotes adverse cardiac remodeling following acute myocardial infarction in the mouse. Proc Natl Acad Sci U S A 2011;108:19725-30.

138. Kawaguchi M, Takahashi M, Hata T et al. Inflammasome activation of cardiac fibroblasts is essential for myocardial ischemia/reperfusion injury. Circulation 2011;123:594-604.

139. Ali SR, Karin M, Nizet V. Signaling cascades and inflammasome activation in microbial infections. Inflammasome 2016;2.

140. Sutterwala FS, Haasken S, Cassel SL. Mechanism of NLRP3 inflammasome activation. Ann N Y Acad Sci 2014;1319:82-95.

141. Karasawa T, Takahashi M. Role of NLRP3 Inflammasomes in Atherosclerosis. J Atheroscler Thromb 2017;24:443-451.

142. Abbate A, Kontos MC, Grizzard JD et al. Interleukin-1 blockade with anakinra to prevent adverse cardiac remodeling after acute myocardial infarction (Virginia Commonwealth University Anakinra Remodeling Trial [VCU-ART] Pilot study). Am J Cardiol 2010;105:1371-1377 e1.

143. Takahashi M. NLRP3 inflammasome as a novel player in myocardial infarction. Int Heart J 2014;55:101-5.

144. Elahi M, Asopa S, Matata B. NO-cGMP and TNF-alpha counter regulatory system in blood: understanding the mechanisms leading to myocardial dysfunction and failure. Biochim Biophys Acta 2007;1772:5-14.

145. Vaduganathan M, Greene SJ, Butler J et al. The immunological axis in heart failure: importance of the leukocyte differential. Heart Fail Rev 2013;18:835-45.

146. Lindner D, Zietsch C, Tank J et al. Cardiac fibroblasts support cardiac inflammation in heart failure. Basic Res Cardiol 2014;109:428.

147. Zhang P, Su J, Mende U. Cross talk between cardiac myocytes and fibroblasts: from multiscale investigative approaches to mechanisms and functional consequences. Am J Physiol Heart Circ Physiol 2012;303:H1385-96.

148. Zhou R, Tardivel A, Thorens B, Choi I, Tschopp J. Thioredoxin-interacting protein links oxidative stress to inflammasome activation. Nat Immunol 2010;11:136-40.

149. Schroder K, Zhou R, Tschopp J. The NLRP3 inflammasome: a sensor for metabolic danger? Science 2010;327:296-300.

150. Tabas I, Glass CK. Anti-inflammatory therapy in chronic disease: challenges and opportunities. Science 2013;339:166-72.

151. Cero FT, Hillestad V, Sjaastad I et al. Absence of the inflammasome adaptor ASC reduces hypoxia-induced pulmonary hypertension in mice. Am J Physiol Lung Cell Mol Physiol 2015;309:L378-87.

152. Marchetti C, Toldo S, Chojnacki J et al. Pharmacologic Inhibition of the NLRP3 Inflammasome Preserves Cardiac Function After Ischemic and Nonischemic Injury in the Mouse. J Cardiovasc Pharmacol 2015;66:1-8.

153. Sivakumar P, Gupta S, Sarkar S, Sen S. Upregulation of lysyl oxidase and MMPs during cardiac remodeling in human dilated cardiomyopathy. Mol Cell Biochem 2008;307:159-67.

154. Timonen P, Magga J, Risteli J et al. Cytokines, interstitial collagen and ventricular remodelling in dilated cardiomyopathy. Int J Cardiol 2008;124:293-300.

155. Lee SB, Kalluri R. Mechanistic connection between inflammation and fibrosis. Kidney Int Suppl 2010:S22-6.

156. Serhan CN, Brain SD, Buckley CD et al. Resolution of inflammation: state of the art, definitions and terms. FASEB J 2007;21:325-32.

157. Segura AM, Frazier OH, Buja LM. Fibrosis and heart failure. Heart failure reviews 2014;19:173-85.

158. Creemers EE, Pinto YM. Molecular mechanisms that control interstitial fibrosis in the pressure-overloaded heart. Cardiovasc Res 2011;89:265-72.

159. Aoyagi T, Matsui T. The Cardiomyocyte as a Source of Cytokines in Cardiac Injury. J Cell Sci Ther 2011;2012.

160. Barin JG, Rose NR, Cihakova D. Macrophage diversity in cardiac inflammation: a review. Immunobiology 2012;217:468-75.

161. Ma F, Li Y, Jia L et al. Macrophage-stimulated cardiac fibroblast production of IL-6 is essential for TGF beta/Smad activation and cardiac fibrosis induced by angiotensin II. PLoS One 2012;7:e35144.

162. Fadok VA, Bratton DL, Konowal A, Freed PW, Westcott JY, Henson PM. Macrophages that have ingested apoptotic cells in vitro inhibit proinflammatory cytokine production through autocrine/paracrine mechanisms involving TGF-beta, PGE2, and PAF. J Clin Invest 1998;101:890-8.

163. Carlson S, Helterline D, Asbe L et al. Cardiac macrophages adopt profibrotic/M2 phenotype in infarcted hearts: Role of urokinase plasminogen activator. J Mol Cell Cardiol 2017;108:42-49.

164. Falkenham A, de Antueno R, Rosin N et al. Nonclassical resident macrophages are important determinants in the development of myocardial fibrosis. Am J Pathol 2015;185:927-42.

165. Sarrazy V, Billet F, Micallef L, Coulomb B, Desmouliere A. Mechanisms of pathological scarring: role of myofibroblasts and current developments. Wound Repair Regen 2011;19 Suppl 1:s10-5.

166. Awad AE, Kandalam V, Chakrabarti S et al. Tumor necrosis factor induces matrix metalloproteinases in cardiomyocytes and cardiofibroblasts differentially via superoxide production in a PI3Kgamma-dependent manner. Am J Physiol Cell Physiol 2010;298:C679-92.

167. Kubota T, McTiernan CF, Frye CS et al. Dilated cardiomyopathy in transgenic mice with cardiac-specific overexpression of tumor necrosis factor-alpha. Circ Res 1997;81:627-35.

168. Bryant D, Becker L, Richardson J et al. Cardiac failure in transgenic mice with myocardial expression of tumor necrosis factor-alpha. Circulation 1998;97:1375-81.

169. Sivasubramanian N, Coker ML, Kurrelmeyer KM et al. Left ventricular remodeling in transgenic mice with cardiac restricted overexpression of tumor necrosis factor. Circulation 2001;104:826-31.

170. Sriramula S, Francis J. Tumor Necrosis Factor - Alpha Is Essential for Angiotensin II-Induced Ventricular Remodeling: Role for Oxidative Stress. PLoS One 2015;10:e0138372.

171. Sun M, Chen M, Dawood F et al. Tumor necrosis factor-alpha mediates cardiac remodeling and ventricular dysfunction after pressure overload state. Circulation 2007;115:1398-407.

172. Frangogiannis NG, Lindsey ML, Michael LH et al. Resident cardiac mast cells degranulate and release preformed TNF-alpha, initiating the cytokine cascade in experimental canine myocardial ischemia/reperfusion. Circulation 1998;98:699-710.

173. Frangogiannis NG. Cardiac fibrosis: Cell biological mechanisms, molecular pathways and therapeutic opportunities. Mol Aspects Med 2019;65:70-99.

174. Green JB, Bethel MA, Armstrong PW et al. Effect of Sitagliptin on Cardiovascular Outcomes in Type 2 Diabetes. N Engl J Med 2015;373:232-42.

175. Scirica BM, Bhatt DL, Braunwald E et al. Saxagliptin and cardiovascular outcomes in patients with type 2 diabetes mellitus. N Engl J Med 2013;369:1317-26.

176. White WB, Pratley R, Fleck P et al. Cardiovascular safety of the dipetidyl peptidase-4 inhibitor alogliptin in type 2 diabetes mellitus. Diabetes Obes Metab 2013;15:668-73.

177. Zinman B, Wanner C, Lachin JM et al. Empagliflozin, Cardiovascular Outcomes, and Mortality in Type 2 Diabetes. N Engl J Med 2015;373:2117-28.

178. Neal B, Perkovic V, Matthews DR. Canagliflozin and Cardiovascular and Renal Events in Type 2 Diabetes. N Engl J Med 2017;377:2099.

179. Wiviott SD, Raz I, Bonaca MP et al. Dapagliflozin and Cardiovascular Outcomes in Type 2 Diabetes. N Engl J Med 2019;380:347-357.

180. Investigators OT, Gerstein HC, Bosch J et al. Basal insulin and cardiovascular and other outcomes in dysglycemia. N Engl J Med 2012;367:319-28.

181. Wright EM, Loo DD, Hirayama BA. Biology of human sodium glucose transporters. Physiol Rev 2011;91:733-94.

182. Vallon V, Platt KA, Cunard R et al. SGLT2 mediates glucose reabsorption in the early proximal tubule. J Am Soc Nephrol 2011;22:104-12.

183. Hediger MA, Rhoads DB. Molecular physiology of sodium-glucose cotransporters. Physiol Rev 1994;74:993-1026.

184. Isaji M. Sodium-glucose cotransporter inhibitors for diabetes. Curr Opin Investig Drugs 2007;8:285-92.

185. Abdul-Ghani MA, Norton L, Defronzo RA. Role of sodium-glucose cotransporter 2 (SGLT 2) inhibitors in the treatment of type 2 diabetes. Endocr Rev 2011;32:515-31.

186. Muskiet MH, van Raalte DH, van Bommel EJ, Smits MM, Tonneijck L. Understanding EMPA-REG OUTCOME. Lancet Diabetes Endocrinol 2015;3:928-9.

187. Ceriello A, Genovese S, Mannucci E, Gronda E. Understanding EMPA-REG OUTCOME. Lancet Diabetes Endocrinol 2015;3:929-30.

188. Gilbert RE, Connelly KA. Understanding EMPA-REG OUTCOME. Lancet Diabetes Endocrinol 2015;3:930-1.

189. DeFronzo RA. The EMPA-REG study: What has it told us? A diabetologist's perspective. J Diabetes Complications 2016;30:1-2.

190. Grempler R, Thomas L, Eckhardt M et al. Empagliflozin, a novel selective sodium glucose cotransporter-2 (SGLT-2) inhibitor: characterisation and comparison with other SGLT-2 inhibitors. Diabetes Obes Metab 2012;14:83-90.

191. Kurosaki E, Ogasawara H. Ipragliflozin and other sodium-glucose cotransporter-2 (SGLT2) inhibitors in the treatment of type 2 diabetes: preclinical and clinical data. Pharmacol Ther 2013;139:51-9.

192. Rieg T, Masuda T, Gerasimova M et al. Increase in SGLT1-mediated transport explains renal glucose reabsorption during genetic and pharmacological SGLT2 inhibition in euglycemia. Am J Physiol Renal Physiol 2014;306:F188-93.

193. Zhou L, Cryan EV, D'Andrea MR, Belkowski S, Conway BR, Demarest KT. Human cardiomyocytes express high level of Na+/glucose cotransporter 1 (SGLT1). J Cell Biochem 2003;90:339-46.

194. Vrhovac I, Balen Eror D, Klessen D et al. Localizations of Na(+)-D-glucose cotransporters SGLT1 and SGLT2 in human kidney and of SGLT1 in human small intestine, liver, lung, and heart. Pflugers Archiv : European journal of physiology 2015;467:1881-98.

195. Heise T, Seman L, Macha S et al. Safety, tolerability, pharmacokinetics, and pharmacodynamics of multiple rising doses of empagliflozin in patients with type 2 diabetes mellitus. Diabetes Ther 2013;4:331-45.

196. Brand T, Macha S, Mattheus M, Pinnetti S, Woerle HJ. Pharmacokinetics of empagliflozin, a sodium glucose cotransporter-2 (SGLT-2) inhibitor, coadministered with sitagliptin in healthy volunteers. Adv Ther 2012;29:889-99.

197. Heise T, Seewaldt-Becker E, Macha S et al. Safety, tolerability, pharmacokinetics and pharmacodynamics following 4 weeks' treatment with empagliflozin once daily in patients with type 2 diabetes. Diabetes Obes Metab 2013;15:613-21.

198. Sarashina A, Koiwai K, Seman LJ et al. Safety, tolerability, pharmacokinetics and pharmacodynamics of single doses of empagliflozin, a sodium glucose cotransporter 2 (SGLT2) inhibitor, in healthy Japanese subjects. Drug Metab Pharmacokinet 2013;28:213-9.

199. Macha S, Mattheus M, Halabi A, Pinnetti S, Woerle HJ, Broedl UC. Pharmacokinetics, pharmacodynamics and safety of empagliflozin, a sodium glucose cotransporter 2

(SGLT2) inhibitor, in subjects with renal impairment. Diabetes Obes Metab 2014;16:215-22.

200. Macha S, Jungnik A, Hohl K, Hobson D, Salsali A, Woerle HJ. Effect of food on the pharmacokinetics of empagliflozin, a sodium glucose cotransporter 2 (SGLT2) inhibitor, and assessment of dose proportionality in healthy volunteers. Int J Clin Pharmacol Ther 2013;51:873-9.

201. Macha S, Rose P, Mattheus M, Pinnetti S, Woerle HJ. Lack of drug-drug interaction between empagliflozin, a sodium glucose cotransporter 2 inhibitor, and warfarin in healthy volunteers. Diabetes Obes Metab 2013;15:316-23.

202. Friedrich C, Metzmann K, Rose P, Mattheus M, Pinnetti S, Woerle HJ. A randomized, open-label, crossover study to evaluate the pharmacokinetics of empagliflozin and linagliptin after coadministration in healthy male volunteers. Clin Ther 2013;35:A33-42.

203. Baartscheer A, Schumacher CA, Wust RC et al. Empagliflozin decreases myocardial cytoplasmic Na(+) through inhibition of the cardiac Na(+)/H(+) exchanger in rats and rabbits. Diabetologia 2017;60:568-573.

204. Uthman L, Nederlof R, Eerbeek O et al. Delayed ischemic contracture onset by Empagliflozin associates with NHE-1 inhibition and is dependent on insulin in isolated mouse hearts. Cardiovasc Res 2019.

205. Uthman L, Baartscheer A, Bleijlevens B et al. Class effects of SGLT2 inhibitors in mouse cardiomyocytes and hearts: inhibition of Na(+)/H(+) exchanger, lowering of cytosolic Na(+) and vasodilation. Diabetologia 2018;61:722-726.

206. Gallo LA, Ward MS, Fotheringham AK et al. Once daily administration of the SGLT2 inhibitor, empagliflozin, attenuates markers of renal fibrosis without improving albuminuria in diabetic db/db mice. Sci Rep 2016;6:26428.

207. Seman L, Macha S, Nehmiz G et al. Empagliflozin (BI 10773), a Potent and Selective SGLT2 Inhibitor, Induces Dose-Dependent Glucosuria in Healthy Subjects. Clin Pharmacol Drug Dev 2013;2:152-61.

208. Hsafety and tolerability of 4 weeks' treatment with empagliflozin in Japanese patientseise T, Seman L, Macha S et al. Safety, tolerability, pharmacokinetics, and pharmacodynamics of multiple rising doses of empagliflozin in patients with type 2 diabetes mellitus. Diabetes Ther 2013;4:331-45.

209. Kanada S, Koiwai K, Taniguchi A, Sarashina A, Seman L, Woerle HJ. Pharmacokinetics, pharmacodynamics, safety and tolerability of 4 weeks' treatment with empagliflozin in Japanese patients with type 2 diabetes mellitus. J Diabetes Investig 2013;4:613-7.

210. Nair AB, Jacob S. A simple practice guide for dose conversion between animals and human. J Basic Clin Pharm 2016;7:27-31.

211. Contrera JF, Matthews EJ, Kruhlak NL, Benz RD. Estimating the safe starting dose in phase I clinical trials and no observed effect level based on QSAR modeling of the human maximum recommended daily dose. Regul Toxicol Pharmacol 2004;40:185-206.

212. Reigner BG, Blesch KS. Estimating the starting dose for entry into humans: principles and practice. Eur J Clin Pharmacol 2002;57:835-45.

213. Komoroski B, Vachharajani N, Feng Y, Li L, Kornhauser D, Pfister M. Dapagliflozin, a novel, selective SGLT2 inhibitor, improved glycemic control over 2 weeks in patients with type 2 diabetes mellitus. Clin Pharmacol Ther 2009;85:513-9.

214. Cherney DZ, Perkins BA, Soleymanlou N et al. Renal hemodynamic effect of sodium-glucose cotransporter 2 inhibition in patients with type 1 diabetes mellitus. Circulation 2014;129:587-97.

215. Mudaliar S, Polidori D, Zambrowicz B, Henry RR. Sodium-Glucose Cotransporter Inhibitors: Effects on Renal and Intestinal Glucose Transport: From Bench to Bedside. Diabetes Care 2015;38:2344-53.

216. Lambers Heerspink HJ, de Zeeuw D, Wie L, Leslie B, List J. Dapagliflozin a glucose-regulating drug with diuretic properties in subjects with type 2 diabetes. Diabetes Obes Metab 2013;15:853-62.

217. Psaty BM, Lumley T, Furberg CD et al. Health outcomes associated with various antihypertensive therapies used as first-line agents: a network meta-analysis. JAMA 2003;289:2534-44.

218. Emdin CA, Rahimi K, Neal B, Callender T, Perkovic V, Patel A. Blood pressure lowering in type 2 diabetes: a systematic review and meta-analysis. JAMA 2015;313:603-15.

219. Olde Engberink RH, Frenkel WJ, van den Bogaard B, Brewster LM, Vogt L, van den Born BJ. Effects of thiazide-type and thiazide-like diuretics on cardiovascular events and mortality: systematic review and meta-analysis. Hypertension 2015;65:1033-40.

220. Yanai H, Hakoshima M, Adachi H et al. Effects of Six Kinds of Sodium-Glucose Cotransporter 2 Inhibitors on Metabolic Parameters, and Summarized Effect and Its Correlations With Baseline Data. J Clin Med Res 2017;9:605-612.

221. Neeland IJ, McGuire DK, Chilton R et al. Empagliflozin reduces body weight and indices of adipose distribution in patients with type 2 diabetes mellitus. Diab Vasc Dis Res 2016;13:119-26.

222. Ridderstrale M, Andersen KR, Zeller C et al. Comparison of empagliflozin and glimepiride as add-on to metformin in patients with type 2 diabetes: a 104-week randomised, active-controlled, double-blind, phase 3 trial. The lancet Diabetes & endocrinology 2014;2:691-700.

223. Murakami T, Kokado H. Abstract 17182: Empagliflozin Early Reverses Metabolic and Cardiac Disturbances in Type-2 Diabetics With Chronic Heart Failure. Circulation 2017;136:A17182-A17182.

224. Haffner SM. Abdominal adiposity and cardiometabolic risk: do we have all the answers? Am J Med 2007;120:S10-6; discussion S16-7.

225. Abdul-Ghani M, Del Prato S, Chilton R, DeFronzo RA. SGLT2 Inhibitors and Cardiovascular Risk: Lessons Learned From the EMPA-REG OUTCOME Study. Diabetes Care 2016;39:717-25.

226. Ferrannini E, Muscelli E, Frascerra S et al. Metabolic response to sodium-glucose cotransporter 2 inhibition in type 2 diabetic patients. J Clin Invest 2014;124:499-508.

227. Merovci A, Solis-Herrera C, Daniele G et al. Dapagliflozin improves muscle insulin sensitivity but enhances endogenous glucose production. J Clin Invest 2014;124:509-14.

228. McGarry JD, Foster DW. Regulation of hepatic fatty acid oxidation and ketone body production. Annu Rev Biochem 1980;49:395-420.

229. Devenny JJ, Godonis HE, Harvey SJ, Rooney S, Cullen MJ, Pelleymounter MA. Weight loss induced by chronic dapagliflozin treatment is attenuated by compensatory hyperphagia in diet-induced obese (DIO) rats. Obesity (Silver Spring) 2012;20:1645-52.

230. Yokono M, Takasu T, Hayashizaki Y et al. SGLT2 selective inhibitor ipragliflozin reduces body fat mass by increasing fatty acid oxidation in high-fat diet-induced obese rats. Eur J Pharmacol 2014;727:66-74.

231. Suzuki M, Takeda M, Kito A et al. Tofogliflozin, a sodium/glucose cotransporter 2 inhibitor, attenuates body weight gain and fat accumulation in diabetic and obese animal models. Nutr Diabetes 2014;4:e125.

232. Tahara A, Kurosaki E, Yokono M et al. Effects of sodium-glucose cotransporter 2 selective inhibitor ipragliflozin on hyperglycaemia, oxidative stress, inflammation and liver injury in streptozotocin-induced type 1 diabetic rats. The Journal of pharmacy and pharmacology 2014;66:975-87.

233. Inagaki N, Kondo K, Yoshinari T, Takahashi N, Susuta Y, Kuki H. Efficacy and safety of canagliflozin monotherapy in Japanese patients with type 2 diabetes inadequately controlled with diet and exercise: a 24-week, randomized, double-blind, placebo-controlled, Phase III study. Expert Opin Pharmacother 2014;15:1501-15.

234. Xu L, Nagata N, Nagashimada M et al. SGLT2 Inhibition by Empagliflozin Promotes Fat Utilization and Browning and Attenuates Inflammation and Insulin Resistance by Polarizing M2 Macrophages in Diet-induced Obese Mice. EBioMedicine 2017;20:137-149.

235. Benetti E, Mastrocola R, Vitarelli G et al. Empagliflozin Protects against Diet-Induced NLRP-3 Inflammasome Activation and Lipid Accumulation. J Pharmacol Exp Ther 2016;359:45-53.

236. Ferrannini E, Baldi S, Frascerra S et al. Shift to Fatty Substrate Utilization in Response to Sodium-Glucose Cotransporter 2 Inhibition in Subjects Without Diabetes and Patients With Type 2 Diabetes. Diabetes 2016;65:1190-5.

237. Ferrannini E, Mark M, Mayoux E. CV Protection in the EMPA-REG OUTCOME Trial: A "Thrifty Substrate" Hypothesis. Diabetes Care 2016;39:1108-14.

238. Mudaliar S, Alloju S, Henry RR. Can a Shift in Fuel Energetics Explain the Beneficial Cardiorenal Outcomes in the EMPA-REG OUTCOME Study? A Unifying Hypothesis. Diabetes Care 2016;39:1115-22.

239. Peters AL, Buschur EO, Buse JB, Cohan P, Diner JC, Hirsch IB. Euglycemic Diabetic Ketoacidosis: A Potential Complication of Treatment With Sodium-Glucose Cotransporter 2 Inhibition. Diabetes Care 2015;38:1687-93.

240. Taylor SI, Blau JE, Rother KI. SGLT2 Inhibitors May Predispose to Ketoacidosis. J Clin Endocrinol Metab 2015;100:2849-52.

241. Administration USFaD. FDA warns that SGLT2 inhibitors for diabetes may result in a serious

condition of too much acid in the blood. 2015.

242. Donnelly RP, Finlay DK. Glucose, glycolysis and lymphocyte responses. Mol Immunol 2015;68:513-9.

243. Lahnwong S, Chattipakorn SC, Chattipakorn N. Potential mechanisms responsible for cardioprotective effects of sodium-glucose co-transporter 2 inhibitors. Cardiovasc Diabetol 2018;17:101.

244. Xu C, Wang W, Zhong J et al. Canagliflozin exerts anti-inflammatory effects by inhibiting intracellular glucose metabolism and promoting autophagy in immune cells. Biochem Pharmacol 2018;152:45-59.

245. Gembardt F, Bartaun C, Jarzebska N et al. The SGLT2 inhibitor empagliflozin ameliorates early features of diabetic nephropathy in BTBR ob/ob type 2 diabetic mice with and without hypertension. American journal of physiology Renal physiology 2014;307:F317-25.

246. Leng W, Ouyang X, Lei X et al. The SGLT-2 Inhibitor Dapagliflozin Has a Therapeutic Effect on Atherosclerosis in Diabetic ApoE(-/-) Mice. Mediators Inflamm 2016;2016:6305735.

247. Birnbaum Y, Bajaj M, Yang HC, Ye Y. Combined SGLT2 and DPP4 Inhibition Reduces the Activation of the Nlrp3/ASC Inflammasome and Attenuates the Development of Diabetic Nephropathy in Mice with Type 2 Diabetes. Cardiovasc Drugs Ther 2018;32:135-145.

248. Chen L, Klein T, Leung PS. Effects of combining linagliptin treatment with BI-38335, a novel SGLT2 inhibitor, on pancreatic islet function and inflammation in db/db mice. Curr Mol Med 2012;12:995-1004.

249. Ye Y, Bajaj M, Yang HC, Perez-Polo JR, Birnbaum Y. SGLT-2 Inhibition with Dapagliflozin Reduces the Activation of the Nlrp3/ASC Inflammasome and Attenuates the Development of Diabetic Cardiomyopathy in Mice with Type 2 Diabetes. Further Augmentation of the Effects with Saxagliptin, a DPP4 Inhibitor. Cardiovasc Drugs Ther 2017;31:119-132.

250. LEE Y-H, KIM SR, BAE J et al. SGLT2 Inhibitors Suppress NLRP3 Inflammasome Activity via Changes in Ketones and Insulin in Type 2 Diabetes and Cardiovascular Diseases. Diabetes 2018;67:164-OR.

251. Joubert M, Jagu B, Montaigne D et al. The Sodium-Glucose Cotransporter 2 Inhibitor Dapagliflozin Prevents Cardiomyopathy in a Diabetic Lipodystrophic Mouse Model. Diabetes 2017;66:1030-1040.

252. Kashiwagi Y, Nagoshi T, Yoshino T et al. Expression of SGLT1 in Human Hearts and Impairment of Cardiac Glucose Uptake by Phlorizin during Ischemia-Reperfusion Injury in Mice. PLoS One 2015;10:e0130605.

253. Bartos DC, Grandi E, Ripplinger CM. Ion Channels in the Heart. Compr Physiol 2015;5:1423-64.

254. Priest BT, McDermott JS. Cardiac ion channels. Channels (Austin) 2015;9:352-9.

255. Mustroph J, Wagemann O, Lucht CM et al. Empagliflozin reduces Ca/calmodulin-dependent kinase II activity in isolated ventricular cardiomyocytes. ESC heart failure 2018;5:642-648.

256. Mustroph J, Lucht CM, Wagemann O et al. Empagliflozin enhances human and murine cardiomyocyte glucose uptake by increased expression of GLUT1. Diabetologia 2019;62:726-729.

257. Pabel S, Wagner S, Bollenberg H et al. Empagliflozin directly improves diastolic function in human heart failure. European journal of heart failure 2018;20:1690-1700.

Chapter Two

Normalization of Cardiac Substrate Utilization and Left Ventricular Hypertrophy Precede Functional Recovery in Heart Failure Regression

Contribution:

Nikole J Byrne: conception and design of the experimental paradigm, organizing all experiments, analysis of echocardiography images, *in vivo* experiments (indirect calorimetry, treadmill running), immunoblot analysis, interpretation of resulting data and manuscript writing
Jody L Levasseur: conception and design of the experimental paradigm, surgeries
Donna Beker: echocardiography
Grant Masson: isolated heart perfusions
Dyck JRB: conception and design of research, intellectual and editorial contribution

Chapter 2 has been published as:

Byrne NJ, Levasseur J, Sung MM, Masson G, Boisvenue J, Young ME, Dyck JRB. Normalization of Cardiac Substrate Utilization and Left Ventricular Hypertrophy Precede Functional Recovery in Heart Failure Regression. *Cardiovascular Research*. 2016; 110(2):249-57.

2.1 Introduction

Increases in aortic pressure resulting from conditions such as hypertension or valvular heart disease often induce compensatory structural remodelling of the LV, presenting as LV hypertrophy (1). These adaptive changes in the heart are necessary for the heart to normalize wall stress and to maintain CO (2). However, if the precipitating condition that increases afterload is not treated, the structural changes occurring within the heart may become maladaptive. This maladaptive remodelling of the LV can worsen over time and eventually transition from a compensated to decompensated hypertrophy and eventually to HF (3,4).

A hallmark of the transition from compensated to decompensated LV hypertrophy is the genetic reprogramming of the metabolic pathways in the cardiomyocyte, which results in impaired cardiac energetics and subsequent impaired cardiac performance (5-8). Since many of these changes occur at the transcriptional level of the metabolic enzymes, it has been proposed that sustained loss of metabolic flexibility of the heart contributes to decreased mitochondrial flux and an energetically compromised heart (9,10). Although impaired cardiac energetics has been shown to be a major contributor to HF (11,12), whether or not this genetic reprogramming of the metabolic pathways can be reversed in established HF has not been extensively investigated. Therefore, to address this, we used a mouse model of severe HF to determine whether metabolic remodelling is reversible and whether regression of LV hypertrophy or improved cardiac performance is preceded by improved cardiac energy metabolism. Overall, we propose that determining the potential reversibility of this previously assumed permanent change in cardiac metabolism has significant clinical implications for the treatment or management of patients with HF.

2.2 Methods

2.2.1 Experimental animals

All protocols involving mice were approved by the University of Alberta Institutional Animal Care and Use Committee and conform with the Guide for the Care and Use of Laboratory Animals published by the United States National Institutes of Health (eighth edition; revised 2011). The University of Alberta adheres to the principles for biomedical research involving animals developed by the Council for International Organizations of Medical Sciences and complies with the Canadian Council on Animal Care guidelines. Male C57Bl/6 mice (7 weeks of age) were obtained from Charles River Laboratories (Sherbrooke, QC). Mice were maintained on a 12:12 h light-dark cycle with free *ad libitum* access to food and drinking water. At 8 weeks of age were randomly assigned to the Sham (n = 9) or TAC (n = 48) group. At 3–4 weeks post-surgery, mice considered to be in severe HF (EF <30%) were then subjected to DB surgery. An additional group of TAC mice served as controls without undergoing a DB surgery.

2.2.2 TAC and DB surgery[b]

TAC surgery was performed as previously described (13). In brief, male eight-week old mice were anaesthetized by an intraperitoneal injection of a cocktail of ketamine (100 mg/kg) and xylazine (10 mg/kg), intubated, and connected to a mouse ventilator (MiniVent, Harvard Apparatus, Holliston, MA, USA). Following midline sternotomy, a double-blunted 27-gauge needle was tied

[b] See Appendix B for additional information regarding TAC surgery.

encircling the aorta between the innominate and left common carotid arteries using a 6/0 silk suture. The needle was then removed, and chest and skin were sutured and closed. HF mice were then subjected to a second surgery re-entering through the original incision site. The TAC suture was carefully removed, and chest and skin were sutured closed (DB). Sham mice also underwent a second open-chest procedure.

2.2.3 Echocardiography

Mice were anaesthetized with isoflurane and *in vivo* cardiac function was assessed by transthoracic echocardiography using a Vevo 770 high-resolution imaging system equipped with a 30-MHz transducer (RMV-707B; VisualSonics, Toronto, Canada), as previously described (14). Pressure-overload was confirmed in all mice at 3-weeks after TAC by measuring trans-stenotic gradient by pulsed-wave Doppler flow. Full systolic and diastolic parameters were measured either at 3–4 weeks TAC or at 1 or 3-weeks following DB. Sham data were collected following two sham procedures.

2.2.4 Metabolic analysis *in vivo*

Total physical activity was measured using the Comprehensive Lab Animal Monitoring System (CLAMS/Oxymax Columbus Instruments, Columbus, OH, USA) and was calculated by adding Z counts (rearing or jumping) to total counts associated with ambulatory movement and stereotypical rodent behaviour (grooming and scratching) as described previously (15). An Oxymax treadmill (Columbis Instruments) was used to determine running capacity in mice before or 1 or 3 weeks

after DB. With a 10° incline, the belt speed was programmed to increase from 10 m/min by 1 m/min every minute, where maximal oxygen consumption (VO_2max) was taken as peak oxygen consumption (VO_2).

2.2.5 Histology

Masson's trichrome staining of paraffin-embedded LV heart sections taken mid-papillary were visualized using a Leica DMLA microscope (Leica Microsystems, Wetzlar, Germany) equipped with a Retiga 1300i FAST 1394 CCD camera (OImaging, Surrey, BC, Canada), as described previously (16). Three representative images were taken from each sample and densitometric analysis was performed using the ImageJ software (National Institutes of Health, Bethesda, MD, USA).

2.2.6 *Ex vivo* heart perfusions

Mice were euthanized with an intraperitoneal injection of euthanyl (120 mg/kg body weight). Hearts were excised and perfused in working heart mode at 11.5 mmHg preload and 50 mmHg afterload with Krebs-Henseleit buffer containing 0.8 mmol/L [9,10-^{3}H]oleate prebound to 3% delipidated bovine serum albumin (BSA), 5 mmol/L [U-^{14}C]glucose, and 50 μU/ml insulin. A sample of perfusate was taken every 10 minutes for a total of 60-min aerobic perfusion, following which hearts were frozen in liquid nitrogen and stored at -80°C. Fatty acid and glucose oxidation rates were calculated based on the collection of myocardial ^{3}H and $^{14}CO_2$ production, respectively (13).

2.2.7 Immunoblot analysis[c]

Frozen heart tissue was homogenized according to the previously reported methods (16), and protein concentration was assayed using the bicinchoninic acid protein assay kit (number 23 255; Pierce, Thermo Fisher Scientific, Rockford, IL, USA). Protein (15–20 μg) was resolved by SDS–PAGE and transferred to a nitrocellulose membrane. Blotted proteins were identified by the following primary antibodies: Akt, mTOR, Raptor, 4E-BP1, S6, GSK3β, phosphorylated-AMPKα (pT172), phosphorylated-ACC (S79). Primary antibodies were purchased from Cell Signaling Technology and secondary antibodies for goat anti-rabbit and donkey anti-goat (Santa Cruz Biotechnology). Densitometric analysis was performed using the ImageJ software (National Institutes of Health) and corrected against Memcode protein stain as a loading control.

2.2.8 Quantitative RT-PCR

Cardiac mRNA expression was determined by real-time polymerase chain reaction (RT-PCR) using Taqman probes. Total ribonucleic acid (RNA) was extracted from heart tissue using the TRIzol RNA extraction method (17). RNA (1 μg) was subjected to reverse transcription to synthesize complementary deoxyribonucleic acid (cDNA). RT-PCR was performed by taking 5 μL of suitable cDNA dilutions from unknown, standard (brain cDNA) and 8 μL of Taqman master-mix (includes primers + probes) that were then loaded on white 384 Light cycler® 480 multiwell plates supplied from Roche. Gene expression of cardiac hypertrophy markers (*Anp*, *Bnp*, *Mhcb*, and *Mhca*), contractility (*Serca2a*), fibrosis (*Col1a1*), glucose metabolism (*Glut4* and *Pdk4*), and

[c] See Appendix C for additional information regarding antibodies used for immunoblot analysis.

FA metabolism (*Ppara*, *Mcd*, *Pgc1a*, and *Mcad*) were analysed. Data are presented as mRNA molecules per nanogram total mRNA relative to the control housekeeping gene (*Cyclophilin*). Primers used for RT-PCR reactions are listed in **Table 2.1**.

2.2.9 Statistical analysis

Data are expressed as mean ± S.E.M. Comparisons between groups (Sham, TAC, and each respective DB group) were performed using one-way analysis of variance (ANOVA) and Tukey's multiple comparisons test. A p value of <0.05 is considered significant.

2.3 Results

2.3.1 Removal of the elevated aortic afterload improves survival and systolic and diastolic cardiac function in mice with pre-existing heart failure

Of the total of 44 male mice that successfully underwent TAC, 35 (79.5%) met criteria of EF <30% by 3–4 weeks following surgery. At this time period, mice with established HF either remained as HF controls or underwent a second surgery to remove the aortic constriction (DB). Doppler echocardiography was used to confirm the presence of an elevated pressure gradient across the transverse aorta at 3-weeks following TAC (TAC: 53.5 ± 3.3 mmHg vs. Sham: 3.6 ± 0.4 mmHg) and subsequent normalization of this gradient following DB (8.4 ± 1.6 mmHg). We have previously shown that without intervention, mice with established HF have a 50% survival rate of

~4 weeks (13), whereas mice with HF that underwent the DB procedure had no complications associated with HF even beyond 4 weeks following DB (data not shown).

To determine whether prolonged survival in DB mice was due to restored cardiac function, mice were subjected to transthoracic echocardiography. At 3–4 weeks post-TAC, mice had a mean EF of 21.73% compared to 52.33% for Sham controls **(Figure 2.1A** and **Table 2.2)**. Moreover, mice subjected to TAC displayed additional impairments in systolic function, such as reductions in CO, SV, and FS **(Figure 2.1A-C** and **Table 2.2)**, as well as diastolic dysfunction evident by an increase in mitral E/A and E/E′ ratios, with a shortened deceleration time (DT) (**Figure 2.1D-F** and **Table 2.2)**. However, as early as 1-week following DB, all parameters of cardiac function showed improvement, with a near full recovery of systolic and diastolic function occurring by 3-weeks **(Figure 2.1A-F** and **Table 2.2)**. To directly assess cardiac function in the absence of potential systemic or haemodynamic effects, mechanical function was also assessed *ex vivo* in the perfused working heart. Consistent with poor function *in vivo*, TAC hearts had reduced CO and aortic flow (58.9 and 44.7%, respectively) *ex vivo*, yet both of these parameters were fully restored to that of Sham-operated mice by 3-weeks post-DB **(Table 2.3)**.

2.3.2 Removal of the elevated aortic afterload restores spontaneous physical activity and maximal exercise capacity in mice with pre-existing heart failure

Exercise intolerance is a hallmark of HF severity in patients with HF (18). Given that both systolic and diastolic dysfunction were returned to normal in hearts following DB of TAC mice, we investigated whether these improvements had any effect on daily physical activity or exercise

capacity. Using the Oxymax laboratory animal monitoring system with *x*-, *y*-, and *z*-axis activity monitors, we determined that Sham and DB mice displayed higher levels of daily physical activity (evident by increased rearing) than did TAC mice **(Figure 2.1G)**. Furthermore, when subjected to an exercise endurance test, DB mice showed fully restored exercise capacity, determined by restored VO_2max by 1-week post-DB **(Figure 2.1H)**.

2.3.3 Removal of elevated aortic afterload causes a regression of left ventricular hypertrophy in mice with pre-existing heart failure

Morphological changes in response to pressure-overload include increased LV hypertrophy, LV dilation, and increased LA diameter **(Table 2.2)**. The presence of pressure-overload-induced LV hypertrophy was evident in the TAC group compared to the Sham group by a 1.5-fold increase in LV mass and a 1.3-fold increase in wall thickness at end-diastole **(Table 2.2)**. Surprisingly, DB mice demonstrate rapid regression of LV hypertrophy, evidenced by significantly reduced LV mass, IVS thickness, and LV posterior wall thickness at end-diastole as early as 1-week following DB **(Figure 2.2A-C** and **Table 2.2)**, which preceded marked improvement in cardiac function. In addition, structural remodelling of the heart following TAC surgery resulted in an increase in LVID, LV volume, and enlarged LA, which were significantly reduced as early as 1-week post-DB. However, LVID and LV volume at end-diastole were not significantly reduced by DB **(Table 2.2)**.

A hallmark of pathological hypertrophy is a shift in gene expression from the MHCα to the MHCβ isoform (19-21). Therefore, in all groups of mice, we measured cardiac transcript levels of these

as well as other molecular markers for LV hypertrophy/HF, which are generally altered in hypertrophied/failing hearts (such as *Anp* and *Bnp*) (22). In agreement with the regression of LV hypertrophy, cardiac expression of these transcripts also returned to near-baseline values of Sham mice post-DB **(Figure 2.2D)**. Furthermore, as reported previously (23), cardiac expression of *Serca2a*, a Ca^{2+}-ATPase that modulates cardiac contractility, was significantly reduced in TAC hearts, but returned to levels close to that of Sham-operated hearts by 3-weeks post-DB **(Figure 2.2D)**.

In addition to changes in transcript levels of stress genes associated with HF and HF regression, previous reports have demonstrated TAC-induced activation of Akt and the mTOR signalling pathway (24). While expression of phosphorylated proteins did not appear to be altered in our HF mice (data not shown), total protein levels of Akt, mTOR, Raptor, 4E-BP1, S6, and GSK3β were significantly increased in response to pressure-overload, as previously described (25). More importantly, we observed normalized cardiac content of these regulators of protein synthesis following DB **(Figure 2.2E-F)**, suggesting that some of the molecular signalling events that control hypertrophic growth have returned to baseline values and that the pro-hypertrophic molecular stimuli have also regressed.

2.3.4 Removal of elevated aortic afterload restores levels of markers of adverse cardiac remodeling without reversing cardiac fibrosis in mice with pre-existing heart failure

Since myocardial stiffness is a major result of pressure-overload due to worsening fibrosis, we investigated whether improved diastolic function in DB mice occurred as a result of reduced

collagen deposition compared to TAC mice. The expression of *Col1a1*, a gene involved in fibrotic remodelling, was increased five-fold in TAC hearts yet it was completely restored to that of Sham-operated mice by 1-week post-DB **(Figure 2.3A)**. Surprisingly, however, despite significant recovery of diastolic function at 3-weeks following DB, Masson's trichrome staining showed a trend towards increased cardiac fibrosis in TAC mice that remained post-DB **(Figure 2.3B-C)**. Taken together, these data suggest that while the potential for continued fibrosis and collagen deposition may be reduced, existing cardiac fibrosis is not degraded following DB.

2.3.5 Removal of elevated aortic afterload normalizes genetic reprogramming and molecular signaling events of the metabolic pathways in mice with pre-existing heart failure

The healthy heart generates the majority of the necessary ATP primarily via the utilization of FAs and glucose. However, it has been shown that HF is associated with alterations at the transcriptional level of metabolic enzymes that contribute to impaired cardiac energetics (12,13). To determine whether these transcriptional changes are permanent, we measured the transcript levels of metabolic genes involved in both glucose and FA metabolism in all hearts. Consistent with the previous work (26-29), numerous genes involved in the regulation of glucose (*Glut4* and *Pdk4*) and FA (*Mcad*, *Pgc1a*, *Mcd*, and *Ppara*) metabolism were significantly reduced in TAC hearts **(Figure 2.4A-B)**. In most instances, unlike markers of cardiac hypertrophy (which were restored by 1–3 weeks following DB), gene expression of several regulators of both glucose and FA transport and utilization (*Pdk4, Glut4, Pgc1a, Mcd,* and *Ppara*) were not significantly different for mice following DB when compared to TAC controls. However, the expression of these markers also did not significantly differ from Sham-operated mice and transcript levels

of *Mcad* were significantly increased **(Figure 2.4A-B)**, suggesting the potential for reversibility of the transcript levels of metabolic enzymes otherwise reduced by HF, beyond 3-weeks following DB.

2.3.6 Removal of elevated aortic afterload improves cardiac oxidative metabolism in mice with pre-existing heart failure

Although we did not observe normalization of transcript levels of metabolic enzymes normally reduced by HF, we directly measured *ex vivo* rates of glucose and FA oxidation in all groups of hearts. Compared to Sham mice, mice with HF demonstrated significantly impaired myocardial glucose oxidation **(Figure 2.4C)** and FA oxidation **(Figure 2.4D)** rates by 75 and 70%, respectively. This is consistent with numerous pervious reports that total myocardial oxidative metabolism is reduced in pressure-overload-induced HF (30,31).

Contrary to our gene expression data, both glucose and FA oxidation levels were restored to that of the Sham-operated group by 1-week post-DB, indicating a very early and remarkable recovery of cardiac energy metabolism following removal of the elevated aortic afterload. Consistent with this, AMPK, which is a metabolic stress kinase and thus an endogenous measure of cardiac myocardial energetic status (7,32-34), was activated in TAC hearts (indicated by phosphorylation of AMPK and its downstream target, ACC), but normalized post-DB **(Figure 2.4E)**. Taken together, these data demonstrate that improved myocardial energetic status precedes cardiac functional recovery in TAC mice following DB.

2.4 Discussion

Here, we present data characterizing a mouse model of reversible HF using a DB surgery of a previously banded transverse aorta and have used this model to better understand the molecular and structural changes that occur in the regression of severe HF. This model is unique as the DB was performed in mice with severe HF (mean EF of 21.73%) and the recovery period was studied for 3-weeks following DB. In addition to significant reductions in EF, prior to DB, there was also a significant diastolic dysfunction, profound cardiac remodelling, and the mice exhibited severe exercise intolerance. Moreover, hearts from these mice demonstrated many of the hallmarks of HF such as increased transcript levels of cardiac stress markers (*Anp* and *Bnp*) as well as decreased expression of transcripts involved in HF (*Serca2a*). Furthermore, molecular signalling pathways that mediate cellular growth in response to stress were also characteristically altered, as was the genetic reprogramming of the pathways controlling glucose and FA oxidation, and an accompanying impairment of cardiac substrate metabolism. Using this model, we investigated whether removal of the elevated aortic afterload in mice with established severe HF would result in the recovery of cardiac function, substrate metabolism, and genetic reprogramming as well as determined the temporal relationship of these changes.

Since our model was designed to determine whether there was functional recovery following intervention after the establishment of severe HF, we first determined whether or not our DB procedure could reverse cardiac dysfunction. Interestingly, as early as 1-week post-DB, hearts from mice with previous HF started to show signs of improved systolic and diastolic function and a near full recovery of cardiac function was observed at 3-weeks post-DB. In fact, the majority of

indices of cardiac function measured, such as CO, SV, mitral E/A ratio, E/E′ ratio, and DT, were returned to near-baseline levels observed in Sham mice. The noticeable exceptions to this were FS and EF, which were only recovered to 76 and 85%, respectively, of Sham controls at 3-weeks following DB. Although we cannot explain this delay in functional recovery compared to other parameters post-DB, it is likely that FS and EF would have returned to normal if the mice were allowed to recover for a longer period of time. Importantly, unlike previous studies where DB occurred at an EF of 39–53% (35-37), we provide evidence that mice with more severe HF are able to fully recover in response to pressure unloading. Importantly, this improved function is manifested in restored physical activity and exercise capacity in mice with pre-existing HF, suggesting that this major symptom of clinical HF also has the potential to be regressed.

As expected with almost complete recovery of heart function, we show that hearts undergo a dramatic beneficial remodelling that involves both concentric LV hypertrophy regression and LA diameter normalization as early as 1-week following DB. While regression of LV hypertrophy has previously been shown in models of compensated hypertrophy (36,38-40), ours is the first to demonstrate complete regression of LV hypertrophy following severe HF. In addition to these morphological changes, the hearts also underwent profound changes in the expression of hypertrophy gene transcripts and the molecular signalling events that are associated with cardiac remodelling. For instance, a marked reversal in the expression of cardiac stress markers (such as *Anp* and *Bnp)* as early as 1-week following DB provides evidence that genetic reprogramming is not irreversible, even following severe HF. In addition, ours is the first study to demonstrate that protein expression of numerous molecules involved in regulating protein synthesis were altered in TAC hearts and normalized following DB. Particularly, the Akt/mTOR signalling pathway, which

mediates cellular growth in response to stress (41), was normalized by 3-weeks following DB, suggesting that these hearts undergo reverse remodelling rapidly following relief of the pressure-overload.

Since myocardial stiffness is a major result of pressure-overload due, in part, to fibrosis, we investigated whether improved cardiac function in DB mice occurred as a result of reduced collagen deposition when compared to TAC mice. The expression of *Col1a1*, a gene involved in fibrotic remodelling, was increased in TAC hearts and was completely restored to that of Sham-operated mice by 1-week post-DB. Interestingly, despite the normalization in *Col1a1* expression and the reduction in myocardial stiffness indicated by improved diastolic relaxation and function, there was a trend towards increased fibrosis in TAC hearts, which was not resolved following DB **(Figure 2.3B-C)**. Thus, it appears that while remodelling and impaired function regress in our model of pressure unloading, residual cardiac fibrosis remains following pressure unloading, suggesting that reduced fibrosis is not responsible for this recovery.

Since we observed a near complete reversal of functional/structural remodelling as well as the reversal of the transcriptional changes observed in HF following DB, we assessed whether or not this was also the case with the significant transcriptional reprogramming of many of the proteins that control cardiac substrate metabolism that occurs in the hypertrophied/failing heart (42). Unlike the reversal of the hypertrophic and cardiac stress markers that occurred rapidly after DB, the altered expression of genes encoding for proteins involved in the regulation of glucose and FA metabolism were either unchanged (*Ppara*), not fully normalized (*Pdk4*, *Glut4*, *Pgc1a*, and *Mcd*), or did not normalize until 3-weeks post-DB (*Mcad*). These data agree with the only partial reversal

of depressed metabolic gene expression in the failing human heart upon implantation of a LV assist device (43), suggesting that the impairment in cardiac energetics that occurs at the transcriptional level in HF is not fully recovered following unloading.

Since it is widely understood that a poor correlation exists between mRNA and protein expression levels (44-46), and cardiac energy metabolism is regulated at multiple levels including many post-translational modifications, we also measured phosphorylation of AMPK, a key regulator of cellular metabolism. Despite not observing dramatic changes in the expression of genes encoding for proteins involved in the regulation of glucose and FA metabolism by 3-weeks following DB, activity of AMPK and its downstream target, ACC, were fully restored. Since activation of the AMPK signalling pathway may not be responsible for the rapid normalization of substrate utilization following DB, we speculate that post-translational modification of specific metabolic enzymes via AMPK-independent mechanisms is likely involved. However, we have not measured the activities of all enzymes involved in regulating glucose and FA oxidation and thus cannot provide data to pinpoint the precise regulatory pathways involved.

While our data show that in response to pressure-overload the heart exhibits severely reduced glucose oxidation, this is not consistent with the work done by Riehle *et al.* (47) that shows increased glucose oxidation and glycolysis rates in hearts subjected to TAC. These discrepancies may be accounted for by the stage of compensation and severity of HF induced in both our model and others who have demonstrated either no change or a decrease in both glucose and FA oxidation in hearts subjected to aortic banding (30,31). In addition, several studies have demonstrated a switch from mitochondrial oxidative metabolism to increased rates of glycolysis in hypertrophied

rodent hearts (7,43,48,49). Although glycolysis was not measured in the current study, we speculate, based on the reversal of cardiac function, regression of LV hypertrophy, and normalization of FA and glucose oxidation, that any potential changes in glycolysis in mice with HF would similarly be restored. Despite not measuring glycolysis in the present study, we did show that there was a striking and rapid normalization of cardiac oxidative metabolism (which is severely impaired in the failing heart) (13) as early as 1-week post-DB. While these data are consistent with normalized baseline cardiac substrate oxidation of dogs recovering from pacing-induced HF (31), this is the first account that fully restored FA and glucose oxidation precedes recovery of cardiac function in the regression of severe HF. While the precise mechanisms responsible for this are unknown, it has been well established that increases in local ADP concentration at the myofilaments occur as a result of depressed energy metabolism in HF (50,51). In fact, Tian *et al.* (51) have shown that a linear relationship exists between adenosine diphosphate (ADP) and LV end-diastolic pressure (LVEDP); therefore, elevated ADP contributes to impaired relaxation. Taken together, these data support the concept that recovered myocardial energy reserve following HF contributes to restored diastolic function. Notwithstanding this, although it is likely that early recovery of energy production may drive the normalization of cardiac function, our data do not provide direct genetic or pharmacological evidence to definitively prove this conclusion. Although previous groups have studied metabolic remodelling in both humans and animal models of HF (43,52), our study is the first to address the temporal recovery of improved substrate oxidation in relationship to both morphological and functional improvements. In addition, while previous studies have assessed the recovery of HF in models exhibiting moderately reduced cardiac function (35-37), we have shown that even in a model of severe HF, the metabolic perturbations are reversible. However, in the current study, we examined the reversibility of

impaired cardiac function and substrate metabolism under normal physiological conditions and whether or not DB hearts respond to a second, delayed stress such as ischemia or pressure-overload have yet to be determined.

2.5 Conclusion

In conclusion, this study indicates that in severe HF, removal of the elevated aortic afterload enables complete restoration of myocardial substrate metabolism, LV hypertrophy regression, and normalization of cardiac function. Importantly, regression of LV hypertrophy and normalization of cardiac energy metabolism occur prior to full functional recovery. Taken together, the data presented here show that impaired myocardial energy metabolism as a result of HF is not permanent and, in fact, suggest that early recovery of substrate utilization along with regression of LV hypertrophy regression may be critical determinants for functional recovery in the failing heart.

2.6 Figures

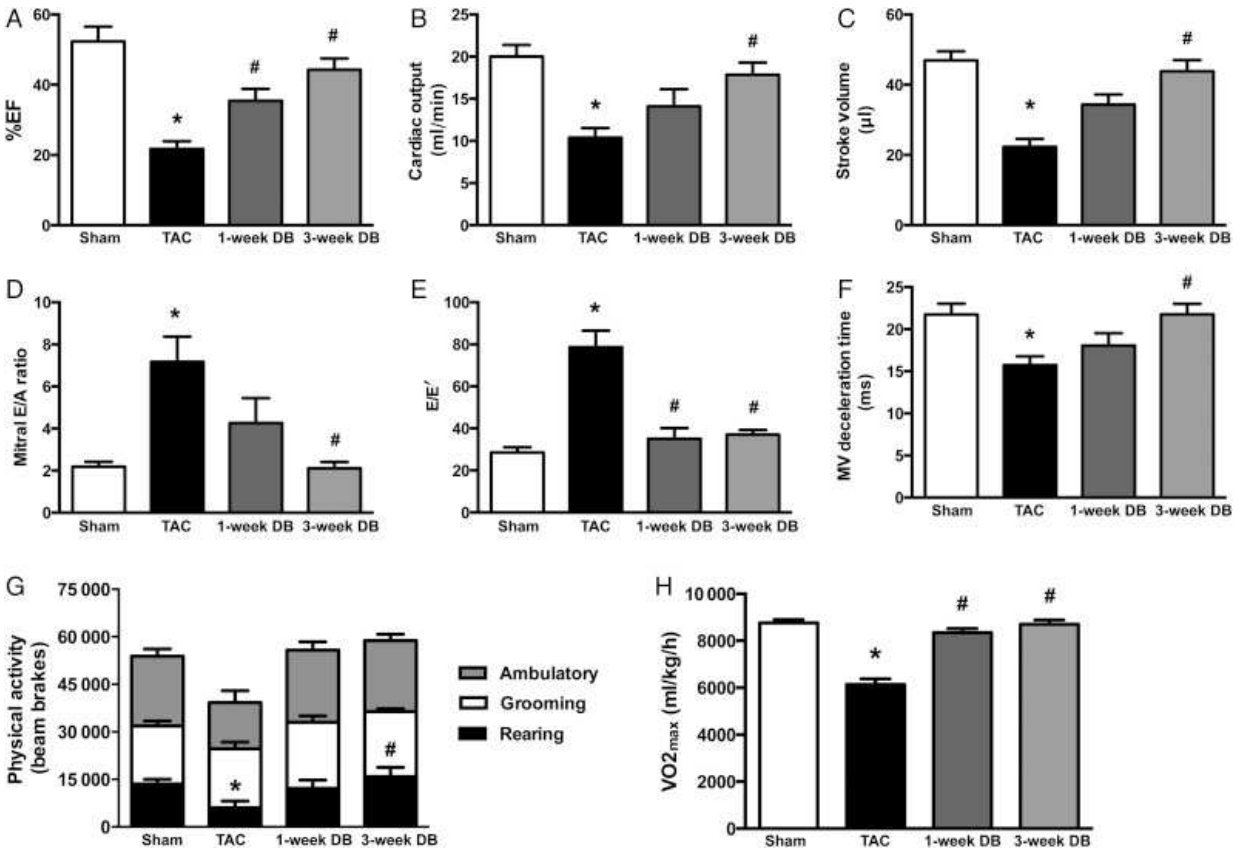

Figure 2.1. Removal of the Elevated Aortic Afterload Improves Systolic and Diastolic Cardiac Function and Restores Spontaneous Physical Activity and Maximal Exercise Capacity in Mice with Pre-existing Heart Failure. EF **(A)** (n = 8–9); cardiac output **(B)** (n = 7–9); SV **(C)** (n = 7–9); mitral E/A ratio **(D)** (n = 5–9); mitral E/E′ ratio **(E)** (n = 5–9); MV DT **(F)** (n = 6–9). Total 12-h rodent physical activity (divided into rearing, ambulatory, and grooming) as measured by metabolic cages **(G)** (n = 4–10); VO_2max during exercise **(H)** (n = 4–9). Results are expressed as mean ± standard error of the mean (SEM). Comparisons between groups were performed using one-way ANOVA and Tukey's multiple comparisons test. ***p<0.05 versus Sham; $^{\#}$p<0.05 versus TAC.** A = late mitral inflow; ANOVA = analysis of variance; DB, debanding; DT = deceleration time; E = early mitral inflow; EF = ejection fraction; E′ = tissue Doppler mitral annulus velocity; MV = mitral valve; SEM = standard error of the mean; SV = stroke volume; TAC = transverse aortic constriction; VO_2max = maximal oxygen consumption.

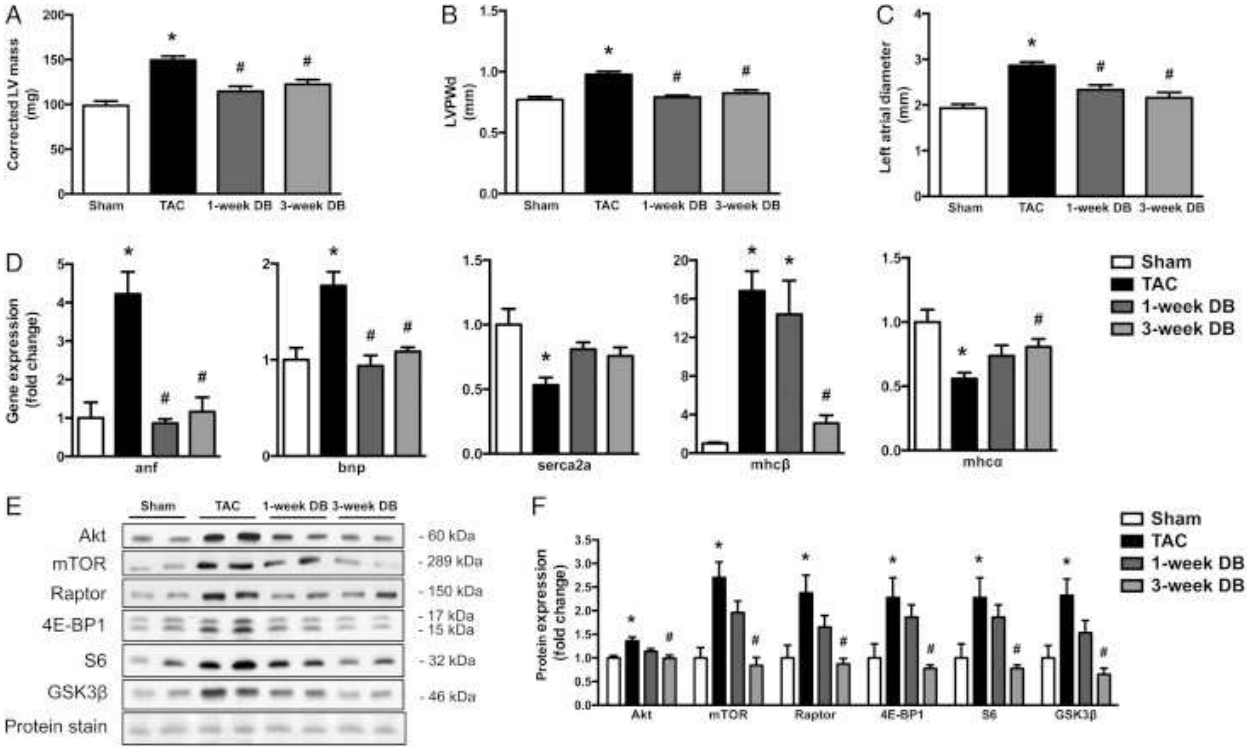

Figure 2.2. Removal of the Elevated Aortic Afterload Restores Cardiac Morphology and Normalizes Gene Expression and Molecular Signalling Events of Left Ventricular Hypertrophy in Mice with Pre-existing Heart Failure. Corrected LV mass **(A)**, LVPW at end-diastole **(B)** and LA diameter **(C)** (n = 5–9). Gene expression of markers of pathological cardiac hypertrophy/HF (*Anp, Bnp, Mhcb, Mhca, and Serca2a*) in ventricular tissue **(D)** (n = 5–7). Representative immunoblot **(E)** and densitometric analysis **(F)** of proteins in the heart involved in protein synthesis (Akt, mTOR, Raptor, 4E-BP1, S6, and GSK3β) (n = 5–7). Results are expressed as mean ± SEM. Comparisons between groups were performed using one-way ANOVA and Tukey's multiple comparisons test. ***p<0.05 versus Sham; #p<0.05 versus TAC.** 4E-BP1 = eukaryotic translation initiation factor 4E; AKT = protein kinase B; ANOVA = analysis of variance; ANP = atrial natriuretic peptide; BNP = brain natriuretic peptide; DB = debanding; GSK3β = glycogen synthase kinase 3-beta; LV = left ventricle; LVPW = LV posterior wall; MHC = myosin heavy

chain; MTOR = mammalian target of rapamycin; RAPTOR = regulatory-associated protein of mTOR; S6 = small subunit ribosomal protein S6; SEM = standard error of the mean; SERCA2a = sarco/endoplasmic reticulum Ca^{2+} adenosine triphosphatase-2a; TAC = transverse aortic constriction.

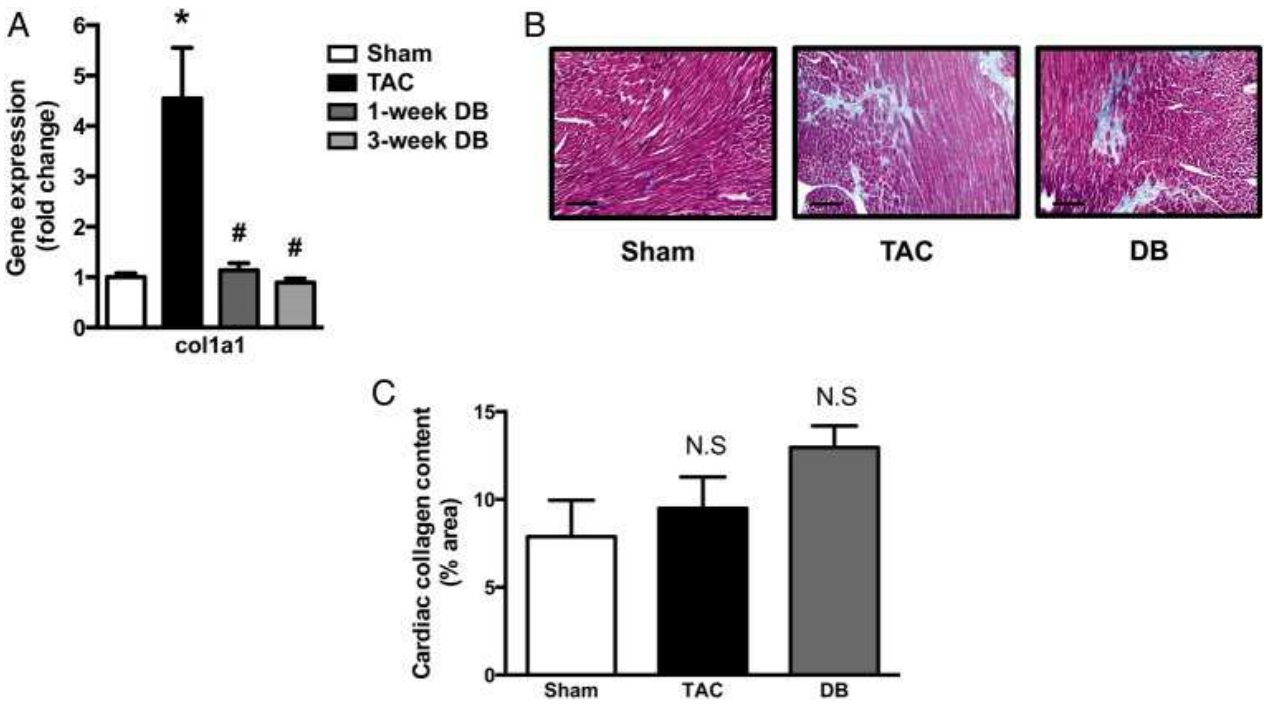

Figure 2.3. Removal of the Elevated Aortic Afterload Restores the Levels of Markers of Adverse Cardiac Remodelling Without Reversing Cardiac Fibrosis in Mice with Pre-existing Heart Failure. Gene expression of the marker of cardiac fibrosis (*Col1a1)* in ventricular tissue **(A)** (n = 5–7); representative images of LV heart sections taken mid-papillary and stained with Masson's trichrome at x 20 magnification **(B)**; and quantification of collagen staining in histological images expressed as % area **(C)** (n = 3–4). Scale bars = 100 μM. Results are expressed as mean ± SEM. Comparisons between groups were performed using one-way ANOVA and Tukey's multiple comparisons test. ***p<0.05 versus Sham; #p<0.05 versus TAC.** ANOVA = analysis of variance; COL1α1 = collagen type I alpha-1; DB = debanding; LV = left ventricle; SEM = standard error of the mean; TAC = transverse aortic constriction.

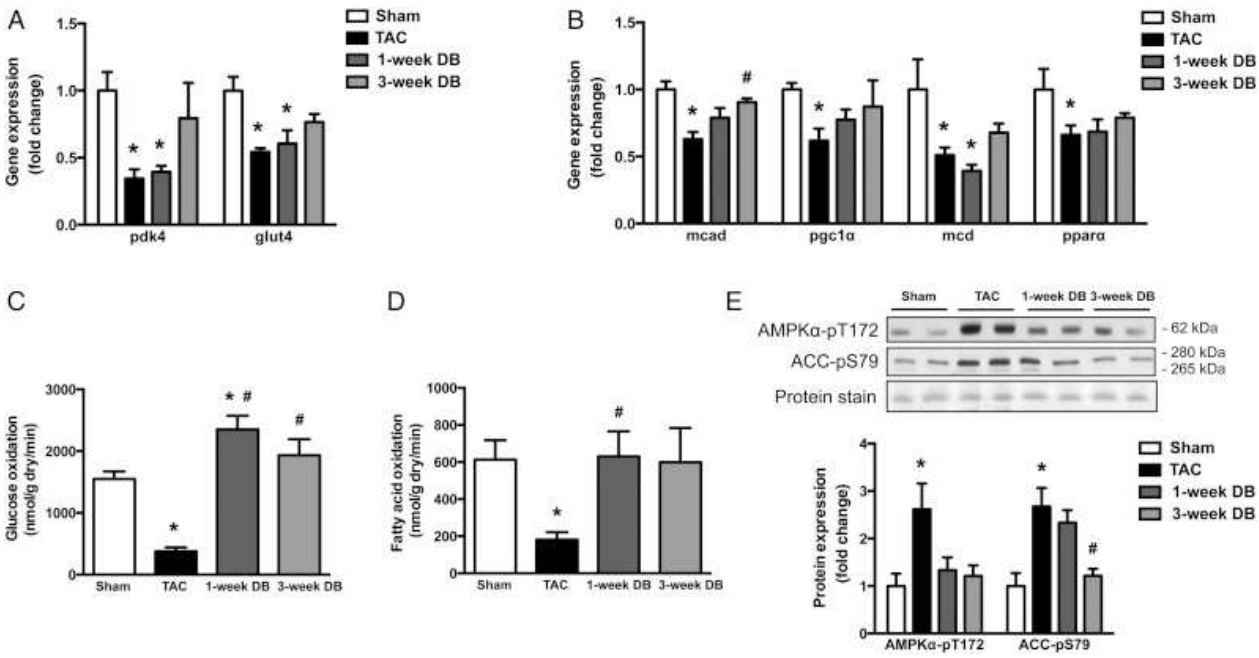

Figure 2.4. Removal of the Elevated Aortic Afterload Normalizes Transcript Levels of Metabolic Enzymes and Restores Cardiac Oxidative Metabolism in Mice with Pre-existing Heart Failure. Gene expression of proteins involved in glucose (*Pdk4 and Glut4*) **(A)** and FA (*Mcad, Pgc1a, Mcd, and Ppara*) uptake and metabolism **(B)** (n = 5–7). Glucose **(C)** and FA **(D)** oxidation rates in hearts from ex vivo perfusions (n = 4–7). Representative images and densitometric analysis of cardiac phosphorylated-AMPKα (Thr 172) and phosphorylated-ACC (Ser 79) in the heart as measured by immunoblot analysis **(B)** (n = 5–7). Results are expressed as mean ± SEM. Comparisons between groups were performed using one-way ANOVA and Tukey's multiple comparisons test. ***p<0.05 versus Sham; #p<0.05 versus TAC.** ACC = acetyl-CoA carboxylase; AMPK = 5′ adenosine monophosphate-activated protein kinase; ANOVA = analysis of variance; DB = debanding; FA = fatty acid; GLUT = glucose transporter; MCAD = medium-chain acyl-CoA dehydrogenase; MCD = malonyl-CoA decarboxylase; PDK = pyruvate dehydrogenase kinase; PGC1α = peroxisomal proliferator activated receptor-g coactivator 1-alpha;

PPARα = peroxisome proliferator activated receptor-alpha; SEM = standard error of the mean; TAC = transverse aortic constriction.

Table 2.1. Primers for RT-PCR Reactions.

gene	Type	Sequence
Anp	Forward: Reverse: Probe:	5′-AGTGCGGTGTCCAACACAG-3′ 5′-CTTCATCGGTCTGCTCGCT-3′ 5′-FAM-TCTGATGGATTTCAAGAACCTGCTAGACCAC-TAMRA-3′
Bnp	Forward: Reverse: Probe:	5'-CTG CTG GAG CTG ATA AGA GA-3' 5'-TGC CCA AAG CAG CTT GAG AT-3' 5'-FAM-CTC AAG GCA GCA CCC TCC GGG-TAMRA-3'
Mhcb	Forward: Reverse: Probe:	5′-TCCTCCCTCAAGCTCCTAAGTAA-3′ 5′-TTTGCCTTTGCCCTTGTCTA-3′ 5′-FAM-CATCAGCICCAGCATAGTTGGCAAACA-TAMRA-3′
Mhca	Forward: Reverse: Probe:	5′-GCTTCTGCTGATACCGGTGA-3′ 5′-GTTCAGATTTTCCCGGTGGA-3′ 5′- FAM-AGCAGACACTGTTTGGAAGGATGAGCCT-TAMRA-3′
Serca2a	Forward: Reverse: Probe:	5′-AAATCTCCTTGCCTGTGATCC-3′ 5′-TGCTAACAACGCACATGCAC-3′ 5′- FAM-ACTACCTGGAACAACCCGCAATACTGGA-TAMRA-3′
Glut4	Forward: Reverse: Probe:	5′-CCCCCGATACCTCTACATCATC-3′ 5′-GCATCAGACACATCAGCCCAG-3′ 5′-FAM-CTGCCCGAAAGAGTCTAAAGCGCCT-TAMRA-3′
Pdk4	Forward: Reverse: Probe:	5′-TTCACACCTTCACCACATGC-3′ 5′-AAAGGGCGGTTTTCTTGATG-3′ 5′-FAM-CGTGGCCCTCATGGCATTCTTG-TAMRA-3′
Ppara	Forward: Reverse: Probe:	5′-ACTACGGAGTTCACGCATGTG-3′ 5′-TTGTCGTACACCAGCTTCAGC-3′ 5′-FAM-AGGCTGTAAGGGCTTCTTTCGGCG-TAMRA-3′
Mcd	Forward: Reverse: Probe	5′-CGGCACCTTCCTCATAAAGC-3′ 5′-GGGTATAGGTGACAGGCTGGA-3′ 5′-FAM-AGTGGTCAAGGAGCTGCAGAAGGAGTTT-TAMRA-3′
Mcad	Forward: Reverse: Probe:	5′-TGGCATATGGGTGTACAGGG-3′ 5′-CCAAATACTTCTTCTTCTGTTGATCA-3′ 5′-FAM-AGGCATTTGCCCCAAAGAATTTGCTTC-TAMRA-3′
Pgc1a	Forward: Reverse: Probe:	5’-AGAAGCGGGAGTCTGAAAGG-3’ 5’-CAGTTCTGTCCGCGTTGTG-3’ 5′- FAM-AGAAAGCAATTGAAGAGCGCCGTGTG-TAMRA-3′

Col1a1	Forward: Reverse: Probe:	5’- CTTCACCTACAGCACCCTTGTG-3’ 5’-TGACTGTCTTGCCCCAAGTTC-3’ 5’-FAM-CTGCACGAGTCACACC-TAMRA-3'

Table 2.2. Cardiac Morphology and Function in TAC and DB Mice.

	Sham		TAC		1-week DB		3-week DB	
HR, bpm	393.77 ± 19.78		464.30 ± 26.47		381.15 ± 14.86	#	388.30 ± 10.50	#
Morphology								
Corr. LV mass, mg	98.58 ± 5.11		149.42 ± 4.39	*	114.63 ± 5.65	#	122.45 ± 5.10	* #
IVS-diastole, mm	0.77 ± 0.02		0.98 ± 0.02	*	0.79 ± 0.02	#	0.82 ± 0.03	#
IVS-systole, mm	1.05 ± 0.04		1.12 ± 0.03	*	0.99 ± 0.04	#	1.04 ± 0.03	#
LVPW-diastole, mm	0.76 ± 0.02		0.98 ± 0.02	*	0.79 ± 0.02	#	0.82 ± 0.03	#
LVPW-systole, mm	1.06 ± 0.04		1.12 ± 0.03		1.00 ± 0.04		1.04 ± 0.03	
LVID-diastole, mm	4.25 ± 0.11		4.49 ± 0.09		4.53 ± 0.07		4.60 ± 0.11	
LVID-systole, mm	2.99 ± 0.13		3.94 ± 0.11	*	3.76 ± 0.10	*	3.55 ± 0.15	
LA diameter, mm	1.93 ± 0.08		2.87 ± 0.08	*	2.33 ± 0.10	#	2.16 ± 0.12	#
Systolic function								
EF, %	52.33 ± 4.19		21.73 ± 2.22	*	35.41 ± 3.41	* #	44.26 ± 3.22	#
FS, %	29.12 ± 1.79		10.40 ± 1.10	*	17.12 ± 1.92	*	22.06 ± 1.83	#
LVEDV, µl	81.49 ± 5.26		94.03 ± 4.86		94.23 ± 3.54		97.71 ± 5.88	
LVESV, µl	35.71 ± 3.96		70.48 ± 4.19	*	61.08 ± 3.86	*	53.75 ± 5.96	
CO, mL/min	20.01 ± 1.38		10.39 ± 1.14	*	14.09 ± 2.04		17.84 ± 1.47	#
SV, µl	46.92 ± 2.59		22.30 ± 2.25	*	34.34 ± 2.88	* #	43.81 ± 3.24	#
Diastolic function								
Mitral E/A ratio	2.19 ± 0.24		7.17 ± 1.20	*	4.27 ± 1.18		2.12 ± 0.30	#
Mitral E velocity, mm/s	652.62 ± 35.63		824.02 ± 55.79		598.76 ± 64.72	#	625.84 ± 36.41	#
Mitral A velocity, mm/s	324.60 ± 36.10		136.35 ± 26.65		232.73 ± 77.39		313.17 ± 30.29	
E/E′	28.58 ± 2.46		78.64 ± 7.89	*	35.01 ± 5.11	#	37.01 ± 2.24	#
DT, ms	21.74 ± 1.29		15.75 ± 1.05	*	18.04 ± 1.50		21.77 ± 1.24	#
IVRT, ms	18.44 ± 1.36		14.42 ± 0.82		20.26 ± 1.01	#	19.17 ± 1.16	
IVCT, ms	17.24 ± 1.34		17.98 ± 3.51		16.12 ± 1.69		14.64 ± 1.21	
ET, ms	49.46 ± 2.22		43.63 ± 6.73		45.10 ± 1.87		48.74 ± 2.05	

n = 7–9 shams; n = 4–10 TAC; n = 7–9 1-week DB; n = 7–9 3-week DB. Results are expressed as mean ± SEM. Comparisons between groups were performed using one-way ANOVA and Tukey's multiple comparisons test. ***p<0.05 versus Sham; #p<0.05 versus TAC.** A = late mitral inflow; ANOVA = analysis of variance; CO = cardiac output; DB = debanding; DT = deceleration time; E = early mitral inflow; EF = ejection fraction; ET = ejection time; E′ = tissue Doppler mitral

annulus velocity; FS = fractional shortening; HR = heart rate; IVCT = isovolumic contraction time; IVRT = isovolumic relaxation time; IVS = interventricular septum; LA = left atrial; LV = left ventricle; LVEDV = LV end-diastolic volume; LVESV = LV end-systolic volume; LVID = LV internal diameter; LVPW = LV posterior wall; MV = mitral valve; SEM = standard error of the mean; SV = stroke volume; TAC = transverse aortic constriction.

Table 2.3. Physical Characteristics and *Ex Vivo* Function in TAC and DB Mice.

	Sham	TAC	1-week DB	3-week DB
Body weight, g	27.10 ± 0.85	23.64 ± 0.47	24.61 ± 0.57	25.65 ± 0.69
Wet lung weight, mg	147.03 ± 4.85	317.50 ± 58.47 *	217.97 ± 9.33	173.48 ± 8.48
Dry heart weight, mg	37.91 ± 1.20	55.91 ± 5.06 *	37.62 ± 1.97 #	39.72 ± 2.61 #
Atria weight, mg	2.85 ± 0.21	6.94 ± 1.32 *	4.30 ± 0.45	2.64 ± 0.21 #
Ex vivo function				
HR, bpm	263.40 ± 11.80	216.71 ± 11.80	268.92 ± 12.00	270.36 ± 28.41
PSP	69.10 ± 0.91	59.00 ± 2.02 *	68.04 ± 1.53 * #	71.24 ± 1.66 * #
HR x PSP (x 10-3)	18.22 ± 0.90	12.81 ± 0.85 *	18.26 ± 0.70 * #	19.18 ± 1.81 * #
DP	19.07 ± 0.50	11.57 ± 0.82 *	14.44 ± 0.83	19.92 ± 1.72
HR x DP (x 10-3)	5.01 ± 0.24	2.52 ± 0.23	3.89 ± 0.31	5.29 ± 0.47
CO, ml/min	7.77 ± 0.70	4.58 ± 0.96	7.42 ± 0.77	9.49 ± 1.40 #
Aortic Flow, ml/min	5.42 ± 0.81	2.42 ± 0.86	5.01 ± 0.75	7.26 ± 1.15 #
Coronary Flow, ml/min	2.35 ± 0.20	2.16 ± 0.20	2.42 ± 0.05	2.23 ± 0.31
Cardiac work, ml*mmHg/min	5.37 ± 0.47	2.73 ± 0.66	5.10 ± 0.60	8.79 ± 1.17 * #

n = 5–9 shams; n = 5–7 TAC; n = 5–6 1-week DB; n = 4–5 3-week DB. Results are expressed as mean ± SEM. Comparisons between groups were performed using one-way ANOVA and Tukey's multiple comparisons test. ***p<0.05 versus Sham; #p<0.05 versus TAC.** ANOVA = analysis of variance; CO = cardiac output; DB = debanding; DP = developed pressure; HR = heart rate; PSP = peak systolic pressure; SEM = standard error of the mean; TAC = transverse aortic constriction.

2.7 References

1. Dorn GW, 2nd, Force T. Protein kinase cascades in the regulation of cardiac hypertrophy. J Clin Invest 2005;115:527-37.
2. Naylor LH, George K, O'Driscoll G, Green DJ. The athlete's heart: a contemporary appraisal of the 'Morganroth hypothesis'. Sports Med 2008;38:69-90.
3. Lorell BH. Transition from hypertrophy to failure. Circulation 1997;96:3824-7.
4. Frey N, Olson EN. Cardiac hypertrophy: the good, the bad, and the ugly. Annu Rev Physiol 2003;65:45-79.
5. Lehman JJ, Kelly DP. Gene regulatory mechanisms governing energy metabolism during cardiac hypertrophic growth. Heart Fail Rev 2002;7:175-85.
6. Allard MF. Energy substrate metabolism in cardiac hypertrophy. Curr Hypertens Rep 2004;6:430-5.
7. Nascimben L, Ingwall JS, Lorell BH et al. Mechanisms for increased glycolysis in the hypertrophied rat heart. Hypertension 2004;44:662-7.
8. Kolwicz SC, Jr., Tian R. Glucose metabolism and cardiac hypertrophy. Cardiovasc Res 2011;90:194-201.
9. Neubauer S, Horn M, Cramer M et al. Myocardial Phosphocreatine-to-ATP Ratio Is a Predictor of Mortality in Patients With Dilated Cardiomyopathy. Circulation 1997;96:2190-2196.
10. Taegtmeyer H. Genetics of energetics: transcriptional responses in cardiac metabolism. Ann Biomed Eng 2000;28:871-6.

11. Sharov VG, Todor AV, Silverman N, Goldstein S, Sabbah HN. Abnormal mitochondrial respiration in failed human myocardium. J Mol Cell Cardiol 2000;32:2361-7.

12. Paolisso G, Gambardella A, Galzerano D et al. Total-body and myocardial substrate oxidation in congestive heart failure. Metabolism 1994;43:174-9.

13. Sung MM, Das SK, Levasseur J et al. Resveratrol treatment of mice with pressure-overload-induced heart failure improves diastolic function and cardiac energy metabolism. Circ Heart Fail 2015;8:128-37.

14. Sung MM, Koonen DP, Soltys CL, Jacobs RL, Febbraio M, Dyck JR. Increased CD36 expression in middle-aged mice contributes to obesity-related cardiac hypertrophy in the absence of cardiac dysfunction. J Mol Med (Berl) 2011;89:459-69.

15. Koonen DP, Sung MM, Kao CK et al. Alterations in skeletal muscle fatty acid handling predisposes middle-aged mice to diet-induced insulin resistance. Diabetes 2010;59:1366-75.

16. Kienesberger PC, Pulinilkunnil T, Sung MM et al. Myocardial ATGL overexpression decreases the reliance on fatty acid oxidation and protects against pressure overload-induced cardiac dysfunction. Mol Cell Biol 2012;32:740-50.

17. Zhong J, Basu R, Guo D et al. Angiotensin-converting enzyme 2 suppresses pathological hypertrophy, myocardial fibrosis, and cardiac dysfunction. Circulation 2010;122:717-28, 18 p following 728.

18. Conraads VM, Van Craenenbroeck EM, De Maeyer C, Van Berendoncks AM, Beckers PJ, Vrints CJ. Unraveling new mechanisms of exercise intolerance in chronic heart failure: role of exercise training. Heart Fail Rev 2013;18:65-77.

19. Kiss E, Ball NA, Kranias EG, Walsh RA. Differential changes in cardiac phospholamban and sarcoplasmic reticular Ca(2+)-ATPase protein levels. Effects on Ca2+ transport and mechanics in compensated pressure-overload hypertrophy and congestive heart failure. Circ Res 1995;77:759-64.

20. Lowes BD, Minobe W, Abraham WT et al. Changes in gene expression in the intact human heart. Downregulation of alpha-myosin heavy chain in hypertrophied, failing ventricular myocardium. J Clin Invest 1997;100:2315-24.

21. Arai M, Matsui H, Periasamy M. Sarcoplasmic reticulum gene expression in cardiac hypertrophy and heart failure. Circ Res 1994;74:555-64.

22. Kehat I, Molkentin JD. Molecular pathways underlying cardiac remodeling during pathophysiological stimulation. Circulation 2010;122:2727-35.

23. Li XM, Ma YT, Yang YN et al. Downregulation of survival signalling pathways and increased apoptosis in the transition of pressure overload-induced cardiac hypertrophy to heart failure. Clin Exp Pharmacol Physiol 2009;36:1054-61.

24. Xu X, Lu Z, Fassett J et al. Metformin protects against systolic overload-induced heart failure independent of AMP-activated protein kinase alpha2. Hypertension 2014;63:723-8.

25. Shende P, Plaisance I, Morandi C et al. Cardiac raptor ablation impairs adaptive hypertrophy, alters metabolic gene expression, and causes heart failure in mice. Circulation 2011;123:1073-82.

26. Razeghi P, Young ME, Alcorn JL, Moravec CS, Frazier OH, Taegtmeyer H. Metabolic gene expression in fetal and failing human heart. Circulation 2001;104:2923-31.

27. Depre C, Shipley GL, Chen W et al. Unloaded heart in vivo replicates fetal gene expression of cardiac hypertrophy. Nat Med 1998;4:1269-75.

28. Arany Z, Novikov M, Chin S, Ma Y, Rosenzweig A, Spiegelman BM. Transverse aortic constriction leads to accelerated heart failure in mice lacking PPAR-gamma coactivator 1alpha. Proc Natl Acad Sci U S A 2006;103:10086-91.

29. Sack MN, Rader TA, Park S, Bastin J, McCune SA, Kelly DP. Fatty acid oxidation enzyme gene expression is downregulated in the failing heart. Circulation 1996;94:2837-42.

30. Zhang L, Jaswal JS, Ussher JR et al. Cardiac insulin-resistance and decreased mitochondrial energy production precede the development of systolic heart failure after pressure-overload hypertrophy. Circ Heart Fail 2013;6:1039-48.

31. Zhabyeyev P, Gandhi M, Mori J et al. Pressure-overload-induced heart failure induces a selective reduction in glucose oxidation at physiological afterload. Cardiovasc Res 2013;97:676-85.

32. Nagendran J, Waller TJ, Dyck JR. AMPK signalling and the control of substrate use in the heart. Mol Cell Endocrinol 2013;366:180-93.

33. Kim TT, Dyck JR. Is AMPK the savior of the failing heart? Trends Endocrinol Metab 2015;26:40-8.

34. Tian R, Musi N, D'Agostino J, Hirshman MF, Goodyear LJ. Increased adenosine monophosphate-activated protein kinase activity in rat hearts with pressure-overload hypertrophy. Circulation 2001;104:1664-9.

35. Andersen NM, Stansfield WE, Tang RH, Rojas M, Patterson C, Selzman CH. Recovery from decompensated heart failure is associated with a distinct, phase-dependent gene expression profile. J Surg Res 2012;178:72-80.

36. Zhang X, Javan H, Li L et al. A modified murine model for the study of reverse cardiac remodelling. Exp Clin Cardiol 2013;18:e115-7.

37. Bjornstad JL, Skrbic B, Sjaastad I, Bjornstad S, Christensen G, Tonnessen T. A mouse model of reverse cardiac remodelling following banding-debanding of the ascending aorta. Acta Physiol (Oxf) 2012;205:92-102.

38. Yang DK, Choi BY, Lee YH et al. Gene profiling during regression of pressure overload-induced cardiac hypertrophy. Physiol Genomics 2007;30:1-7.

39. Stansfield WE, Charles PC, Tang RH et al. Regression of pressure-induced left ventricular hypertrophy is characterized by a distinct gene expression profile. J Thorac Cardiovasc Surg 2009;137:232-8, 238e1-8.

40. Gao XM, Kiriazis H, Moore XL et al. Regression of pressure overload-induced left ventricular hypertrophy in mice. Am J Physiol Heart Circ Physiol 2005;288:H2702-7.

41. Chaanine AH, Hajjar RJ. AKT signalling in the failing heart. Eur J Heart Fail 2011;13:825-9.

42. Lai L, Leone TC, Keller MP et al. Energy metabolic reprogramming in the hypertrophied and early stage failing heart: a multisystems approach. Circ Heart Fail 2014;7:1022-31.

43. Razeghi P, Young ME, Ying J et al. Downregulation of metabolic gene expression in failing human heart before and after mechanical unloading. Cardiology 2002;97:203-9.

44. Vogel C, Marcotte EM. Insights into the regulation of protein abundance from proteomic and transcriptomic analyses. Nat Rev Genet 2012;13:227-32.

45. Guo Y, Xiao P, Lei S et al. How is mRNA expression predictive for protein expression? A correlation study on human circulating monocytes. Acta Biochim Biophys Sin (Shanghai) 2008;40:426-36.

46. de Sousa Abreu R, Penalva LO, Marcotte EM, Vogel C. Global signatures of protein and mRNA expression levels. Mol Biosyst 2009;5:1512-26.

47. Riehle C, Wende AR, Zaha VG et al. PGC-1beta deficiency accelerates the transition to heart failure in pressure overload hypertrophy. Circ Res 2011;109:783-93.

48. Leong HN, Ang B, Earnest A, Teoh C, Xu W, Leo YS. Investigational use of ribavirin in the treatment of severe acute respiratory syndrome, Singapore, 2003. Trop Med Int Health 2004;9:923-7.

49. Lei B, Lionetti V, Young ME et al. Paradoxical downregulation of the glucose oxidation pathway despite enhanced flux in severe heart failure. J Mol Cell Cardiol 2004;36:567-76.

50. Spindler M, Saupe KW, Christe ME et al. Diastolic dysfunction and altered energetics in the alphaMHC403/+ mouse model of familial hypertrophic cardiomyopathy. J Clin Invest 1998;101:1775-83.

51. Tian R, Nascimben L, Ingwall JS, Lorell BH. Failure to maintain a low ADP concentration impairs diastolic function in hypertrophied rat hearts. Circulation 1997;96:1313-9.

52. Qanud K, Mamdani M, Pepe M et al. Reverse changes in cardiac substrate oxidation in dogs recovering from heart failure. Am J Physiol Heart Circ Physiol 2008;295:H2098-105.

Chapter Three

Empagliflozin Prevents Worsening of Cardiac Function in an Experimental Model of Pressure Overload-Induced Heart Failure

Contribution:

Nikole J Byrne: conception and design of the experimental paradigm, organizing all experiments, analysis of echocardiography images, interpretation of resulting data and manuscript writing
Jody L Levasseur: conception and design of the experimental paradigm, surgeries
Donna Beker: echocardiography
Grant Masson: isolated heart perfusions
Dyck JRB: conception and design of research, intellectual and editorial contribution

Chapter 3 has been published as:

Byrne NJ, Parajuli N, Levasseur JL, Boisvenue J, Beker DL, Masson G, Fedak PWM, Verma S and Dyck JRB. Empagliflozin Prevents Worsening of Cardiac Function in an Experimental Model of Pressure Overload-Induced Heart Failure. *JACC: Basic to Translational Science*. 2017;2:347-354.

3.1 Introduction

Recent findings from the EMPA-REG OUTCOME trial demonstrated that the SGLT2 inhibitor empagliflozin markedly reduced CV death and HF hospitalization in subjects with type 2 diabetes (1). Despite the profound and precocious efficacy, the physiological and biomolecular mechanisms responsible for this ~40% reduction in CV mortality and HF are not known. Interestingly, intrinsic changes to the cardiac tissue itself have largely been ruled out because SGLT2 receptors are not known to be present in the heart (2). Based in part on this fact, the prevailing theories explaining how empagliflozin may exert its beneficial effects in HF involve either improved hemodynamics through osmotic diuresis and natriuresis or by promoting enhanced ketone oxidation by the heart through increased ketone concentrations in the blood (3). However, these theories have not been fully investigated. In addition, because empagliflozin is used to treat diabetes, it is not known whether the drug is capable of eliciting equally beneficial effects on HF outcomes in nondiabetic patients.

3.2 Methods

3.2.1 Experimental animals

All protocols involving mice were approved by the University of Alberta Institutional Animal Care and Use Committee and conform to the Guide for the Care and Use of Laboratory Animals published by the U.S. National Institutes of Health (8th edition, revised 2011). The University of

Alberta adheres to the principles for biomedical research involving animals developed by the Council for International Organizations of Medical Sciences and complies with the Canadian Council on Animal Care guidelines. Eight-week old male C57Bl/6 mice underwent TAC surgery to induce pressure overload. At 2 to 3 weeks post-surgery, most of the mice transitioned into HFrEF. Mice considered to be in HF (EF <45%) were randomly assigned to receive either vehicle (0.5% hydroxyethyl cellulose [Natrosol]) (Sigma-Aldrich, Ontario, Canada) or empagliflozin (MedChemExpress, Princeton, New Jersey) (10 mg/kg/day) for 2 weeks by oral gavage.

3.2.2 TAC surgery[b]

TAC surgery was performed as previously described (4,5). Briefly, male eight-week old mice were anesthetized by intraperitoneal injection of a cocktail of ketamine (100 mg/kg) and xylazine (10 mg/kg), intubated, and connected to a mouse ventilator (MiniVent; Harvard Apparatus, Holliston, Massachusetts). Following midline sternotomy, a double-blunted 27-gauge needle was tied encircling the aorta between the innominate and left common carotid arteries using a 6/0 silk suture. The needle was then removed, and chest and skin were sutured and closed.

3.2.3 Echocardiography

Mice were anesthetized with 1.0% to 1.5% isoflurane with 1 to 1.5 l/min 100% oxygen, and in vivo cardiac function was assessed by transthoracic echocardiography using a Vevo 3100 high-

[b] See Appendix B for additional information regarding TAC surgery.

resolution imaging system equipped with a 30-MHz transducer (model RMV-707B, VisualSonics, Toronto, Ontario, Canada), as previously described (4,5). Pressure overload was confirmed in all mice at 2 weeks after TAC by measuring trans-stenotic gradient by pulsed-wave Doppler flow. Full systolic and diastolic parameters were measured prior to and following 2-week oral gavage of vehicle or empagliflozin.

3.2.4 Histology

Masson's trichrome and hematoxylin-eosin stains of paraffin-embedded left ventricular heart sections taken mid-papillary were visualized using microscopy (DMLA microscope, Leica Microsystems, Wetzlar, Germany; equipped with a Retiga 1300i FAST 1394 charge-coupled device camera, OImaging, Surrey, British Columbia, Canada), as described previously (6). Three representative images were taken of each sample.

3.2.5 *Ex vivo* heart perfusions

Hearts were perfused in the working heart mode at 11.5 mm Hg preload and 50 mm Hg afterload with Krebs-Henseleit buffer containing 0.8 mmol/l oleate prebound to 3% delipidated BSA, 5 mmol/l glucose, and 50 μU/ml insulin, as described previously (4,7).

3.2.6 Statistical analysis

Results are expressed as mean ± SEM. Statistical analyses were performed using Prism software (GraphPad Corp., La Jolla, California). Comparisons between groups were performed by Wilcoxon signed-rank test, Mann-Whitney *U* test, or repeated measures two-way ANOVA, followed by Sidak multiple comparisons test where appropriate. Wilcoxon signed rank test was used to evaluate pre- versus post-gavage data **(Figure 3.1)**. A p value of <0.05 was considered significant.

3.3 Results

3.3.1 Empagliflozin treatment prevents worsening of cardiac function in mice with heart failure

In order to help address the effects of empagliflozin in HF in the absence of diabetes, we subjected healthy C57Bl/6 mice to TAC surgery to induce HF as described previously (7). Following TAC surgery, mice were subjected to pulsed wave Doppler M-mode echocardiography. Mice demonstrating an EF of <45% were subsequently randomized and treated with either vehicle (0.5% hydroxyethyl cellulose) or empagliflozin (10 mg/kg) by daily oral gavage for a period of 2 weeks **(Figure 3.1A)**. As expected, empagliflozin significantly increased glucose concentrations in the urine during the treatment period **(Figure 3.1B)**. In addition, whereas vehicle-treated mice HF continued to display a significant drop in EF over the 2-week treatment period **(Figure 3.1C,E,F)**, empagliflozin-treated mice maintained stable cardiac function **(Figure 3.1D-F)**. In order to account for dependent data, a repeated measures two-way ANOVA was used to show that a statistically significant interaction existed between the effect of time and treatment on EF

(p=0.011). There were no statistically significant differences in treatment (p=0.230), but there were statistically significant differences between baseline and post-gavage times (p=0.033). Interestingly, empagliflozin prevented the time-dependent decline in systolic function without significantly affecting body weight (23.79 ± 0.45 g vs. 24.41 ± 0.54 g for vehicle and empagliflozin-treated mice with HF, respectively), or without changing measurements of corrected LV mass **(Figure 3.2A)** or wet ventricle weight normalized to tibia length (VW/TL) **(Figure 3.2B)**. Furthermore, other indices of structural remodeling, such as LV end-diastolic volume (LVEDV) **(Figure 3.2C)**, LVID at end-diastole **(Figure 3.2D)**, LVPW at end-diastole **(Figure 3.2E)**, and LA diameter **(Figure 3.2F)**, were also similar between groups.

3.3.2 Cardiac structural remodeling, diastolic function, cardiac fibrosis, and macrophage infiltration showed no differences in mice with HF treated with empagliflozin

In addition to development of cardiac hypertrophy, we also measured indices of diastolic function such as LV filling pressure (E/E′ ratio) (**Figure 3.3A**) and the mitral E/A ratio **(Figure 3.3B)**, which were also not significantly changed between groups. Furthermore, because excessive myocardial fibrosis is a major result of pressure overload-induced HF (8,9), we used Masson trichrome staining to investigate whether treatment with empagliflozin reduced cardiac collagen content. Consistent with our observation that empagliflozin did not reduce myocardial stiffness, there was no obvious reduction in cardiac fibrosis compared to vehicle-treated mice with HF **(Figure 3.3C)**. Furthermore, we also investigated the presence of macrophage infiltration in hearts from vehicle- and empagliflozin-treated mice with HF to assess the effect of empagliflozin on the inflammatory response to pressure overload. Interestingly, there was no obvious presence

of macrophage infiltration in either group **(Figure 3.3D)**, suggesting that the inflammatory response to pressure overload had likely resolved prior to when the mice were euthanized, and hearts used for histology.

3.3.3 Improved *in vivo* cardiac function in empagliflozin-treated mice with heart failure is preserved *ex vivo*

To ascertain whether or not the protective effects observed in the empagliflozin-treated mice with HF were related to extrinsic factors that controlled cardiac function (such as hemodynamics or ketone oxidation), we subjected vehicle- and empagliflozin-treated mice to *ex vivo* functional assessment using an isolated perfused working heart system (4,7). In the presence of matching pre-load and after-load pressures, identical concentrations of insulin, fatty acids, and glucose, as well as in the absence of ketones (4,7), *ex vivo* perfused hearts still demonstrated significantly improved *ex vivo* cardiac output **(Figure 3.4A)** and cardiac work **(Figure 3.4B)** without any differences in HR **(Figure 3.4C)**. This ability of empagliflozin to provide a sustained benefit in isolated hearts suggests that the empagliflozin-mediated prevention of worsening cardiac function in mice with HF may be due to an intrinsic and sustained cardiac effect and is not based on potential hemodynamic changes or a potentially confounding blood-based environmental milieu associated with HF and other factors related to empagliflozin treatment.

3.4 Discussion

Together, our data show for the first time that empagliflozin treatment of nondiabetic mice with HFrEF blunts the progressive decline in cardiac function both *in vivo* and *ex vivo*. Interestingly, although SGLT1 mRNA is abundantly expressed in the human heart as well as in other tissues, SGLT2, the selective target of empagliflozin, has been identified in skeletal muscle and kidney but not in heart (10,11). Thus, our findings introduce a completely novel concept that empagliflozin can directly influence cardiac function despite no definitive evidence of molecular targets in cardiac tissue.

Based on the results of EMPA-REG OUTCOMES and other studies that have primarily shown a lower incidence of hospitalization for HF and death in patients with type 2 diabetes treated with empagliflozin (1) and other SGLT2 inhibitors (12-14) several theories have been put forward to explain the beneficial effects of SGLT2 inhibition. Theories include natriuresis/diuresis, improved myocardial energetics through increases in ketone oxidation (15,16), and more recently, through a direct effect that inhibits the NHE1 in cardiomyocytes (17). Interestingly, numerous studies propose that empagliflozin may reduce cardiometabolic risk in diabetic patients by significantly reducing body weight and adiposity (18,19); however, no changes in body weight were found in our study. Although it has also been suggested that the glucose-lowering effects of empagliflozin may reduce the cardiac effects of glucotoxicity (20,21), our data suggest that empagliflozin has cardioprotective benefits even in the absence of elevated blood glucose. Furthermore, despite previous findings that empagliflozin mildly reduces cardiac hypertrophy, improves diastolic function, and reduces collagen deposition in female mice with diabetes and obesity (22), these improvements were not apparent in our study using a mouse model of HF without impaired glucose handling.

3.4.1 Study limitations

Although it was not measured in the current study, the effect of empagliflozin on the abnormal ventricular electrophysiological profile exists in cardiac hypertrophy and failure (23-25) may offer insight into the mechanism of action and would therefore be an area to explore in future studies. Furthermore, although we observed increased cardiac function both *in vivo* and *ex vivo*, another limitation of our study is that we do not know whether empagliflozin improves cardiomyocyte contractility, which could provide additional insight into potential mechanism of action.

3.5 Conclusion

Although there are no data for biomarkers in patients with HF treated with SGLT2 inhibitors, preliminary data suggest that SGLT2 inhibition can reduce ANP and BNP peptide in zebrafish models of HF (26) and improve measurements of diastolic function in humans with diabetes and clinical CVD (27). Based on these results, clinical trials have been initiated to investigate the role of SGLT2 inhibitors in the treatment of patients with established HF where diabetes is not an inclusion criterion per se [*i.e.* EMPEROR-Reduced (Empagliflozin Outcome Trial in Patients With Chronic HF With Reduced Ejection Fraction; NCT03057977), EMPEROR-Preserved (EMPagliflozin outcomE tRial in Patients with chrOnic heaRt Failure With Preserved Ejection Fraction; NCT03057951), and Dapa-HF (Study to Evaluate the Effect of Dapagliflozin on the Incidence of Worsening Heart Failure or Cardiovascular Death in Patients with Chronic Heart

Failure; NCT03036124)]. However, the scientific community has been waiting for translational and mechanistic studies to elucidate if this strategy is associated with a change in LV mass, remodeling, and cardiac function. Although human cardiac magnetic resonance studies are also currently underway [EMPA-HEART (Effects of Empagliflozin on Cardiac Structure in Patients with Type 2 Diabetes; NCT02998970)], these studies also are being carried out in subjects with diabetes and previous MI. Therefore, the novelty of our work underscores a potential application of this therapy in established HF without diabetes.

3.6 Figures

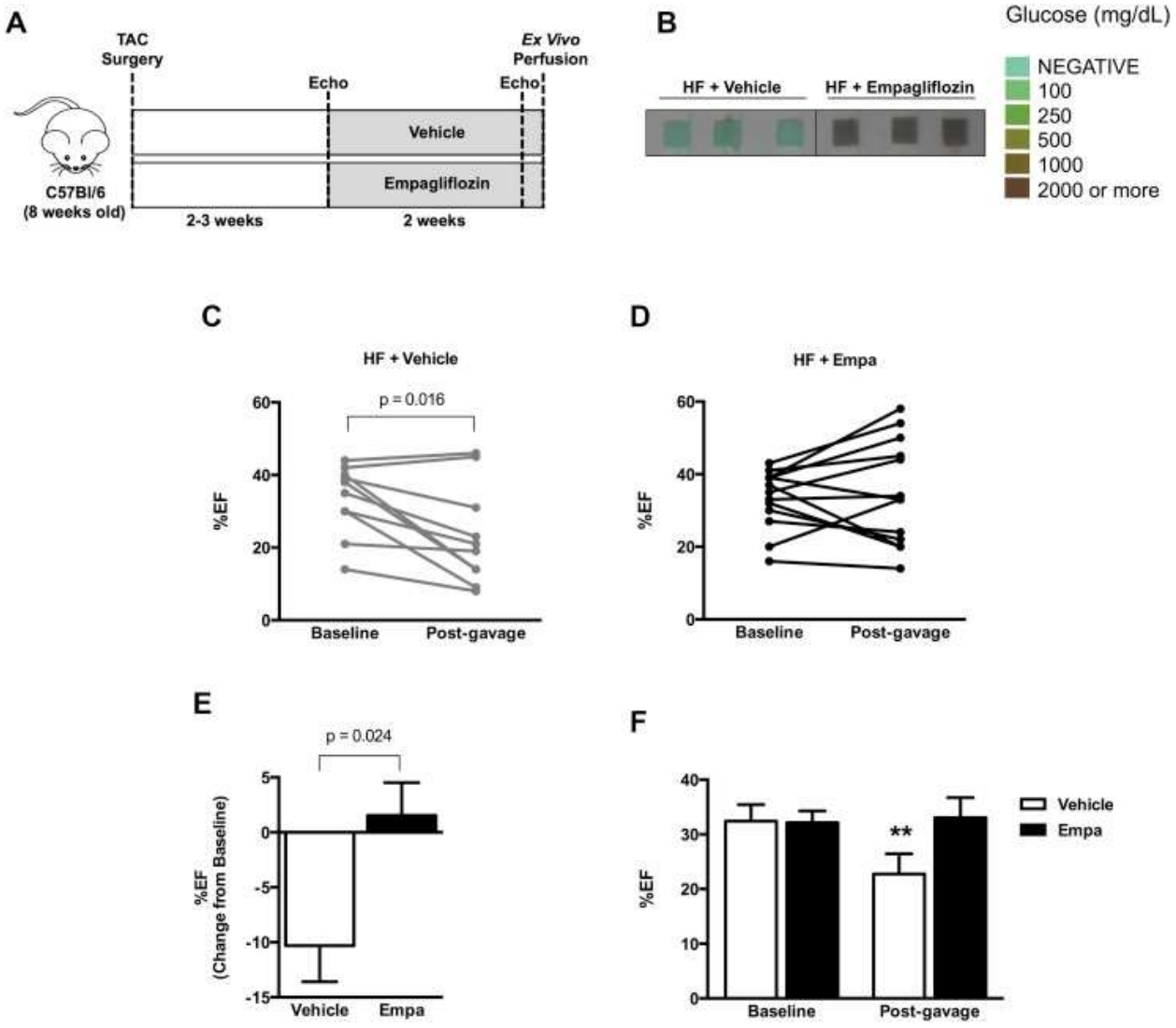

Figure 3.1. Empagliflozin Treatment Prevents Worsening of Cardiac Function in Mice with Heart Failure. Experimental design of empa treatment in mice in which HF was induced using TAC **(A).** Urine glucose levels are shown for vehicle-treated and Empa-treated HF mice **(B)** (n = 3). EF of vehicle-treated **(C)** and Empa-treated **(D)** mice with HF and expressed as change from baseline **(E)** and pre- and post- gavage **(F)** based on echocardiographic assessment (n = 10–13). Results are expressed as mean ± SEM. Comparisons between groups were performed using Wilcoxon signed rank test for pre- versus post-gavage data **(C, D)**, Mann-Whitney U test **(E)** and repeated measures two-way ANOVA followed by Sidak multiple comparisons tests **(F)**. ****p<0.01**

versus baseline. ANOVA = analysis of variance; ECHO = echocardiography; EF = ejection fraction; EMPA = empagliflozin; HF = heart failure; SEM = standard error of the mean; TAC = transverse aortic constriction.

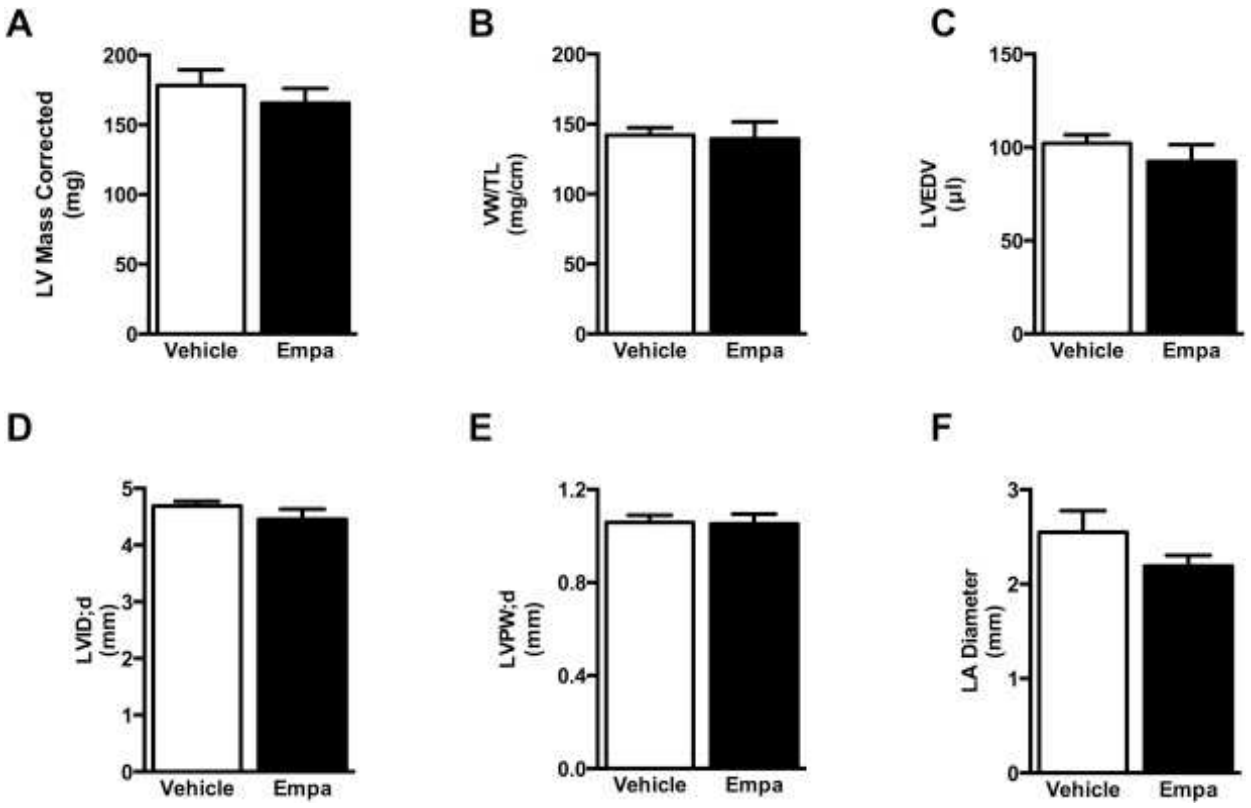

Figure 3.2. Cardiac Structural Remodeling Showed No Differences in Mice with Heart Failure Treated with Empagliflozin. Hearts from vehicle- and empa-treated mice with HF displayed no significant changes in corrected LV mass **(A)**, wet VW-to-TL ratio **(B)**, LV end-diastolic volume **(C)**, LVID at end-diastole **(D)**, LVPW at end-diastole **(E)**, and LA diameter **(F)** (n = 6–10). Results are expressed as mean ± SEM. Comparisons between groups were performed using Mann-Whitney U test. ECHO = echocardiography; EF = ejection fraction; EMPA = empagliflozin; HF = heart failure; LA = left atrial; LV = left ventricular; LVEDV = LV end-diastolic volume; LVID = LV internal diameter; LVPW = LV posterior wall; SEM = standard error of the mean; VW/TL = ventricle weight normalized to tibia length.

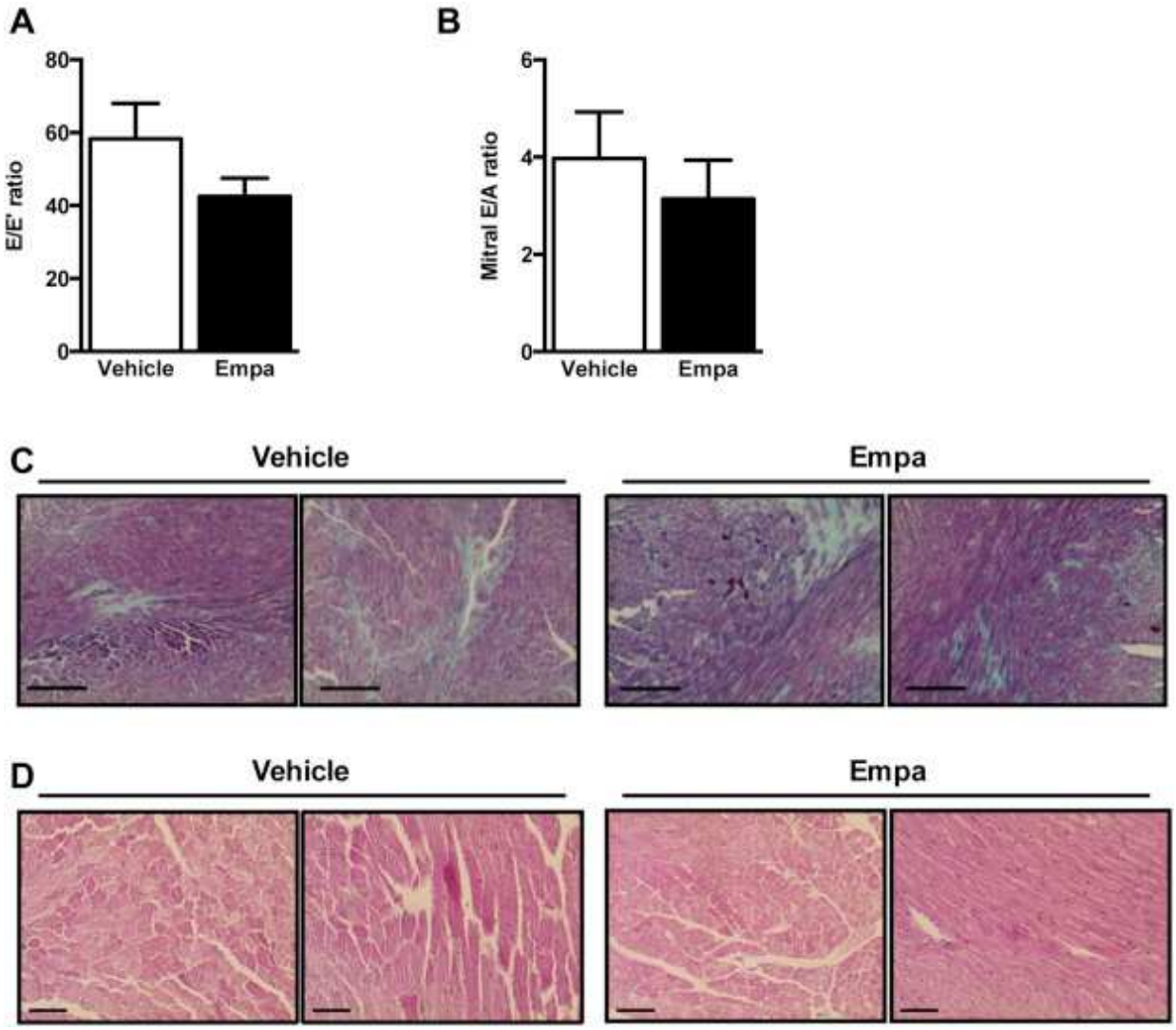

Figure 3.3. Diastolic Function, Cardiac Fibrosis, and Macrophage Infiltration Showed No Differences in Mice with Heart Failure Treated with Empagliflozin. Hearts from vehicle- and Empa-treated mice with HF displayed no significant changes in indices of diastolic function such as the left ventricular filling ratio E/E′ **(A)** and mitral E/A ratio **(B)** (n = 6–10). Representative images of left ventricular heart sections taken mid-papillary and stained with Masson's trichrome at x 20 magnification **(C)** and hematoxylin-eosin stain **(D)** (n = 5–7). Scale bars = 100 μM. Results are expressed as mean ± SEM. Comparisons between groups were performed using Mann-Whitney

U test. A = late mitral inflow; E = early mitral inflow; EMPA = empagliflozin; E′ = tissue Doppler mitral annulus velocity; HF = heart failure; SEM = standard error of the mean.

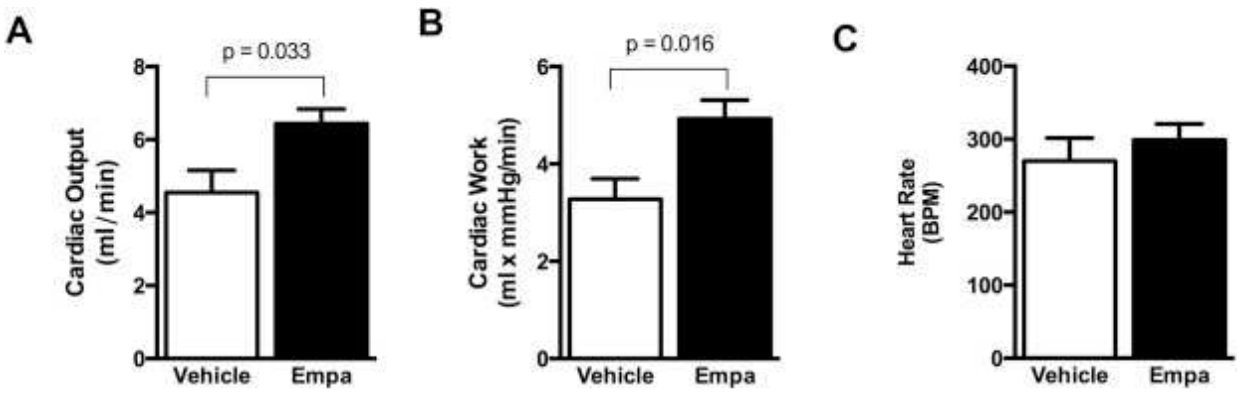

Figure 3.4. Improved *In Vivo* Cardiac Function in Empagliflozin-Treated Mice with Heart Failure Is Preserved *Ex Vivo*. Hearts from vehicle- and empa-treated mice with HF were perfused *ex vivo* to measure cardiac function. CO **(A)**, cardiac work **(B)**, and HR **(C)** were measured using *ex vivo* perfused working hearts (n = 9–10). Results are expressed as mean ± SEM. CO = Cardiac output; EMPA = empagliflozin; HF = heart failure; HR = heart rate; SEM = standard error of the mean.

3.7 References

1. Zinman B, Wanner C, Lachin JM et al. Empagliflozin, Cardiovascular Outcomes, and Mortality in Type 2 Diabetes. N Engl J Med 2015;373:2117-28.
2. von Lewinski D, Rainer PP, Gasser R et al. Glucose-transporter-mediated positive inotropic effects in human myocardium of diabetic and nondiabetic patients. Metabolism 2010;59:1020-8.
3. Sattar N, McLaren J, Kristensen SL, Preiss D, McMurray JJ. SGLT2 Inhibition and cardiovascular events: why did EMPA-REG Outcomes surprise and what were the likely mechanisms? Diabetologia 2016;59:1333-1339.
4. Byrne NJ, Levasseur J, Sung MM et al. Normalization of cardiac substrate utilization and left ventricular hypertrophy precede functional recovery in heart failure regression. Cardiovasc Res 2016;110:249-57.
5. Sung MM, Byrne NJ, Robertson IM et al. Resveratrol improves exercise performance and skeletal muscle oxidative capacity in heart failure. Am J Physiol Heart Circ Physiol 2017;312:H842-H853.
6. Kienesberger PC, Pulinilkunnil T, Sung MM et al. Myocardial ATGL overexpression decreases the reliance on fatty acid oxidation and protects against pressure overload-induced cardiac dysfunction. Mol Cell Biol 2012;32:740-50.
7. Sung MM, Das SK, Levasseur J et al. Resveratrol treatment of mice with pressure-overload-induced heart failure improves diastolic function and cardiac energy metabolism. Circ Heart Fail 2015;8:128-37.

8. Segura AM, Frazier OH, Buja LM. Fibrosis and heart failure. Heart failure reviews 2014;19:173-85.

9. Creemers EE, Pinto YM. Molecular mechanisms that control interstitial fibrosis in the pressure-overloaded heart. Cardiovasc Res 2011;89:265-72.

10. Wright EM, Loo DD, Hirayama BA. Biology of human sodium glucose transporters. Physiol Rev 2011;91:733-94.

11. Zhou L, Cryan EV, D'Andrea MR, Belkowski S, Conway BR, Demarest KT. Human cardiomyocytes express high level of Na+/glucose cotransporter 1 (SGLT1). J Cell Biochem 2003;90:339-46.

12. Kosiborod M, Cavender MA, Fu AZ et al. Lower Risk of Heart Failure and Death in Patients Initiated on Sodium-Glucose Cotransporter-2 Inhibitors Versus Other Glucose-Lowering Drugs: The CVD-REAL Study (Comparative Effectiveness of Cardiovascular Outcomes in New Users of Sodium-Glucose Cotransporter-2 Inhibitors). Circulation 2017;136:249-259.

13. Neal B, Perkovic V, Matthews DR. Canagliflozin and Cardiovascular and Renal Events in Type 2 Diabetes. N Engl J Med 2017;377:2099.

14. Wiviott SD, Raz I, Bonaca MP et al. Dapagliflozin and Cardiovascular Outcomes in Type 2 Diabetes. N Engl J Med 2019;380:347-357.

15. Lopaschuk GD, Verma S. Empagliflozin's Fuel Hypothesis: Not so Soon. Cell Metab 2016;24:200-2.

16. Ferrannini E, Mark M, Mayoux E. CV Protection in the EMPA-REG OUTCOME Trial: A "Thrifty Substrate" Hypothesis. Diabetes Care 2016;39:1108-14.

17. Baartscheer A, Schumacher CA, Wust RC et al. Empagliflozin decreases myocardial cytoplasmic Na(+) through inhibition of the cardiac Na(+)/H(+) exchanger in rats and rabbits. Diabetologia 2017;60:568-573.

18. Yanai H, Hakoshima M, Adachi H et al. Effects of Six Kinds of Sodium-Glucose Cotransporter 2 Inhibitors on Metabolic Parameters, and Summarized Effect and Its Correlations With Baseline Data. J Clin Med Res 2017;9:605-612.

19. Neeland IJ, McGuire DK, Chilton R et al. Empagliflozin reduces body weight and indices of adipose distribution in patients with type 2 diabetes mellitus. Diab Vasc Dis Res 2016;13:119-26.

20. Ferrannini E, Muscelli E, Frascerra S et al. Metabolic response to sodium-glucose cotransporter 2 inhibition in type 2 diabetic patients. J Clin Invest 2014;124:499-508.

21. Abdul-Ghani M, Al Jobori H, Daniele G et al. Inhibition of Renal Sodium-Glucose Cotransport With Empagliflozin Lowers Fasting Plasma Glucose and Improves beta-Cell Function in Subjects With Impaired Fasting Glucose. Diabetes 2017;66:2495-2502.

22. Habibi J, Aroor AR, Sowers JR et al. Sodium glucose transporter 2 (SGLT2) inhibition with empagliflozin improves cardiac diastolic function in a female rodent model of diabetes. Cardiovasc Diabetol 2017;16:9.

23. Boulaksil M, Winckels SK, Engelen MA et al. Heterogeneous Connexin43 distribution in heart failure is associated with dispersed conduction and enhanced susceptibility to ventricular arrhythmias. Eur J Heart Fail 2010;12:913-21.

24. Boulaksil M, Noorman M, Engelen MA et al. Longitudinal arrhythmogenic remodelling in a mouse model of longstanding pressure overload. Neth Heart J 2010;18:509-15.

25. Anastasiou-Nana MI, Nanas JN, Karagounis LA et al. Relation of dispersion of QRS and QT in patients with advanced congestive heart failure to cardiac and sudden death mortality. Am J Cardiol 2000;85:1212-7.

26. Shi X, Verma S, Yun J et al. Effect of empagliflozin on cardiac biomarkers in a zebrafish model of heart failure: clues to the EMPA-REG OUTCOME trial? Mol Cell Biochem 2017;433:97-102.

27. Verma S, Garg A, Yan AT et al. Effect of Empagliflozin on Left Ventricular Mass and Diastolic Function in Individuals With Diabetes: An Important Clue to the EMPA-REG OUTCOME Trial? Diabetes Care 2016;39:e212-e213.

Chapter Four

Empagliflozin Improves Cardiac Function in Heart Failure by Suppressing Activation of the NLRP3 Inflammasome

Contribution:

Nikole J Byrne: conception and design of the experimental paradigm, organizing all experiments, *in vivo* mouse work (urine collection, blood glucose and ketone measurements and indirect calorimetry), echocardiography analysis, interpretation of resulting data and manuscript writing
Jody L Levasseur: conception and design of the experimental paradigm, surgeries
Nobu Matsumura: *in vivo* rat work
Donna Beker: echocardiography
Grant Masson: isolated heart perfusions
Wenqing Zhuang: flame photometry
James Won Suk Jahng: confocal immunofluorescence
Ahmed M Darwesh: Langendorff heart perfusions, immunoblot analysis
Zaid Alma'ayah: cell culture, quantitative RT-PCR, immunoblot analysis
Ferdaoussi M: cell culture, quantitative RT-PCR, immunoblot analysis
Dyck JRB: conception and design of research, intellectual and editorial contribution

A version of Chapter 4 has been submitted for publication as:

Byrne NJ, Matsumura N, Alma'ayah Z, Ferdaoussi M, Takahara S, Darwesh AM, Levasseur JL, Jahng JWS, Vos D, Parajuli N, El-Kadi AOS, Braam B, Young ME, Light PE, Verma S, Sweeney G, Seubert JM, Dyck JRB.

4.1 Introduction

Recently, the new class of oral anti-hyperglycemic agents, SGLT2 inhibitors, was associated with marked reductions in CV death and HF hospitalization in subjects with type 2 diabetes (1,2). Since the CV outcomes seen upon treatment with empagliflozin in the EMPA-REG OUTCOME trial appear to be irrespective of glycemic control (3), it stands to reason that empagliflozin may exert cardiac benefit in the ~60% of patients with HF that do not have diabetes as a comorbidity (4,5). In support of this, we have recently shown that empagliflozin treatment can also blunt the decline in cardiac function in non-diabetic mice with established HFrEF (6) demonstrating that treating diabetes may not be a pre-requisite for empagliflozin improving HF outcomes. In addition, the mechanism(s) responsible for these beneficial cardiac effects in the setting of diabetes as well as independent of diabetes remains unknown. For instance, although it has been proposed that empagliflozin elevates circulating ketones and that enhanced ketone oxidation in the heart can improve function (7), this notion has been challenged, at least conceptually (8). Furthermore, while the benefits of empagliflozin observed in HFrEF are profound (6), it is unknown if empagliflozin can also be used to help treat patients with HFpEF in the absence of diabetes. Moreover, the mechanism(s) responsible for the beneficial effects of empagliflozin observed in both sub-types of HF remains unknown.

Although it was originally thought that inflammation was a secondary symptom of HF pathogenesis, it has more recently become accepted that cytokine signaling may play a mechanistic role in the development and progression of cardiac dysfunction (9). However, the role of the inflammation in HF is far from understood. Of importance, several studies have demonstrated that

SGLT2 inhibition reduces inflammation in the liver and kidney (10-12). In addition, empagliflozin has been shown to modulate activation of the NLRP3 inflammasome in the kidney (13). Moreover, another SGLT2 inhibitor (dapagliflozin) was found to attenuate cardiac inflammation associated with activation of the NLRP3 inflammasome and reduce cardiac dysfunction in obese mice with diabetes. Although these are important findings, what is still lacking is a clear explanation about how empagliflozin works in HF in the absence of diet-induced obesity and/or diabetes. As a result of this, we investigated the effects of empagliflozin on the NLRP3 inflammasome in the heart in rodent models of HF in the absence of diabetes, in order to ascertain if mediating NLRP3 activation is a potential mechanism contributing to the cardiac benefit of empagliflozin use in HF. Furthermore, in order to provide a more fulsome understanding of the ability of empagliflozin to treat HF in the absence of diabetes, we also investigated the effects of empagliflozin in a rat model of HFpEF, in the absence of obesity and/or diabetes as well as the involvement of the NLRP3 inflammasome in this model.

4.2 Methods

4.2.1 Experimental animals

All protocols involving rodents were approved by the University of Alberta Institutional Animal Care and Use Committee and conform to the Guide for the Care and Use of Laboratory Animals published by the United States National Institutes of Health (eighth edition; revised 2011). The University of Alberta adheres to the principles for biomedical research involving animals

developed by the Council for International Organizations of Medical Sciences and complies with the Canadian Council on Animal Care guidelines.

Eight-week old male C57Bl/6 mice underwent TAC surgery to induce pressure overload. At 2 to 3 weeks post-surgery, the majority of the mice presented with established HF, evident by an EF of <45% (as assessed using echocardiography). Mice considered to be in HF were randomly assigned to receive either vehicle (0.5% hydroxyethyl cellulose [Natrosol]) (Sigma-Aldrich, Ontario, Canada) or empagliflozin (MedChemExpress, Princeton, New Jersey) (10 mg/kg/day) for 2 weeks by oral gavage. Body weight was measured before and after 2-week oral gavage. Following the treatment period, 24-hour food and water consumption were monitored, and body composition was assessed by EchoMRI (Echo Medical System, Houston, Texas).

As a separate cohort, 8 weeks old male Dahl salt-sensitive rats were fed a diet with either low salt (0.3% NaCl) or high salt (8% NaCl) to induce clinical signs of HFpEF, including diastolic cardiac dysfunction and pathophysiological cardiac remodeling. After 6 weeks of high salt feeding, the HFpEF group was randomly assigned to receive either vehicle (0.5% Natrosol) or empagliflozin (10 mg/kg/day) for 2 weeks via oral gavage in the presence of continuous high salt diet feeding.

4.2.2 TAC surgery[b]

TAC surgery was performed as previously described (6,14). Briefly, male eight-week old mice were anesthetized by intraperitoneal injection of a cocktail of ketamine (100 mg/kg) and xylazine

[b] See Appendix B for additional information regarding TAC surgery.

(10 mg/kg), intubated, and connected to a mouse ventilator (MiniVent; Harvard Apparatus, Holliston, Massachusetts). Following midline sternotomy, a double-blunted 27-gauge needle was tied encircling the aorta between the innominate and left common carotid arteries using a 6/0 silk suture. The needle was then removed, and chest and skin were sutured and closed.

4.2.3 Echocardiography

Rodents were anaesthetized with 1.0-1.5% isoflurane with 1-1.5L/min 100% oxygen and *in vivo* cardiac function was assessed by transthoracic echocardiography using a Vevo 3100 high-resolution imaging system equipped with a 30-MHz transducer (RMV-707B; VisualSonics, Toronto, Canada) for mice and using a Vevo 2100 high-resolution imaging system equipped with a 21-MHz transducer (MS250; VisualSonics, Toronto, Canada) for rats, as previously described (15). Pressure overload was confirmed in all TAC mice by measuring trans-stenotic gradient by pulsed-wave Doppler flow. Full systolic and diastolic parameters were measured prior to and following 2-week oral gavage.

4.2.4 Blood glucose and ketone levels

Following 2-week oral gavage of vehicle or empagliflozin, rodents were fed or fasted for 16 hours and a drop of blood from tail vein was analyzed for glucose and ketone levels using Accu-Check Aviva glucose meter (Roche Diabetes Care Inc., Mannheim, Germany) and Freestyle Precision Neo blood ketone meter (Abbott Diabetes Care Ltd., Mississauga, ON, Canada), respectively.

4.2.5 Metabolic analysis *in vivo*

Indirect calorimetry was performed using the Comprehensive Laboratory Animal Monitoring System (Oxymax/CLAMS; Columbus Instruments, Columbus, OH) as previously described (16,17). Following a 24-h acclimatization period, mice were monitored for a full 12:12-h dark (active)-light (inactive) cycle. The respiratory exchange ratio [RER; carbon dioxide production (VCO_2)/VO_2] was used to estimate the percent contribution of fat and carbohydrates to whole body energy metabolism in mice *in vivo*. Lipid and glucose oxidation rates ($ml \cdot kg^{-1} \cdot h^{-1}$) were calculated based on validated equations (18):

Glucose oxidation = $4.55VCO_2 – 3.21VO_2 – 2.87N$

Lipid oxidation = $1.67(VO_2 – VCO_2) – 1.92N$

4.2.6 Flame photometry

24-urinary samples were collected from mice using metabolic cages, snap frozen in liquid nitrogen and stored in -80°C until further processing. Samples were then thawed at room temperature and diluted to 1:200 or 1:800 for sodium and potassium ion (Na^+ and K^+, respectively) detection, respectively. The flame photometer (Jenway PFP7/C) was with either standard (Bibby Scientific, Stone Engineering) and color value recorded at a flame emission wavelength of 589 nm or 766 nm for Na^+ and K^+, respectively.

4.2.7 *Ex vivo* heart perfusions

Following 2-weeks oral gavage with vehicle or empagliflozin, TAC mice were sacrificed and hearts with excised and blood collected for plasma isolation. The hearts were perfused in working heart mode for 60 min at 11.5 mm Hg preload and 50 mm Hg afterload with Krebs-Henseleit solution containing 0.8 mmol/l oleate (prebound to 3% delipidated BSA), 5 mmol/l glucose, and 50 μU/ml insulin, as described previously (14,19) or with the addition of 0.5 mmol/l βOHB. At the end of the perfusion protocol, the left ventricles were snap-frozen with liquid nitrogen and stored at 80 C. Oleate, βOHB and glucose were labeled using [9,10-^{3}H]oleate, [3-^{14}C]βOHB and [5-^{3}H/ U-^{14}C]glucose for the metabolic determination of FA oxidation, ketone oxidation, glycolysis and glucose oxidation rates, respectively.

4.2.8 Langendorff heart perfusions

Hearts were isolated from 12-13-week old male C57Bl/6 mice and perfused in the Langendorff mode (20-22). Briefly, mouse hearts were perfused in the retrograde mode at a constant flow-rate for 40 min of baseline (stabilization) and then subjected to 30 min of global no flow ischemia followed by 40 min of reperfusion. Hearts were perfused with either vehicle (dimethyl sulfoxide; DMSO) or empagliflozin (1 μM); the concentrations utilized in the current study were based on previously published data from cell culture experiments, which demonstrate effects in isolated ventricular myocytes at similar concentrations (23). In all experiments, chemicals were added 20 min before ischemia and were present in the heart throughout the reperfusion period. After 40 min of reperfusion, hearts were immediately frozen and stored below −80°C.

4.2.9 Histology

Heart tissues were fixed in 10% neutral buffered formalin overnight and embedded in paraffin blocks after serial dehydration with ascending grades of ethanol. Heart paraffin blocks were sectioned at 5um on a Leica RM2125 RTS microtome. The sections were de-paraffinized and re-hydrated with descending grades of ethanol, and antigens were retrieved with citrate buffer (pH 6.0). The sections were permeabilized with 0.3% Triton X-100 in TBS and blocked with blocking solution [2% BSA and 5% goat serum in phosphate buffered saline (PBS)]. The sections were incubated overnight at 4°C with IL-18 (D046-3, MBL), F4/80 (ab6640, Abcam) at 1:200 concentration, then incubated with Alexa secondary antibodies (Invitrogen) at 1:1000. Sections were then mounted with coverslip on 1:1 mixture of Vectashield Mounting medium with 4′,6-diamidino-2-phenylindole (DAPI) (VectorLabs) and ProLong Gold (Life Technologies). The images were captured using 20X objective with confocal microscope (LSM700, Zeiss).

4.2.10 Cell culture and treatments

Human cardiomyocyte RL-14 cells (American Type Cell Culture Patent Deposit Deposit Designation No. PTA-1499, Manassas, VA), were maintained in DMEM/F-12, with phenol red supplemented with 12.5% fetal BSA, 20 M l-glutamine, 100 IU/ml penicillin G and 100 g/ml streptomycin. Cells were grown in 75 cm^2 tis- sue culture flasks at 37 ° C under a 5% CO_2 humidified environment (24). The cells were seeded in 12- and 6-well cell culture plates in F12/DMEM culture media for RNA and protein assays, respectively. In all experiments, the cells were washed with PBS and then treated for the indicated time intervals in serum-free media with test compounds as indicated. The effect of LPS (25 μg/ml) and empagliflozin (1 μM) on RL-14 cell viability was determined by measuring the capacity of reducing enzymes to convert 3-[4,5-

dimethylthiazol-2-yl]-2,5-diphenyltetrazoliumbromide (MTT) to colored formazan crystals as described previously (25,26). Intracellular Ca^{2+} concentration was determined after 120 minutes incubation using the Fluo-8 Calcium Flux Assay Kit (Abcam), according to the manufacturer's instructions. Twenty-four hours after incubation with 25 μg/ml LPS in the presence and absence of empagliflozin (1 μM) and/or Ca^{2+} ionophore (A23187; 10 μM), approximately 1.5×10^6 cells per six-well culture plate were collected in 100 l lysis buffer (50mM HEPES, 0.5M sodium chloride, 1.5mM magnesium chloride, 1 mM EDTA, 10% glycerol (v/v), 1% Triton X-100, and 5 l/ml of protease inhibitor cocktail). Total cellular proteins were obtained by incubating the cell lysates on ice for 1 h, with intermittent vortex mixing every 10 min, followed by centrifugation at 12,000 × g for 10min at 4°C. To determine the effect of LPS (25 μg/ml) and empagliflozin (1-10 μM) on activation of inflammation in macrophages, we used a commercially available reporter macrophage cell line (RAW-Blue cells; InvivoGen, San Diego, CA). Cells were derived from murine RAW 264.7 macrophages with chromosomal integration of a secreted embryonic alkaline phosphatase reporter construct, induced by NFκB and activator protein 1 transcriptional activation.

4.2.11 Quantitative RT-PCR

Total RNA from frozen tissues or treated cells was isolated using TRIzol reagent (Invitrogen®) according to the manufacturer's instructions and quantified by measuring the absorbance at 260 nm. RNA purity was determined by measuring the 260/280 ratio (>1.8). Thereafter, first strand cDNA synthesis was performed using 5X All-In-One RT MasterMix, according to the manufacturer's instructions (Applied biological, abm) (27). Briefly, 1.5 μg of total RNA from each sample was added to a mixture of 2.0 μl of 10 × reverse transcriptase buffer, 0.8 l of 25 ×

dNTP mix (100 mM), 2.0 µl of 10 × reverse transcriptase random primers, 1.0 µl of MultiScribe reverse transcriptase, and 4.2 µl of nuclease-free water. The final reaction mixture was kept at 25°C for 10 min, heated to 37°C for 120 min, heated for 85°C for 5 min, and finally cooled to 4°C. Quantitative analysis of specific mRNA expression was performed by RT-PCR by subjecting the resulting 1.5 µg cDNA to PCR amplification using 96-well optical reaction plates in the ABI Prism 7500 System (Applied Biosystems) (25). The 25 µl reaction mixture contained 0.1 µl of 10 µM forward primer and 0.1 µl of 10 µM reverse primer (40 nM final concentration of each primer), 12.5 µl of SYBR Green Universal Master mix, 11.05 µl of nuclease-free water, and 1.25 µl of cDNA sample. Mouse, rat and human primers sequences and probes are illustrated in **Table 4.1**. These primers were purchased from Integrated DNA technologies (IDT, Coralville, IA). The RT-PCR data was analyzed using the relative gene expression (*i.e.* Ct) method, as described and explained previously (28). Briefly, the fold change in the level of target genes between treated and untreated cells, corrected for the level of β-actin, was determined using the following equation: fold change = $2^{-(Ct)}$, where $Ct = Ct_{(target)} - Ct_{(\beta\text{-actin})}$ and $(Ct) = Ct_{(treated)} - Ct_{(untreated)}$

4.2.12 Immunoblot analysis[c]

Briefly, hearts were snap-frozen in liquid nitrogen, subsequently homogenized and prepared according to previously reported methods (20,29). 25-50 µg of protein was resolved by electrophoresis on (10–15%) SDS-polyacrylamide gels and transferred onto membrane which was probed with antibodies to glyceraldehyde 3-phosphate dehydrogenase (GAPDH) (1:1000; Cell Signaling Technology and Calbiochem), IL-1β (1:1000, Abcam and Cell Signaling Technology),

[c] See Appendix C for additional information regarding antibodies used for immunoblot analysis.

NLRP3 protein (1:500; Abcam) and Txnip (1:500, MBL International). After washing, membranes were incubated with the corresponding secondary antibodies (1:5000). The blots were visualized with ECL reagent and densitometric analysis was performed using ImageJ software (National Institutes of Health, Bethesda, MD). The activity of caspase-1 was determined by a commercial kit (Abcam, ab39412) according to the manufacturer's instructions.

4.2.13 Statistical analysis

Results are expressed as mean ± SEM. Comparisons between groups were performed using Wilcoxon signed rank test**,** repeated measures two-way ANOVA followed by Sidak multiple comparisons test**,** Mann-Whitney U test or Kruskal-Wallis followed by Dunn's multiple comparisons test**.** A p value of <0.05 was considered significant.

4.3 Results

4.3.1 Empagliflozin blunts the decline in cardiac function in heart failure in the absence of diabetes without increasing circulating ketone bodies or altering urinary electrolyte excretion

Since the reduction in the risk of hospitalization for HF in diabetic patients treated with empagliflozin occurs irrespective of alterations in HbA1c, it suggests that the beneficial effects were not driven by glycaemic control (30). As such, we subjected C57Bl/6 mice to TAC surgery

to induce HF [as described previously (6)] in the absence of diet-induced obesity or diabetes, in order to explore current hypotheses of potential mechanisms involved in the CV effects of empagliflozin.

At 2 to 3 weeks following TAC surgery, mice were subjected to pulsed wave Doppler M-mode echocardiography and those demonstrating an EF of <45% were subsequently randomized and treated with either vehicle (0.5% hydroxyethyl cellulose) or empagliflozin (10 mg/kg) by daily oral gavage for a period of 2 weeks. In order to confirm our previous findings in this cohort of mice, we demonstrate that vehicle-treated mice with HF displayed a significant decline in systolic cardiac function between pre-treatment (Baseline) and following 2-week oral gavage **(Figure 4.1A-B;** 32.5% vs 24.7%; p=0.0003). Importantly, this is not the case for empagliflozin-treated mice who maintain stable cardiac function over the treatment period **(Figure 4.1A-B;** 33.6% vs 30.62%; p=0.2224). As expected with empagliflozin treatment, urinary glucose excretion was increased upon SGLT2 inhibition **(Figure 4.1C)**. While empagliflozin significantly reduced fasting (16 hours) blood glucose levels in mice with HF **(Figure 4.1D)** changes in blood glucose levels were not observed in the fed state **(Figure 4.1E)**. Since it has been proposed that hypoglycemia induced my empagliflozin increases circulating ketone levels that would improve cardiac energetics in HF (7), we also measured ketone levels in these mice. Interestingly, although there were no differences in blood βOHB between any groups of mice during the fed state **(Figure 4.1F)**, mice with HF had significantly reduced fasted blood βOHB levels than control mice, which was not significantly altered by empagliflozin treatment **(Figure 4.1G)**. Together, these data suggest that changes in circulating ketones may not contribute directly to the beneficial effects of empagliflozin in HF.

To explore whether the diuretic effect of SGLT2 inhibition (1,31-34) are sustained in the absence of diabetes, 24-hour urinary output was measured in all groups of mice. Although urinary output was found to significantly decrease in HF mice versus control, the volume of urine was significantly increased in empagliflozin-treated HF mice after a single treatment (data not shown) and maintained after 2 weeks of oral gavage **(Figure 4.1I)**. Nonetheless, this increase in urinary output was not associated with any alterations in electrolyte balance, as demonstrated by no significant changes in urinary Na^+ **(Figure 4.1I-J)**, urinary K^+ **(Figure 4.1K-L)** or blood Na^+ or K^+ concentrations **(Figure 4.1M-N)**. Lastly, there appeared to be a trend toward increased water intake in empagliflozin- versus vehicle-treated HF mice **(Figure 4.1O;** $p<0.07$). Together, these data suggest that the beneficial effects of empagliflozin treatment in HF are not reliant on natriuresis in our model, and that both of these processes may play a role in maintaining cardiac function.

In order to ascertain whether the ability of empagliflozin to reduce visceral fat in patients with type 2 diabetes (35-37) contributes to the beneficial effects of empagliflozin observed in our non-diabetic model of HF, we subjected all groups of mice to body composition analysis. In contrast to that observed in humans, there were no significant differences in body weight **(Figure 4.2A)**, fat mass **(Figure 4.2B)** or lean mass **(Figure 4.2C)** amongst control and HF mice treated with vehicle or empagliflozin. Empagliflozin also had no effect on food intake compared to vehicle, which otherwise tended to decrease in HF versus control **(Figure 4.2D;** $p<0.07$).

4.3.2 Empagliflozin shifts whole body substrate utilization without altering cardiac energy metabolism in heart failure in the absence of diabetes

As a result of empagliflozin-induced glucose excreted in the urine, there appears to be a progressive shift in whole-body metabolism away from carbohydrate to fatty substrate use in diabetic patients and to a lesser extent nondiabetic controls (38,39). While it has been proposed that glucose lowering without associated inhibition of lipid oxidation may be beneficial to the failing heart (40), whether or not empagliflozin exerts such a shift in whole-body metabolism in HF in the absence of diabetes is currently unknown. As such, we subjected mice with HF to indirect calorimetry following 2-week treatment with vehicle or empagliflozin. Interestingly, empagliflozin-treated mice with HF showed an acute response to oral gavage, evident by reduced RER during the dark phase (active; 6PM-6AM) **(Figure 4.3A-B)**. However, calculated rates of whole-body carbohydrate **(Figure 4.3C)** and FA utilization **(Figure 4.3D)** during the dark phase were not significantly changed in empagliflozin-treated HF mice. Together, our data suggests that alterations in systemic substrate utilization are unlikely to contribute to the CV benefit of empagliflozin (40) even in HF in the absence of diabetes.

Since SGLT2 inhibitors have been shown to increase the level of circulating ketones (12), it has also been proposed that empagliflozin may exert its beneficial effects in HF as a consequence of promoting enhanced ketone oxidation by the heart, and thus improve cardiac bioenergetics (7). While dramatic changes in circulating ketones were not observed in our mouse model, we still explored the role of substrate utilization (FAs, glucose and ketone bodies) in the failing heart in response to treatment with empagliflozin. Hearts from mice with HF treated with vehicle or

empagliflozin for 2 weeks were subjected to *ex vivo* working heart perfusions, using physiological levels of glucose, FAs and ketones. Consistent with our previous findings (6), cardiac work was significantly improved in hearts from empagliflozin-treated mice with HF compared to vehicle-treated mice **(Figure 4.3E-F)**. Interestingly, myocardial oleate oxidation rates of hearts from empagliflozin-treated HF mice were 140% that of vehicle-treated HF mice **(Figure 4.3G)**, although these changes did not reach statistical significance. Furthermore, glucose oxidation **(Figure 4.3H)**, glycolysis **(Figure 4.3I)** and βOHB oxidation **(Figure 4.3J)** rates were unchanged upon treatment with empagliflozin. More importantly, there was no change in overall cardiac ATP production **(Figure 4.3K)** or cardiac ATP production per unit work **(Figure 4.3L)** in hearts from HF mice treated with empagliflozin versus vehicle, suggesting that improved cardiac energetics are not necessary for the cardiac benefit of empagliflozin in HF in the absence of diabetes.

4.3.3 Empagliflozin blunts inflammasome priming in heart failure in the absence of diabetes

SGLT2 inhibitors have been reported to have anti-inflammatory properties in experimental models (11) and *in vitro* studies (41) of type 1 and type 2 diabetes. Furthermore, empagliflozin has been found to attenuate activation of the NLRP3 inflammasome in the kidney (13), although the effect of empagliflozin on the failing heart in the absence of diet-induced obesity or diabetes has yet to be elucidated. As such, we utilized both confocal immunofluorescence and gene expression quantification in cardiac tissue sections/tissues from control and vehicle- or empagliflozin-treated HF mice to explore the effects of empagliflozin on cardiac inflammation. In agreement with previous studies (42), our results demonstrate that *Il-18* **(Figure 4.4A-B)** and *Il-1b* **(Figure 4.4C-D)**, two markers of inflammation, were significantly increased in hearts from mice with HF

compared to hearts from healthy control mice. Furthermore, infiltration of macrophages into cardiac tissue, as indicated by immunofluorescence **(Figure 4.4E)** and gene expression of lysosomal-associated membrane protein 2 (*Mac3*) **(Figure 4.4F)**, as well as quantification of F4/80+ cells **(Figure 4.4G-H)**, increased in HF. Of importance, following 2-week treatment, both markers of inflammation (*Il-18* and *Il-Ib*) **(Figure 4.4A-D)** and markers of macrophage infiltration (*Mac3* and F4/80+ cells) **(Figure 4.4E-H)** were significantly reduced in cardiac tissue from mice with HF treated with empagliflozin to an amount comparable to that of control. Furthermore, inflammasome-priming, measured via gene expression levels of *Nlrp3, Nfkb, Caspase-1* and *Tnfa* **(Figure 4.4I-L)** indicate increases in these transcript levels observed in vehicle-treated HF mice were blunted in mice treated with empagliflozin.

4.3.4 Empagliflozin improves diastolic function and blunts inflammasome priming in HFpEF

Recent clinical results have shown that empagliflozin reduces LV mass and improves diastolic function in subjects with type 2 diabetes (43). As such, we next sought to determine whether empagliflozin could have beneficial effects in an experimental model of HFpEF, in the absence of diabetes. In order to test the efficacy of empagliflozin in HFpEF, we first validated the cardiac phenotype of Dahl salt-sensitive rats that were administered either 0.3% salt (Control) or 8.0% salt for a period of 6 weeks to induce HFpEF, as previously described (44,45). Following this feeding period, rats with HFpEF displayed significantly elevated systolic BP compared to the control group (180.8 ± 0.9 mmHg, $n = 21$ vs. 160.2 ± 1.3 mmHg, $n = 25$, $p<0.001$). Since it has been reported that empagliflozin treatment improves diastolic function and reduces LV mass in diabetic patients with established CVD (43), rats with HFpEF were then randomly selected to receive either vehicle-

or empagliflozin (10 mg/kg/day) for and additional 2 weeks via oral gavage in the presence of continuous high salt diet feeding. Echocardiographic assessment confirmed that the rise in BP in HFpEF rats produced no overt systolic dysfunction (*i.e.* no decreased in EF) and thus empagliflozin treatment had no effect on EF **(Figure 4.5A)**. However, HFpEF rats showed signs of diastolic dysfunction with significantly reduced mitral E/A wave ratio (1.32 ± 0.11, n = 8 vs. 0.92 ± 0.07, n = 6 $p<0.03$), elevated E/E′ ratios **(Figure 4.5B)** and resulting decrease in cardiac output (89.4 ± 6.1 ml/min, n = 8 vs. 65.3 ± 7.5 ml/min, n = 6 $p<0.03$), characteristic of patients with HF (46). Indeed, while the mitral E/A ratio was not significantly different with empagliflozin treatment (data not shown), the more sensitive index of diastolic function, E/E′, tended to reduce in rats with HFpEF compared to vehicle-treated rats with HFpEF, comparable to that of controls **(Figure 4.5B;** $p<0.07$). In agreement with the pathophysiological adaptations to elevated BP and the onset of HFpEF, compared to controls, hearts from rats with HFpEF remodeled and displayed increased LA diameter (4.24 ± 0.17 mm, n = 7 vs. 5.85 ± 0.35 mm, n = 6 $p<0.01$), and increased LV wall thickness **(Figure 4.5C)** and wet heart weight normalized to tibia length (HW/TL) (26.8 ± 0.8 mg/mm, n = 6 vs. 33.3 ± 0.9 mg/mm, n = 8 $p<0.001$), indicative of cardiac hypertrophy. Surprisingly, radiotelemetric monitoring of systolic BP in rats with HFpEF demonstrates that empagliflozin-treated rats actually have slightly elevated BPs compared to vehicle controls (209.5 ± 17.2 mmHg, n = 3 vs. 184.9 ± 1.8 mmHg, n = 2 $p<0.20$), demonstrating that, at the very least, empagliflozin does not decrease hemodynamic load. Nonetheless, despite no reduction in BP or improvements in cardiac output and LA diameter (data not shown), empagliflozin treatment reduced LV wall thickness **(Figure 4.5C)**, reduced cardiomyocyte cell size **(Figure 4.5D)** and reduced wet HW/TL **(Figure 4.5E)**, suggesting that empagliflozin improves diastolic function by preventing a worsening of cardiac hypertrophy and detrimental cardiac remodeling. Furthermore,

since cardiac fibrosis is another major factor shown to induce diastolic dysfunction (47), we also demonstrate that empagliflozin reduces the volume of collagen deposits **(Figure 4.5F)** as well as gene expression of the marker of interstitial fibrosis, *Col3a1* **(Figure 4.5G)**, in hearts from rats with HFpEF.

In addition to these structural and functional cardiac effects, empagliflozin dramatically increased urine glucose levels compared to vehicle-treated rats with HFpEF **(Figure 4.5H)**. In agreement with our results in mice with HFrEF, fed blood glucose concentrations were unchanged while fasted blood glucose concentrations were modestly but significantly decreased in empagliflozin- versus vehicle-treated rats with HFpEF **(Figure 4.5I-J)**. Interestingly, while fed blood βOHB levels were also unchanged, fasted blood βOHB levels were significantly increased in empagliflozin- compared to vehicle-treated rats with HFpEF **(Figure 4.5K-L)**. This is consistent with the physiological response to the glucose lowering effects and entirely consistent with that is observed in diabetic patients treated with empagliflozin (48) but is not consistent with the findings in our mouse model of HFrEF. Nonetheless, HFpEF rats showed no changes in body weight after 2-week treatment with empagliflozin **(Figure 4.5M)**, which agrees with our model of HFrEF.

Lastly, in order to determine whether the beneficial effect of empagliflozin in HFpEF is also associated with reduced cardiac inflammation, we also quantified expression of several markers of inflammation and activation of the NLRP3 inflammasome. As expected, 2-week treatment with empagliflozin was found to reduce the gene expression levels of markers of inflammation (*Il-6* and *Il-1b*) **(Figure 4.5N)** and several markers of inflammasome-priming (*Nlrp3, Caspase-1*

and *Tnfa)* **(Figure 4.5O),** except expression of *Nfkb*. Furthermore, immunoblot analysis revealed that expression of IL-Iβ and TXNIP, a protein involved in mediating activation of NLRP3 inflammasome (49), were significantly decreased in cardiac tissue from HFpEF rats treated with empagliflozin versus vehicle-treated rats **(Figure 4.5P-Q)**. Moreover, caspase-1 enzyme activity was significantly increased in hearts from HFpEF rats compared to controls (data not shown) and this was significantly reduced in hearts from HFpEF rats treated with empagliflozin versus vehicle **(Figure 4.5R)**.

4.3.5 Empagliflozin blunts NLRP3 activation in isolated hearts and inflammation in cardiomyocytes

Since SGTL2 is not expressed at any significant levels in the heart (50), we explored whether empagliflozin had SGLT2-independent effects on the heart using our isolated heart perfusion system. Mouse hearts were perfused in a crystalloid perfusion buffer and subjected to I/R in order to induce NLRP3 activation as previously shown (29). To determine the ability of empagliflozin to blunt NLRP3 inflammasome-priming, the expression levels of the inflammasome component; NLRP3 and TXNIP were assessed. Immunoblot analysis revealed that I/R injury significantly upregulated active NLRP3 and this was blunted in hearts perfused with empagliflozin (1 μM) **(Figure 4.6A-B)**. Similarly, protein expression of TXNIP was significantly decreased in I/R injured hearts treated with empagliflozin **(Figure 4.6A-B)**. This was further supported by the finding that empagliflozin blunted the increase in caspase-1 activity seen in cardiac tissue of I/R injured hearts compared to aerobic controls **(Figure 4.6C)**. More importantly, the attenuation of NLRP3 inflammasome activity directly in the heart by empagliflozin was associated with

improved contractile recovery following I/R injury. This was evident by significantly improved post-ischemic recovery of LV developed pressure (LVDP) compared with vehicle-treated hearts **(Figure 4.6D)**. Consistent with this, hearts perfused with empagliflozin demonstrated improved rates of contraction **(Figure 4.6E)** and relaxation **(Figure 4.6F)** compared to vehicle-treated I/R hearts. As such, these studies show that empagliflozin can act directly on the heart to blunt NLRP3 activation and that this is associated with improved cardiac function. Of importance, since empagliflozin did not alter the coronary flow rates (data not shown), the improved post-ischemia function recovery observed upon treatment with empagliflozin is not attributed to alterations in hemodynamics in the isolated heart. Furthermore, since it has been previously shown that activation of NLRP3 inflammasome is dependent on calcium ion (Ca^{2+}) mobilization (51), we conducted *in vitro* experiments to test the effect of empagliflozin on intracellular Ca^{2+} and inflammasome-priming in isolated human cardiomyocytes (RL-14 cells) after stimulation with 25 μg/ml lipopolysaccharide (LPS). Interestingly, intracellular Ca^{2+} was significantly increased in cardiomyocytes following 2 h incubation with LPS and this was significantly decreased with empagliflozin pre-treatment, comparable to that of vehicle-treated cells **(Figure 4.6G)**. In order to further elucidate the role of Ca^{2+} mobilization in NLRP3 inflammasome-priming, we also subjected human cardiomyocytes to treatment with the Ca^{2+} ionophore, A23187, in the presence of LPS +/- empagliflozin. Our results first showed that none of the aforementioned treatment combinations significantly affected cell viability **(Figure 4.6H)**. In agreement with our animal models, empagliflozin appeared to reduce gene expression of numerous markers of inflammation (*IL-18, IL-1B, TNFA*); however, this ability of empagliflozin to prevent inflammation was completely blunted by the Ca^{2+} ionophore **(Figure 4.6I-L)**. Interestingly, LPS-induced inflammation and suppression of TXNIP were shown in isolated macrophages **(Figure 4.6M-N)**,

as previously described (52), and this was unchanged with empagliflozin, thus ruling out the potential that the effects of empagliflozin observed *in vivo* are due to reduced NLRP3 activation in macrophages. Taken together, these data suggest that empagliflozin directly attenuates NLRP3 inflammasome priming in cardiomyocytes in a Ca^{2+}-dependent manner, irrespective of its glucose-lowering effects.

4.4 Discussion

While the mechanism of action of empagliflozin remains elusive (53), one focus of this study was to explore whether the metabolic and diuretic effects of SGLT2 inhibition were apparent in our non-diabetic experimental model of HF. Previous studies have shown that empagliflozin induces moderate weight loss in diabetic patients (54), and that this is associated with decreased CV risk (55). Furthermore, studies of SGLT2 inhibitors have consistently reported reductions in visceral fat, which accounts for the majority of the total weight loss (37,56,57). Based on this, ongoing studies aim to explore the possible role of reductions in epicardial adipose tissue on improved cardiac function in patients treated with SGLT2 inhibitors [*i.e.* Dapagliflozin Effects on Epicardial Fat (NCT02235298)]. Of importance to these studies, we clearly show that no weight loss or changes in body composition occur in our non-diabetic mice with HF treated with empagliflozin. While weight loss and/or decreased adipose tissue mass may result from treatment with empagliflozin for a longer period of time or in patients with diabetic, our data suggests that this potential mechanism is not essential for the beneficial cardiac effects of empagliflozin seen in our experimental model of HF.

In addition to weight loss, it has also been proposed that SGLT2 inhibitors cause osmotic diuresis without activation of neurohormonal factors, and therefore may be beneficial for HF (58). Interestingly, the beneficial effects of SGLT2 inhibitors were prominent in patients who were not treated in combination with diuretics, loop diuretics, or mineralocorticoid receptor antagonists (59), suggesting that improved CV outcomes by empagliflozin may be driven by their diuretic action. Particularly, SGLT2 inhibitors have been thought to combat fluid retention by increasing excretion of both water and sodium. Notably, this is thought to lead to reduced plasma volume and contribute to reductions in BP, thereby resulting in a lower cardiac preload and afterload and reducing risk of pulmonary congestion and peripheral edema (3,7). Previous studies have reported either no significant changes in urine volume (60-62) or increased urinary output peaks during the first 24 hours following treatment with empagliflozin which returns to a new "set point" within a few days of treatment (62). However, neither of these was the case in mice with HF in the absence of diabetes, which showed that increased urinary output following treatment with empagliflozin was sustained for the duration of the treatment period (2 weeks). Interestingly, urine volume has also been shown to decrease upon treatment with the SGLT2 inhibitor, dapagliflozin, in streptozotocin-induced diabetic rats, unlike the notable increase seen in our model of HF (63). Furthermore, since diuretics such as bumetanide, have been known to stimulate thirst, our results suggest that the excess in water excretion may be merely compensated by increased water intake, although the potential contribution of a diuretic effect and ventricular unloading cannot be overlooked. Nonetheless, while the diuretic effects of empagliflozin were confirmed in our model of HF in the absence of diabetes, there appeared to be no difference in electrolyte balance, which was within the published range (64,65). Although this is not consistent with previous studies that

have shown SGLT2 inhibitors to blunt the decline in serum electrolytes that occurs as a result of diabetes (63), it should be noted that hyponatremia and hypokalemia were not evident on our model of HF. Furthermore, although changes in plasma electrolyte concentrations have been proposed as a potential mechanism contributing to reduced CV mortality with empagliflozin, there were no significant changes in plasma Na^+, K^+ or Ca^{2+} observed in the EMPA-REG Outcome study (1) or in diabetic patients with hypertension treated with empagliflozin (66). Altogether, while this does not rule out the potential role of a shift in sodium distribution from the intracellular to extracellular space (67), alterations in electrolyte concentration and distribution are unlikely to explain the rapid CV benefits seen with empagliflozin. Furthermore, since the CV benefit of empagliflozin does not exactly match the profile of antihypertensive and diuretic therapy, which show smaller reductions in HF and mortality and a clear risk reduction in stroke than observed in the EMPA-REG Outcomes trial (68-70), it stands to reason that other mechanisms in addition to the diuretic effect must be at play. Nonetheless, clinical trials have been designed to further evaluate the effect of empagliflozin on serum sodium levels [*i.e.* the SAND Study (Effect of the SGLT2-inhibitor Empagliflozin on Patients with SIADH; NCT02874807)].

Of the prevailing theories explaining how SGLT2 inhibitors exert their beneficial effects in HF (7,53,71,72), one theory implicates the increased circulating ketone body concentrations induced by empagliflozin. Indeed, it has been proposed that elevated circulating ketones may improve cardiac bioenergetics by enhancing cardiac ketone oxidation rates, thereby increasing cardiac efficiency and aiding in the prevention of HF (7). This increase in circulating ketone bodies in response to empagliflozin was observed only modestly in our model of HFpEF but was absent in our model of HFrEF, thus challenging the "thrifty fuel hypothesis" (7) in explaining the beneficial

cardiac effects of SGLT2 inhibition. In fact, our data show for the first time that empagliflozin blunts the decline in cardiac function in mice with pressure overload-induced HF even in the absence of increased circulating ketone bodies or increased cardiac ketone body oxidation. This is consistent with a recent study that demonstrated the decline in overall ATP production in hearts from diabetic mice was blunted upon treatment with empagliflozin, without associated increases in myocardial ketone oxidation or cardiac efficiency (73). Furthermore, empagliflozin was also recently shown to reduce myocardial ketone body utilization in diabetic hypertensive rats with mild HF using a novel hyperpolarized [3-^{13}C]acetoacetate, despite increased circulating ketone bodies (74). Taken together, these findings suggest that a switch in myocardial utilization of ketone bodies may not play a major role in contributing to the beneficial cardiac effects of empagliflozin in HF. However, a recent study reported that empagliflozin induced a shift toward ketone body, FA and branched-chain amino acid metabolism in a porcine model of MI (75), highlighting that the metabolic effect of empagliflozin has yet to be fully elucidated.

Although the majority of the studies have focused on the effects of SGLT2 inhibition in the setting of obesity and diabetes, there has been less work identifying other patient populations who may benefit from empagliflozin treatment, even in the absence of hyperglycemia. However, empagliflozin was previously shown to reduce diastolic tension in ventricular trabecular isolated from human failing hearts as well as in cardiomyocytes from both diabetic and non-diabetic mice (76). Furthermore, early treatment with empagliflozin protected from cardiorenal syndrome induced by 5/6 subtotal nephrectomy and doxorubicin treatment (77). Of importance, the favorable effects of empagliflozin on aortic stiffness, vascular resistance and diastolic function (78-80) are encouraging for patients who present with HFpEF. Indeed, the beneficial cardiac effects in absence

of diabetes were preserved *in vivo* in our model of HFpEF as well others' (81). Importantly, our current study shows that in the absence of diabetes, empagliflozin blunts worsening diastolic dysfunction and reduces myocardial mass in HFpEF without changes in BP or atrial reverse-remodeling. These data are in agreement with other pre-clinical studies that have shown that empagliflozin increased diastolic relaxation in obese db/db mice even in the absence of any changes in BP (79). While the mechanism of action of empagliflozin continues to evolve (53), we conclude that empagliflozin, and possibly other gliflozins, have beneficial effects in HFpEF in the absence of diabetes and/or decreased BP.

Since increased inflammation is linked with the development of HF (82), it is not surprising that interventions that reduce inflammation are being explored as potential treatment in HF. Particularly, the NLRP3 inflammasome has been implicated as a significant contributor to chronic inflammation and the development of HF (83). Of note, inhibition of SGLT2 has been associated with reduced inflammation (10-12) and reduced activation of the NLRP3 inflammasome in the kidney (13) and heart (41). Firstly, ipragliflozin was shown to reduce markers of inflammation in liver and plasma in type 1 and 2 diabetes (11,12). Similarly, empagliflozin was shown to reduce renal tubular damage in mice fed a high-fat diet and this was associated with decreased activation of NLRP3 inflammasome in the kidney (13); however, cardiac NLRP3 inflammasome was not found to be activated in response to high fat diet in these mice. Furthermore, dapagliflozin was shown to attenuate the development of fibrosis and LV dysfunction as well as suppress activation of NLRP3 inflammasome in hearts of type 2 diabetic mice and isolated cardiac fibroblasts (41). Altogether, attenuated cardiac NLRP3 inflammasome priming, inflammatory cytokines and macrophage infiltration upon treatment with SGTL2 inhibitors have been well-documented in

experimental models of obesity/diabetes (41,84,85). Thus, our current study significantly advances these previous studies and show for the first time that empagliflozin blunts NLRP3 inflammasome priming and subsequent inflammation in the heart in 2 experimental models of HF in the absence of diabetes. In addition, to our knowledge, our study shows for the first time that the NLRP3 pathway is also activated in the heart in a model of HFpEF. As such, it is tempting to speculate that inhibition of the cardiac NLRP3 inflammasome may be an important mechanism of action of empagliflozin that contributes to the therapeutic benefit of empagliflozin in HF.

The SLGT2 inhibitor, dapagliflozin, was previously shown to attenuate NLRP3 inflammasome priming in cardiofibroblasts isolated from diabetic mice, suggesting an SGLT2-independent and glucose-lowering-independent effect (41). In support of our previous findings that the beneficial functional effects of empagliflozin are sustained in hearts *ex vivo* (6), we also demonstrate herein that empagliflozin exerts functional benefit via suppression of NLRP3 inflammasome signalling in the isolated perfused heart and isolated human cardiomyocytes, independent of SGTL2 and glucose-lowering effects. Furthermore, since mobilization of Ca^{2+} has been recently implicated in the activation of NLRP3 inflammasome (51), we also explored whether the ability of empagliflozin to attenuate activation of NLRP3 inflammasome in the heart was dependent on Ca^{2+}. Indeed, the Ca^{2+} ionophore, A23187, was sufficient to blunt the anti-inflammatory effect of empagliflozin on human cardiomyocytes. Interestingly, this is contrary to the work by Pabel et al (76), which showed that Ca^{2+} transient amplitude and diastolic Ca^{2+} levels were not altered by empagliflozin. This may be explained by differences in Ca^{2+} handling in failing cardiomyocytes compared to an LPS-induced inflammatory reaction. Nonetheless, in support of our findings, empagliflozin has also been recently shown to reduce sarcoplasmic reticulum Ca^{2+} leak in failing

ventricular myocytes and decrease cytosolic Ca^{2+} and increase mitochondrial Ca^{2+} in isolated ventricular myocytes (23,86). Lastly, although SGLT2 inhibitors have also been found to attenuate activation of the NLRP3 inflammasome in human macrophages (87), our study shows that empagliflozin has no effect on LPS-induced inflammation in isolated macrophages, similar to that observed with other SGLT2 inhibitors (88). Together, these data suggest that the beneficial cardiac effect of empagliflozin occurs, at least in part, due to reduced cardiac inflammation upon Ca^{2+}-dependent modulation of the NLRP3 inflammasome in the cardiomyocytes.

4.4.1 Study limitations

Firstly, although the treatment period utilized in both experimental models of rodents in our study is much shorter than in humans, our results, nonetheless, demonstrate a dramatic effectiveness of empagliflozin treatment in HF in 2 models of HF resulting from diverse etiologies. More importantly, these beneficial effects of empagliflozin occurred in established HF, as opposed to preventing the onset of HF, which has important implications in HF therapy.

Furthermore, although one theory suggests that empagliflozin improves cardiac function upon reducing hemodynamic load, we did not measure whether this was the case in our mouse model of HFrEF. Nonetheless, improvements in diastolic cardiac function in our rat model of HFpEF occurred regardless of any changes in systolic BP. In addition, although empagliflozin induced diuresis in the non-diabetic mice with HF, whether or not this is the mechanism responsible for the improved cardiac function remains unknown. However, it should be noted that post-ischemic functional recovery was also significantly improved *ex vivo* and empagliflozin exerted direct

effects on isolated cardiomyocytes, highlighting that empagliflozin has beneficial cardiac effects irrespective of diuretic and hemodynamic variables.

Furthermore, while our data clearly demonstrates that inhibition of the cardiac NLRP3 inflammasome occurs in response to empagliflozin, whether this is a direct or indirect effect remains unknown. However, given the fact that empagliflozin modulates NLRP3 signaling in isolated hearts and in cultured cardiac myocytes, we have evidence that there is a direct effect on the heart. In addition, we provide data that show that the inhibition of NLRP3 signaling in the heart is tightly coupled to improved cardiac function, it is tempting to speculate that the regulation of this pathway by empagliflozin in HF contributes to improved cardiac outcomes.

4.5 Conclusion

In summary, the SGLT2 inhibitor, empagliflozin, attenuated cardiac dysfunction in two experimental models of HF in the absence of hyperglycemia or diabetes. These beneficial cardiac effects were associated with the reduction of the activation of myocardial NLRP3 inflammasome pathway and downstream cytokine signaling. Furthermore, we show that the beneficial effect of empagliflozin occurs directly on the cardiomyocytes and is dependent on Ca^{2+} mobilization, suggesting that ionic homeostasis may play a role in the effects associated with empagliflozin. Together, these data provide important translational clues for the ongoing studies of SGLT2 inhibition in patients with and without diabetes who have HFrEF [*i.e.* EMPEROR-Reduced (Empagliflozin Outcome Trial in Patients with Chronic Heart Failure with Reduced Ejection

Fraction; NCT03057977)] and HFpEF [*i.e.* EMPEROR-Preserved (EMPagliflozin outcomE tRial in Patients with chrOnic heaRt Failure with Preserved Ejection Fraction); NCT03057951].

4.6 Figures

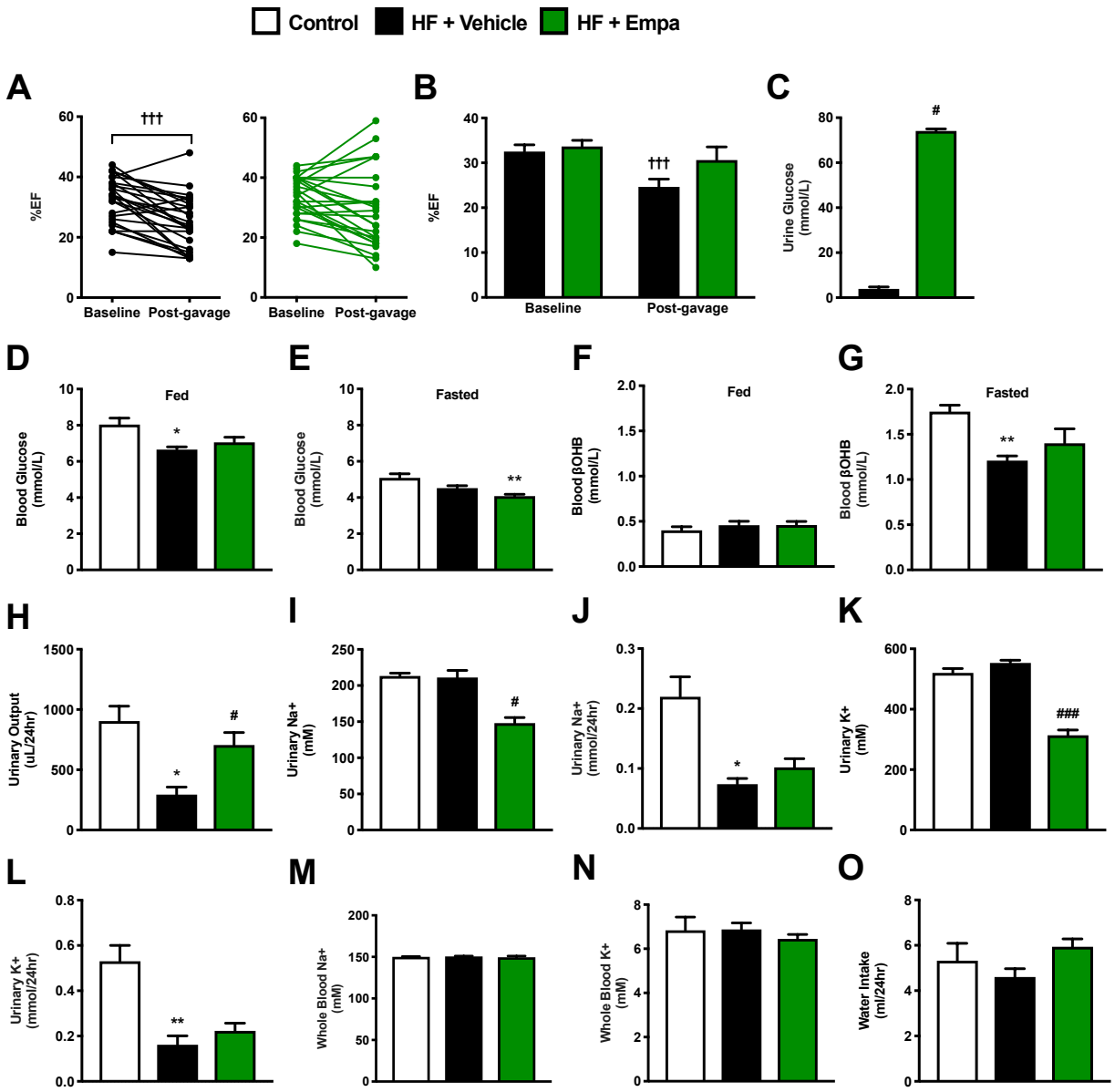

Figure 4.1. Empagliflozin Blunts the Decline in Cardiac Function in Heart Failure in the Absence of Diabetes Without Increasing Circulating Ketone Bodies or Altering Urinary Electrolyte Excretion. EF **(A-B)** based on echocardiographic assessment of vehicle- and empagliflozin-treated HF mice (n = 26). Urinary glucose concentration **(C)** (n = 3–4). Circulating glucose **(D-E)** and βOHB levels **(F-G)** under fed conditions or following a 16-hour overnight fast, respectively (n = 6–19). 24-hour urinary output **(H)**, urinary Na^+ **(I-J)** and K^+ **(K-L)** excretion (n = 3–9). Blood Na^+ **(H)** and K^+ **(I)** concentrations following a 16-hour overnight fast (n = 3–4). 24-hour water **(D)** intake (n = 4–11).

Results are expressed as mean ± SEM. Comparisons between groups were performed using Wilcoxon signed rank test **(A),** repeated measures two-way ANOVA followed by Sidak multiple comparisons test **(B),** Mann-Whitney U test **(C)** and Kruskal-Wallis followed by Dunn's multiple comparisons test **(D-O). †††p<0.001 versus baseline; *p<0.05, **p<0.01 versus control; #p<0.05, ##p<0.01, ###p<0.001 versus HF vehicle.** ANOVA = analysis of variance; βOHB = β-hydroxybutyrate; EF = ejection fraction; EMPA = empagliflozin; HF = heart failure; Na^+ = sodium ion; K^+ = potassium ion; SEM = standard error of the mean.

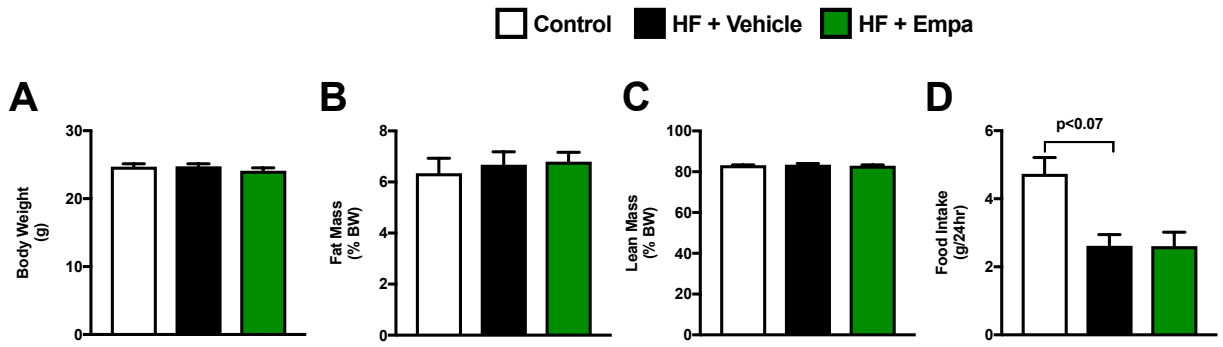

Figure 4.2. Empagliflozin Does Not Alter Body Composition in Heart Failure in the Absence of Diabetes. Body weight **(A)** (n = 27–29), fat mass **(B)** and lean mass **(C)** (n = 10–11) for control and vehicle- or empagliflozin-treated HF mice following 2-week treatment. 24-hour food **(D)** (n = 3–13). Results are expressed as mean ± SEM. Comparisons between groups were performed using Kruskal-Wallis followed by Dunn's multiple comparisons test. BW = body weight; EMPA = empagliflozin; HF = heart failure; SEM = standard error of the mean.

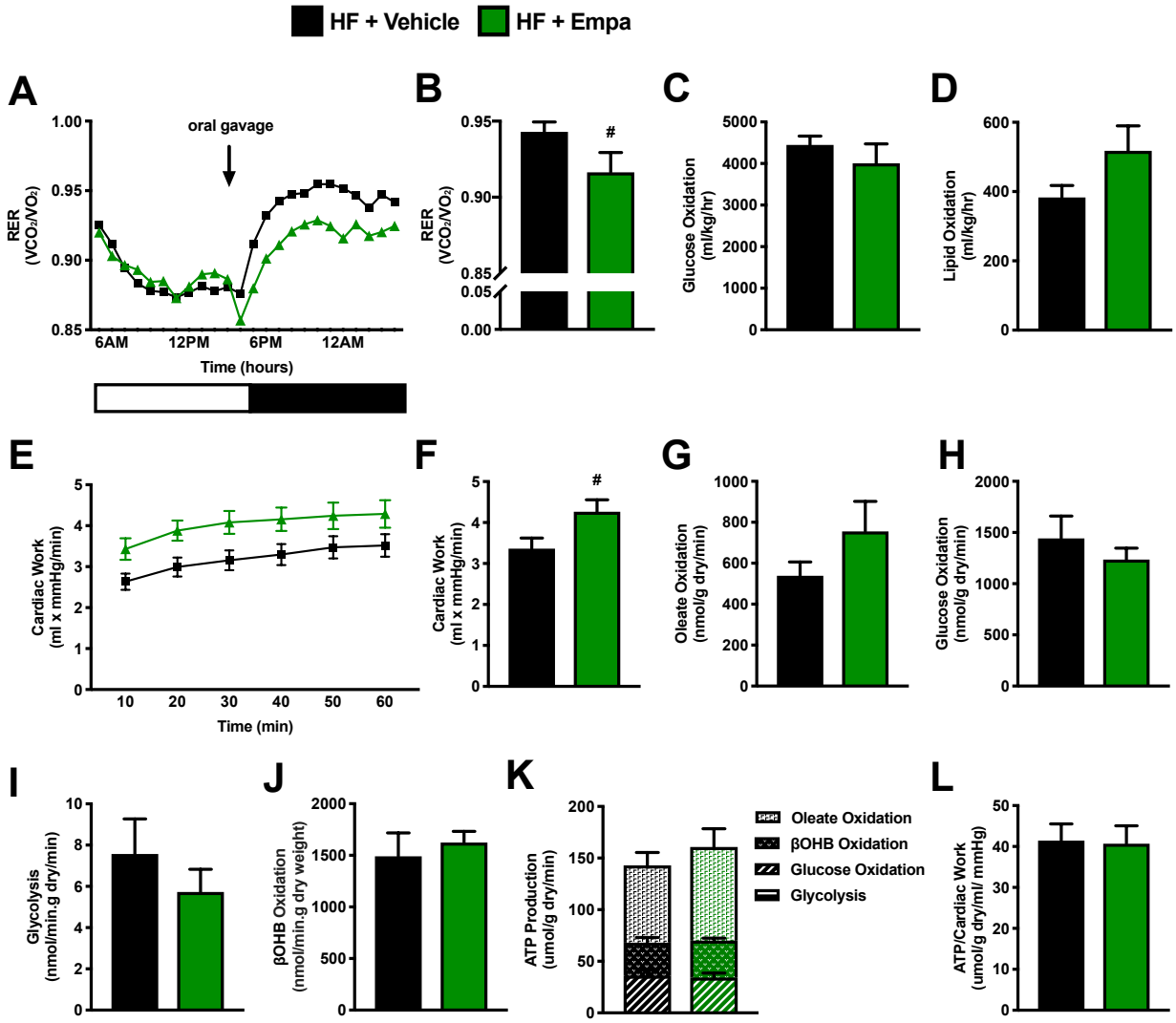

Figure 4.3. Empagliflozin Shifts Whole Body Substrate Utilization Without Improving Cardiac Energy Production in Heart Failure in the Absence of Diabetes. RER during a 24-h cycle **(A)** and during dark (active) phase post-gavage **(B)** for vehicle- and empagliflozin-treated HF mice (n = 8–10). Calculated whole glucose oxidation **(C)** and lipid oxidation **(D)** rates during dark (active; 6PM-6AM) phase post-gavage (n = 8–10). Hearts from vehicle- and empagliflozin-treated HF mice perfused *ex vivo* to measure cardiac work **(E-F)** (n = 21–24), oleate oxidation **(G)** (n = 11), glucose oxidation **(H)** (n = 8–10), glycolysis **(I)** (n = 8–9) and βOHB oxidation **(J)** (n = 8–11) and total ATP production **(K-L)** (n = 21–24). Results are expressed as mean ± SEM. Comparisons between groups were performed

using Mann-Whitney U test**. #p<0.05 versus HF vehicle.** ATP = adenosine triphosphate; βOHB = β-hydroxybutyrate; EMPA = empagliflozin; HF = heart failure; RER = respiratory exchange ratio; SEM = standard error of the mean.

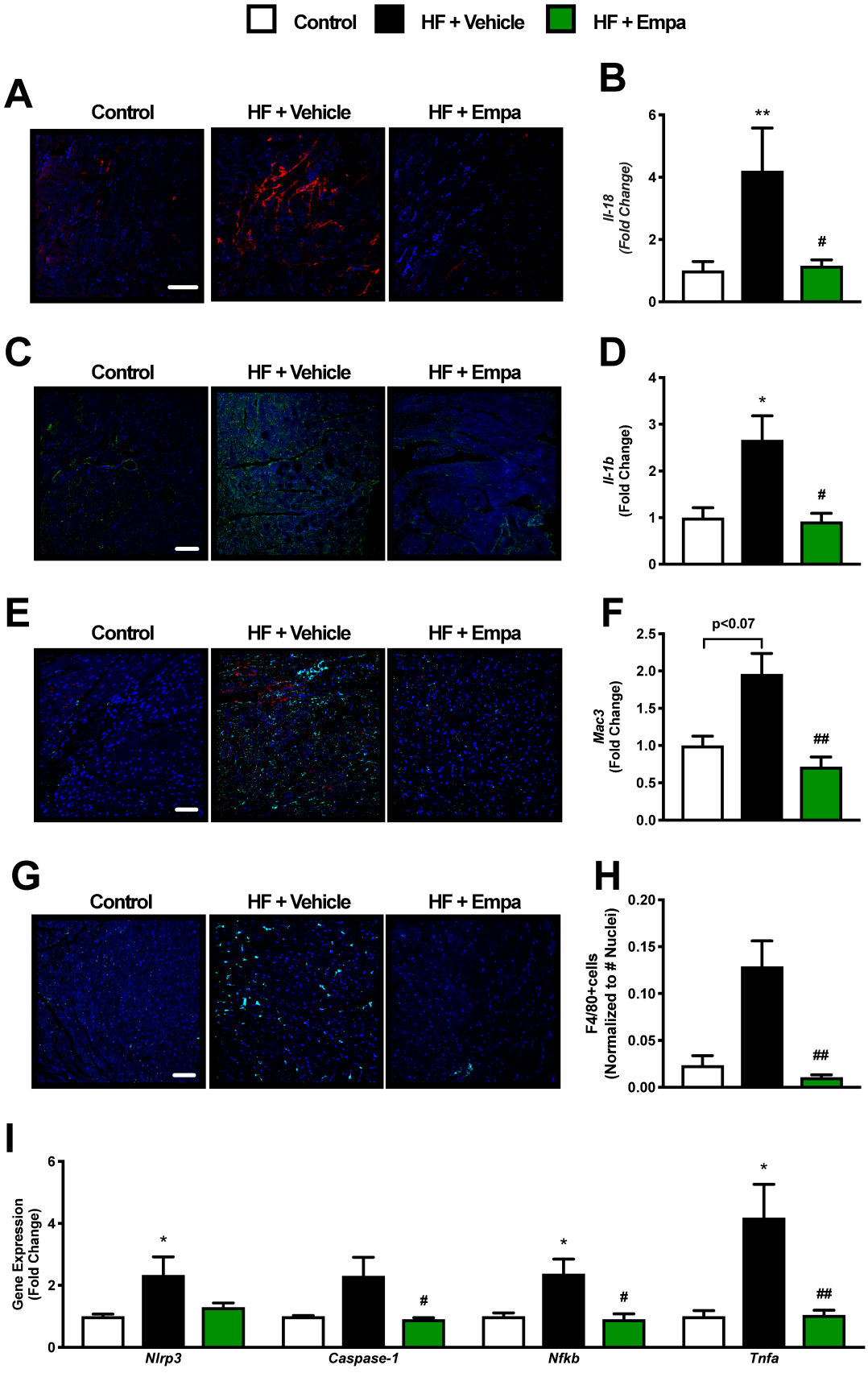
Control
HF + Vehicle
HF + Empa
A
Control
HF + Vehicle
HF + Empa
B
Il-18
(Fold Change)
**
#
C
Control
HF + Vehicle
HF + Empa
D
Il-1b
(Fold Change)
*
#
E
Control
HF + Vehicle
HF + Empa
F
Mac3
(Fold Change)
p<0.07
##
G
Control
HF + Vehicle
HF + Empa
H
F4/80+cells
(Normalized to # Nuclei)
##
I
Gene Expression
(Fold Change)
Nlrp3
Caspase-1
Nfkb
Tnfa

Figure 4.4. Empagliflozin Blunts Inflammasome Priming in Heart Failure in the Absence of Diabetes. Representative images of LV heart sections taken mid-papillary for control and vehicle- or empa-treated HF mice with immuno-staining **(A, C, E, G)** and gene expression **(B, D, F)** for *Il-18* **(A-B)**, *Il-1b* **(C-D)**, and *Mac3* **(E-F)** (n = 4–6)**.** Representative immunofluorescence images and quantification of F4/80 puncta per field of view normalized to number of DAPI **(G-H).** Gene expression of markers of NLRP3 inflammasome (*Nlrp3, Caspase-1, Nfkb* and *Tnfa*) **(L)** (n = 4–6). Gene expression normalized to *Gapdh.* Results are expressed as mean ± SEM. Comparisons between groups were performed using Kruskal-Wallis followed by Dunn's multiple comparisons test**. *p<0.05, **p<0.01 versus control; #p<0.05, ##p<0.01 versus HF vehicle.** EMPA = empagliflozin; DAPI = 4′,6-diamidino-2-phenylindole; GAPDH = glyceraldehyde 3-phosphate dehydrogenase; HF = heart failure; IL = interleukin; LV = left ventricular; MAC3 = lysosomal-associated membrane protein 2; NLRP3 = nucleotide-binding domain-like receptor protein 3; NFκB = nuclear factor kappa-light-chain-enhancer of activated B cells; SEM = standard error of the mean; TNFα = tumor necrosis factor-alpha. Scale bar = 50 μM. Blue = DAPI; Red = IL-18 **(A)**; Green = IL1β **(C)**; Cyan = Mac3 **(E)** or F4/80 **(G)**.

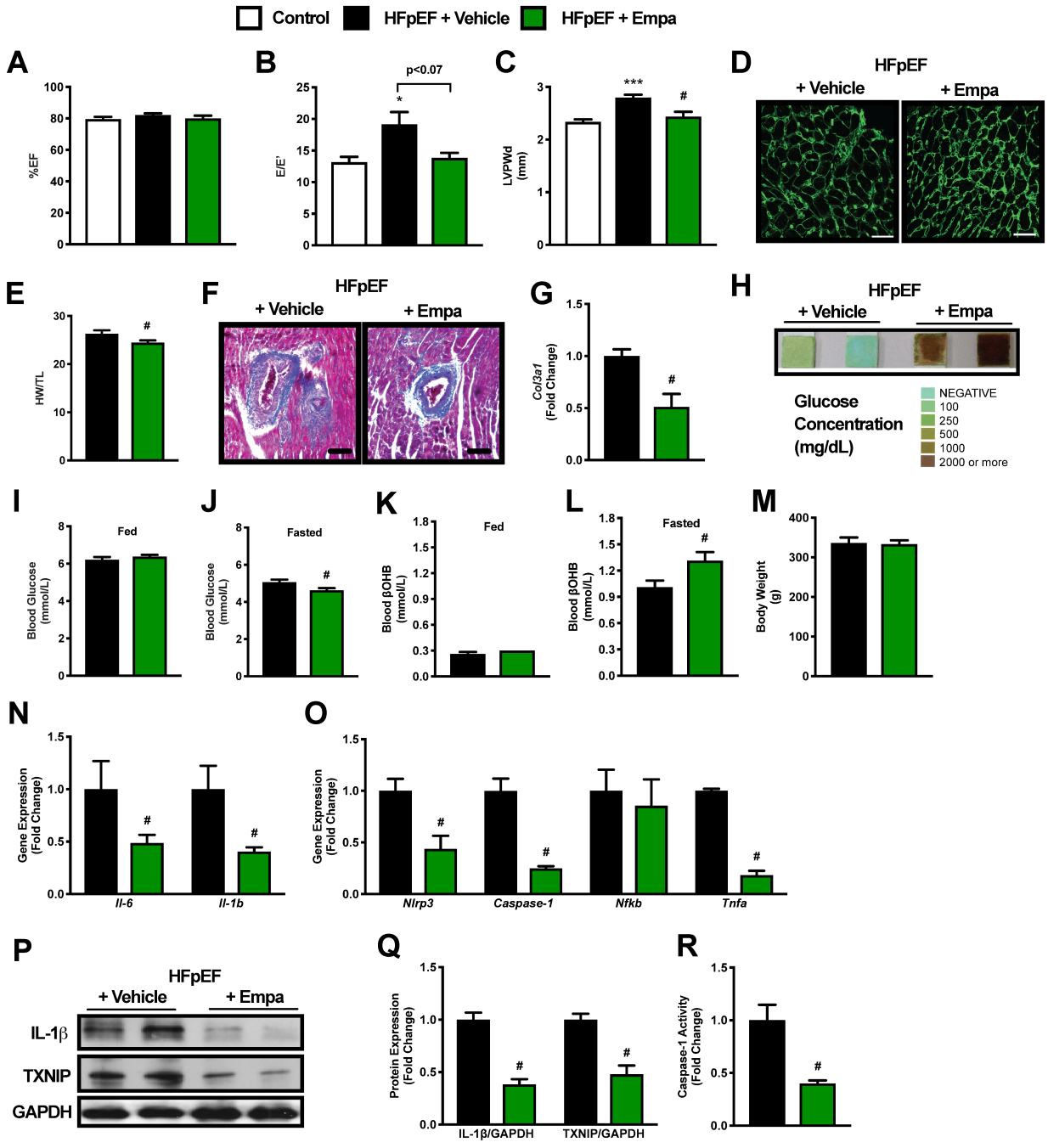

Figure 4.5. Empagliflozin Improves Diastolic Function and Blunts Inflammasome Priming in Heart Failure with Preserved Ejection Fraction. EF **(A)**, E/E′ ratio **(B)**, and LVPW at end-diastole **(C)** based on echocardiographic assessment of control and vehicle- or empagliflozin-treated rats with

HFpEF (n = 8–10). Representative images of WGA stain of LV heart sections taken mid-papillary **(D)** (n = 5) and HW/TL **(E)** (n = 9–10). Masson's Trichrome stain of LV heart sections taken mid-papillary **(F)** (n = 5) and gene expression of a marker of fibrosis (*Col3a1*) **(G)** (n = 4). Estimation of 24-hour urine glucose concentration **(H)** for vehicle- or empagliflozin-treated rats with HFpEF. Circulating glucose **(I-J)** and βOHB levels **(K-L)** under fed conditions or following a 16-hour overnight fast, respectively (n = 7–9). Body weight following 2-week treatment **(M)** (n = 9). Gene expression of markers of inflammation (*Il-6* and *Il-1b*) **(N)** and NLRP3 inflammasome (*Nlrp3, Caspase-1, Nfkb,* and *Tnfa*) **(O)** in heart tissue (n = 4–5). Representative immunoblots **(P)** and quantification of protein expression of markers of inflammation (TXNIP and IL-1β) **(Q)** in heart tissue (n = 4). Caspase-1 protein activity determined in heart tissue **(R)** (n = 4–5). Gene expression normalized to *Gapdh.* Results are expressed as mean ± SEM. Comparisons between groups were performed using Kruskal-Wallis followed by Dunn's multiple comparisons test **(A-C)** or Mann-Whitney U test **(E, G, I-O, Q, R). *p<0.05, ***p<0.001 versus control; #p<0.05 versus HFpEF vehicle.** βOHB = β-hydroxybutyrate; COL3α1 = collagen type III alpha-1; E = early mitral inflow; E′ = tissue Doppler mitral annulus velocity; EMPA = empagliflozin; EF = ejection fraction; GAPDH = glyceraldehyde 3-phosphate dehydrogenase; HF = heart failure; HFpEF = HF with preserved EF; HW/TL = heart weight normalized to tibia length; IL = interleukin; LV = left ventricular; LVPW = LV posterior wall; NFκB = nuclear factor kappa-light-chain-enhancer of activated B cells; NLRP3 = nucleotide-binding domain-like receptor protein 3; SEM = standard error of the mean; TNFα = tumor necrosis factor-alpha; TXNIP = thioredoxin-interacting protein; WGA = wheat germ agglutinin. Scale bars = 50 μM.

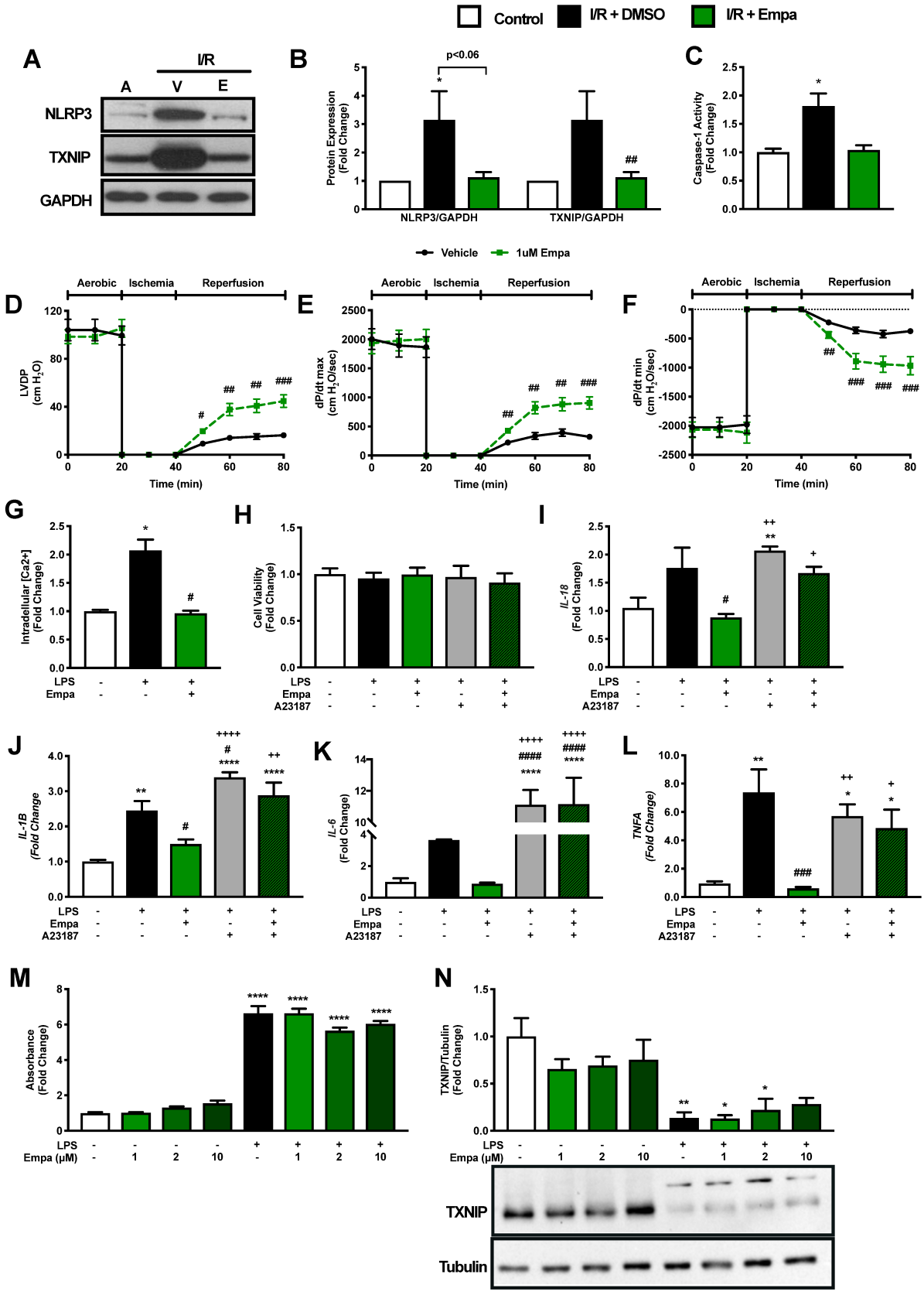
Control
I/R + DMSO
I/R + Empa
A
I/R
A
V
E
NLRP3
TXNIP
GAPDH
B
p<0.06
Protein Expression (Fold Change)
NLRP3/GAPDH
TXNIP/GAPDH
C
Caspase-1 Activity (Fold Change)
Vehicle
1uM Empa
D
Aerobic
Ischemia
Reperfusion
LVDP (cm H2O)
Time (min)
E
dP/dt max (cm H2O/sec)
F
dP/dt min (cm H2O/sec)
G
Intradellular [Ca2+] (Fold Change)
H
Cell Viability (Fold Change)
I
IL-18 (Fold Change)
LPS
Empa
A23187
J
IL-1B (Fold Change)
K
IL-6 (Fold Change)
L
TNFA (Fold Change)
M
Absorbance (Fold Change)
Empa (μM)
N
TXNIP/Tubulin (Fold Change)
TXNIP
Tubulin

Figure 4.6. Empagliflozin Blunts NLRP3 Activation in Isolated Hearts and Inflammation in Cardiomyocytes. Isolated mouse hearts were perfused in the Langendorff mode subjected to 30 min ischemia followed by 40 min of reperfusion to induce activation of NLRP3 inflammasome. Representative immunoblots **(A)** and quantification of protein expression of NLRP3 and TXNIP **(B)** and caspase-1 protein activity **(C)** determined in hearts treated with DMSO with or without empagliflozin (1 μM) during I/R-induced NLRP3 activation (n = 3–5). LVDP **(D)**, dP/dTmax **(E)** and dP/dTmin **(F)** in hearts treated with DMSO with or without empagliflozin (1 μM) during I/R-induced NLRP3 activation (n = 9–10). Intracellular Ca^{2+} concentration of human cardiomyocytes untreated or exposed to LPS (25 μg/ml) with or without empagliflozin (1 μM) **(G)**. Effect of 1 μM empagliflozin on cell viability **(H)** and gene expression for markers of inflammation (*IL-18*, *IL-1B*, *IL-8*, *IL-6* and *TNFA)* **(I-L)** in human cardiomyocytes untreated or exposed to LPS (25 μg/ml) with or without Ca^{2+} ionophore (A23187; 10 μM) (n = 4–6)**.** Murine macrophages were left untreated or exposed to LPS (25 μg/ml) with or without 1 μM, 2 μM or 10 μM empagliflozin. NFκB activation upon Dectin-1 stimulation was determined using QUANTI-Blue (absorbance at 620 nm) **(M)**. Representative immunoblots and quantification of protein expression of TXNIP from RAW-Blue Cells media **(N)**. Gene expression normalized to *B-ACTIN*. Results are expressed as mean ± SEM. Comparisons between groups were performed using Kruskal-Wallis followed by Dunn's multiple comparisons test (**B, C, G-N**) or multiple t-tests (**D-F**)**. *p<0.05, **p<0.001 ****p<0.0001 versus control; #p<0.05, ##p<0.01, ###p<0.001, ####p<0.0001 versus I/R+DMSO or +LPS; +p<0.05, ++p<0.01, +++p<0.0001 versus +LPS/+Empa. Ca^{2+} = calcium ion;** DMSO = dimethyl sulfoxide; DP/DT_{MAX} = rate of contraction; DP/DT_{MIN} = rate of relaxation; EMPA = empagliflozin; I/R = ischemia/reperfusion; IL = interleukin; LPS = lipopolysaccharide; LV = left ventricular; LVDP = LV

developed pressure; NLRP3 = nucleotide-binding domain-like receptor protein 3; SEM = standard error of the mean; TNFα = tumor necrosis factor-alpha; TXNIP = thioredoxin-interacting protein.

Table 4.1. Mouse, Rat and Human Primer Sequences for RT-PCR Reactions.

Gene	Forward primer	Reverse primer
Human B-ACTIN	CTGGCACCCAGCACAATG	GCCGATCCACACGGAGTACT
Human IL-1B	CCAGGGACAGGATATGGAGCA	TTCAACACGCAGGACAGGTACAG
Human IL-18	CATTGACCAAGGAAATCGGC	CACAGAGATAGTTACAGCCATACC
Human IL-8	CTCTTGGCAGCCTTCCTGATT	TATGCACTGACATCTAAGTTCTTTAGCA
Human IL-6	GGTACATCCTCGACGGCATCT	GTGCCTCTTTGCTGCTTTCAC
Human TNFA	GAGGCCAAGCCCTGGTATG	CGGGCCGATTGATCTCAGC
Rat Gapdh	CAAGGTCATCCATGACAACTTTG	GGGCCATCCACAGTCTTCTG
Rat Nfkb	CACTGCTCAGGTCCACTGTC	CTGTCACTATCCCGGAGTTCA
Rat Il-1b	CACCTCTCAAGCAGAGCACAG	GGGTTCCATGGTGAAGTCAAC
Rat Nlrp3	CCAGGGCTCTGTTCATTG	CCTTGGCTTTCACTTCG
Rat Casp1	AGGAGGGAATATGTGGG	AACCTTGGGCTTGTCTT
Rat Pro I	TATGCTTGATCTGTATCTGCCACAAT	TCGCCCTCCCGTTTTTG
Rat Pro III	CAGCTGGCCTTCCTCAGACT	TGCTGTTTTTGCAGTGGTATGTAA
Rat Il-6	GTCAACTCCATCTGCCCTTCA	GGCAGTGGCTGTCAACAT
Rat Tnfa	ACAAGGCTGCCCCGACTAT	CTCCTGGTATGAAGTGGCAAATC
Mouse Gapdh	GCCTTCCGTGTTCCTACCC	TGCCTGCTTCACCACCTTC
Mouse Nfkb	AGCTGCAGAGCCTTCTCAAG	GCCACCTTTTGACAGTGATGAG
Mouse Il-1b	GCCACCTTTTGACAGTGATGAG	AAGGTCCACGGGAAAGACAC
Mouse Nlrp3	GACACGAGTCCTGGTGACTT	GTCCACACAGAAAGTTCTCTTAGC
Mouse Casp1	AACGCCATGGCTGACAAGA	TGATCACATAGGTCCCGTGC
Mouse Il-18	GCCTCAAACCTTCCAAATCA	TGGATCCATTTCCTCAAAGG
Mouse Tnfa	CATCTTCTCAAAATTCGAGTGACAA	TGGGAGTAGACAAGGTACAACCC
Mouse Mac3	CTAGGAGCCGTTCAGTCCAA	CTTGCAGGTGAATACCCCAA

4.7 References

1. Zinman B, Wanner C, Lachin JM et al. Empagliflozin, Cardiovascular Outcomes, and Mortality in Type 2 Diabetes. The New England journal of medicine 2015;373:2117-28.
2. Neal B, Perkovic V, Mahaffey KW et al. Canagliflozin and Cardiovascular and Renal Events in Type 2 Diabetes. The New England journal of medicine 2017;377:644-657.
3. Butler J, Hamo CE, Filippatos G et al. The potential role and rationale for treatment of heart failure with sodium-glucose co-transporter 2 inhibitors. European journal of heart failure 2017;19:1390-1400.
4. McAlister FA, Teo KK, Taher M et al. Insights into the contemporary epidemiology and outpatient management of congestive heart failure. American heart journal 1999;138:87-94.
5. Thomas MC. Type 2 Diabetes and Heart Failure: Challenges and Solutions. Current cardiology reviews 2016;12:249-55.
6. Byrne NJ, Parajuli N, Levasseur JL et al. Empagliflozin Prevents Worsening of Cardiac Function in an Experimental Model of Pressure Overload-Induced Heart Failure. JACC Basic to translational science 2017;2:347-354.
7. Ferrannini E, Mark M, Mayoux E. CV Protection in the EMPA-REG OUTCOME Trial: A "Thrifty Substrate" Hypothesis. Diabetes care 2016;39:1108-14.
8. Lopaschuk GD, Verma S. Empagliflozin's Fuel Hypothesis: Not so Soon. Cell metabolism 2016;24:200-2.

9. von Haehling S, Schefold JC, Lainscak M, Doehner W, Anker SD. Inflammatory biomarkers in heart failure revisited: much more than innocent bystanders. Heart Fail Clin 2009;5:549-60.

10. Gembardt F, Bartaun C, Jarzebska N et al. The SGLT2 inhibitor empagliflozin ameliorates early features of diabetic nephropathy in BTBR ob/ob type 2 diabetic mice with and without hypertension. American journal of physiology Renal physiology 2014;307:F317-25.

11. Tahara A, Kurosaki E, Yokono M et al. Effects of SGLT2 selective inhibitor ipragliflozin on hyperglycemia, hyperlipidemia, hepatic steatosis, oxidative stress, inflammation, and obesity in type 2 diabetic mice. European journal of pharmacology 2013;715:246-55.

12. Tahara A, Kurosaki E, Yokono M et al. Effects of sodium-glucose cotransporter 2 selective inhibitor ipragliflozin on hyperglycaemia, oxidative stress, inflammation and liver injury in streptozotocin-induced type 1 diabetic rats. The Journal of pharmacy and pharmacology 2014;66:975-87.

13. Benetti E, Mastrocola R, Vitarelli G et al. Empagliflozin Protects against Diet-Induced NLRP-3 Inflammasome Activation and Lipid Accumulation. The Journal of pharmacology and experimental therapeutics 2016;359:45-53.

14. Byrne NJ, Levasseur J, Sung MM et al. Normalization of cardiac substrate utilization and left ventricular hypertrophy precede functional recovery in heart failure regression. Cardiovascular research 2016;110:249-57.

15. Matsumura N, Takahara S, Maayah ZH et al. Resveratrol improves cardiac function and exercise performance in MI-induced heart failure through the inhibition of cardiotoxic HETE metabolites. Journal of molecular and cellular cardiology 2018;125:162-173.

16. Sung MM, Byrne NJ, Robertson IM et al. Resveratrol improves exercise performance and skeletal muscle oxidative capacity in heart failure. American journal of physiology Heart and circulatory physiology 2017;312:H842-H853.

17. Koonen DP, Sung MM, Kao CK et al. Alterations in skeletal muscle fatty acid handling predisposes middle-aged mice to diet-induced insulin resistance. Diabetes 2010;59:1366-75.

18. Ferrannini E. The theoretical bases of indirect calorimetry: a review. Metabolism: clinical and experimental 1988;37:287-301.

19. Sung MM, Das SK, Levasseur J et al. Resveratrol treatment of mice with pressure-overload-induced heart failure improves diastolic function and cardiac energy metabolism. Circulation Heart failure 2015;8:128-37.

20. Batchu SN, Law E, Brocks DR, Falck JR, Seubert JM. Epoxyeicosatrienoic acid prevents postischemic electrocardiogram abnormalities in an isolated heart model. Journal of molecular and cellular cardiology 2009;46:67-74.

21. Darwesh AM, El-Azab MF, Abo-Gresha NM, El-Sayed NM, Moustafa YM. Cardioprotective Mechanisms of Exenatide in Isoprenaline-induced Myocardial Infarction: Novel Effects on Myocardial alpha-Estrogen Receptor Expression and IGF-1/IGF-2 System. Journal of cardiovascular pharmacology 2018;71:160-173.

22. Seubert J, Yang B, Bradbury JA et al. Enhanced postischemic functional recovery in CYP2J2 transgenic hearts involves mitochondrial ATP-sensitive K+ channels and p42/p44 MAPK pathway. Circulation research 2004;95:506-14.

23. Baartscheer A, Schumacher CA, Wust RC et al. Empagliflozin decreases myocardial cytoplasmic Na(+) through inhibition of the cardiac Na(+)/H(+) exchanger in rats and rabbits. Diabetologia 2017;60:568-573.

24. Maayah ZH, Elshenawy OH, Althurwi HN, Abdelhamid G, El-Kadi AO. Human fetal ventricular cardiomyocyte, RL-14 cell line, is a promising model to study drug metabolizing enzymes and their associated arachidonic acid metabolites. Journal of pharmacological and toxicological methods 2015;71:33-41.

25. Maayah ZH, El Gendy MA, El-Kadi AO, Korashy HM. Sunitinib, a tyrosine kinase inhibitor, induces cytochrome P450 1A1 gene in human breast cancer MCF7 cells through ligand-independent aryl hydrocarbon receptor activation. Archives of toxicology 2013;87:847-56.

26. Liu Y, Peterson DA, Kimura H, Schubert D. Mechanism of cellular 3-(4,5-dimethylthiazol-2-yl)-2,5-diphenyltetrazolium bromide (MTT) reduction. Journal of neurochemistry 1997;69:581-93.

27. Zordoky BN, Aboutabl ME, El-Kadi AO. Modulation of cytochrome P450 gene expression and arachidonic acid metabolism during isoproterenol-induced cardiac hypertrophy in rats. Drug metabolism and disposition: the biological fate of chemicals 2008;36:2277-86.

28. Livak KJ, Schmittgen TD. Analysis of relative gene expression data using real-time quantitative PCR and the 2(-Delta Delta C(T)) Method. Methods 2001;25:402-8.

29. Darwesh AM, Jamieson KL, Wang C, Samokhvalov V, Seubert JM. Cardioprotective effects of CYP-derived epoxy metabolites of docosahexaenoic acid involve limiting NLRP3 inflammasome activation. Can J Physiol Pharmacol 2019;97:544-556.

30. Wanner C, Lachin JM, Inzucchi SE et al. Empagliflozin and Clinical Outcomes in Patients With Type 2 Diabetes Mellitus, Established Cardiovascular Disease, and Chronic Kidney Disease. Circulation 2018;137:119-129.

31. Komoroski B, Vachharajani N, Feng Y, Li L, Kornhauser D, Pfister M. Dapagliflozin, a novel, selective SGLT2 inhibitor, improved glycemic control over 2 weeks in patients with type 2 diabetes mellitus. Clin Pharmacol Ther 2009;85:513-9.

32. Cherney DZ, Perkins BA, Soleymanlou N et al. Renal hemodynamic effect of sodium-glucose cotransporter 2 inhibition in patients with type 1 diabetes mellitus. Circulation 2014;129:587-97.

33. Mudaliar S, Polidori D, Zambrowicz B, Henry RR. Sodium-Glucose Cotransporter Inhibitors: Effects on Renal and Intestinal Glucose Transport: From Bench to Bedside. Diabetes Care 2015;38:2344-53.

34. Lambers Heerspink HJ, de Zeeuw D, Wie L, Leslie B, List J. Dapagliflozin a glucose-regulating drug with diuretic properties in subjects with type 2 diabetes. Diabetes Obes Metab 2013;15:853-62.

35. Yanai H, Hakoshima M, Adachi H et al. Effects of Six Kinds of Sodium-Glucose Cotransporter 2 Inhibitors on Metabolic Parameters, and Summarized Effect and Its Correlations With Baseline Data. J Clin Med Res 2017;9:605-612.

36. Neeland IJ, McGuire DK, Chilton R et al. Empagliflozin reduces body weight and indices of adipose distribution in patients with type 2 diabetes mellitus. Diab Vasc Dis Res 2016;13:119-26.

37. Ridderstrale M, Andersen KR, Zeller C et al. Comparison of empagliflozin and glimepiride as add-on to metformin in patients with type 2 diabetes: a 104-week

randomised, active-controlled, double-blind, phase 3 trial. The lancet Diabetes & endocrinology 2014;2:691-700.

38. Daniele G, Xiong J, Solis-Herrera C et al. Dapagliflozin Enhances Fat Oxidation and Ketone Production in Patients With Type 2 Diabetes. Diabetes care 2016;39:2036-2041.

39. Ferrannini E, Baldi S, Frascerra S et al. Shift to Fatty Substrate Utilization in Response to Sodium-Glucose Cotransporter 2 Inhibition in Subjects Without Diabetes and Patients With Type 2 Diabetes. Diabetes 2016;65:1190-5.

40. Jorgensen NB, Pedersen J, Vaag AA. EMPA-REG: Glucose excretion and lipid mobilization - not storage - saves lives. Journal of diabetes and its complications 2016;30:753.

41. Ye Y, Bajaj M, Yang HC, Perez-Polo JR, Birnbaum Y. SGLT-2 Inhibition with Dapagliflozin Reduces the Activation of the Nlrp3/ASC Inflammasome and Attenuates the Development of Diabetic Cardiomyopathy in Mice with Type 2 Diabetes. Further Augmentation of the Effects with Saxagliptin, a DPP4 Inhibitor. Cardiovascular drugs and therapy 2017;31:119-132.

42. Li R, Lu K, Wang Y et al. Triptolide attenuates pressure overload-induced myocardial remodeling in mice via the inhibition of NLRP3 inflammasome expression. Biochemical and biophysical research communications 2017;485:69-75.

43. Verma S, Garg A, Yan AT et al. Effect of Empagliflozin on Left Ventricular Mass and Diastolic Function in Individuals With Diabetes: An Important Clue to the EMPA-REG OUTCOME Trial? Diabetes Care 2016.

44. Doi R, Masuyama T, Yamamoto K et al. Development of different phenotypes of hypertensive heart failure: systolic versus diastolic failure in Dahl salt-sensitive rats. Journal of hypertension 2000;18:111-20.

45. Klotz S, Hay I, Zhang G, Maurer M, Wang J, Burkhoff D. Development of heart failure in chronic hypertensive Dahl rats: focus on heart failure with preserved ejection fraction. Hypertension 2006;47:901-11.

46. Ponikowski P, Voors AA, Anker SD et al. 2016 ESC Guidelines for the diagnosis and treatment of acute and chronic heart failure: The Task Force for the diagnosis and treatment of acute and chronic heart failure of the European Society of Cardiology (ESC)Developed with the special contribution of the Heart Failure Association (HFA) of the ESC. European heart journal 2016;37:2129-2200.

47. Segura AM, Frazier OH, Buja LM. Fibrosis and heart failure. Heart failure reviews 2014;19:173-85.

48. Sattar N, McLaren J, Kristensen SL, Preiss D, McMurray JJ. SGLT2 Inhibition and cardiovascular events: why did EMPA-REG Outcomes surprise and what were the likely mechanisms? Diabetologia 2016;59:1333-1339.

49. Liu Y, Lian K, Zhang L et al. TXNIP mediates NLRP3 inflammasome activation in cardiac microvascular endothelial cells as a novel mechanism in myocardial ischemia/reperfusion injury. Basic research in cardiology 2014;109:415.

50. Vrhovac I, Balen Eror D, Klessen D et al. Localizations of Na(+)-D-glucose cotransporters SGLT1 and SGLT2 in human kidney and of SGLT1 in human small intestine, liver, lung, and heart. Pflugers Archiv : European journal of physiology 2015;467:1881-98.

51. Murakami T, Ockinger J, Yu J et al. Critical role for calcium mobilization in activation of the NLRP3 inflammasome. Proceedings of the National Academy of Sciences of the United States of America 2012;109:11282-7.

52. Forrester MT, Seth D, Hausladen A et al. Thioredoxin-interacting protein (Txnip) is a feedback regulator of S-nitrosylation. J Biol Chem 2009;284:36160-6.

53. Verma S, McMurray JJV, Cherney DZI. The Metabolodiuretic Promise of Sodium-Dependent Glucose Cotransporter 2 Inhibition: The Search for the Sweet Spot in Heart Failure. JAMA cardiology 2017;2:939-940.

54. Rosenstock J, Jelaska A, Zeller C et al. Impact of empagliflozin added on to basal insulin in type 2 diabetes inadequately controlled on basal insulin: a 78-week randomized, double-blind, placebo-controlled trial. Diabetes, obesity & metabolism 2015;17:936-48.

55. Wilson PW, Kannel WB, Silbershatz H, D'Agostino RB. Clustering of metabolic factors and coronary heart disease. Archives of internal medicine 1999;159:1104-9.

56. Bolinder J, Ljunggren O, Johansson L et al. Dapagliflozin maintains glycaemic control while reducing weight and body fat mass over 2 years in patients with type 2 diabetes mellitus inadequately controlled on metformin. Diabetes, obesity & metabolism 2014;16:159-69.

57. Cefalu WT, Leiter LA, Yoon KH et al. Efficacy and safety of canagliflozin versus glimepiride in patients with type 2 diabetes inadequately controlled with metformin (CANTATA-SU): 52 week results from a randomised, double-blind, phase 3 non-inferiority trial. Lancet 2013;382:941-50.

58. Heerspink HJ, Perkins BA, Fitchett DH, Husain M, Cherney DZ. Sodium Glucose Cotransporter 2 Inhibitors in the Treatment of Diabetes Mellitus: Cardiovascular and

Kidney Effects, Potential Mechanisms, and Clinical Applications. Circulation 2016;134:752-72.

59. Fitchett D, Zinman B, Wanner C et al. Heart failure outcomes with empagliflozin in patients with type 2 diabetes at high cardiovascular risk: results of the EMPA-REG OUTCOME(R) trial. Eur Heart J 2016;37:1526-34.

60. Heise T, Seewaldt-Becker E, Macha S et al. Safety, tolerability, pharmacokinetics and pharmacodynamics following 4 weeks' treatment with empagliflozin once daily in patients with type 2 diabetes. Diabetes Obes Metab 2013;15:613-21.

61. Heise T, Seman L, Macha S et al. Safety, tolerability, pharmacokinetics, and pharmacodynamics of multiple rising doses of empagliflozin in patients with type 2 diabetes mellitus. Diabetes Ther 2013;4:331-45.

62. Heise T, Jordan J, Wanner C et al. Pharmacodynamic Effects of Single and Multiple Doses of Empagliflozin in Patients With Type 2 Diabetes. Clinical therapeutics 2016;38:2265-2276.

63. Chen L, LaRocque LM, Efe O, Wang J, Sands JM, Klein JD. Effect of Dapagliflozin Treatment on Fluid and Electrolyte Balance in Diabetic Rats. Am J Med Sci 2016;352:517-523.

64. Stender RN, Engler WJ, Braun TM, Hankenson FC. Establishment of blood analyte intervals for laboratory mice and rats by use of a portable clinical analyzer. J Am Assoc Lab Anim Sci 2007;46:47-52.

65. Stechman MJ, Ahmad BN, Loh NY et al. Establishing normal plasma and 24-hour urinary biochemistry ranges in C3H, BALB/c and C57BL/6J mice following acclimatization in metabolic cages. Lab Anim 2010;44:218-25.

66. Tikkanen I, Narko K, Zeller C et al. Empagliflozin reduces blood pressure in patients with type 2 diabetes and hypertension. Diabetes Care 2015;38:420-8.

67. Levelt E, Mahmod M, Piechnik SK et al. Relationship Between Left Ventricular Structural and Metabolic Remodeling in Type 2 Diabetes. Diabetes 2016;65:44-52.

68. Psaty BM, Lumley T, Furberg CD et al. Health outcomes associated with various antihypertensive therapies used as first-line agents: a network meta-analysis. JAMA 2003;289:2534-44.

69. Emdin CA, Rahimi K, Neal B, Callender T, Perkovic V, Patel A. Blood pressure lowering in type 2 diabetes: a systematic review and meta-analysis. JAMA 2015;313:603-15.

70. Olde Engberink RH, Frenkel WJ, van den Bogaard B, Brewster LM, Vogt L, van den Born BJ. Effects of thiazide-type and thiazide-like diuretics on cardiovascular events and mortality: systematic review and meta-analysis. Hypertension 2015;65:1033-40.

71. Verma S, McMurray JJV. SGLT2 inhibitors and mechanisms of cardiovascular benefit: a state-of-the-art review. Diabetologia 2018;61:2108-2117.

72. Shi X, Verma S, Yun J et al. Effect of empagliflozin on cardiac biomarkers in a zebrafish model of heart failure: clues to the EMPA-REG OUTCOME trial? Molecular and cellular biochemistry 2017;433:97-102.

73. Verma S, Rawat S, Ho KL et al. Empagliflozin Increases Cardiac Energy Production in Diabetes: Novel Translational Insights Into the Heart Failure Benefits of SGLT2 Inhibitors. JACC Basic to translational science 2018;3:575-587.

74. Abdurrachim D, Teo XQ, Woo CC et al. Empagliflozin reduces myocardial ketone utilization while preserving glucose utilization in diabetic hypertensive heart disease: A

hyperpolarized (13) C magnetic resonance spectroscopy study. Diabetes, obesity & metabolism 2018.

75. Santos-Gallego CG, Requena-Ibanez JA, San Antonio R et al. Empagliflozin Ameliorates Adverse Left Ventricular Remodeling in Nondiabetic Heart Failure by Enhancing Myocardial Energetics. J Am Coll Cardiol 2019;73:1931-1944.

76. Pabel S, Wagner S, Bollenberg H et al. Empagliflozin directly improves diastolic function in human heart failure. European journal of heart failure 2018;20:1690-1700.

77. Yang CC, Chen YT, Wallace CG et al. Early administration of empagliflozin preserved heart function in cardiorenal syndrome in rat. Biomed Pharmacother 2019;109:658-670.

78. Chilton R, Tikkanen I, Cannon CP et al. Effects of empagliflozin on blood pressure and markers of arterial stiffness and vascular resistance in patients with type 2 diabetes. Diabetes Obes Metab 2015;17:1180-93.

79. Habibi J, Aroor AR, Sowers JR et al. Sodium glucose transporter 2 (SGLT2) inhibition with empagliflozin improves cardiac diastolic function in a female rodent model of diabetes. Cardiovascular diabetology 2017;16:9.

80. Verma S, Garg A, Yan AT et al. Effect of Empagliflozin on Left Ventricular Mass and Diastolic Function in Individuals With Diabetes: An Important Clue to the EMPA-REG OUTCOME Trial? Diabetes Care 2016;39:e212-e213.

81. Connelly KA, Zhang Y, Visram A et al. Empagliflozin Improves Diastolic Function in a Nondiabetic Rodent Model of Heart Failure With Preserved Ejection Fraction. JACC Basic Transl Sci 2019;4:27-37.

82. Van Linthout S, Tschope C. Inflammation - Cause or Consequence of Heart Failure or Both? Current heart failure reports 2017;14:251-265.

83. Butts B, Gary RA, Dunbar SB, Butler J. The Importance of NLRP3 Inflammasome in Heart Failure. J Card Fail 2015;21:586-93.

84. Kusaka H, Koibuchi N, Hasegawa Y, Ogawa H, Kim-Mitsuyama S. Empagliflozin lessened cardiac injury and reduced visceral adipocyte hypertrophy in prediabetic rats with metabolic syndrome. Cardiovasc Diabetol 2016;15:157.

85. Lin B, Koibuchi N, Hasegawa Y et al. Glycemic control with empagliflozin, a novel selective SGLT2 inhibitor, ameliorates cardiovascular injury and cognitive dysfunction in obese and type 2 diabetic mice. Cardiovasc Diabetol 2014;13:148.

86. Mustroph J, Wagemann O, Lucht CM et al. Empagliflozin reduces Ca/calmodulin-dependent kinase II activity in isolated ventricular cardiomyocytes. ESC heart failure 2018;5:642-648.

87. LEE Y-H, KIM SR, BAE J et al. SGLT2 Inhibitors Suppress NLRP3 Inflammasome Activity via Changes in Ketones and Insulin in Type 2 Diabetes and Cardiovascular Diseases. Diabetes 2018;67.

88. Leng W, Ouyang X, Lei X et al. The SGLT-2 Inhibitor Dapagliflozin Has a Therapeutic Effect on Atherosclerosis in Diabetic ApoE(-/-) Mice. Mediators of inflammation 2016;2016:6305735.

Chapter Five

General Discussion

5.1 Overview

Although current therapeutic options have improved outcomes and increased survival, the prognosis of patients with HF remains low. Pharmacotherapies that may improve or restore cardiac ATP production, which is otherwise impaired in HF, have recently gained popularity. Nonetheless, our understanding of the changes in myocardial energetics, and therefore altered production of ATP, during the development, progression and regression of HF is still poorly understood. A such, this has made it difficult to develop ideal pharmacological targets. That being said, since changes in myocardial fuel selection appear to occur at the transcriptional level of the metabolic enzymes, it remains questionable whether the resulting impairments in FA and glucose oxidation rates are reversible in HF and can therefore be corrected by interventions. Our results suggest that even following severe HF (EF <30%), LV hypertrophy, systolic and diastolic dysfunction are nearly entirely reversed upon removal of the elevated aortic afterload. This is not surprising considering the potential of reverse remodeling and reversal of contractile dysfunction in patients following long-term mechanical unloading upon implantation of LV assist devices (1-5). Interestingly, the expression of AMPK, which is widely recognized as a key sensor of cellular energy status (6-9), was completely restored following normalization of the aortic afterload. In addition to its role in metabolism, AMPK is known to regulate cardiac remodeling, autophagy and endoplasmic reticulum stress (10); as such, normalization of its expression in the regressed heart may also be indicative of other pathways that have recovered following DB.

Nonetheless, we also provide evidence that myocardial FA and glucose oxidation rates and associated gene expression are similarly reversed in the regression of HF. Consistent with our

findings, expression of key transcriptional regulators of myocardial metabolism appears to be restored following mechanical unloading in humans (11), although this finding has been challenged (12). Cardiac substrate oxidation was also restored following recovery from borderline HF (EF ~40%) induced by pacing in dogs (13). However, our results further explored the temporal profile of restored cardiac energetics following regression from decompensated hypertrophy and severe HF (EF <30%) to show that improved FA and glucose oxidation precede improvement in cardiac contractility. Interestingly, the findings by Qanud *et al.* also suggest that recovered hearts fail to increase FA and glucose oxidation in response to acute pacing stress compared to controls, suggesting that following HF, cardiac energetics may only be restored during normal physiological conditions. Overall, these studies highlight the metabolic resilience of the heart and provide evidence that recovery of impaired substrate utilization occurs prior to recovery of contractile function. It is tempting to speculate, therefore, that improved myocardial energetics is essential to restoring proper mechanical function, providing rationale for novel drug targets aimed at increasing energy production of the failing heart.

Of note, the anti-diabetic drug, empagliflozin, has recently gained extreme popularity for its potential in improving cardiac energy production, thereby reducing CV complications. Based on the fact that empagliflozin, and other SGLT2 inhibitors, increase the production of βOHB in the setting of diabetes, it has been proposed that it enhances myocardial ketone body metabolism, thereby enhancing cardiac efficiency (14,15). Importantly, infusion of βOHB was recently shown to partially mimic the improvements in cardiac energetics and survival seen with empagliflozin (16). Interestingly, however, the beneficial hemodynamic effects of βOHB infusion occurred without alterations in myocardial external energy efficiency (MEE) (17). The theory that

empagliflozin's benefits are mediated through βOHB is further supported by the recent finding that increased availability of βOHB increases rates of myocardial ketone oxidation and overall energy production in the isolated failing mouse heart (18). Regardless of the potential beneficial effects of elevated circulating ketone bodies, empagliflozin failed to increase circulating βOHB in HF the absence of diabetes in our study. Contrary to our findings, others have demonstrated that empagliflozin increases circulating ketone levels in a non-diabetic models of ischemic heart disease in rats (19) and pigs (20). These differences may be explained by the 3-times higher dose of empagliflozin administered in the first study (19) and longer duration of treatment in the latter (20) and/or the type of HF in question in both studies. Of note, fasting βOHB levels were significantly elevated following chronic, but not acute, treatment with empagliflozin and this was more pronounced in type 2 diabetics than nondiabetic patients (21). In support of our findings, the cardioprotective effects of empagliflozin have otherwise been shown to be mediated by improved mitochondrial function, in the absence of βOHB (22). We also conducted experiments to determine whether empagliflozin induced changes in myocardial oxidation rates of ketone bodies, glucose or FAs and found there to be no significant alterations in the energetic profile of the failing heart in response to empagliflozin-treatment. Interestingly, this is also contrary to recent findings that provide indirect measure of enhanced cardiac ketone utilization by empagliflozin in both rats with MI (19) and diabetic patients (23) and increased myocardial uptake of ketones and FAs in nondiabetic pigs with MI (20). However, none of the aforementioned studies provide direct measurement of ketone body oxidation in hearts treated with empagliflozin. Interestingly, empagliflozin was also recently shown to reduce myocardial utilization of the ketone body, acetoacetate, despite increasing fasting blood βOHB levels (24). Moreover, another study reported empagliflozin increased overall ATP production in a diabetic heart (25). It is important to mention

that the decrease in ATP production in the diabetic model was accompanied by reduced cardiac ketone oxidation in this study (18). This is a clear and noteworthy difference to the failing heart, which has been shown to increase reliance on ketone bodies (18,26). Therefore, it is stands to reason that the potential of empagliflozin to increase cardiac ketone oxidation may be limited in the failing heart, which is thought to already have an elevated ketone oxidation profile and may explain the differences between these findings. Of note, these data are contrary to our earlier results suggesting that normalization of cardiac energetics are required to drive improvements in cardiac mechanical function. Overall, these findings suggest that enhanced myocardial energy production is not imperative for improved cardiac systolic function, as seen upon treatment with empagliflozin **(Figure 5.1)**.

Importantly, although direct action in the heart was previously considered unlikely due to negligible expression of SGTL2 in the heart (27) and low binding affinity of empagliflozin to SGTL1 (28), recent findings have suggested that empagliflozin may target other ion channels. Empagliflozin was shown to reduce myocardial Na^+, which is otherwise elevated in the failing heart (29,30), via NHE1 and subsequently increase mitochondrial Ca^{2+} and decrease cytoplasmic Ca^{2+} concentrations (31). This is further supported by the finding that empagliflozin reduces sarcoplasmic reticulum Ca^{2+} leak in failing ventricular myocytes (32). Altogether, these effects are thought to occur secondary to NHE1 inhibition, mediated by the sarcolemmal and mitochondrial Na^+/Ca^{2+} exchanger (NCX) (33,34). This direct inhibitory effect of NHE1 in the heart appears to be consistent with other SGTL2 inhibitors and is thought to promote vasodilation in the healthy heart (35). It is also possible that inhibition of NHE by empagliflozin in endothelial cells and/or vascular smooth muscle cells induces lowering of cytoplasmic Ca^{2+}, thereby explaining these

beneficial vasodilator effects. In addition, empagliflozin was shown to delay ischaemic contracture, without reducing I/R injury, through inhibition of NHE1 in an isolated murine heart (36). The possibility that empagliflozin has direct interaction with the NHE1 in the heart is further supported by the fact that SGLT2 colocalizes with the renal NHE3 (31,37). Interestingly, activity of NHE1 (31,38,39) and expression of NHE3 (40,41) have both been shown to be increased in HF. Of importance, elevated NHE1 may explain the rise in increased intracellular Ca^{2+} and resulting contractile dysfunction, which are both improved upon treatment with empagliflozin in our studies. Furthermore, since increased mitochondrial Ca^{2+} has been shown to prevent sudden cardiac death in a swine model of HF (42), the effects of empagliflozin on myocardial NHE1 may also explain the reductions in sudden cardiac death reported in the EMPA-REG Outcomes trial (43). In support of this potential mechanism of empagliflozin, inhibition of NHE1 has shown to improve cardiac remodeling and contractile function in cardiac hypertrophy/HF (44-49). Lastly, although not measured in our study, SGLT2 inhibitors have also been shown to increase activity of SERCA2a associated with improved cardiac contractility in diabetic mice (50,51). Altogether, these data indicate the possibility of an empagliflozin-mediated cardiac benefit through improved Ca^{2+} handling in the heart in an SGLT2-independent manner, perhaps via NHE1.

Furthermore, based on the fact that empagliflozin is highly selective for SGLT2 over SGLT1 (28,52) and the dose utilized in our studies is well below the IC_{50} of SGLT1 (52), it is similarly unlikely that the direct effects seen in isolated cardiomyocytes are a result of empagliflozin action on SGLT1. Moreover, given that SGLT1 is not particularly localized to the cardiomyocytes but rather in the capillaries in the human heart (27), the inhibition of cardiac inflammation by empagliflozin ought to be mediated through an SGLT1/2-independent pathway. In addition, one

would expect that dual inhibition of SGLT1/2 would have a negative, not positive, myocardial effect (53,54). Particularly, although canagliflozin is considered to exert substantial inhibition of SGLT1 based on plasma concentrations resulting from commonly used oral dosages (55), this is not the case for empagliflozin (56).

Attenuation of pressure overload-induced cardiac remodeling, fibrosis and dysfunction has been previously associated with inhibition of the NLRP3 inflammasome (57-59). Moreover, deletion of NLRP3 has been shown to protect against I/R injury in isolated mouse hearts (60). However, NLRP3 expression is down-regulated in the heart following aortic banding and global NLRP3 deficiency was shown to accelerate resulting cardiac dysfunction (61). As such, the role of the inflammasome in cardiac injury is far from understood. Perhaps NLRP3 inflammasome priming is crucial during the early adaptive cardiac remodeling and therefore early NLRP3 deletion has detrimental consequences, but inhibition at a later stage may have beneficial effects. In our study, empagliflozin treatment was initiated 2 weeks post-TAC, once HF was already established, and the reduction in NLRP3 inflammasome priming was associated with lessened cardiac dysfunction. However, whether or not this is a causal relationship requires additional studies.

As the role of the immune system in HF continues to evolve, mechanisms of NLRP3 inflammasome activation are a matter of debate. It should be noted that nutrient-state may be involved in regulating activation of the NLRP3 inflammasome (62). Particularly, high-glucose concentrations are thought to facilitate the production of IL-1β (63,64) and may regulate activation of the NLRP3 inflammasome and resulting inflammation during diabetes (65,66). Furthermore, activation of the NLRP3 inflammasome has been shown to contribute to insulin resistance and

glucose intolerance (67). In contrast, diabetic patients have been reported to have defective IL-1β production (68), particular in patients with poor metabolic control (65), nevertheless suggesting that glycemic control may be essential for proper immune function. As such, it has been proposed that aberrant NLRP3 inflammasome priming and immune response is induced by the diabetic condition and regulation by SGLT2 inhibitors is mediated through improved glycemic control. In fact, SGLT2 inhibitors may modulate NRLP3-mediated inflammation through regulating blood glucose and lipid levels, independent of direct action of macrophages (69,70). In support of this, canagliflozin has been shown to exert anti-inflammatory properties in macrophage and monocyte cells as well as immunodeficient mice, which is thought to be mediated through inhibition of intracellular glucose metabolism (71). However, the data presented herein provides evidence that cardiac NLRP3 inflammasome activation occurs in HF regardless of the presence of hyperglycemia **(Figure 5.1)**. In addition, the ability of empagliflozin to modulate cardiac inflammation occurred without any changes in cardiac glucose utilization, suggesting that empagliflozin mediates inflammation via NLRP3 inflammasome independent of glycemic control.

It is noteworthy that these anti-inflammatory properties are considered to be a class effect, as another SGTL2 inhibitor, dapagliflozin, attenuated expression of NLRP3 inflammasome complex in the aortic root of diabetic mice with atherosclerosis (69). Altogether, attenuated cardiac NLRP3 inflammasome priming, inflammatory cytokines and macrophage infiltration upon treatments with SGTL2 inhibitors have been well-documented in experimental models of obesity/diabetes (51,72). Lastly, empagliflozin reduced cardiac biomarkers of HF in zebrafish associated with attenuated inflammation; although NLRP3 inflammasome was not measured (73). As such, our data show for

the first time that reductions in NLRP3 inflammasome-mediated inflammation are associated with reduced cardiac dysfunction in HF in the absence of diabetes and obesity.

The ability of SGLT2 inhibitors to reduce cardiac fibrosis has been well documented in experimental models of obesity/diabetes (72,74,75), but is less clear in the absence of hyperglycemia. Particularly, while both empagliflozin (20) and dapagliflozin (76) were shown to attenuate fibrotic remodeling in the infarcted, nondiabetic heart, empagliflozin failed to reduce cardiac fibrosis in a nondiabetic rat model of HFpEF (77). Interestingly, our results show that collagen deposit is significantly reduced in the heart following treatment with empagliflozin in an experimental model of HFpEF, but not HFrEF. Furthermore, diastolic dysfunction was similarly only improved in our model of HFpEF, suggesting that cardiac fibrosis is tightly coupled with diastolic, but not systolic, dysfunction. Importantly, is has been proposed that cardiac fibrosis occurs as a result of chronic inflammation (78,79), thereby exacerbating cardiac dysfunction and HF (80,81). In fact, inhibition of the NLRP3 inflammasome has been associated with attenuated myocardial remodeling and fibrosis (57-59,82). In addition, various SGLT2 inhibitors have been reported to slightly reduce biomarkers of inflammation, particularly TNFα, in type 2 diabetic patients (83-85), as well as in the kidney (86) and heart (87) of mice. In agreement, our results suggest that cardiac inflammation is reduced upon treatment with empagliflozin, evident by attenuated expression of NLRP3 complex, pro-inflammatory cytokines, and macrophage infiltration. While others have suggested that SGLT2 inhibitors may mediate their anti-inflammatory effects via cardiac fibroblasts (72), we highlight a novel role of cardiomyocytes. Interestingly, despite evident reductions in cardiac inflammation in both experimental models of HF upon treatment with empagliflozin, this was not associated with reductions in cardiac fibrotic

remodeling in HFrEF. Meanwhile, it is important to note that elevated fibrotic remodeling was not resolved in our experimental model of regressed HF, despite complete restoration of diastolic and systolic cardiac function. Altogether, these data suggest that reducing myocardial fibrosis is not pertinent to improving cardiac function in HF.

Of importance, since SGLT2 inhibitors have been shown to elevated circulating ketone bodies (88) and βOHB has been shown to inhibit the NLRP3 inflammasome (89), it stands to reason that the anti-inflammatory potential of empagliflozin may be mediated through the signaling properties of ketone bodies. Importantly, these signaling properties occur without oxidation of βOHB in the TCA cycle (89). Particularly, elevated circulating βOHB has been shown to reduce expression of NLRP3 complex and associated pro-inflammatory cytokines *in vivo* in the spinal cord of mice (90) and in retina of diabetic mice (91), as well as blunt NLRP3-mediated neutrophil and/or macrophage infiltration into the peritoneum (89), spinal cord (90), liver (92) and kidney (93,94) of experimental models. Concurrently, ketogenic diet, but not necessarily βOHB specifically, was similarly shown to decrease NLRP3 inflammasome activation in the brain of a murine model of ischemic stroke (95). In addition, βOHB has also been shown to inhibit NLRP3-mediated inflammation in isolated murine microglia cells (96), bone marrow-derived dendritic cells (93) and macrophages (89,97), murine and human neutrophils (97) and monocytes (89), human and rat glioblastoma cells (98) and human neuroblastoma (95) and hepatoma (92) cells. Altogether, these data indicate the potential of elevated ketone bodies, particularly βOHB, in counteracting inflammatory-related organ dysfunction. Interestingly, the ability of βOHB to mediate anti-inflammatory effects via inhibition of the NLRP3 inflammasome has been challenged by Neudorf et al. (99) who showed that a rise in blood βOHB upon exogenous administration of either ketone

salt or ketone monoester supplementation was associated with activation of caspase-1 and expression of IL-1β in whole blood of healthy humans. Regardless of the potential effect of in ketone bodies on inflammation, we did not observe elevated βOHB in response to treatment with empagliflozin in our model of HFrEF, despite reductions in cardiac inflammation and dysfunction. Together, this suggests that the beneficial anti-inflammation properties of empagliflozin are not mediated through elevated circulating ketones. Nonetheless, the possible effects of βOHB on NLRP3-mediated inflammation in the heart are less well-characterize than other tissues including the kidneys and brain. Therefore, this potential therapeutic benefit of βOHB in the heart should be further explored using ketogenic diets as well as diets supplemented with 1,3-butanediol (93,94) and other sources of βOHB, such as ketone esters (100), particularly in states of energy deficiency such as HF.

Although majority of the studies have focused on the effects of SGLT2 inhibition in the setting of obesity and diabetes, there has been less work identifying other clinical groups who may benefit from treatment with empagliflozin, for example in the absence of hyperglycemia. Interestingly, empagliflozin was found to delay ischaemic contracture, without reducing cardiac injury, through inhibition of NHE1 in an isolate mouse heart (36). Furthermore, empagliflozin improved mitochondrial respiration in a nondiabetic isolated perfused heart subjected to I/R injury, despite no reductions in infarct size (22). These findings are consistent with no reductions in MI in EMPA-REG Outcomes but shed light on potential mechanisms for long term protection from development of HF. Additionally, early treatment with empagliflozin protected from cardiorenal syndrome (87). Of importance, the favorable effects of empagliflozin on aortic stiffness, vascular resistance and diastolic function (75,101,102) are encouraging for patients who present with HFpEF. Indeed, the

beneficial cardiac effects in absence of diabetes were preserved in our model of HFpEF as well others' (77), without any effect on systolic BP. These improvements are thought to occur upon improving myofilament passive stiffness, without any changes to Ca^{2+} cycling (103). Altogether, our data supports the effectiveness of treatment with empagliflozin in HF resulting from diverse etiologies and demonstrate, for the first time, that these beneficial effects are mediated through immune regulation, independent of glycemic control.

While designing pharmacological therapies to target the metabolic inflexibility of the heart seems promising, our findings suggest that improved substrate utilization is not pertinent to improving HF. Rather, strategies that reduce cardiac inflammation, such as SGLT2-inhibitors, may be effective in treating a broad range of CVD. This begs the question: are SGLT2 inhibitors the new line of treatment for both diabetic and nondiabetic heart disease?

5.2 Limitations

A major limitation of these studies is the use of experimental models in attempt to recapitulate human disease. First off, considering that the murine heart is highly glycolytic (104), up-regulation of glycolysis rates may not be detected in our mouse model of HF (105-107). It should be noted that rodents used in these studies are relatively young compared to the typical age of onset of HF in humans, particularly due to the more desirable level of cardiac dysfunction achieved in an 8-week old mouse. Furthermore, the high rates of intraoperative mortality that exist with this technically demanding procedure only worsen in aged mice. As such, the finding that cardiac

dysfunction and more importantly, impaired cardiac energy production, are completely reversible following normalization of the elevated aortic afterload leading to severe HF, may be limited to a young, murine heart. As mentioned previously, the sudden onset of HF is a major restriction of the TAC model of HF, which does not entirely mimic the gradual progression of pressure-overload and transition from hypertrophy that occurs over decades in patients. Lastly, BP is often controlled in the clinical setting; however, pressure-overload is maintained for the duration of the study, which may limit the potential of cardiac improvement in these models. Nonetheless, the use of these animal models in these studies has provided specific insight into the potential mechanisms involved in the regression of HF as well the potential cardiac benefit of empagliflozin, particularly in the absence of diabetes or other comorbidities.

It should be highlighted that there were notable differences between the degree of cardiac dysfunction and impaired energetics measured in our studies. Although both *in vivo* and *ex vivo* cardiac function were only slightly worse in our TAC control group in the DB study compared to TAC vehicle group in empagliflozin study (EF of ~22% vs 27% and cardiac work of 2.71 vs 3.3 ml*mmHg/min, respectively), there appeared to be a profound difference in substrate use between the two studies. Particularly, while the *ex vivo* cardiac work of the TAC hearts in DB study was only ~27% reduced compared to those of the empagliflozin study, FA and glucose use were ~60-70% reduced, which may suggest that the failing hearts in the DB study were more efficient (producing less ATP for work required). This is unlikely the case and may be explained by measurement differences in *ex vivo* substrate flux between cohorts and is therefore a major limitation in our studies. However, it should be noted that ATP production is not entirely coupled to mechanical function, as ATP is utilized in the heart for basic function of membrane transport

systems (such as Na^+/K^+-ATPase) in addition to its role in contraction/relaxation of the sarcomere. Nonetheless, since we did not include a healthy control heart in the *ex vivo* experiments for the empagliflozin study, we cannot discuss these rates as a matter of relative decline from control.

5.3 Future Directions

We demonstrate that complete recovery of impaired cardiac substrate metabolism precedes the restoration of impaired cardiac contractile function in severe HF. However, whether or not regressed hearts exert a normal response to a second, delayed stress such as ischemia or reoccurring pressure-overload has yet to be determined. As such, we intend to further explore the resilience of the heart upon subjecting regressed (DB) hearts to additional testing in order to elucidate whether HF pre-disposes or protects the heart to future stressors.

One finding of our study was that treatment with empagliflozin resulted in diuretic effects without accompanying reductions in BP in HF the absence of diabetes. Although we show that empagliflozin exerts direct benefits to the isolated heart and cardiomyocytes, irrespective of diuretic and hemodynamic variables, a primary focus of future studies will be to explore the role of osmotic diuresis in regulating the beneficial effects of empagliflozin in nondiabetic HF.

Nevertheless, while our results suggest an association between improved cardiac function and reduced NLRP3-mediated cardiac inflammation in the setting of nondiabetic HF, whether this is a cause or effect relationship remains to be elucidated. As such, the ability of empagliflozin to exert

direct cardiac action via the NLRP3 inflammasome signaling cascade will be further explored using transgenic mice (such as NLRP3 knockout (KO) mice) (108) and specific overexpression and/or inhibitions of NLRP3 (109-115).

Finally, while our data clearly demonstrates that inhibition of the cardiac NLRP3 inflammasome occurs in response to empagliflozin, whether or not this is related to the effects of empagliflozin on NHE1 as previously suggested (31) or to effects on other ion channels and/or Ca^{2+} handling proteins is currently under investigation.

5.4 Figures

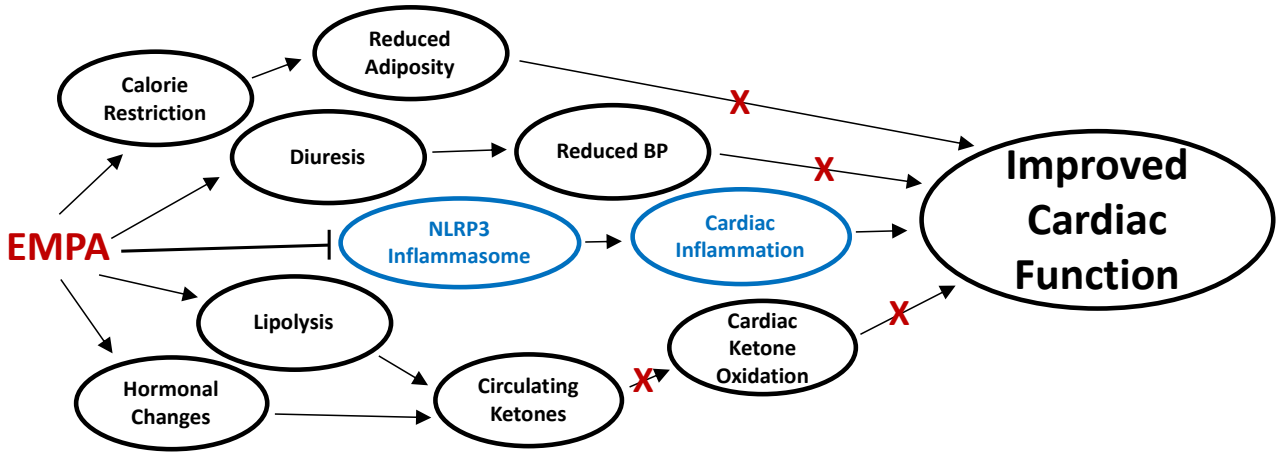

Figure 5.1. Mechanism(s) Responsible for Beneficial Cardiac Effects in Heart Failure in the Absence of Diabetes. Our results clearly demonstrate that empagliflozin does not reduce adiposity or alter BP in the setting of nondiabetic HF. In addition, empagliflozin failed to elevate circulating ketones and had no effect on cardiac ketone oxidation rates or overall ATP production in HF. However, empagliflozin blunted NLRP3-mediated inflammation directly in the heart, thus providing insight to the potential of an SGLT2-independent effect of empagliflozin in HF. BP = blood pressure; EMPA = empagliflozin; HF = heart failure.

5.5 References

1. Drakos SG, Terrovitis JV, Anastasiou-Nana MI, Nanas JN. Reverse remodeling during long-term mechanical unloading of the left ventricle. J Mol Cell Cardiol 2007;43:231-42.
2. Mudd JO, Kass DA. Reversing chronic remodeling in heart failure. Expert Rev Cardiovasc Ther 2007;5:585-98.
3. Soliman OI, Geleijnse ML, Theuns DA et al. Reverse of left ventricular volumetric and structural remodeling in heart failure patients treated with cardiac resynchronization therapy. Am J Cardiol 2008;101:651-7.
4. Birks EJ, Tansley PD, Hardy J et al. Left ventricular assist device and drug therapy for the reversal of heart failure. N Engl J Med 2006;355:1873-84.
5. Heerdt PM, Holmes JW, Cai B et al. Chronic unloading by left ventricular assist device reverses contractile dysfunction and alters gene expression in end-stage heart failure. Circulation 2000;102:2713-9.
6. Nascimben L, Ingwall JS, Lorell BH et al. Mechanisms for increased glycolysis in the hypertrophied rat heart. Hypertension 2004;44:662-7.
7. Nagendran J, Waller TJ, Dyck JR. AMPK signalling and the control of substrate use in the heart. Mol Cell Endocrinol 2013;366:180-93.
8. Kim TT, Dyck JR. Is AMPK the savior of the failing heart? Trends Endocrinol Metab 2015;26:40-8.
9. Tian R, Musi N, D'Agostino J, Hirshman MF, Goodyear LJ. Increased adenosine monophosphate-activated protein kinase activity in rat hearts with pressure-overload hypertrophy. Circulation 2001;104:1664-9.

10. Li C, Zhang J, Xue M et al. SGLT2 inhibition with empagliflozin attenuates myocardial oxidative stress and fibrosis in diabetic mice heart. Cardiovasc Diabetol 2019;18:15.
11. Gupte AA, Hamilton DJ, Cordero-Reyes AM et al. Mechanical unloading promotes myocardial energy recovery in human heart failure. Circ Cardiovasc Genet 2014;7:266-76.
12. Razeghi P, Young ME, Ying J et al. Downregulation of metabolic gene expression in failing human heart before and after mechanical unloading. Cardiology 2002;97:203-9.
13. Qanud K, Mamdani M, Pepe M et al. Reverse changes in cardiac substrate oxidation in dogs recovering from heart failure. Am J Physiol Heart Circ Physiol 2008;295:H2098-105.
14. Ferrannini E, Mark M, Mayoux E. CV Protection in the EMPA-REG OUTCOME Trial: A "Thrifty Substrate" Hypothesis. Diabetes Care 2016;39:1108-14.
15. Mudaliar S, Alloju S, Henry RR. Can a Shift in Fuel Energetics Explain the Beneficial Cardiorenal Outcomes in the EMPA-REG OUTCOME Study? A Unifying Hypothesis. Diabetes Care 2016;39:1115-22.
16. Oshima H, Miki T, Kuno A et al. Empagliflozin, an SGLT2 Inhibitor, Reduced the Mortality Rate after Acute Myocardial Infarction with Modification of Cardiac Metabolomes and Antioxidants in Diabetic Rats. J Pharmacol Exp Ther 2019;368:524-534.
17. Nielsen R, Moller N, Gormsen LC et al. Cardiovascular Effects of Treatment with the Ketone Body 3-Hydroxybutyrate in Chronic Heart Failure Patients. Circulation 2019.
18. Ho KL, Zhang L, Wagg C et al. Increased ketone body oxidation provides additional energy for the failing heart without improving cardiac efficiency. Cardiovasc Res 2019.

19. Yurista SR, Sillje HHW, Oberdorf-Maass SU et al. Sodium-glucose co-transporter 2 inhibition with empagliflozin improves cardiac function in non-diabetic rats with left ventricular dysfunction after myocardial infarction. Eur J Heart Fail 2019.

20. Santos-Gallego CG, Requena-Ibanez JA, San Antonio R et al. Empagliflozin Ameliorates Adverse Left Ventricular Remodeling in Nondiabetic Heart Failure by Enhancing Myocardial Energetics. J Am Coll Cardiol 2019;73:1931-1944.

21. Ferrannini E, Baldi S, Frascerra S et al. Shift to Fatty Substrate Utilization in Response to Sodium-Glucose Cotransporter 2 Inhibition in Subjects Without Diabetes and Patients With Type 2 Diabetes. Diabetes 2016;65:1190-5.

22. Nr J, Tr L, Mv H, Nb S, He B. Sodium Glucose Transporter 2 (SGLT2) Inhibition does not Protect the Myocardium from Acute Ischemic Reperfusion Injury but Modulates Post- Ischemic Mitochondrial Function. Cardiovascular Pharmacology: Open Access 2017;06.

23. Kappel BA, Lehrke M, Schutt K et al. Effect of Empagliflozin on the Metabolic Signature of Patients With Type 2 Diabetes Mellitus and Cardiovascular Disease. Circulation 2017;136:969-972.

24. Abdurrachim D, Teo XQ, Woo CC et al. Empagliflozin reduces myocardial ketone utilization while preserving glucose utilization in diabetic hypertensive heart disease: A hyperpolarized (13) C magnetic resonance spectroscopy study. Diabetes, obesity & metabolism 2018.

25. Verma S, Rawat S, Ho KL et al. Empagliflozin Increases Cardiac Energy Production in Diabetes: Novel Translational Insights Into the Heart Failure Benefits of SGLT2 Inhibitors. JACC Basic to translational science 2018;3:575-587.

26. Aubert G, Martin OJ, Horton JL et al. The Failing Heart Relies on Ketone Bodies as a Fuel. Circulation 2016;133:698-705.

27. Vrhovac I, Balen Eror D, Klessen D et al. Localizations of Na(+)-D-glucose cotransporters SGLT1 and SGLT2 in human kidney and of SGLT1 in human small intestine, liver, lung, and heart. Pflugers Archiv : European journal of physiology 2015;467:1881-98.

28. Kurosaki E, Ogasawara H. Ipragliflozin and other sodium-glucose cotransporter-2 (SGLT2) inhibitors in the treatment of type 2 diabetes: preclinical and clinical data. Pharmacol Ther 2013;139:51-9.

29. Despa S, Islam MA, Weber CR, Pogwizd SM, Bers DM. Intracellular Na(+) concentration is elevated in heart failure but Na/K pump function is unchanged. Circulation 2002;105:2543-8.

30. Baartscheer A, Schumacher CA, van Borren MM, Belterman CN, Coronel R, Fiolet JW. Increased Na+/H+-exchange activity is the cause of increased [Na+]i and underlies disturbed calcium handling in the rabbit pressure and volume overload heart failure model. Cardiovasc Res 2003;57:1015-24.

31. Baartscheer A, Schumacher CA, Wust RC et al. Empagliflozin decreases myocardial cytoplasmic Na(+) through inhibition of the cardiac Na(+)/H(+) exchanger in rats and rabbits. Diabetologia 2017;60:568-573.

32. Mustroph J, Wagemann O, Lucht CM et al. Empagliflozin reduces Ca/calmodulin-dependent kinase II activity in isolated ventricular cardiomyocytes. ESC heart failure 2018;5:642-648.

33. Liu T, O'Rourke B. Enhancing mitochondrial Ca2+ uptake in myocytes from failing hearts restores energy supply and demand matching. Circ Res 2008;103:279-88.

34. Pogwizd SM, Sipido KR, Verdonck F, Bers DM. Intracellular Na in animal models of hypertrophy and heart failure: contractile function and arrhythmogenesis. Cardiovasc Res 2003;57:887-96.

35. Uthman L, Baartscheer A, Bleijlevens B et al. Class effects of SGLT2 inhibitors in mouse cardiomyocytes and hearts: inhibition of Na(+)/H(+) exchanger, lowering of cytosolic Na(+) and vasodilation. Diabetologia 2018;61:722-726.

36. Uthman L, Nederlof R, Eerbeek O et al. Delayed ischemic contracture onset by Empagliflozin associates with NHE-1 inhibition and is dependent on insulin in isolated mouse hearts. Cardiovasc Res 2019.

37. Pessoa TD, Campos LC, Carraro-Lacroix L, Girardi AC, Malnic G. Functional role of glucose metabolism, osmotic stress, and sodium-glucose cotransporter isoform-mediated transport on Na+/H+ exchanger isoform 3 activity in the renal proximal tubule. J Am Soc Nephrol 2014;25:2028-39.

38. Yokoyama H, Gunasegaram S, Harding SE, Avkiran M. Sarcolemmal Na+/H+ exchanger activity and expression in human ventricular myocardium. J Am Coll Cardiol 2000;36:534-40.

39. hui Y, junzhu C, jianhua Z. Gap junction and Na+-H+ exchanger alternations in fibrillating and failing atrium. Int J Cardiol 2008;128:147-9.

40. Inoue BH, dos Santos L, Pessoa TD et al. Increased NHE3 abundance and transport activity in renal proximal tubule of rats with heart failure. Am J Physiol Regul Integr Comp Physiol 2012;302:R166-74.

41. Lutken SC, Kim SW, Jonassen T et al. Changes of renal AQP2, ENaC, and NHE3 in experimentally induced heart failure: response to angiotensin II AT1 receptor blockade. Am J Physiol Renal Physiol 2009;297:F1678-88.

42. Liu T, Takimoto E, Dimaano VL et al. Inhibiting mitochondrial Na+/Ca2+ exchange prevents sudden death in a Guinea pig model of heart failure. Circ Res 2014;115:44-54.

43. Zinman B, Wanner C, Lachin JM et al. Empagliflozin, Cardiovascular Outcomes, and Mortality in Type 2 Diabetes. N Engl J Med 2015;373:2117-28.

44. Karmazyn M. NHE-1: still a viable therapeutic target. J Mol Cell Cardiol 2013;61:77-82.

45. Aker S, Snabaitis AK, Konietzka I et al. Inhibition of the Na+/H+ exchanger attenuates the deterioration of ventricular function during pacing-induced heart failure in rabbits. Cardiovasc Res 2004;63:273-82.

46. Kilic A, Huang CX, Rajapurohitam V, Madwed JB, Karmazyn M. Early and transient sodium-hydrogen exchanger isoform 1 inhibition attenuates subsequent cardiac hypertrophy and heart failure following coronary artery ligation. J Pharmacol Exp Ther 2014;351:492-9.

47. Baartscheer A, Schumacher CA, van Borren MM et al. Chronic inhibition of Na+/H+-exchanger attenuates cardiac hypertrophy and prevents cellular remodeling in heart failure. Cardiovasc Res 2005;65:83-92.

48. Baartscheer A, Hardziyenka M, Schumacher CA et al. Chronic inhibition of the Na+/H+ -exchanger causes regression of hypertrophy, heart failure, and ionic and electrophysiological remodelling. Br J Pharmacol 2008;154:1266-75.

49. Engelhardt S, Hein L, Keller U, Klambt K, Lohse MJ. Inhibition of Na(+)-H(+) exchange prevents hypertrophy, fibrosis, and heart failure in beta(1)-adrenergic receptor transgenic mice. Circ Res 2002;90:814-9.

50. Hammoudi N, Jeong D, Singh R et al. Empagliflozin Improves Left Ventricular Diastolic Dysfunction in a Genetic Model of Type 2 Diabetes. Cardiovasc Drugs Ther 2017;31:233-246.

51. Joubert M, Jagu B, Montaigne D et al. The Sodium-Glucose Cotransporter 2 Inhibitor Dapagliflozin Prevents Cardiomyopathy in a Diabetic Lipodystrophic Mouse Model. Diabetes 2017;66:1030-1040.

52. Grempler R, Thomas L, Eckhardt M et al. Empagliflozin, a novel selective sodium glucose cotransporter-2 (SGLT-2) inhibitor: characterisation and comparison with other SGLT-2 inhibitors. Diabetes Obes Metab 2012;14:83-90.

53. Connelly KA, Zhang Y, Desjardins JF, Thai K, Gilbert RE. Dual inhibition of sodium-glucose linked cotransporters 1 and 2 exacerbates cardiac dysfunction following experimental myocardial infarction. Cardiovasc Diabetol 2018;17:99.

54. Kashiwagi Y, Nagoshi T, Yoshino T et al. Expression of SGLT1 in Human Hearts and Impairment of Cardiac Glucose Uptake by Phlorizin during Ischemia-Reperfusion Injury in Mice. PLoS One 2015;10:e0130605.

55. Polidori D, Sha S, Mudaliar S et al. Canagliflozin lowers postprandial glucose and insulin by delaying intestinal glucose absorption in addition to increasing urinary glucose excretion: results of a randomized, placebo-controlled study. Diabetes Care 2013;36:2154-61.

56. Faillie JL. Pharmacological aspects of the safety of gliflozins. Pharmacol Res 2017;118:71-81.

57. Song E, Jahng JW, Chong LP et al. Lipocalin-2 induces NLRP3 inflammasome activation via HMGB1 induced TLR4 signaling in heart tissue of mice under pressure overload challenge. Am J Transl Res 2017;9:2723-2735.

58. Li R, Lu K, Wang Y et al. Triptolide attenuates pressure overload-induced myocardial remodeling in mice via the inhibition of NLRP3 inflammasome expression. Biochemical and biophysical research communications 2017;485:69-75.

59. Wang Y, Wu Y, Chen J, Zhao S, Li H. Pirfenidone attenuates cardiac fibrosis in a mouse model of TAC-induced left ventricular remodeling by suppressing NLRP3 inflammasome formation. Cardiology 2013;126:1-11.

60. Sandanger O, Gao E, Ranheim T et al. NLRP3 inflammasome activation during myocardial ischemia reperfusion is cardioprotective. Biochem Biophys Res Commun 2016;469:1012-20.

61. Li F, Zhang H, Yang L et al. NLRP3 deficiency accelerates pressure overload-induced cardiac remodeling via increased TLR4 expression. J Mol Med (Berl) 2018;96:1189-1202.

62. Traba J, Kwarteng-Siaw M, Okoli TC et al. Fasting and refeeding differentially regulate NLRP3 inflammasome activation in human subjects. J Clin Invest 2015;125:4592-600.

63. Sanchez-Lopez E, Rodriguez-Vita J, Cartier C et al. Inhibitory effect of interleukin-1beta on angiotensin II-induced connective tissue growth factor and type IV collagen production in cultured mesangial cells. Am J Physiol Renal Physiol 2008;294:F149-60.

64. Larsen CM, Faulenbach M, Vaag A et al. Interleukin-1-receptor antagonist in type 2 diabetes mellitus. N Engl J Med 2007;356:1517-26.

65. Iannantuoni F, Diaz-Morales N, Escribano-Lopez I et al. Does Glycemic Control Modulate the Impairment of NLRP3 Inflammasome Activation in Type 2 Diabetes? Antioxid Redox Signal 2018.

66. Feng H, Gu J, Gou F et al. High Glucose and Lipopolysaccharide Prime NLRP3 Inflammasome via ROS/TXNIP Pathway in Mesangial Cells. J Diabetes Res 2016;2016:6973175.

67. Wen H, Gris D, Lei Y et al. Fatty acid-induced NLRP3-ASC inflammasome activation interferes with insulin signaling. Nat Immunol 2011;12:408-15.

68. Kousathana F, Georgitsi M, Lambadiari V, Giamarellos-Bourboulis EJ, Dimitriadis G, Mouktaroudi M. Defective production of interleukin-1 beta in patients with type 2 diabetes mellitus: Restoration by proper glycemic control. Cytokine 2017;90:177-184.

69. Leng W, Ouyang X, Lei X et al. The SGLT-2 Inhibitor Dapagliflozin Has a Therapeutic Effect on Atherosclerosis in Diabetic ApoE(-/-) Mice. Mediators Inflamm 2016;2016:6305735.

70. Dandona P, Chaudhuri A, Ghanim H, Mohanty P. Proinflammatory effects of glucose and anti-inflammatory effect of insulin: relevance to cardiovascular disease. Am J Cardiol 2007;99:15B-26B.

71. Xu C, Wang W, Zhong J et al. Canagliflozin exerts anti-inflammatory effects by inhibiting intracellular glucose metabolism and promoting autophagy in immune cells. Biochem Pharmacol 2018;152:45-59.

72. Ye Y, Bajaj M, Yang HC, Perez-Polo JR, Birnbaum Y. SGLT-2 Inhibition with Dapagliflozin Reduces the Activation of the Nlrp3/ASC Inflammasome and Attenuates the Development of Diabetic Cardiomyopathy in Mice with Type 2 Diabetes. Further Augmentation of the Effects with Saxagliptin, a DPP4 Inhibitor. Cardiovascular drugs and therapy 2017;31:119-132.

73. Shi X, Verma S, Yun J et al. Effect of empagliflozin on cardiac biomarkers in a zebrafish model of heart failure: clues to the EMPA-REG OUTCOME trial? Mol Cell Biochem 2017;433:97-102.

74. Kusaka H, Koibuchi N, Hasegawa Y, Ogawa H, Kim-Mitsuyama S. Empagliflozin lessened cardiac injury and reduced visceral adipocyte hypertrophy in prediabetic rats with metabolic syndrome. Cardiovasc Diabetol 2016;15:157.

75. Habibi J, Aroor AR, Sowers JR et al. Sodium glucose transporter 2 (SGLT2) inhibition with empagliflozin improves cardiac diastolic function in a female rodent model of diabetes. Cardiovasc Diabetol 2017;16:9.

76. Lee TM, Chang NC, Lin SZ. Dapagliflozin, a selective SGLT2 Inhibitor, attenuated cardiac fibrosis by regulating the macrophage polarization via STAT3 signaling in infarcted rat hearts. Free Radic Biol Med 2017;104:298-310.

77. Connelly KA, Zhang Y, Visram A et al. Empagliflozin Improves Diastolic Function in a Nondiabetic Rodent Model of Heart Failure With Preserved Ejection Fraction. JACC Basic Transl Sci 2019;4:27-37.

78. Lee SB, Kalluri R. Mechanistic connection between inflammation and fibrosis. Kidney Int Suppl 2010:S22-6.

79. Serhan CN, Brain SD, Buckley CD et al. Resolution of inflammation: state of the art, definitions and terms. FASEB J 2007;21:325-32.

80. Segura AM, Frazier OH, Buja LM. Fibrosis and heart failure. Heart failure reviews 2014;19:173-85.

81. Creemers EE, Pinto YM. Molecular mechanisms that control interstitial fibrosis in the pressure-overloaded heart. Cardiovasc Res 2011;89:265-72.

82. Marchetti C, Toldo S, Chojnacki J et al. Pharmacologic Inhibition of the NLRP3 Inflammasome Preserves Cardiac Function After Ischemic and Nonischemic Injury in the Mouse. J Cardiovasc Pharmacol 2015;66:1-8.

83. Tan SA, Tan L. Empagliflozin and Canagliflozin Attenuate Inflammatory Cytokines Interferon-λ, Tumor Necrosis Factor-α, Interleukin-6: Possible Mechanism of Decreasing Cardiovascular Risk in Diabetes Mellitus. Journal of the American College of Cardiology 2018;71.

84. Matsumura M, Nakatani Y, Tanka S et al. Efficacy of Additional Canagliflozin Administration to Type 2 Diabetes Patients Receiving Insulin Therapy: Examination of Diurnal Glycemic Patterns Using Continuous Glucose Monitoring (CGM). Diabetes Ther 2017;8:821-827.

85. Sato T, Aizawa Y, Yuasa S et al. The effect of dapagliflozin treatment on epicardial adipose tissue volume. Cardiovasc Diabetol 2018;17:6.

86. Birnbaum Y, Bajaj M, Yang HC, Ye Y. Combined SGLT2 and DPP4 Inhibition Reduces the Activation of the Nlrp3/ASC Inflammasome and Attenuates the Development of Diabetic Nephropathy in Mice with Type 2 Diabetes. Cardiovasc Drugs Ther 2018;32:135-145.

87. Yang CC, Chen YT, Wallace CG et al. Early administration of empagliflozin preserved heart function in cardiorenal syndrome in rat. Biomed Pharmacother 2019;109:658-670.

88. Tahara A, Kurosaki E, Yokono M et al. Effects of sodium-glucose cotransporter 2 selective inhibitor ipragliflozin on hyperglycaemia, oxidative stress, inflammation and liver injury in streptozotocin-induced type 1 diabetic rats. The Journal of pharmacy and pharmacology 2014;66:975-87.

89. Youm YH, Nguyen KY, Grant RW et al. The ketone metabolite beta-hydroxybutyrate blocks NLRP3 inflammasome-mediated inflammatory disease. Nat Med 2015;21:263-9.

90. Qian J, Zhu W, Lu M, Ni B, Yang J. D-beta-hydroxybutyrate promotes functional recovery and relieves pain hypersensitivity in mice with spinal cord injury. Br J Pharmacol 2017;174:1961-1971.

91. Trotta MC, Maisto R, Guida F et al. The activation of retinal HCA2 receptors by systemic beta-hydroxybutyrate inhibits diabetic retinal damage through reduction of endoplasmic reticulum stress and the NLRP3 inflammasome. PLoS One 2019;14:e0211005.

92. Bae HR, Kim DH, Park MH et al. beta-Hydroxybutyrate suppresses inflammasome formation by ameliorating endoplasmic reticulum stress via AMPK activation. Oncotarget 2016;7:66444-66454.

93. Anders HJ, Suarez-Alvarez B, Grigorescu M et al. The macrophage phenotype and inflammasome component NLRP3 contributes to nephrocalcinosis-related chronic kidney disease independent from IL-1-mediated tissue injury. Kidney Int 2018;93:656-669.

94. Chakraborty S, Galla S, Cheng X et al. Salt-Responsive Metabolite, beta-Hydroxybutyrate, Attenuates Hypertension. Cell Rep 2018;25:677-689 e4.

95. Guo M, Wang X, Zhao Y et al. Ketogenic Diet Improves Brain Ischemic Tolerance and Inhibits NLRP3 Inflammasome Activation by Preventing Drp1-Mediated Mitochondrial Fission and Endoplasmic Reticulum Stress. Front Mol Neurosci 2018;11:86.

96. Fu SP, Li SN, Wang JF et al. BHBA suppresses LPS-induced inflammation in BV-2 cells by inhibiting NF-kappaB activation. Mediators Inflamm 2014;2014:983401.

97. Goldberg EL, Asher JL, Molony RD et al. beta-Hydroxybutyrate Deactivates Neutrophil NLRP3 Inflammasome to Relieve Gout Flares. Cell Rep 2017;18:2077-2087.

98. Shang S, Wang L, Zhang Y, Lu H, Lu X. The Beta-Hydroxybutyrate Suppresses the Migration of Glioma Cells by Inhibition of NLRP3 Inflammasome. Cell Mol Neurobiol 2018;38:1479-1489.

99. Neudorf H, Durrer C, Myette-Cote E, Makins C, O'Malley T, Little JP. Oral Ketone Supplementation Acutely Increases Markers of NLRP3 Inflammasome Activation in Human Monocytes. Mol Nutr Food Res 2019;63:e1801171.

100. Cox PJ, Kirk T, Ashmore T et al. Nutritional Ketosis Alters Fuel Preference and Thereby Endurance Performance in Athletes. Cell Metab 2016;24:256-68.

101. Chilton R, Tikkanen I, Cannon CP et al. Effects of empagliflozin on blood pressure and markers of arterial stiffness and vascular resistance in patients with type 2 diabetes. Diabetes Obes Metab 2015;17:1180-93.

102. Verma S, Garg A, Yan AT et al. Effect of Empagliflozin on Left Ventricular Mass and Diastolic Function in Individuals With Diabetes: An Important Clue to the EMPA-REG OUTCOME Trial? Diabetes Care 2016;39:e212-e213.

103. Pabel S, Wagner S, Bollenberg H et al. Empagliflozin directly improves diastolic function in human heart failure. Eur J Heart Fail 2018;20:1690-1700.

104. Aasum E, Hafstad AD, Larsen TS. Changes in substrate metabolism in isolated mouse hearts following ischemia-reperfusion. Mol Cell Biochem 2003;249:97-103.

105. Zhabyeyev P, Gandhi M, Mori J et al. Pressure-overload-induced heart failure induces a selective reduction in glucose oxidation at physiological afterload. Cardiovasc Res 2013;97:676-85.

106. Zhang L, Jaswal JS, Ussher JR et al. Cardiac insulin-resistance and decreased mitochondrial energy production precede the development of systolic heart failure after pressure-overload hypertrophy. Circ Heart Fail 2013;6:1039-48.

107. Fillmore N, Levasseur JL, Fukushima A et al. Uncoupling of glycolysis from glucose oxidation accompanies the development of heart failure with preserved ejection fraction. Mol Med 2018;24:3.

108. Kim HJ, Lee DW, Ravichandran K et al. NLRP3 inflammasome knockout mice are protected against ischemic but not cisplatin-induced acute kidney injury. J Pharmacol Exp Ther 2013;346:465-72.

109. Coll RC, Robertson AA, Chae JJ et al. A small-molecule inhibitor of the NLRP3 inflammasome for the treatment of inflammatory diseases. Nat Med 2015;21:248-55.

110. Stutz A, Kolbe CC, Stahl R et al. NLRP3 inflammasome assembly is regulated by phosphorylation of the pyrin domain. J Exp Med 2017;214:1725-1736.

111. Krishnan SM, Dowling JK, Ling YH et al. Inflammasome activity is essential for one kidney/deoxycorticosterone acetate/salt-induced hypertension in mice. Br J Pharmacol 2016;173:752-65.

112. Primiano MJ, Lefker BA, Bowman MR et al. Efficacy and Pharmacology of the NLRP3 Inflammasome Inhibitor CP-456,773 (CRID3) in Murine Models of Dermal and Pulmonary Inflammation. J Immunol 2016;197:2421-33.

113. Tate MD, Ong JD, Dowling JK et al. Reassessing the role of the NLRP3 inflammasome during pathogenic influenza A virus infection via temporal inhibition. Sci Rep 2016;6:27912.

114. Tucey TM, Verma-Gaur J, Nguyen J et al. The Endoplasmic Reticulum-Mitochondrion Tether ERMES Orchestrates Fungal Immune Evasion, Illuminating Inflammasome Responses to Hyphal Signals. mSphere 2016;1.

115. van Hout GP, Bosch L, Ellenbroek GH et al. The selective NLRP3-inflammasome inhibitor MCC950 reduces infarct size and preserves cardiac function in a pig model of myocardial infarction. Eur Heart J 2016.

Bibliography

Aasum E, Hafstad AD, Larsen TS. Changes in substrate metabolism in isolated mouse hearts following ischemia-reperfusion. Mol Cell Biochem 2003;249:97-103.

Abbate A, Kontos MC, Grizzard JD et al. Interleukin-1 blockade with anakinra to prevent adverse cardiac remodeling after acute myocardial infarction (Virginia Commonwealth University Anakinra Remodeling Trial [VCU-ART] Pilot study). Am J Cardiol 2010;105:1371-1377 e1.

Abdul-Ghani M, Al Jobori H, Daniele G et al. Inhibition of Renal Sodium-Glucose Cotransport With Empagliflozin Lowers Fasting Plasma Glucose and Improves beta-Cell Function in Subjects With Impaired Fasting Glucose. Diabetes 2017;66:2495-2502.

Abdul-Ghani M, Del Prato S, Chilton R, DeFronzo RA. SGLT2 Inhibitors and Cardiovascular Risk: Lessons Learned From the EMPA-REG OUTCOME Study. Diabetes Care 2016;39:717-25.

Abdul-Ghani MA, Norton L, Defronzo RA. Role of sodium-glucose cotransporter 2 (SGLT 2) inhibitors in the treatment of type 2 diabetes. Endocr Rev 2011;32:515-31.

Abdurrachim D, Teo XQ, Woo CC et al. Empagliflozin reduces myocardial ketone utilization while preserving glucose utilization in diabetic hypertensive heart disease: A hyperpolarized (13) C magnetic resonance spectroscopy study. Diabetes, obesity & metabolism 2018.

Administration USFaD. FDA warns that SGLT2 inhibitors for diabetes may result in a serious condition of too much acid in the blood. 2015: Available from: http://www.fda.gov/Drugs/DrugSafety/ucm446845.htm.

Aker S, Snabaitis AK, Konietzka I et al. Inhibition of the Na+/H+ exchanger attenuates the deterioration of ventricular function during pacing-induced heart failure in rabbits. Cardiovasc Res 2004;63:273-82.

Akki A, Smith K, Seymour AM. Compensated cardiac hypertrophy is characterised by a decline in palmitate oxidation. Mol Cell Biochem 2008;311:215-24.

Ali SR, Karin M, Nizet V. Signaling cascades and inflammasome activation in microbial infections. Inflammasome 2016;2.

Allard MF, Schonekess BO, Henning SL, English DR, Lopaschuk GD. Contribution of oxidative metabolism and glycolysis to ATP production in hypertrophied hearts. Am J Physiol 1994;267:H742-50.

Allard MF. Energy substrate metabolism in cardiac hypertrophy. Curr Hypertens Rep 2004;6:430-5.

Anastasiou-Nana MI, Nanas JN, Karagounis LA et al. Relation of dispersion of QRS and QT in patients with advanced congestive heart failure to cardiac and sudden death mortality. Am J Cardiol 2000;85:1212-7.

Anders HJ, Suarez-Alvarez B, Grigorescu M et al. The macrophage phenotype and inflammasome component NLRP3 contributes to nephrocalcinosis-related chronic kidney disease independent from IL-1-mediated tissue injury. Kidney Int 2018;93:656-669.

Andersen NM, Stansfield WE, Tang RH, Rojas M, Patterson C, Selzman CH. Recovery from decompensated heart failure is associated with a distinct, phase-dependent gene expression profile. J Surg Res 2012;178:72-80.

Andreadou I, Efentakis P, Balafas E et al. Empagliflozin Limits Myocardial Infarction in Vivo and Cell Death in Vitro: Role of STAT3, Mitochondria, and Redox Aspects. Front Physiol 2017;8:1077.

Aoyagi T, Matsui T. The Cardiomyocyte as a Source of Cytokines in Cardiac Injury. J Cell Sci Ther 2011;2012.

Arad M, Seidman CE, Seidman JG. AMP-activated protein kinase in the heart: role during health and disease. Circ Res 2007;100:474-88.

Arai M, Matsui H, Periasamy M. Sarcoplasmic reticulum gene expression in cardiac hypertrophy and heart failure. Circ Res 1994;74:555-64.

Arany Z, Novikov M, Chin S, Ma Y, Rosenzweig A, Spiegelman BM. Transverse aortic constriction leads to accelerated heart failure in mice lacking PPAR-gamma coactivator 1alpha. Proc Natl Acad Sci U S A 2006;103:10086-91.

Aubert G, Martin OJ, Horton JL et al. The Failing Heart Relies on Ketone Bodies as a Fuel. Circulation 2016;133:698-705.

Aukrust P, Ueland T, Lien E et al. Cytokine network in congestive heart failure secondary to ischemic or idiopathic dilated cardiomyopathy. Am J Cardiol 1999;83:376-82.

Awad AE, Kandalam V, Chakrabarti S et al. Tumor necrosis factor induces matrix metalloproteinases in cardiomyocytes and cardiofibroblasts differentially via superoxide production in a PI3Kgamma-dependent manner. Am J Physiol Cell Physiol 2010;298:C679-92.

Baartscheer A, Hardziyenka M, Schumacher CA et al. Chronic inhibition of the Na+/H+ -exchanger causes regression of hypertrophy, heart failure, and ionic and electrophysiological remodelling. Br J Pharmacol 2008;154:1266-75.

Baartscheer A, Schumacher CA, van Borren MM et al. Chronic inhibition of Na+/H+-exchanger attenuates cardiac hypertrophy and prevents cellular remodeling in heart failure. Cardiovasc Res 2005;65:83-92.

Baartscheer A, Schumacher CA, van Borren MM, Belterman CN, Coronel R, Fiolet JW. Increased Na+/H+-exchange activity is the cause of increased [Na+]i and underlies disturbed calcium handling in the rabbit pressure and volume overload heart failure model. Cardiovasc Res 2003;57:1015-24.

Baartscheer A, Schumacher CA, Wust RC et al. Empagliflozin decreases myocardial cytoplasmic Na(+) through inhibition of the cardiac Na(+)/H(+) exchanger in rats and rabbits. Diabetologia 2017;60:568-573.

Bae HR, Kim DH, Park MH et al. beta-Hydroxybutyrate suppresses inflammasome formation by ameliorating endoplasmic reticulum stress via AMPK activation. Oncotarget 2016;7:66444-66454.

Balasse EO, Fery F. Ketone body production and disposal: effects of fasting, diabetes, and exercise. Diabetes Metab Rev 1989;5:247-70.

Barger PM, Brandt JM, Leone TC, Weinheimer CJ, Kelly DP. Deactivation of peroxisome proliferator-activated receptor-alpha during cardiac hypertrophic growth. J Clin Invest 2000;105:1723-30.

Barin JG, Rose NR, Cihakova D. Macrophage diversity in cardiac inflammation: a review. Immunobiology 2012;217:468-75.

Barry SP, Davidson SM, Townsend PA. Molecular regulation of cardiac hypertrophy. Int J Biochem Cell Biol 2008;40:2023-39.

Bartos DC, Grandi E, Ripplinger CM. Ion Channels in the Heart. Compr Physiol 2015;5:1423-64.

Batchu SN, Law E, Brocks DR, Falck JR, Seubert JM. Epoxyeicosatrienoic acid prevents postischemic electrocardiogram abnormalities in an isolated heart model. Journal of molecular and cellular cardiology 2009;46:67-74.

Bedi KC, Jr., Snyder NW, Brandimarto J et al. Evidence for Intramyocardial Disruption of Lipid Metabolism and Increased Myocardial Ketone Utilization in Advanced Human Heart Failure. Circulation 2016;133:706-16.

Benetti E, Mastrocola R, Vitarelli G et al. Empagliflozin Protects against Diet-Induced NLRP-3 Inflammasome Activation and Lipid Accumulation. J Pharmacol Exp Ther 2016;359:45-53.

Bing OH, Brooks WW, Robinson KG et al. The spontaneously hypertensive rat as a model of the transition from compensated left ventricular hypertrophy to failure. J Mol Cell Cardiol 1995;27:383-96.

Birks EJ, Tansley PD, Hardy J et al. Left ventricular assist device and drug therapy for the reversal of heart failure. N Engl J Med 2006;355:1873-84.

Birnbaum Y, Bajaj M, Yang HC, Ye Y. Combined SGLT2 and DPP4 Inhibition Reduces the Activation of the Nlrp3/ASC Inflammasome and Attenuates the Development of Diabetic Nephropathy in Mice with Type 2 Diabetes. Cardiovasc Drugs Ther 2018;32:135-145.

Bjornstad JL, Skrbic B, Sjaastad I, Bjornstad S, Christensen G, Tonnessen T. A mouse model of reverse cardiac remodelling following banding-debanding of the ascending aorta. Acta Physiol (Oxf) 2012;205:92-102.

Bleumink GS, Knetsch AM, Sturkenboom MC et al. Quantifying the heart failure epidemic: prevalence, incidence rate, lifetime risk and prognosis of heart failure The Rotterdam Study. Eur Heart J 2004;25:1614-9.

Bolinder J, Ljunggren O, Johansson L et al. Dapagliflozin maintains glycaemic control while reducing weight and body fat mass over 2 years in patients with type 2 diabetes mellitus inadequately controlled on metformin. Diabetes, obesity & metabolism 2014;16:159-69.

Boulaksil M, Noorman M, Engelen MA et al. Longitudinal arrhythmogenic remodelling in a mouse model of longstanding pressure overload. Neth Heart J 2010;18:509-15.

Boulaksil M, Winckels SK, Engelen MA et al. Heterogeneous Connexin43 distribution in heart failure is associated with dispersed conduction and enhanced susceptibility to ventricular arrhythmias. Eur J Heart Fail 2010;12:913-21.

Bracey NA, Beck PL, Muruve DA et al. The Nlrp3 inflammasome promotes myocardial dysfunction in structural cardiomyopathy through interleukin-1beta. Exp Physiol 2013;98:462-72.

Brand T, Macha S, Mattheus M, Pinnetti S, Woerle HJ. Pharmacokinetics of empagliflozin, a sodium glucose cotransporter-2 (SGLT-2) inhibitor, coadministered with sitagliptin in healthy volunteers. Adv Ther 2012;29:889-99.

Bryant D, Becker L, Richardson J et al. Cardiac failure in transgenic mice with myocardial expression of tumor necrosis factor-alpha. Circulation 1998;97:1375-81.

Butler J, Hamo CE, Filippatos G et al. The potential role and rationale for treatment of heart failure with sodium-glucose co-transporter 2 inhibitors. European journal of heart failure 2017;19:1390-1400.

Butts B, Gary RA, Dunbar SB, Butler J. The Importance of NLRP3 Inflammasome in Heart Failure. J Card Fail 2015;21:586-93.

Byrne NJ, Levasseur J, Sung MM et al. Normalization of cardiac substrate utilization and left ventricular hypertrophy precede functional recovery in heart failure regression. Cardiovascular research 2016;110:249-57.

Byrne NJ, Parajuli N, Levasseur JL et al. Empagliflozin Prevents Worsening of Cardiac Function in an Experimental Model of Pressure Overload-Induced Heart Failure. JACC Basic to translational science 2017;2:347-354.

Cahill GF, Jr. Fuel metabolism in starvation. Annu Rev Nutr 2006;26:1-22.

Calligaris SD, Lecanda M, Solis F et al. Mice long-term high-fat diet feeding recapitulates human cardiovascular alterations: an animal model to study the early phases of diabetic cardiomyopathy. PLoS One 2013;8:e60931.

Camici PG, Marraccini P, Lorenzoni R et al. Coronary hemodynamics and myocardial metabolism in patients with syndrome X: response to pacing stress. J Am Coll Cardiol 1991;17:1461-70.

Cappola TP. Molecular remodeling in human heart failure. J Am Coll Cardiol 2008;51:137-8.

Carlson S, Helterline D, Asbe L et al. Cardiac macrophages adopt profibrotic/M2 phenotype in infarcted hearts: Role of urokinase plasminogen activator. J Mol Cell Cardiol 2017;108:42-49.

Carniel E, Taylor MR, Sinagra G et al. Alpha-myosin heavy chain: a sarcomeric gene associated with dilated and hypertrophic phenotypes of cardiomyopathy. Circulation 2005;112:54-9.

Cefalu WT, Leiter LA, Yoon KH et al. Efficacy and safety of canagliflozin versus glimepiride in patients with type 2 diabetes inadequately controlled with metformin (CANTATA-SU): 52 week results from a randomised, double-blind, phase 3 non-inferiority trial. Lancet 2013;382:941-50.

Ceriello A, Genovese S, Mannucci E, Gronda E. Understanding EMPA-REG OUTCOME. Lancet Diabetes Endocrinol 2015;3:929-30.

Cero FT, Hillestad V, Sjaastad I et al. Absence of the inflammasome adaptor ASC reduces hypoxia-induced pulmonary hypertension in mice. Am J Physiol Lung Cell Mol Physiol 2015;309:L378-87.

Chaanine AH, Hajjar RJ. AKT signalling in the failing heart. Eur J Heart Fail 2011;13:825-9.

Chakraborty S, Galla S, Cheng X et al. Salt-Responsive Metabolite, beta-Hydroxybutyrate, Attenuates Hypertension. Cell Rep 2018;25:677-689 e4.

Chen L, Klein T, Leung PS. Effects of combining linagliptin treatment with BI-38335, a novel SGLT2 inhibitor, on pancreatic islet function and inflammation in db/db mice. Curr Mol Med 2012;12:995-1004.

Chen L, LaRocque LM, Efe O, Wang J, Sands JM, Klein JD. Effect of Dapagliflozin Treatment on Fluid and Electrolyte Balance in Diabetic Rats. Am J Med Sci 2016;352:517-523.

Cherney DZ, Perkins BA, Soleymanlou N et al. Renal hemodynamic effect of sodium-glucose cotransporter 2 inhibition in patients with type 1 diabetes mellitus. Circulation 2014;129:587-97.

Chilton R, Tikkanen I, Cannon CP et al. Effects of empagliflozin on blood pressure and markers of arterial stiffness and vascular resistance in patients with type 2 diabetes. Diabetes Obes Metab 2015;17:1180-93.

Coll RC, Robertson AA, Chae JJ et al. A small-molecule inhibitor of the NLRP3 inflammasome for the treatment of inflammatory diseases. Nat Med 2015;21:248-55.

Connelly KA, Zhang Y, Desjardins JF, Thai K, Gilbert RE. Dual inhibition of sodium-glucose linked cotransporters 1 and 2 exacerbates cardiac dysfunction following experimental myocardial infarction. Cardiovasc Diabetol 2018;17:99.

Connelly KA, Zhang Y, Visram A et al. Empagliflozin Improves Diastolic Function in a Nondiabetic Rodent Model of Heart Failure With Preserved Ejection Fraction. JACC Basic Transl Sci 2019;4:27-37.

Conraads VM, Van Craenenbroeck EM, De Maeyer C, Van Berendoncks AM, Beckers PJ, Vrints CJ. Unraveling new mechanisms of exercise intolerance in chronic heart failure: role of exercise training. Heart Fail Rev 2013;18:65-77.

Contrera JF, Matthews EJ, Kruhlak NL, Benz RD. Estimating the safe starting dose in phase I clinical trials and no observed effect level based on QSAR modeling of the human maximum recommended daily dose. Regul Toxicol Pharmacol 2004;40:185-206.

Cotter DG, Schugar RC, Crawford PA. Ketone body metabolism and cardiovascular disease. Am J Physiol Heart Circ Physiol 2013;304:H1060-76.

Cox PJ, Kirk T, Ashmore T et al. Nutritional Ketosis Alters Fuel Preference and Thereby Endurance Performance in Athletes. Cell Metab 2016;24:256-68.

Creemers EE, Pinto YM. Molecular mechanisms that control interstitial fibrosis in the pressure-overloaded heart. Cardiovasc Res 2011;89:265-72.

Currie S, Smith GL. Enhanced phosphorylation of phospholamban and downregulation of sarco/endoplasmic reticulum Ca2+ ATPase type 2 (SERCA 2) in cardiac sarcoplasmic reticulum from rabbits with heart failure. Cardiovasc Res 1999;41:135-46.

Dandona P, Chaudhuri A, Ghanim H, Mohanty P. Proinflammatory effects of glucose and anti-inflammatory effect of insulin: relevance to cardiovascular disease. Am J Cardiol 2007;99:15B-26B.

Daniele G, Xiong J, Solis-Herrera C et al. Dapagliflozin Enhances Fat Oxidation and Ketone Production in Patients With Type 2 Diabetes. Diabetes care 2016;39:2036-2041.

Darwesh AM, El-Azab MF, Abo-Gresha NM, El-Sayed NM, Moustafa YM. Cardioprotective Mechanisms of Exenatide in Isoprenaline-induced Myocardial Infarction: Novel Effects on Myocardial alpha-Estrogen Receptor Expression and IGF-1/IGF-2 System. Journal of cardiovascular pharmacology 2018;71:160-173.

Darwesh AM, Jamieson KL, Wang C, Samokhvalov V, Seubert JM. Cardioprotective effects of CYP-derived epoxy metabolites of docosahexaenoic acid involve limiting NLRP3 inflammasome activation. Can J Physiol Pharmacol 2019;97:544-556.

Dass S, Holloway CJ, Cochlin LE et al. No Evidence of Myocardial Oxygen Deprivation in Nonischemic Heart Failure. Circ Heart Fail 2015;8:1088-93.

Davila-Roman VG, Vedala G, Herrero P et al. Altered myocardial fatty acid and glucose metabolism in idiopathic dilated cardiomyopathy. J Am Coll Cardiol 2002;40:271-7.

de Sousa Abreu R, Penalva LO, Marcotte EM, Vogel C. Global signatures of protein and mRNA expression levels. Mol Biosyst 2009;5:1512-26.

DeFronzo RA. The EMPA-REG study: What has it told us? A diabetologist's perspective. J Diabetes Complications 2016;30:1-2.

Degens H, de Brouwer KF, Gilde AJ et al. Cardiac fatty acid metabolism is preserved in the compensated hypertrophic rat heart. Basic Res Cardiol 2006;101:17-26.

Dennis SC, Gevers W, Opie LH. Protons in ischemia: where do they come from; where do they go to? J Mol Cell Cardiol 1991;23:1077-86.

Depre C, Shipley GL, Chen W et al. Unloaded heart in vivo replicates fetal gene expression of cardiac hypertrophy. Nat Med 1998;4:1269-75.

Depre C, Vanoverschelde JL, Taegtmeyer H. Glucose for the heart. Circulation 1999;99:578-88.

Despa S, Islam MA, Weber CR, Pogwizd SM, Bers DM. Intracellular Na(+) concentration is elevated in heart failure but Na/K pump function is unchanged. Circulation 2002;105:2543-8.

Devenny JJ, Godonis HE, Harvey SJ, Rooney S, Cullen MJ, Pelleymounter MA. Weight loss induced by chronic dapagliflozin treatment is attenuated by compensatory hyperphagia in diet-induced obese (DIO) rats. Obesity (Silver Spring) 2012;20:1645-52.

Diakos NA, Navankasattusas S, Abel ED et al. Evidence of Glycolysis Up-Regulation and Pyruvate Mitochondrial Oxidation Mismatch During Mechanical Unloading of the Failing Human

Heart: Implications for Cardiac Reloading and Conditioning. JACC Basic Transl Sci 2016;1:432-444.

Doenst T, Pytel G, Schrepper A et al. Decreased rates of substrate oxidation ex vivo predict the onset of heart failure and contractile dysfunction in rats with pressure overload. Cardiovasc Res 2010;86:461-70.

Doi R, Masuyama T, Yamamoto K et al. Development of different phenotypes of hypertensive heart failure: systolic versus diastolic failure in Dahl salt-sensitive rats. Journal of hypertension 2000;18:111-20.

Donnelly RP, Finlay DK. Glucose, glycolysis and lymphocyte responses. Mol Immunol 2015;68:513-9.

Dorn GW, 2nd, Force T. Protein kinase cascades in the regulation of cardiac hypertrophy. J Clin Invest 2005;115:527-37.

Drakos SG, Terrovitis JV, Anastasiou-Nana MI, Nanas JN. Reverse remodeling during long-term mechanical unloading of the left ventricle. J Mol Cell Cardiol 2007;43:231-42.

Du Z, Shen A, Huang Y et al. 1H-NMR-based metabolic analysis of human serum reveals novel markers of myocardial energy expenditure in heart failure patients. PLoS One 2014;9:e88102.

Dyck JR, Cheng JF, Stanley WC et al. Malonyl coenzyme a decarboxylase inhibition protects the ischemic heart by inhibiting fatty acid oxidation and stimulating glucose oxidation. Circ Res 2004;94:e78-84.

Dyck JR, Lopaschuk GD. AMPK alterations in cardiac physiology and pathology: enemy or ally? J Physiol 2006;574:95-112.

Elahi M, Asopa S, Matata B. NO-cGMP and TNF-alpha counter regulatory system in blood: understanding the mechanisms leading to myocardial dysfunction and failure. Biochim Biophys Acta 2007;1772:5-14.

Emdin CA, Rahimi K, Neal B, Callender T, Perkovic V, Patel A. Blood pressure lowering in type 2 diabetes: a systematic review and meta-analysis. JAMA 2015;313:603-15.

Engelhardt S, Hein L, Keller U, Klambt K, Lohse MJ. Inhibition of Na(+)-H(+) exchange prevents hypertrophy, fibrosis, and heart failure in beta(1)-adrenergic receptor transgenic mice. Circ Res 2002;90:814-9.

Fadok VA, Bratton DL, Konowal A, Freed PW, Westcott JY, Henson PM. Macrophages that have ingested apoptotic cells in vitro inhibit proinflammatory cytokine production through autocrine/paracrine mechanisms involving TGF-beta, PGE2, and PAF. J Clin Invest 1998;101:890-8.

Faillie JL. Pharmacological aspects of the safety of gliflozins. Pharmacol Res 2017;118:71-81.

Falkenham A, de Antueno R, Rosin N et al. Nonclassical resident macrophages are important determinants in the development of myocardial fibrosis. Am J Pathol 2015;185:927-42.

Feng H, Gu J, Gou F et al. High Glucose and Lipopolysaccharide Prime NLRP3 Inflammasome via ROS/TXNIP Pathway in Mesangial Cells. J Diabetes Res 2016;2016:6973175.

Ferrannini E, Baldi S, Frascerra S et al. Shift to Fatty Substrate Utilization in Response to Sodium-Glucose Cotransporter 2 Inhibition in Subjects Without Diabetes and Patients With Type 2 Diabetes. Diabetes 2016;65:1190-5.

Ferrannini E, Mark M, Mayoux E. CV Protection in the EMPA-REG OUTCOME Trial: A "Thrifty Substrate" Hypothesis. Diabetes care 2016;39:1108-14.

Ferrannini E, Muscelli E, Frascerra S et al. Metabolic response to sodium-glucose cotransporter 2 inhibition in type 2 diabetic patients. J Clin Invest 2014;124:499-508.

Ferrannini E, Santoro D, Bonadonna R, Natali A, Parodi O, Camici PG. Metabolic and hemodynamic effects of insulin on human hearts. Am J Physiol 1993;264:E308-15.

Ferrannini E. The theoretical bases of indirect calorimetry: a review. Metabolism: clinical and experimental 1988;37:287-301.

Fillmore N, Levasseur JL, Fukushima A et al. Uncoupling of glycolysis from glucose oxidation accompanies the development of heart failure with preserved ejection fraction. Mol Med 2018;24:3.

Fitchett D, Zinman B, Wanner C et al. Heart failure outcomes with empagliflozin in patients with type 2 diabetes at high cardiovascular risk: results of the EMPA-REG OUTCOME(R) trial. Eur Heart J 2016;37:1526-34.

Forrester MT, Seth D, Hausladen A et al. Thioredoxin-interacting protein (Txnip) is a feedback regulator of S-nitrosylation. J Biol Chem 2009;284:36160-6.

Fragasso G, Palloshi A, Puccetti P et al. A randomized clinical trial of trimetazidine, a partial free fatty acid oxidation inhibitor, in patients with heart failure. J Am Coll Cardiol 2006;48:992-8.

Fragasso G, Perseghin G, De Cobelli F et al. Effects of metabolic modulation by trimetazidine on left ventricular function and phosphocreatine/adenosine triphosphate ratio in patients with heart failure. Eur Heart J 2006;27:942-8.

Frangogiannis NG, Lindsey ML, Michael LH et al. Resident cardiac mast cells degranulate and release preformed TNF-alpha, initiating the cytokine cascade in experimental canine myocardial ischemia/reperfusion. Circulation 1998;98:699-710.

Frangogiannis NG. Cardiac fibrosis: Cell biological mechanisms, molecular pathways and therapeutic opportunities. Mol Aspects Med 2019;65:70-99.

Frank A, Bonney M, Bonney S, Weitzel L, Koeppen M, Eckle T. Myocardial ischemia reperfusion injury: from basic science to clinical bedside. Semin Cardiothorac Vasc Anesth 2012;16:123-32.

Frey N, Olson EN. Cardiac hypertrophy: the good, the bad, and the ugly. Annu Rev Physiol 2003;65:45-79.

Friedrich C, Metzmann K, Rose P, Mattheus M, Pinnetti S, Woerle HJ. A randomized, open-label, crossover study to evaluate the pharmacokinetics of empagliflozin and linagliptin after coadministration in healthy male volunteers. Clin Ther 2013;35:A33-42.

Fu SP, Li SN, Wang JF et al. BHBA suppresses LPS-induced inflammation in BV-2 cells by inhibiting NF-kappaB activation. Mediators Inflamm 2014;2014:983401.

Fukao T, Lopaschuk GD, Mitchell GA. Pathways and control of ketone body metabolism: on the fringe of lipid biochemistry. Prostaglandins Leukot Essent Fatty Acids 2004;70:243-51.

Funada J, Betts TR, Hodson L et al. Substrate utilization by the failing human heart by direct quantification using arterio-venous blood sampling. PLoS One 2009;4:e7533.

Gallo LA, Ward MS, Fotheringham AK et al. Once daily administration of the SGLT2 inhibitor, empagliflozin, attenuates markers of renal fibrosis without improving albuminuria in diabetic db/db mice. Sci Rep 2016;6:26428.

Gambhir D, Ananth S, Veeranan-Karmegam R et al. GPR109A as an anti-inflammatory receptor in retinal pigment epithelial cells and its relevance to diabetic retinopathy. Invest Ophthalmol Vis Sci 2012;53:2208-17.

Gambhir V, Yildiz C, Mulder R et al. The TLR2 agonists lipoteichoic acid and Pam3CSK4 induce greater pro-inflammatory responses than inactivated Mycobacterium butyricum. Cell Immunol 2012;280:101-7.

Gao XM, Kiriazis H, Moore XL et al. Regression of pressure overload-induced left ventricular hypertrophy in mice. Am J Physiol Heart Circ Physiol 2005;288:H2702-7.

Garnier A, Fortin D, Delomenie C, Momken I, Veksler V, Ventura-Clapier R. Depressed mitochondrial transcription factors and oxidative capacity in rat failing cardiac and skeletal muscles. J Physiol 2003;551:491-501.

Gembardt F, Bartaun C, Jarzebska N et al. The SGLT2 inhibitor empagliflozin ameliorates early features of diabetic nephropathy in BTBR ob/ob type 2 diabetic mice with and without hypertension. American journal of physiology Renal physiology 2014;307:F317-25.

Gilbert RE, Connelly KA. Understanding EMPA-REG OUTCOME. Lancet Diabetes Endocrinol 2015;3:930-1.

Gilbert RE, Krum H. Heart failure in diabetes: effects of anti-hyperglycaemic drug therapy. Lancet 2015;385:2107-17.

Goldberg EL, Asher JL, Molony RD et al. beta-Hydroxybutyrate Deactivates Neutrophil NLRP3 Inflammasome to Relieve Gout Flares. Cell Rep 2017;18:2077-2087.

Goldberg RJ, Spencer FA, Yarzebski J et al. A 25-year perspective into the changing landscape of patients hospitalized with acute myocardial infarction (the Worcester Heart Attack Study). Am J Cardiol 2004;94:1373-8.

Green JB, Bethel MA, Armstrong PW et al. Effect of Sitagliptin on Cardiovascular Outcomes in Type 2 Diabetes. N Engl J Med 2015;373:232-42.

Greenberg H, McMaster P, Dwyer EM, Jr. Left ventricular dysfunction after acute myocardial infarction: results of a prospective multicenter study. J Am Coll Cardiol 1984;4:867-74.

Grempler R, Thomas L, Eckhardt M et al. Empagliflozin, a novel selective sodium glucose cotransporter-2 (SGLT-2) inhibitor: characterisation and comparison with other SGLT-2 inhibitors. Diabetes Obes Metab 2012;14:83-90.

Guo M, Wang X, Zhao Y et al. Ketogenic Diet Improves Brain Ischemic Tolerance and Inhibits NLRP3 Inflammasome Activation by Preventing Drp1-Mediated Mitochondrial Fission and Endoplasmic Reticulum Stress. Front Mol Neurosci 2018;11:86.

Guo Y, Xiao P, Lei S et al. How is mRNA expression predictive for protein expression? A correlation study on human circulating monocytes. Acta Biochim Biophys Sin (Shanghai) 2008;40:426-36.

Gupte AA, Hamilton DJ, Cordero-Reyes AM et al. Mechanical unloading promotes myocardial energy recovery in human heart failure. Circ Cardiovasc Genet 2014;7:266-76.

Habibi J, Aroor AR, Sowers JR et al. Sodium glucose transporter 2 (SGLT2) inhibition with empagliflozin improves cardiac diastolic function in a female rodent model of diabetes. Cardiovasc Diabetol 2017;16:9.

Haffner SM. Abdominal adiposity and cardiometabolic risk: do we have all the answers? Am J Med 2007;120:S10-6; discussion S16-7.

Hammoudi N, Jeong D, Singh R et al. Empagliflozin Improves Left Ventricular Diastolic Dysfunction in a Genetic Model of Type 2 Diabetes. Cardiovasc Drugs Ther 2017;31:233-246.

Hara M, Ono K, Hwang MW et al. Evidence for a role of mast cells in the evolution to congestive heart failure. J Exp Med 2002;195:375-81.

Hardie DG. Minireview: the AMP-activated protein kinase cascade: the key sensor of cellular energy status. Endocrinology 2003;144:5179-83.

Heather LC, Howell NJ, Emmanuel Y et al. Changes in cardiac substrate transporters and metabolic proteins mirror the metabolic shift in patients with aortic stenosis. PLoS One 2011;6:e26326.

Hediger MA, Rhoads DB. Molecular physiology of sodium-glucose cotransporters. Physiol Rev 1994;74:993-1026.

Heerdt PM, Holmes JW, Cai B et al. Chronic unloading by left ventricular assist device reverses contractile dysfunction and alters gene expression in end-stage heart failure. Circulation 2000;102:2713-9.

Heerspink HJ, Perkins BA, Fitchett DH, Husain M, Cherney DZ. Sodium Glucose Cotransporter 2 Inhibitors in the Treatment of Diabetes Mellitus: Cardiovascular and Kidney Effects, Potential Mechanisms, and Clinical Applications. Circulation 2016;134:752-72.

Heise T, Jordan J, Wanner C et al. Pharmacodynamic Effects of Single and Multiple Doses of Empagliflozin in Patients With Type 2 Diabetes. Clinical therapeutics 2016;38:2265-2276.

Heise T, Seewaldt-Becker E, Macha S et al. Safety, tolerability, pharmacokinetics and pharmacodynamics following 4 weeks' treatment with empagliflozin once daily in patients with type 2 diabetes. Diabetes Obes Metab 2013;15:613-21.

Heise T, Seman L, Macha S et al. Safety, tolerability, pharmacokinetics, and pharmacodynamics of multiple rising doses of empagliflozin in patients with type 2 diabetes mellitus. Diabetes Ther 2013;4:331-45.

Heyen JR, Blasi ER, Nikula K et al. Structural, functional, and molecular characterization of the SHHF model of heart failure. Am J Physiol Heart Circ Physiol 2002;283:H1775-84.

Ho KL, Zhang L, Wagg C et al. Increased ketone body oxidation provides additional energy for the failing heart without improving cardiac efficiency. Cardiovasc Res 2019; [Epub ahead of print].

Hsafety and tolerability of 4 weeks' treatment with empagliflozin in Japanese patientseise T, Seman L, Macha S et al. Safety, tolerability, pharmacokinetics, and pharmacodynamics of multiple rising doses of empagliflozin in patients with type 2 diabetes mellitus. Diabetes Ther 2013;4:331-45.

Hu P, Zhang D, Swenson L, Chakrabarti G, Abel ED, Litwin SE. Minimally invasive aortic banding in mice: effects of altered cardiomyocyte insulin signaling during pressure overload. Am J Physiol Heart Circ Physiol 2003;285:H1261-9.

hui Y, junzhu C, jianhua Z. Gap junction and Na+-H+ exchanger alternations in fibrillating and failing atrium. Int J Cardiol 2008;128:147-9.

Huss JM, Kelly DP. Mitochondrial energy metabolism in heart failure: a question of balance. J Clin Invest 2005;115:547-55.

Iannantuoni F, Diaz-Morales N, Escribano-Lopez I et al. Does Glycemic Control Modulate the Impairment of NLRP3 Inflammasome Activation in Type 2 Diabetes? Antioxid Redox Signal 2018; [Epub ahead of print].

Inagaki N, Kondo K, Yoshinari T, Takahashi N, Susuta Y, Kuki H. Efficacy and safety of canagliflozin monotherapy in Japanese patients with type 2 diabetes inadequately controlled with

diet and exercise: a 24-week, randomized, double-blind, placebo-controlled, Phase III study. Expert Opin Pharmacother 2014;15:1501-15.

Ingelsson E, Bjorklund-Bodegard K, Lind L, Arnlov J, Sundstrom J. Diurnal blood pressure pattern and risk of congestive heart failure. JAMA 2006;295:2859-66.

Inoko M, Kihara Y, Morii I, Fujiwara H, Sasayama S. Transition from compensatory hypertrophy to dilated, failing left ventricles in Dahl salt-sensitive rats. The American journal of physiology 1994;267:H2471-82.

Inoue BH, dos Santos L, Pessoa TD et al. Increased NHE3 abundance and transport activity in renal proximal tubule of rats with heart failure. Am J Physiol Regul Integr Comp Physiol 2012;302:R166-74.

Investigators OT, Gerstein HC, Bosch J et al. Basal insulin and cardiovascular and other outcomes in dysglycemia. N Engl J Med 2012;367:319-28.

Isaji M. Sodium-glucose cotransporter inhibitors for diabetes. Curr Opin Investig Drugs 2007;8:285-92.

Janardhan A, Chen J, Crawford PA. Altered systemic ketone body metabolism in advanced heart failure. Tex Heart Inst J 2011;38:533-8.

Jaswal JS, Keung W, Wang W, Ussher JR, Lopaschuk GD. Targeting fatty acid and carbohydrate oxidation--a novel therapeutic intervention in the ischemic and failing heart. Biochim Biophys Acta 2011;1813:1333-50.

Jorgensen NB, Pedersen J, Vaag AA. EMPA-REG: Glucose excretion and lipid mobilization - not storage - saves lives. Journal of diabetes and its complications 2016;30:753.

Joubert M, Jagu B, Montaigne D et al. The Sodium-Glucose Cotransporter 2 Inhibitor Dapagliflozin Prevents Cardiomyopathy in a Diabetic Lipodystrophic Mouse Model. Diabetes 2017;66:1030-1040.

Kanada S, Koiwai K, Taniguchi A, Sarashina A, Seman L, Woerle HJ. Pharmacokinetics, pharmacodynamics, safety and tolerability of 4 weeks' treatment with empagliflozin in Japanese patients with type 2 diabetes mellitus. J Diabetes Investig 2013;4:613-7.

Kappel BA, Lehrke M, Schutt K et al. Effect of Empagliflozin on the Metabolic Signature of Patients With Type 2 Diabetes Mellitus and Cardiovascular Disease. Circulation 2017;136:969-972.

Karasawa T, Takahashi M. Role of NLRP3 Inflammasomes in Atherosclerosis. J Atheroscler Thromb 2017;24:443-451.

Karmazyn M. NHE-1: still a viable therapeutic target. J Mol Cell Cardiol 2013;61:77-82.

Karwi QG, Uddin GM, Ho KL, Lopaschuk GD. Loss of Metabolic Flexibility in the Failing Heart. Front Cardiovasc Med 2018;5:68.

Karwi QG, Zhang L, Wagg CS et al. Targeting the glucagon receptor improves cardiac function and enhances insulin sensitivity following a myocardial infarction. Cardiovasc Diabetol 2019;18:1.

Kashiwagi Y, Nagoshi T, Yoshino T et al. Expression of SGLT1 in Human Hearts and Impairment of Cardiac Glucose Uptake by Phlorizin during Ischemia-Reperfusion Injury in Mice. PLoS One 2015;10:e0130605.

Kashiwaya Y, King MT, Veech RL. Substrate signaling by insulin: a ketone bodies ratio mimics insulin action in heart. Am J Cardiol 1997;80:50A-64A.

Kato T, Niizuma S, Inuzuka Y et al. Analysis of metabolic remodeling in compensated left ventricular hypertrophy and heart failure. Circ Heart Fail 2010;3:420-30.

Kawaguchi M, Takahashi M, Hata T et al. Inflammasome activation of cardiac fibroblasts is essential for myocardial ischemia/reperfusion injury. Circulation 2011;123:594-604.

Kehat I, Molkentin JD. Molecular pathways underlying cardiac remodeling during pathophysiological stimulation. Circulation 2010;122:2727-35.

Kemppainen J, Fujimoto T, Kalliokoski KK, Viljanen T, Nuutila P, Knuuti J. Myocardial and skeletal muscle glucose uptake during exercise in humans. J Physiol 2002;542:403-12.

Kienesberger PC, Pulinilkunnil T, Sung MM et al. Myocardial ATGL overexpression decreases the reliance on fatty acid oxidation and protects against pressure overload-induced cardiac dysfunction. Mol Cell Biol 2012;32:740-50.

Kilic A, Huang CX, Rajapurohitam V, Madwed JB, Karmazyn M. Early and transient sodium-hydrogen exchanger isoform 1 inhibition attenuates subsequent cardiac hypertrophy and heart failure following coronary artery ligation. J Pharmacol Exp Ther 2014;351:492-9.

Kim HJ, Lee DW, Ravichandran K et al. NLRP3 inflammasome knockout mice are protected against ischemic but not cisplatin-induced acute kidney injury. J Pharmacol Exp Ther 2013;346:465-72.

Kim M, Shen M, Ngoy S, Karamanlidis G, Liao R, Tian R. AMPK isoform expression in the normal and failing hearts. J Mol Cell Cardiol 2012;52:1066-73.

Kim TT, Dyck JR. Is AMPK the savior of the failing heart? Trends Endocrinol Metab 2015;26:40-8.

Kiss E, Ball NA, Kranias EG, Walsh RA. Differential changes in cardiac phospholamban and sarcoplasmic reticular Ca(2+)-ATPase protein levels. Effects on Ca2+ transport and mechanics in compensated pressure-overload hypertrophy and congestive heart failure. Circ Res 1995;77:759-64.

Klotz S, Hay I, Zhang G, Maurer M, Wang J, Burkhoff D. Development of heart failure in chronic hypertensive Dahl rats: focus on heart failure with preserved ejection fraction. Hypertension 2006;47:901-11.

Kolwicz SC, Jr., Tian R. Glucose metabolism and cardiac hypertrophy. Cardiovasc Res 2011;90:194-201.

Komoroski B, Vachharajani N, Feng Y, Li L, Kornhauser D, Pfister M. Dapagliflozin, a novel, selective SGLT2 inhibitor, improved glycemic control over 2 weeks in patients with type 2 diabetes mellitus. Clin Pharmacol Ther 2009;85:513-9.

Koonen DP, Sung MM, Kao CK et al. Alterations in skeletal muscle fatty acid handling predisposes middle-aged mice to diet-induced insulin resistance. Diabetes 2010;59:1366-75.

Kosiborod M, Cavender MA, Fu AZ et al. Lower Risk of Heart Failure and Death in Patients Initiated on Sodium-Glucose Cotransporter-2 Inhibitors Versus Other Glucose-Lowering Drugs: The CVD-REAL Study (Comparative Effectiveness of Cardiovascular Outcomes in New Users of Sodium-Glucose Cotransporter-2 Inhibitors). Circulation 2017;136:249-259.

Kousathana F, Georgitsi M, Lambadiari V, Giamarellos-Bourboulis EJ, Dimitriadis G, Mouktaroudi M. Defective production of interleukin-1 beta in patients with type 2 diabetes mellitus: Restoration by proper glycemic control. Cytokine 2017;90:177-184.

Krishnan SM, Dowling JK, Ling YH et al. Inflammasome activity is essential for one kidney/deoxycorticosterone acetate/salt-induced hypertension in mice. Br J Pharmacol 2016;173:752-65.

Kubota T, McTiernan CF, Frye CS et al. Dilated cardiomyopathy in transgenic mice with cardiac-specific overexpression of tumor necrosis factor-alpha. Circ Res 1997;81:627-35.

Kurosaki E, Ogasawara H. Ipragliflozin and other sodium-glucose cotransporter-2 (SGLT2) inhibitors in the treatment of type 2 diabetes: preclinical and clinical data. Pharmacol Ther 2013;139:51-9.

Kusaka H, Koibuchi N, Hasegawa Y, Ogawa H, Kim-Mitsuyama S. Empagliflozin lessened cardiac injury and reduced visceral adipocyte hypertrophy in prediabetic rats with metabolic syndrome. Cardiovasc Diabetol 2016;15:157.

Lahnwong S, Chattipakorn SC, Chattipakorn N. Potential mechanisms responsible for cardioprotective effects of sodium-glucose co-transporter 2 inhibitors. Cardiovasc Diabetol 2018;17:101.

Lai L, Leone TC, Keller MP et al. Energy metabolic reprogramming in the hypertrophied and early stage failing heart: a multisystems approach. Circ Heart Fail 2014;7:1022-31.

Lambers Heerspink HJ, de Zeeuw D, Wie L, Leslie B, List J. Dapagliflozin a glucose-regulating drug with diuretic properties in subjects with type 2 diabetes. Diabetes Obes Metab 2013;15:853-62.

Landesberg G, Gilon D, Meroz Y et al. Diastolic dysfunction and mortality in severe sepsis and septic shock. Eur Heart J 2012;33:895-903.

Larsen CM, Faulenbach M, Vaag A et al. Interleukin-1-receptor antagonist in type 2 diabetes mellitus. N Engl J Med 2007;356:1517-26.

Lee SB, Kalluri R. Mechanistic connection between inflammation and fibrosis. Kidney Int Suppl 2010:S22-6.

Lee TM, Chang NC, Lin SZ. Dapagliflozin, a selective SGLT2 Inhibitor, attenuated cardiac fibrosis by regulating the macrophage polarization via STAT3 signaling in infarcted rat hearts. Free Radic Biol Med 2017;104:298-310.

LEE Y-H, KIM SR, BAE J et al. SGLT2 Inhibitors Suppress NLRP3 Inflammasome Activity via Changes in Ketones and Insulin in Type 2 Diabetes and Cardiovascular Diseases. Diabetes 2018;67:164-OR.

LEE Y-H, KIM SR, BAE J et al. SGLT2 Inhibitors Suppress NLRP3 Inflammasome Activity via Changes in Ketones and Insulin in Type 2 Diabetes and Cardiovascular Diseases. Diabetes 2018;67.

Lehman JJ, Kelly DP. Gene regulatory mechanisms governing energy metabolism during cardiac hypertrophic growth. Heart Fail Rev 2002;7:175-85.

Lei B, Lionetti V, Young ME et al. Paradoxical downregulation of the glucose oxidation pathway despite enhanced flux in severe heart failure. J Mol Cell Cardiol 2004;36:567-76.

Leng W, Ouyang X, Lei X et al. The SGLT-2 Inhibitor Dapagliflozin Has a Therapeutic Effect on Atherosclerosis in Diabetic ApoE(-/-) Mice. Mediators of inflammation 2016;2016:6305735.

Leong HN, Ang B, Earnest A, Teoh C, Xu W, Leo YS. Investigational use of ribavirin in the treatment of severe acute respiratory syndrome, Singapore, 2003. Trop Med Int Health 2004;9:923-7.

Levelt E, Mahmod M, Piechnik SK et al. Relationship Between Left Ventricular Structural and Metabolic Remodeling in Type 2 Diabetes. Diabetes 2016;65:44-52.

Li C, Zhang J, Xue M et al. SGLT2 inhibition with empagliflozin attenuates myocardial oxidative stress and fibrosis in diabetic mice heart. Cardiovasc Diabetol 2019;18:15.

Li F, Zhang H, Yang L et al. NLRP3 deficiency accelerates pressure overload-induced cardiac remodeling via increased TLR4 expression. J Mol Med (Berl) 2018;96:1189-1202.

Li R, Lu K, Wang Y et al. Triptolide attenuates pressure overload-induced myocardial remodeling in mice via the inhibition of NLRP3 inflammasome expression. Biochemical and biophysical research communications 2017;485:69-75.

Li S, Wu H, Han D et al. ZP2495 Protects against Myocardial Ischemia/Reperfusion Injury in Diabetic Mice through Improvement of Cardiac Metabolism and Mitochondrial Function: The Possible Involvement of AMPK-FoxO3a Signal Pathway. Oxid Med Cell Longev 2018;2018:6451902.

Li XM, Ma YT, Yang YN et al. Downregulation of survival signalling pathways and increased apoptosis in the transition of pressure overload-induced cardiac hypertrophy to heart failure. Clin Exp Pharmacol Physiol 2009;36:1054-61.

Lin B, Koibuchi N, Hasegawa Y et al. Glycemic control with empagliflozin, a novel selective SGLT2 inhibitor, ameliorates cardiovascular injury and cognitive dysfunction in obese and type 2 diabetic mice. Cardiovasc Diabetol 2014;13:148.

Lindner D, Zietsch C, Tank J et al. Cardiac fibroblasts support cardiac inflammation in heart failure. Basic Res Cardiol 2014;109:428.

Liu T, O'Rourke B. Enhancing mitochondrial Ca2+ uptake in myocytes from failing hearts restores energy supply and demand matching. Circ Res 2008;103:279-88.

Liu T, Takimoto E, Dimaano VL et al. Inhibiting mitochondrial Na+/Ca2+ exchange prevents sudden death in a Guinea pig model of heart failure. Circ Res 2014;115:44-54.

Liu Y, Lian K, Zhang L et al. TXNIP mediates NLRP3 inflammasome activation in cardiac microvascular endothelial cells as a novel mechanism in myocardial ischemia/reperfusion injury. Basic research in cardiology 2014;109:415.

Liu Y, Peterson DA, Kimura H, Schubert D. Mechanism of cellular 3-(4,5-dimethylthiazol-2-yl)-2,5-diphenyltetrazolium bromide (MTT) reduction. Journal of neurochemistry 1997;69:581-93.

Livak KJ, Schmittgen TD. Analysis of relative gene expression data using real-time quantitative PCR and the 2(-Delta Delta C(T)) Method. Methods 2001;25:402-8.

Lommi J, Kupari M, Koskinen P et al. Blood ketone bodies in congestive heart failure. J Am Coll Cardiol 1996;28:665-72.

Lommi J, Kupari M, Yki-Jarvinen H. Free fatty acid kinetics and oxidation in congestive heart failure. Am J Cardiol 1998;81:45-50.

Lopaschuk GD, Ussher JR, Folmes CD, Jaswal JS, Stanley WC. Myocardial fatty acid metabolism in health and disease. Physiol Rev 2010;90:207-58.

Lopaschuk GD, Verma S. Empagliflozin's Fuel Hypothesis: Not so Soon. Cell metabolism 2016;24:200-2.

Lorell BH. Transition from hypertrophy to failure. Circulation 1997;96:3824-7.

Lowes BD, Minobe W, Abraham WT et al. Changes in gene expression in the intact human heart. Downregulation of alpha-myosin heavy chain in hypertrophied, failing ventricular myocardium. J Clin Invest 1997;100:2315-24.

Lu TM, Tsai JY, Chen YC et al. Downregulation of Sirt1 as aging change in advanced heart failure. J Biomed Sci 2014;21:57.

Lutken SC, Kim SW, Jonassen T et al. Changes of renal AQP2, ENaC, and NHE3 in experimentally induced heart failure: response to angiotensin II AT1 receptor blockade. Am J Physiol Renal Physiol 2009;297:F1678-88.

Ma F, Li Y, Jia L et al. Macrophage-stimulated cardiac fibroblast production of IL-6 is essential for TGF beta/Smad activation and cardiac fibrosis induced by angiotensin II. PLoS One 2012;7:e35144.

Maayah ZH, El Gendy MA, El-Kadi AO, Korashy HM. Sunitinib, a tyrosine kinase inhibitor, induces cytochrome P450 1A1 gene in human breast cancer MCF7 cells through ligand-independent aryl hydrocarbon receptor activation. Archives of toxicology 2013;87:847-56.

Maayah ZH, Elshenawy OH, Althurwi HN, Abdelhamid G, El-Kadi AO. Human fetal ventricular cardiomyocyte, RL-14 cell line, is a promising model to study drug metabolizing enzymes and their associated arachidonic acid metabolites. Journal of pharmacological and toxicological methods 2015;71:33-41.

Macha S, Jungnik A, Hohl K, Hobson D, Salsali A, Woerle HJ. Effect of food on the pharmacokinetics of empagliflozin, a sodium glucose cotransporter 2 (SGLT2) inhibitor, and assessment of dose proportionality in healthy volunteers. Int J Clin Pharmacol Ther 2013;51:873-9.

Macha S, Mattheus M, Halabi A, Pinnetti S, Woerle HJ, Broedl UC. Pharmacokinetics, pharmacodynamics and safety of empagliflozin, a sodium glucose cotransporter 2 (SGLT2) inhibitor, in subjects with renal impairment. Diabetes Obes Metab 2014;16:215-22.

Macha S, Rose P, Mattheus M, Pinnetti S, Woerle HJ. Lack of drug-drug interaction between empagliflozin, a sodium glucose cotransporter 2 inhibitor, and warfarin in healthy volunteers. Diabetes Obes Metab 2013;15:316-23.

Marchetti C, Toldo S, Chojnacki J et al. Pharmacologic Inhibition of the NLRP3 Inflammasome Preserves Cardiac Function After Ischemic and Nonischemic Injury in the Mouse. J Cardiovasc Pharmacol 2015;66:1-8.

Martin MA, Gomez MA, Guillen F et al. Myocardial carnitine and carnitine palmitoyltransferase deficiencies in patients with severe heart failure. Biochim Biophys Acta 2000;1502:330-6.

Matsumura M, Nakatani Y, Tanka S et al. Efficacy of Additional Canagliflozin Administration to Type 2 Diabetes Patients Receiving Insulin Therapy: Examination of Diurnal Glycemic Patterns Using Continuous Glucose Monitoring (CGM). Diabetes Ther 2017;8:821-827.

Matsumura N, Takahara S, Maayah ZH et al. Resveratrol improves cardiac function and exercise performance in MI-induced heart failure through the inhibition of cardiotoxic HETE metabolites. Journal of molecular and cellular cardiology 2018;125:162-173.

McAlister FA, Teo KK, Taher M et al. Insights into the contemporary epidemiology and outpatient management of congestive heart failure. American heart journal 1999;138:87-94.

McGarry JD, Brown NF. The mitochondrial carnitine palmitoyltransferase system. From concept to molecular analysis. Eur J Biochem 1997;244:1-14.

McGarry JD, Foster DW. Regulation of hepatic fatty acid oxidation and ketone body production. Annu Rev Biochem 1980;49:395-420.

Merovci A, Solis-Herrera C, Daniele G et al. Dapagliflozin improves muscle insulin sensitivity but enhances endogenous glucose production. J Clin Invest 2014;124:509-14.

Mezzaroma E, Toldo S, Farkas D et al. The inflammasome promotes adverse cardiac remodeling following acute myocardial infarction in the mouse. Proc Natl Acad Sci U S A 2011;108:19725-30.

Mizuno M, Kuno A, Yano T et al. Empagliflozin normalizes the size and number of mitochondria and prevents reduction in mitochondrial size after myocardial infarction in diabetic hearts. Physiol Rep 2018;6:e13741.

Monnet E, Chachques JC. Animal models of heart failure: what is new? Ann Thorac Surg 2005;79:1445-53.

Mori J, Alrob OA, Wagg CS, Harris RA, Lopaschuk GD, Oudit GY. ANG II causes insulin resistance and induces cardiac metabolic switch and inefficiency: a critical role of PDK4. Am J Physiol Heart Circ Physiol 2013;304:H1103-13.

Mori J, Basu R, McLean BA et al. Agonist-induced hypertrophy and diastolic dysfunction are associated with selective reduction in glucose oxidation: a metabolic contribution to heart failure with normal ejection fraction. Circ Heart Fail 2012;5:493-503.

Mudaliar S, Alloju S, Henry RR. Can a Shift in Fuel Energetics Explain the Beneficial Cardiorenal Outcomes in the EMPA-REG OUTCOME Study? A Unifying Hypothesis. Diabetes Care 2016;39:1115-22.

Mudaliar S, Polidori D, Zambrowicz B, Henry RR. Sodium-Glucose Cotransporter Inhibitors: Effects on Renal and Intestinal Glucose Transport: From Bench to Bedside. Diabetes Care 2015;38:2344-53.

Mudd JO, Kass DA. Reversing chronic remodeling in heart failure. Expert Rev Cardiovasc Ther 2007;5:585-98.

Murakami T, Kokado H. Abstract 17182: Empagliflozin Early Reverses Metabolic and Cardiac Disturbances in Type-2 Diabetics With Chronic Heart Failure. Circulation 2017;136:A17182-A17182.

Murakami T, Ockinger J, Yu J et al. Critical role for calcium mobilization in activation of the NLRP3 inflammasome. Proceedings of the National Academy of Sciences of the United States of America 2012;109:11282-7.

Murthy MS, Pande SV. Malonyl-CoA binding site and the overt carnitine palmitoyltransferase activity reside on the opposite sides of the outer mitochondrial membrane. Proc Natl Acad Sci U S A 1987;84:378-82.

Muskiet MH, van Raalte DH, van Bommel EJ, Smits MM, Tonneijck L. Understanding EMPA-REG OUTCOME. Lancet Diabetes Endocrinol 2015;3:928-9.

Mustroph J, Lucht CM, Wagemann O et al. Empagliflozin enhances human and murine cardiomyocyte glucose uptake by increased expression of GLUT1. Diabetologia 2019;62:726-729.

Mustroph J, Wagemann O, Lucht CM et al. Empagliflozin reduces Ca/calmodulin-dependent kinase II activity in isolated ventricular cardiomyocytes. ESC heart failure 2018;5:642-648.

Nagao M, Toh R, Irino Y et al. beta-Hydroxybutyrate elevation as a compensatory response against oxidative stress in cardiomyocytes. Biochem Biophys Res Commun 2016;475:322-8.

Nagendran J, Waller TJ, Dyck JR. AMPK signalling and the control of substrate use in the heart. Mol Cell Endocrinol 2013;366:180-93.

Nagueh SF, Smiseth OA, Appleton CP et al. Recommendations for the Evaluation of Left Ventricular Diastolic Function by Echocardiography: An Update from the American Society of Echocardiography and the European Association of Cardiovascular Imaging. Eur Heart J Cardiovasc Imaging 2016;17:1321-1360.

Nair AB, Jacob S. A simple practice guide for dose conversion between animals and human. J Basic Clin Pharm 2016;7:27-31.

Nascimben L, Ingwall JS, Lorell BH et al. Mechanisms for increased glycolysis in the hypertrophied rat heart. Hypertension 2004;44:662-7.

Naylor LH, George K, O'Driscoll G, Green DJ. The athlete's heart: a contemporary appraisal of the 'Morganroth hypothesis'. Sports Med 2008;38:69-90.

Neal B, Perkovic V, Mahaffey KW et al. Canagliflozin and Cardiovascular and Renal Events in Type 2 Diabetes. The New England journal of medicine 2017;377:644-657.

Neal B, Perkovic V, Matthews DR. Canagliflozin and Cardiovascular and Renal Events in Type 2 Diabetes. N Engl J Med 2017;377:2099.

Neeland IJ, McGuire DK, Chilton R et al. Empagliflozin reduces body weight and indices of adipose distribution in patients with type 2 diabetes mellitus. Diab Vasc Dis Res 2016;13:119-26.

Neglia D, De Caterina A, Marraccini P et al. Impaired myocardial metabolic reserve and substrate selection flexibility during stress in patients with idiopathic dilated cardiomyopathy. Am J Physiol Heart Circ Physiol 2007;293:H3270-8.

Neubauer S, Horn M, Cramer M et al. Myocardial Phosphocreatine-to-ATP Ratio Is a Predictor of Mortality in Patients With Dilated Cardiomyopathy. Circulation 1997;96:2190-2196.

Neubauer S. The failing heart--an engine out of fuel. N Engl J Med 2007;356:1140-51.

Neudorf H, Durrer C, Myette-Cote E, Makins C, O'Malley T, Little JP. Oral Ketone Supplementation Acutely Increases Markers of NLRP3 Inflammasome Activation in Human Monocytes. Mol Nutr Food Res 2019;63:e1801171.

Nielsen R, Moller N, Gormsen LC et al. Cardiovascular Effects of Treatment with the Ketone Body 3-Hydroxybutyrate in Chronic Heart Failure Patients. Circulation 2019; [Epub ahead of print].

Norrelund H, Wiggers H, Halbirk M et al. Abnormalities of whole body protein turnover, muscle metabolism and levels of metabolic hormones in patients with chronic heart failure. J Intern Med 2006;260:11-21.

Nr J, Tr L, Mv H, Nb S, He B. Sodium Glucose Transporter 2 (SGLT2) Inhibition does not Protect the Myocardium from Acute Ischemic Reperfusion Injury but Modulates Post- Ischemic Mitochondrial Function. Cardiovascular Pharmacology: Open Access 2017;06.

Oh JK, Appleton CP, Hatle LK, Nishimura RA, Seward JB, Tajik AJ. The noninvasive assessment of left ventricular diastolic function with two-dimensional and Doppler echocardiography. J Am Soc Echocardiogr 1997;10:246-70.

Olde Engberink RH, Frenkel WJ, van den Bogaard B, Brewster LM, Vogt L, van den Born BJ. Effects of thiazide-type and thiazide-like diuretics on cardiovascular events and mortality: systematic review and meta-analysis. Hypertension 2015;65:1033-40.

Oshima H, Miki T, Kuno A et al. Empagliflozin, an SGLT2 Inhibitor, Reduced the Mortality Rate after Acute Myocardial Infarction with Modification of Cardiac Metabolomes and Antioxidants in Diabetic Rats. J Pharmacol Exp Ther 2019;368:524-534.

Osorio JC, Stanley WC, Linke A et al. Impaired myocardial fatty acid oxidation and reduced protein expression of retinoid X receptor-alpha in pacing-induced heart failure. Circulation 2002;106:606-12.

Owan TE, Redfield MM. Epidemiology of diastolic heart failure. Prog Cardiovasc Dis 2005;47:320-32.

Pabel S, Wagner S, Bollenberg H et al. Empagliflozin directly improves diastolic function in human heart failure. Eur J Heart Fail 2018;20:1690-1700.

Paolisso G, Gambardella A, Galzerano D et al. Total-body and myocardial substrate oxidation in congestive heart failure. Metabolism 1994;43:174-9.

Parati G, Esler M. The human sympathetic nervous system: its relevance in hypertension and heart failure. Eur Heart J 2012;33:1058-66.

Paulson DJ, Ward KM, Shug AL. Malonyl CoA inhibition of carnitine palmityltransferase in rat heart mitochondria. FEBS Lett 1984;176:381-4.

Pessoa TD, Campos LC, Carraro-Lacroix L, Girardi AC, Malnic G. Functional role of glucose metabolism, osmotic stress, and sodium-glucose cotransporter isoform-mediated transport on Na+/H+ exchanger isoform 3 activity in the renal proximal tubule. J Am Soc Nephrol 2014;25:2028-39.

Peters AL, Buschur EO, Buse JB, Cohan P, Diner JC, Hirsch IB. Euglycemic Diabetic Ketoacidosis: A Potential Complication of Treatment With Sodium-Glucose Cotransporter 2 Inhibition. Diabetes Care 2015;38:1687-93.

Pogwizd SM, Sipido KR, Verdonck F, Bers DM. Intracellular Na in animal models of hypertrophy and heart failure: contractile function and arrhythmogenesis. Cardiovasc Res 2003;57:887-96.

Polidori D, Sha S, Mudaliar S et al. Canagliflozin lowers postprandial glucose and insulin by delaying intestinal glucose absorption in addition to increasing urinary glucose excretion: results of a randomized, placebo-controlled study. Diabetes Care 2013;36:2154-61.

Ponikowski P, Voors AA, Anker SD et al. 2016 ESC Guidelines for the diagnosis and treatment of acute and chronic heart failure: The Task Force for the diagnosis and treatment of acute and chronic heart failure of the European Society of Cardiology (ESC)Developed with the special contribution of the Heart Failure Association (HFA) of the ESC. European heart journal 2016;37:2129-2200.

Priest BT, McDermott JS. Cardiac ion channels. Channels (Austin) 2015;9:352-9.

Primiano MJ, Lefker BA, Bowman MR et al. Efficacy and Pharmacology of the NLRP3 Inflammasome Inhibitor CP-456,773 (CRID3) in Murine Models of Dermal and Pulmonary Inflammation. J Immunol 2016;197:2421-33.

Psaty BM, Lumley T, Furberg CD et al. Health outcomes associated with various antihypertensive therapies used as first-line agents: a network meta-analysis. JAMA 2003;289:2534-44.

Qanud K, Mamdani M, Pepe M et al. Reverse changes in cardiac substrate oxidation in dogs recovering from heart failure. Am J Physiol Heart Circ Physiol 2008;295:H2098-105.

Qian J, Zhu W, Lu M, Ni B, Yang J. D-beta-hydroxybutyrate promotes functional recovery and relieves pain hypersensitivity in mice with spinal cord injury. Br J Pharmacol 2017;174:1961-1971.

Rahman M, Muhammad S, Khan MA et al. The beta-hydroxybutyrate receptor HCA2 activates a neuroprotective subset of macrophages. Nat Commun 2014;5:3944.

Rajabi M, Kassiotis C, Razeghi P, Taegtmeyer H. Return to the fetal gene program protects the stressed heart: a strong hypothesis. Heart Fail Rev 2007;12:331-43.

Randle PJ, Garland PB, Hales CN, Newsholme EA. The glucose fatty-acid cycle. Its role in insulin sensitivity and the metabolic disturbances of diabetes mellitus. Lancet 1963;1:785-9.

Razeghi P, Young ME, Alcorn JL, Moravec CS, Frazier OH, Taegtmeyer H. Metabolic gene expression in fetal and failing human heart. Circulation 2001;104:2923-31.

Razeghi P, Young ME, Ying J et al. Downregulation of metabolic gene expression in failing human heart before and after mechanical unloading. Cardiology 2002;97:203-9.

Regan JA, Mauro AG, Carbone S et al. A mouse model of heart failure with preserved ejection fraction due to chronic infusion of a low subpressor dose of angiotensin II. Am J Physiol Heart Circ Physiol 2015;309:H771-8.

Reichert K, Colantuono B, McCormack I, Rodrigues F, Pavlov V, Abid MR. Murine Left Anterior Descending (LAD) Coronary Artery Ligation: An Improved and Simplified Model for Myocardial Infarction. J Vis Exp 2017.

Reigner BG, Blesch KS. Estimating the starting dose for entry into humans: principles and practice. Eur J Clin Pharmacol 2002;57:835-45.

Ridderstrale M, Andersen KR, Zeller C et al. Comparison of empagliflozin and glimepiride as add-on to metformin in patients with type 2 diabetes: a 104-week randomised, active-controlled, double-blind, phase 3 trial. The lancet Diabetes & endocrinology 2014;2:691-700.

Ridker PM, Everett BM, Thuren T et al. Antiinflammatory Therapy with Canakinumab for Atherosclerotic Disease. N Engl J Med 2017;377:1119-1131.

Rieg T, Masuda T, Gerasimova M et al. Increase in SGLT1-mediated transport explains renal glucose reabsorption during genetic and pharmacological SGLT2 inhibition in euglycemia. Am J Physiol Renal Physiol 2014;306:F188-93.

Riehle C, Wende AR, Zaha VG et al. PGC-1beta deficiency accelerates the transition to heart failure in pressure overload hypertrophy. Circ Res 2011;109:783-93.

Rosano GM, Fini M, Caminiti G, Barbaro G. Cardiac metabolism in myocardial ischemia. Curr Pharm Des 2008;14:2551-62.

Rosenstock J, Jelaska A, Zeller C et al. Impact of empagliflozin added on to basal insulin in type 2 diabetes inadequately controlled on basal insulin: a 78-week randomized, double-blind, placebo-controlled trial. Diabetes, obesity & metabolism 2015;17:936-48.

Rudolph W, Maas D, Richter J, Hasinger F, Hofmann H, Dohrn P. [on the Significance of Acetoacetate and Beta-Hydroxybutyrate in Human Myocardial Metabolism]. Klin Wochenschr 1965;43:445-51.

Russell RR, 3rd, Li J, Coven DL et al. AMP-activated protein kinase mediates ischemic glucose uptake and prevents postischemic cardiac dysfunction, apoptosis, and injury. J Clin Invest 2004;114:495-503.

Russell RR, 3rd, Taegtmeyer H. Changes in citric acid cycle flux and anaplerosis antedate the functional decline in isolated rat hearts utilizing acetoacetate. J Clin Invest 1991;87:384-90.

Sack MN, Rader TA, Park S, Bastin J, McCune SA, Kelly DP. Fatty acid oxidation enzyme gene expression is downregulated in the failing heart. Circulation 1996;94:2837-42.

Sanchez-Lopez E, Rodriguez-Vita J, Cartier C et al. Inhibitory effect of interleukin-1beta on angiotensin II-induced connective tissue growth factor and type IV collagen production in cultured mesangial cells. Am J Physiol Renal Physiol 2008;294:F149-60.

Sandanger O, Gao E, Ranheim T et al. NLRP3 inflammasome activation during myocardial ischemia reperfusion is cardioprotective. Biochem Biophys Res Commun 2016;469:1012-20.

Santos-Gallego CG, Requena-Ibanez JA, San Antonio R et al. Empagliflozin Ameliorates Adverse Left Ventricular Remodeling in Nondiabetic Heart Failure by Enhancing Myocardial Energetics. J Am Coll Cardiol 2019;73:1931-1944.

Sarashina A, Koiwai K, Seman LJ et al. Safety, tolerability, pharmacokinetics and pharmacodynamics of single doses of empagliflozin, a sodium glucose cotransporter 2 (SGLT2) inhibitor, in healthy Japanese subjects. Drug Metab Pharmacokinet 2013;28:213-9.

Sarrazy V, Billet F, Micallef L, Coulomb B, Desmouliere A. Mechanisms of pathological scarring: role of myofibroblasts and current developments. Wound Repair Regen 2011;19 Suppl 1:s10-5.

Sato K, Kashiwaya Y, Keon CA et al. Insulin, ketone bodies, and mitochondrial energy transduction. FASEB J 1995;9:651-8.

Sato T, Aizawa Y, Yuasa S et al. The effect of dapagliflozin treatment on epicardial adipose tissue volume. Cardiovasc Diabetol 2018;17:6.

Sattar N, McLaren J, Kristensen SL, Preiss D, McMurray JJ. SGLT2 Inhibition and cardiovascular events: why did EMPA-REG Outcomes surprise and what were the likely mechanisms? Diabetologia 2016;59:1333-1339.

Savarese G, Lund LH. Global Public Health Burden of Heart Failure. Card Fail Rev 2017;3:7-11.

Schroder K, Zhou R, Tschopp J. The NLRP3 inflammasome: a sensor for metabolic danger? Science 2010;327:296-300.

Scirica BM, Bhatt DL, Braunwald E et al. Saxagliptin and cardiovascular outcomes in patients with type 2 diabetes mellitus. N Engl J Med 2013;369:1317-26.

Segura AM, Frazier OH, Buja LM. Fibrosis and heart failure. Heart failure reviews 2014;19:173-85.

Seman L, Macha S, Nehmiz G et al. Empagliflozin (BI 10773), a Potent and Selective SGLT2 Inhibitor, Induces Dose-Dependent Glucosuria in Healthy Subjects. Clin Pharmacol Drug Dev 2013;2:152-61.

Serhan CN, Brain SD, Buckley CD et al. Resolution of inflammation: state of the art, definitions and terms. FASEB J 2007;21:325-32.

Seubert J, Yang B, Bradbury JA et al. Enhanced postischemic functional recovery in CYP2J2 transgenic hearts involves mitochondrial ATP-sensitive K+ channels and p42/p44 MAPK pathway. Circulation research 2004;95:506-14.

Shah KS, Xu H, Matsouaka RA et al. Heart Failure With Preserved, Borderline, and Reduced Ejection Fraction: 5-Year Outcomes. J Am Coll Cardiol 2017;70:2476-2486.

Shang S, Wang L, Zhang Y, Lu H, Lu X. The Beta-Hydroxybutyrate Suppresses the Migration of Glioma Cells by Inhibition of NLRP3 Inflammasome. Cell Mol Neurobiol 2018;38:1479-1489.

Sharov VG, Todor AV, Silverman N, Goldstein S, Sabbah HN. Abnormal mitochondrial respiration in failed human myocardium. J Mol Cell Cardiol 2000;32:2361-7.

Shende P, Plaisance I, Morandi C et al. Cardiac raptor ablation impairs adaptive hypertrophy, alters metabolic gene expression, and causes heart failure in mice. Circulation 2011;123:1073-82.

Shi X, Verma S, Yun J et al. Effect of empagliflozin on cardiac biomarkers in a zebrafish model of heart failure: clues to the EMPA-REG OUTCOME trial? Mol Cell Biochem 2017;433:97-102.

Shimazu T, Hirschey MD, Newman J et al. Suppression of oxidative stress by beta-hydroxybutyrate, an endogenous histone deacetylase inhibitor. Science 2013;339:211-4.

Sivakumar P, Gupta S, Sarkar S, Sen S. Upregulation of lysyl oxidase and MMPs during cardiac remodeling in human dilated cardiomyopathy. Mol Cell Biochem 2008;307:159-67.

Sivasubramanian N, Coker ML, Kurrelmeyer KM et al. Left ventricular remodeling in transgenic mice with cardiac restricted overexpression of tumor necrosis factor. Circulation 2001;104:826-31.

Soliman OI, Geleijnse ML, Theuns DA et al. Reverse of left ventricular volumetric and structural remodeling in heart failure patients treated with cardiac resynchronization therapy. Am J Cardiol 2008;101:651-7.

Song E, Jahng JW, Chong LP et al. Lipocalin-2 induces NLRP3 inflammasome activation via HMGB1 induced TLR4 signaling in heart tissue of mice under pressure overload challenge. Am J Transl Res 2017;9:2723-2735.

Spindler M, Saupe KW, Christe ME et al. Diastolic dysfunction and altered energetics in the alphaMHC403/+ mouse model of familial hypertrophic cardiomyopathy. J Clin Invest 1998;101:1775-83.

Sriramula S, Francis J. Tumor Necrosis Factor - Alpha Is Essential for Angiotensin II-Induced Ventricular Remodeling: Role for Oxidative Stress. PLoS One 2015;10:e0138372.

Stanley WC, Meadows SR, Kivilo KM, Roth BA, Lopaschuk GD. beta-Hydroxybutyrate inhibits myocardial fatty acid oxidation in vivo independent of changes in malonyl-CoA content. Am J Physiol Heart Circ Physiol 2003;285:H1626-31.

Stanley WC, Recchia FA, Lopaschuk GD. Myocardial substrate metabolism in the normal and failing heart. Physiol Rev 2005;85:1093-129.

Stansfield WE, Charles PC, Tang RH et al. Regression of pressure-induced left ventricular hypertrophy is characterized by a distinct gene expression profile. J Thorac Cardiovasc Surg 2009;137:232-8, 238e1-8.

Stechman MJ, Ahmad BN, Loh NY et al. Establishing normal plasma and 24-hour urinary biochemistry ranges in C3H, BALB/c and C57BL/6J mice following acclimatization in metabolic cages. Lab Anim 2010;44:218-25.

Stender RN, Engler WJ, Braun TM, Hankenson FC. Establishment of blood analyte intervals for laboratory mice and rats by use of a portable clinical analyzer. J Am Assoc Lab Anim Sci 2007;46:47-52.

Stutz A, Kolbe CC, Stahl R et al. NLRP3 inflammasome assembly is regulated by phosphorylation of the pyrin domain. J Exp Med 2017;214:1725-1736.

Sun M, Chen M, Dawood F et al. Tumor necrosis factor-alpha mediates cardiac remodeling and ventricular dysfunction after pressure overload state. Circulation 2007;115:1398-407.

Sung MM, Byrne NJ, Kim TT et al. Cardiomyocyte-specific ablation of CD36 accelerates the progression from compensated cardiac hypertrophy to heart failure. Am J Physiol Heart Circ Physiol 2017;312:H552-H560.

Sung MM, Byrne NJ, Robertson IM et al. Resveratrol improves exercise performance and skeletal muscle oxidative capacity in heart failure. American journal of physiology Heart and circulatory physiology 2017;312:H842-H853.

Sung MM, Das SK, Levasseur J et al. Resveratrol treatment of mice with pressure-overload-induced heart failure improves diastolic function and cardiac energy metabolism. Circulation Heart failure 2015;8:128-37.

Sung MM, Koonen DP, Soltys CL, Jacobs RL, Febbraio M, Dyck JR. Increased CD36 expression in middle-aged mice contributes to obesity-related cardiac hypertrophy in the absence of cardiac dysfunction. J Mol Med (Berl) 2011;89:459-69.

Sutterwala FS, Haasken S, Cassel SL. Mechanism of NLRP3 inflammasome activation. Ann N Y Acad Sci 2014;1319:82-95.

Suzuki M, Takeda M, Kito A et al. Tofogliflozin, a sodium/glucose cotransporter 2 inhibitor, attenuates body weight gain and fat accumulation in diabetic and obese animal models. Nutr Diabetes 2014;4:e125.

Tabas I, Glass CK. Anti-inflammatory therapy in chronic disease: challenges and opportunities. Science 2013;339:166-72.

Taegtmeyer H. Genetics of energetics: transcriptional responses in cardiac metabolism. Ann Biomed Eng 2000;28:871-6.

Tahara A, Kurosaki E, Yokono M et al. Effects of SGLT2 selective inhibitor ipragliflozin on hyperglycemia, hyperlipidemia, hepatic steatosis, oxidative stress, inflammation, and obesity in type 2 diabetic mice. European journal of pharmacology 2013;715:246-55.

Tahara A, Kurosaki E, Yokono M et al. Effects of sodium-glucose cotransporter 2 selective inhibitor ipragliflozin on hyperglycaemia, oxidative stress, inflammation and liver injury in streptozotocin-induced type 1 diabetic rats. The Journal of pharmacy and pharmacology 2014;66:975-87.

Takahashi M. NLRP3 inflammasome as a novel player in myocardial infarction. Int Heart J 2014;55:101-5.

Tan SA, Tan L. Empagliflozin and Canagliflozin Attenuate Inflammatory Cytokines Interferon-λ, Tumor Necrosis Factor-α, Interleukin-6: Possible Mechanism of Decreasing Cardiovascular Risk in Diabetes Mellitus. Journal of the American College of Cardiology 2018;71.

Tate MD, Ong JD, Dowling JK et al. Reassessing the role of the NLRP3 inflammasome during pathogenic influenza A virus infection via temporal inhibition. Sci Rep 2016;6:27912.

Taylor M, Wallhaus TR, Degrado TR et al. An evaluation of myocardial fatty acid and glucose uptake using PET with [18F]fluoro-6-thia-heptadecanoic acid and [18F]FDG in Patients with Congestive Heart Failure. J Nucl Med 2001;42:55-62.

Taylor SI, Blau JE, Rother KI. SGLT2 Inhibitors May Predispose to Ketoacidosis. J Clin Endocrinol Metab 2015;100:2849-52.

Testa M, Yeh M, Lee P et al. Circulating levels of cytokines and their endogenous modulators in patients with mild to severe congestive heart failure due to coronary artery disease or hypertension. J Am Coll Cardiol 1996;28:964-71.

Thomas MC. Type 2 Diabetes and Heart Failure: Challenges and Solutions. Current cardiology reviews 2016;12:249-55.

Tian R, Musi N, D'Agostino J, Hirshman MF, Goodyear LJ. Increased adenosine monophosphate-activated protein kinase activity in rat hearts with pressure-overload hypertrophy. Circulation 2001;104:1664-9.

Tian R, Nascimben L, Ingwall JS, Lorell BH. Failure to maintain a low ADP concentration impairs diastolic function in hypertrophied rat hearts. Circulation 1997;96:1313-9.

Tikkanen I, Narko K, Zeller C et al. Empagliflozin reduces blood pressure in patients with type 2 diabetes and hypertension. Diabetes Care 2015;38:420-8.

Timonen P, Magga J, Risteli J et al. Cytokines, interstitial collagen and ventricular remodelling in dilated cardiomyopathy. Int J Cardiol 2008;124:293-300.

Torre-Amione G, Kapadia S, Benedict C, Oral H, Young JB, Mann DL. Proinflammatory cytokine levels in patients with depressed left ventricular ejection fraction: a report from the Studies of Left Ventricular Dysfunction (SOLVD). J Am Coll Cardiol 1996;27:1201-6.

Traba J, Kwarteng-Siaw M, Okoli TC et al. Fasting and refeeding differentially regulate NLRP3 inflammasome activation in human subjects. J Clin Invest 2015;125:4592-600.

Trotta MC, Maisto R, Guida F et al. The activation of retinal HCA2 receptors by systemic beta-hydroxybutyrate inhibits diabetic retinal damage through reduction of endoplasmic reticulum stress and the NLRP3 inflammasome. PLoS One 2019;14:e0211005.

Tucey TM, Verma-Gaur J, Nguyen J et al. The Endoplasmic Reticulum-Mitochondrion Tether ERMES Orchestrates Fungal Immune Evasion, Illuminating Inflammasome Responses to Hyphal Signals. mSphere 2016;1.

Tuunanen H, Engblom E, Naum A et al. Decreased myocardial free fatty acid uptake in patients with idiopathic dilated cardiomyopathy: evidence of relationship with insulin resistance and left ventricular dysfunction. J Card Fail 2006;12:644-52.

Tuunanen H, Ukkonen H, Knuuti J. Myocardial fatty acid metabolism and cardiac performance in heart failure. Curr Cardiol Rep 2008;10:142-8.

Umbarawan Y, Syamsunarno M, Koitabashi N et al. Myocardial fatty acid uptake through CD36 is indispensable for sufficient bioenergetic metabolism to prevent progression of pressure overload-induced heart failure. Sci Rep 2018;8:12035.

Ussher JR, Wang W, Gandhi M et al. Stimulation of glucose oxidation protects against acute myocardial infarction and reperfusion injury. Cardiovasc Res 2012;94:359-69.

Uthman L, Baartscheer A, Bleijlevens B et al. Class effects of SGLT2 inhibitors in mouse cardiomyocytes and hearts: inhibition of Na(+)/H(+) exchanger, lowering of cytosolic Na(+) and vasodilation. Diabetologia 2018;61:722-726.

Uthman L, Nederlof R, Eerbeek O et al. Delayed ischemic contracture onset by Empagliflozin associates with NHE-1 inhibition and is dependent on insulin in isolated mouse hearts. Cardiovasc Res 2019.

Vaduganathan M, Greene SJ, Butler J et al. The immunological axis in heart failure: importance of the leukocyte differential. Heart Fail Rev 2013;18:835-45.

Vallon V, Platt KA, Cunard R et al. SGLT2 mediates glucose reabsorption in the early proximal tubule. J Am Soc Nephrol 2011;22:104-12.

van Hout GP, Bosch L, Ellenbroek GH et al. The selective NLRP3-inflammasome inhibitor MCC950 reduces infarct size and preserves cardiac function in a pig model of myocardial infarction. Eur Heart J 2016.

Van Linthout S, Tschope C. Inflammation - Cause or Consequence of Heart Failure or Both? Current heart failure reports 2017;14:251-265.

Velagaleti RS, Pencina MJ, Murabito JM et al. Long-term trends in the incidence of heart failure after myocardial infarction. Circulation 2008;118:2057-62.

Verma S, Garg A, Yan AT et al. Effect of Empagliflozin on Left Ventricular Mass and Diastolic Function in Individuals With Diabetes: An Important Clue to the EMPA-REG OUTCOME Trial? Diabetes Care 2016;39:e212-e213.

Verma S, Garg A, Yan AT et al. Effect of Empagliflozin on Left Ventricular Mass and Diastolic Function in Individuals With Diabetes: An Important Clue to the EMPA-REG OUTCOME Trial? Diabetes Care 2016.

Verma S, McMurray JJV, Cherney DZI. The Metabolodiuretic Promise of Sodium-Dependent Glucose Cotransporter 2 Inhibition: The Search for the Sweet Spot in Heart Failure. JAMA cardiology 2017;2:939-940.

Verma S, McMurray JJV. SGLT2 inhibitors and mechanisms of cardiovascular benefit: a state-of-the-art review. Diabetologia 2018;61:2108-2117.

Verma S, Rawat S, Ho KL et al. Empagliflozin Increases Cardiac Energy Production in Diabetes: Novel Translational Insights Into the Heart Failure Benefits of SGLT2 Inhibitors. JACC Basic to translational science 2018;3:575-587.

Vogel C, Marcotte EM. Insights into the regulation of protein abundance from proteomic and transcriptomic analyses. Nat Rev Genet 2012;13:227-32.

von Haehling S, Schefold JC, Lainscak M, Doehner W, Anker SD. Inflammatory biomarkers in heart failure revisited: much more than innocent bystanders. Heart Fail Clin 2009;5:549-60.

von Lewinski D, Rainer PP, Gasser R et al. Glucose-transporter-mediated positive inotropic effects in human myocardium of diabetic and nondiabetic patients. Metabolism 2010;59:1020-8.

Vrhovac I, Balen Eror D, Klessen D et al. Localizations of Na(+)-D-glucose cotransporters SGLT1 and SGLT2 in human kidney and of SGLT1 in human small intestine, liver, lung, and heart. Pflugers Archiv : European journal of physiology 2015;467:1881-98.

Wang Y, Wu Y, Chen J, Zhao S, Li H. Pirfenidone attenuates cardiac fibrosis in a mouse model of TAC-induced left ventricular remodeling by suppressing NLRP3 inflammasome formation. Cardiology 2013;126:1-11.

Wanner C, Lachin JM, Inzucchi SE et al. Empagliflozin and Clinical Outcomes in Patients With Type 2 Diabetes Mellitus, Established Cardiovascular Disease, and Chronic Kidney Disease. Circulation 2018;137:119-129.

Wen H, Gris D, Lei Y et al. Fatty acid-induced NLRP3-ASC inflammasome activation interferes with insulin signaling. Nat Immunol 2011;12:408-15.

Wettschureck N, Rutten H, Zywietz A et al. Absence of pressure overload induced myocardial hypertrophy after conditional inactivation of Galphaq/Galpha11 in cardiomyocytes. Nat Med 2001;7:1236-40.

White WB, Pratley R, Fleck P et al. Cardiovascular safety of the dipetidyl peptidase-4 inhibitor alogliptin in type 2 diabetes mellitus. Diabetes Obes Metab 2013;15:668-73.

Wilson PW, Kannel WB, Silbershatz H, D'Agostino RB. Clustering of metabolic factors and coronary heart disease. Archives of internal medicine 1999;159:1104-9.

Winder WW, Hardie DG. AMP-activated protein kinase, a metabolic master switch: possible roles in type 2 diabetes. Am J Physiol 1999;277:E1-10.

Wiviott SD, Raz I, Bonaca MP et al. Dapagliflozin and Cardiovascular Outcomes in Type 2 Diabetes. N Engl J Med 2019;380:347-357.

Wright EM, Loo DD, Hirayama BA. Biology of human sodium glucose transporters. Physiol Rev 2011;91:733-94.

Xu C, Wang W, Zhong J et al. Canagliflozin exerts anti-inflammatory effects by inhibiting intracellular glucose metabolism and promoting autophagy in immune cells. Biochem Pharmacol 2018;152:45-59.

Xu L, Nagata N, Nagashimada M et al. SGLT2 Inhibition by Empagliflozin Promotes Fat Utilization and Browning and Attenuates Inflammation and Insulin Resistance by Polarizing M2 Macrophages in Diet-induced Obese Mice. EBioMedicine 2017;20:137-149.

Xu X, Lu Z, Fassett J et al. Metformin protects against systolic overload-induced heart failure independent of AMP-activated protein kinase alpha2. Hypertension 2014;63:723-8.

Yanai H, Hakoshima M, Adachi H et al. Effects of Six Kinds of Sodium-Glucose Cotransporter 2 Inhibitors on Metabolic Parameters, and Summarized Effect and Its Correlations With Baseline Data. J Clin Med Res 2017;9:605-612.

Yancy CW, Jessup M, Bozkurt B et al. 2013 ACCF/AHA guideline for the management of heart failure: a report of the American College of Cardiology Foundation/American Heart Association Task Force on Practice Guidelines. J Am Coll Cardiol 2013;62:e147-239.

Yang CC, Chen YT, Wallace CG et al. Early administration of empagliflozin preserved heart function in cardiorenal syndrome in rat. Biomed Pharmacother 2019;109:658-670.

Yang DK, Choi BY, Lee YH et al. Gene profiling during regression of pressure overload-induced cardiac hypertrophy. Physiol Genomics 2007;30:1-7.

Ye Y, Bajaj M, Yang HC, Perez-Polo JR, Birnbaum Y. SGLT-2 Inhibition with Dapagliflozin Reduces the Activation of the Nlrp3/ASC Inflammasome and Attenuates the Development of Diabetic Cardiomyopathy in Mice with Type 2 Diabetes. Further Augmentation of the Effects with Saxagliptin, a DPP4 Inhibitor. Cardiovascular drugs and therapy 2017;31:119-132.

Yokono M, Takasu T, Hayashizaki Y et al. SGLT2 selective inhibitor ipragliflozin reduces body fat mass by increasing fatty acid oxidation in high-fat diet-induced obese rats. Eur J Pharmacol 2014;727:66-74.

Yokoyama H, Gunasegaram S, Harding SE, Avkiran M. Sarcolemmal Na+/H+ exchanger activity and expression in human ventricular myocardium. J Am Coll Cardiol 2000;36:534-40.

Youm YH, Nguyen KY, Grant RW et al. The ketone metabolite beta-hydroxybutyrate blocks NLRP3 inflammasome-mediated inflammatory disease. Nat Med 2015;21:263-9.

Yurista SR, Sillje HHW, Oberdorf-Maass SU et al. Sodium-glucose co-transporter 2 inhibition with empagliflozin improves cardiac function in non-diabetic rats with left ventricular dysfunction after myocardial infarction. Eur J Heart Fail 2019.

Zhabyeyev P, Gandhi M, Mori J et al. Pressure-overload-induced heart failure induces a selective reduction in glucose oxidation at physiological afterload. Cardiovasc Res 2013;97:676-85.

Zhang L, Jaswal JS, Ussher JR et al. Cardiac insulin-resistance and decreased mitochondrial energy production precede the development of systolic heart failure after pressure-overload hypertrophy. Circ Heart Fail 2013;6:1039-48.

Zhang P, Su J, Mende U. Cross talk between cardiac myocytes and fibroblasts: from multiscale investigative approaches to mechanisms and functional consequences. Am J Physiol Heart Circ Physiol 2012;303:H1385-96.

Zhang X, Javan H, Li L et al. A modified murine model for the study of reverse cardiac remodelling. Exp Clin Cardiol 2013;18:e115-7.

Zhong J, Basu R, Guo D et al. Angiotensin-converting enzyme 2 suppresses pathological hypertrophy, myocardial fibrosis, and cardiac dysfunction. Circulation 2010;122:717-28, 18 p following 728.

Zhou L, Cryan EV, D'Andrea MR, Belkowski S, Conway BR, Demarest KT. Human cardiomyocytes express high level of Na+/glucose cotransporter 1 (SGLT1). J Cell Biochem 2003;90:339-46.

Zhou R, Tardivel A, Thorens B, Choi I, Tschopp J. Thioredoxin-interacting protein links oxidative stress to inflammasome activation. Nat Immunol 2010;11:136-40.

Zinman B, Wanner C, Lachin JM et al. Empagliflozin, Cardiovascular Outcomes, and Mortality in Type 2 Diabetes. N Engl J Med 2015;373:2117-28.

Zordoky BN, Aboutabl ME, El-Kadi AO. Modulation of cytochrome P450 gene expression and arachidonic acid metabolism during isoproterenol-induced cardiac hypertrophy in rats. Drug metabolism and disposition: the biological fate of chemicals 2008;36:2277-86.

Zordoky BN, Sung MM, Ezekowitz J et al. Metabolomic fingerprint of heart failure with preserved ejection fraction. PLoS One 2015;10:e0124844.

Appendices

Appendix A

Animal dose calculation (Nair and Jacob 2016):

Allometric scaling is a technique used in research to extrapolate drug dose between animals and humans based on differences in body surface area. This approach is recommended by the US Food and Drug Administration's current guidelines when estimating the maximum dose for clinical studies, by accounting for the fact that larger animals (or humans) have lower metabolic rates and a slower physiological process and therefore require a smaller drug dose based on body weight.

Human dose range (empagliflozin- based on 60 kg human): 10-100 mg daily

10 mg/day / 60 kg = 0.167 mg/kg/day

100 mg/day / 60 kg = 1.67 mg/kg/day

Mouse dose = Human equivalent dose (HED) **x 12.3** (Nair and Jacob 2016)

0.167 mg/kg/day **x 12.3** = 2.05 mg/kg/day

1.67 mg/kg/day **x 12.3** = 20.5 mg/kg/day

Mouse range = 2.05-20.5 mg/kg/day

Rat dose = Human equivalent dose (HED) **x 6.2** (Nair and Jacob 2016)

0.167 mg/kg/day **x 6.2** = 1.03 mg/kg/day

1.67 mg/kg/day **x 6.2** = 10.3 mg/kg/day

Rat range = 1.03-10.3 mg/kg/day

Appendix B

Details of TAC surgery:

Mice were anaesthetized by an intraperitoneal injection of a cocktail of ketamine (100 mg/kg) and xylazine (20 mg/kg); surgical plane of anesthesia was confirmed by lack of reflex or response to toe-pinching. Endotracheal intubation was performed using 22G tubing, which was then connected to a ventilator (Hugo-Sachs Electronik Mini-Vent, Harvard Apparatus Canada) and ventilated at 200-250ul SV and 150 breaths/min. A topical agent was applied to chest area to remove fur surrounding the incision area, skin was cleaned with topical antiseptic and Liquid Tears applies to eyes. A pre-operative analgesia, Meloxicam (1-2mg/kg), was injected subcutaneously prior to surgery and body temperature was maintained at 37°C by use of a heating pad. A vertical skin incision was made from the suprasternal notch to mid-sternum, and then straight blunt scissors used to cut the sternum to the 3 or 4^{th} rib. Mini-Goldstein (FST) spreaders are used to retract the ribs. The thymus was blunt dissected and the aortic arch visualized. The transverse arch was carefully dissected free of connective tissue and a 6/0 silk suture was passed under the aortic arch between the innominate and left common carotid arteries and tied encircling the aorta around a double-blunted 27-gauge (0.4mm) needle. The needle, used to standardize the stenosis, was quickly removed allowing the suture to constrict the aorta. The thymus is gently replaced, and retractors removed, 2 sutures are placed in sternum, and skin incision was closed using 6/0 vicryl suture continuous pattern. Sham operated animals underwent the same procedure without banding. Animals were removed from ventilator, given a post-operative analgesia , Meloxicam (1-2mg/kg), and monitored throughout recovery in a pre-warmed cage with food and water ad libitum.

Appendix C

Antibodies used for Immunoblot analysis:

Anti-	Protein	Company	Product Number	Clonality	MW (kDa)	Source (IgG)	WB Dilution
4E-BP1 (53H11)	eukaryotic translation initiation factor 4E-binding protein	Cell Signaling Technology	9644	monoclonal	15-20	Rabbit	1:1000
Akt	protein kinase B	Cell Signaling Technology	9272	polyclonal	60	Rabbit	1:500
GAPDH (14C10)	glyceraldehyde 3-phosphate dehydrogenase	Cell Signaling Technology	2118	monoclonal	37	Rabbit	1:1000
GAPDH (6C5)	glyceraldehyde 3-phosphate dehydrogenase	Calbiochem	CB1001	monoclonal	36	Mouse	1:1000
GSK3β (27C10)	glycogen synthase kinase-3 beta	Cell Signaling Technology	9315	monoclonal	46	Rabbit	1:1000
IL-1β	interleukin-1 beta	Abcam	ab9722	polyclonal	31	Rabbit	1:1000
IL-1β (3A6)	interleukin-1 beta	Cell Signaling Technology	12242	monoclonal	17,31	Mouse	1:1000
mTOR	mechanistic target of rapamycin	Cell Signaling Technology	2972	polyclonal	289	Rabbit	1:1000
NLRP3	nucleotide-binding domain-like receptor protein 3	Abcam	ab214185	polyclonal	114	Rabbit	1:500
phospho-ACC (Ser79)	phosphorylated acetyl-coA carboxylase	Cell Signaling Technology	3661	polyclonal	280	Rabbit	1:1000
phospho-AMPKα (Thr172)	phosphorylated AMP-activated protein kinase-alpha	Cell Signaling Technology	2531	polyclonal	62	Rabbit	1:1000
Raptor (24C12)	regulatory associated protein of mTOR	Cell Signaling Technology	2280	monoclonal	150	Rabbit	1:1000
S6 Ribosomal Protein (5G10)	ribosomal protein S6	Cell Signaling Technology	2217	monoclonal	32	Rabbit	1:1000
Txnip (JY2)	thioredoxin-interacting protein	MBL International	K0205-3	monoclonal	50	Mouse	1:500

MW = molecular weight; WB = western blotting